



## **Terms and Conditions of Use of Digitised Theses from Trinity College Library Dublin**

### **Copyright statement**

All material supplied by Trinity College Library is protected by copyright (under the Copyright and Related Rights Act, 2000 as amended) and other relevant Intellectual Property Rights. By accessing and using a Digitised Thesis from Trinity College Library you acknowledge that all Intellectual Property Rights in any Works supplied are the sole and exclusive property of the copyright and/or other IPR holder. Specific copyright holders may not be explicitly identified. Use of materials from other sources within a thesis should not be construed as a claim over them.

A non-exclusive, non-transferable licence is hereby granted to those using or reproducing, in whole or in part, the material for valid purposes, providing the copyright owners are acknowledged using the normal conventions. Where specific permission to use material is required, this is identified and such permission must be sought from the copyright holder or agency cited.

### **Liability statement**

By using a Digitised Thesis, I accept that Trinity College Dublin bears no legal responsibility for the accuracy, legality or comprehensiveness of materials contained within the thesis, and that Trinity College Dublin accepts no liability for indirect, consequential, or incidental, damages or losses arising from use of the thesis for whatever reason. Information located in a thesis may be subject to specific use constraints, details of which may not be explicitly described. It is the responsibility of potential and actual users to be aware of such constraints and to abide by them. By making use of material from a digitised thesis, you accept these copyright and disclaimer provisions. Where it is brought to the attention of Trinity College Library that there may be a breach of copyright or other restraint, it is the policy to withdraw or take down access to a thesis while the issue is being resolved.

### **Access Agreement**

By using a Digitised Thesis from Trinity College Library you are bound by the following Terms & Conditions. Please read them carefully.

I have read and I understand the following statement: All material supplied via a Digitised Thesis from Trinity College Library is protected by copyright and other intellectual property rights, and duplication or sale of all or part of any of a thesis is not permitted, except that material may be duplicated by you for your research use or for educational purposes in electronic or print form providing the copyright owners are acknowledged using the normal conventions. You must obtain permission for any other use. Electronic or print copies may not be offered, whether for sale or otherwise to anyone. This copy has been supplied on the understanding that it is copyright material and that no quotation from the thesis may be published without proper acknowledgement.

**MECHANICAL TESTING PROTOCOLS AS PERFORMANCE INDICATORS FOR  
GLASS-IONOMERS**

**A thesis submitted to the University of Dublin in fulfilment of the requirements for  
The degree of Doctor of Philosophy by**

**Mirza Shahzad Baig**

**May 2015**

**Materials Science Unit**

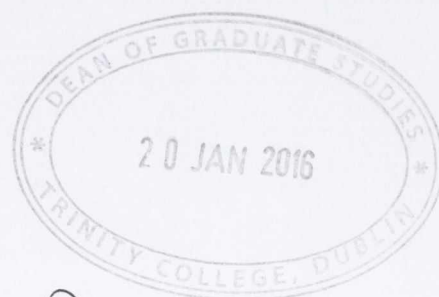
**Division of Oral Biosciences**

**School of Dentistry**

**Dublin Dental University Hospital**

**Trinity College Dublin**

**University of Dublin**



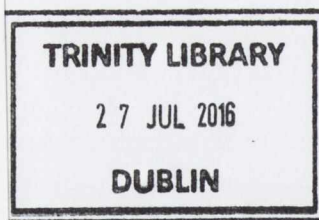
*M.D.*  
*School of Dental Science*

## DECLARATION

I declare that this thesis has not been submitted as an exercise for a degree at this or any other University and it is entirely my own work.

I agree to deposit this thesis in the University's open access institutional repository or allow the library to do so on my behalf, subject to Irish Copyright Legislation and Trinity College Dublin Library conditions of use and acknowledgement.

The mentoring contribution of my supervisor in the preparation of the publications presented herein is respectfully acknowledged.



*Thesis 11038*

## SUMMARY

The aim of the current investigation was to identify a reproducible and discriminatory mechanical testing methodology to act as a performance indicator for glass-ionomers (GIs). The investigation is presented as a series of manuscripts. The dental literature was reviewed to highlight developments in GI powder and liquid constituents since their inception and adoption into the dental field in the early 1970's (Manuscript 3.1). The various reinforcement strategies employed in the dental literature were highlighted to assess the mechanical properties of GIs with their corresponding levels of success or failure (Manuscript 3.1). The mixing and testing conditions employed by investigators for each GI reinforcement strategy were critically reviewed and all experimental short-comings were highlighted (Manuscript 3.1). The GI dental literature was identified to be replete with studies failing to report the mixing and testing conditions employed and with many failing to follow the specifications prescribed in ISO 9917-1:2007 for compressive fracture strength (CFS) testing of GIs which produced an impossibility for comparison between studies (Manuscript 3.1). Previously, the three-point flexure strength (TFS) and biaxial flexure strength (BFS) tests failed to discriminate between three encapsulated GI products when performed under standardised mixing and testing conditions despite the compositional and powder content variations between the three GI products, although differences in CFS were evident. To identify the discriminatory ability of other testing methodologies identified for GIs in the dental literature, the current study investigated the Hertzian Indentation (HI) test (Manuscript 3.2) for reasons of clinical relevance and the fracture toughness ( $K_{IC}$ ) test (Manuscript 3.3) as  $K_{IC}$  is an intrinsic material property by using the same encapsulated GI products (to eliminate product variability between the studies). The HI test was identified as the most clinically relevant testing methodology owing to simulation of occlusal loading conditions and was able to

discriminate between the encapsulated GI products investigated (Manuscript 3.2), although the Hertzian load bearing capacity was recorded as the maximum load-to-failure (Wang and Darvell, 2007) which was not an intrinsic material property. The  $K_{IC}$  test failed to discriminate between the encapsulated GIs investigated, despite  $K_{IC}$  being an intrinsic material property (Manuscript 3.3) and examination of the load-to-failure data revealed that the load-to-failure values were too low to be discriminatory. The GI developmental process involves hand-mixing the GI liquid with varying powder contents and performing preliminary mechanical tests to establish the optimum powder:liquid mixing ratio, such that the mechanical testing protocol of choice must be discriminatory between GIs manipulated with varying powder contents. The CFS, TFS, BFS, HI (Manuscript 3.4) and  $K_{IC}$  (Manuscript 3.3) testing methodologies for GI restoratives were revisited using a hand-mixed GI restorative prepared with varying powder content for a constant weight of liquid. When employed for hand-mixed GIs, the CFS test was identified as the only 'truly' discriminatory testing methodology by identifying a linear deterioration in CFS as the amount of the reinforcing glass filler content was progressively reduced. The TFS and BFS tests failed to discriminate between the GI groups, owing to a uniform surface finishing condition for all specimens irrespective of the powder content. The HI test failed to act as a discriminatory performance indicator owing to indenter penetration and transition in failure mode for GIs prepared with reduced powder contents. The  $K_{IC}$  test also failed to act as discriminatory performance indicator owing to the low load-to-failure values identified for all GI powder:liquid mixing ratio groups. Therefore, the CFS test remains the only mechanical testing methodology that could be advocated for testing GIs during novel GI development.

## ACKNOWLEDGEMENTS

I am thankful to God for the health, patience and countless blessings bestowed upon me during the time of this PhD.

I acknowledge my indebtedness to my supervisor, Dr. Garry JP Fleming, for his unwavering support and guidance throughout this PhD. I am grateful to Garry for the scientific writing skills I acquired over the years as his exceptional attention to detail was a real inspiration which has made this a rewarding journey. I would like to express my gratitude for the opportunity to work with him in the Materials Science Unit which was a real honour. His friendship over the years is graciously appreciated.

I would like to acknowledge the financial assistance received from the Dublin Dental University Hospital, Trinity College Dublin.

To Dr. Adam Dowling for his assistance during the initial stages of the PhD. His help during my early days in Ireland is cordially recognised.

To Dr. Paul Hooi for a great friendship and his invaluable advice throughout my time at the Materials Science Unit. His help and endless support at all times is gratefully acknowledged.

A special thanks to Dr. Emma Louise McGinley for her positive encouragement, in particular during the later and more stressful stages of this PhD, thank you.

To Dr. Charles Lloyd for the generous donation of the fracture toughness moulds. His contribution in the preparation of the fracture toughness testing manuscript is respectfully acknowledged.

To Kevin, it has been a pleasure working with him. To Mustafa for being a true friend over the years. To Aoife for her continuous support and encouragement.

Lastly, I am indebted to my parents and siblings, who endured it all.

## CONTENTS

<b>1. INTRODUCTION</b>	<b>1</b>
1.1 Historical development of glass-ionomers	1
1.2 Developments in GI powder	4
1.2.1 Glass structure	4
1.2.2 Glass composition	8
1.3 Developments in GI liquid	13
1.3.1 Acrylic acid and itaconic or maleic acid copolymers	14
1.3.2 GIs as thermoplastic polymers	15
1.3.3 Molecular weight and concentration of polyacrylic acid	18
1.4 Strategies of reinforcement	26
1.4.1 Fibres	27
1.4.2 Metallic powders	30
1.4.3 Hydroxyapatite	35
1.4.4 Bioactive glass particles	38
1.4.5 Montmorillonite clay	38
1.4.6 Novel polyacids	39
1.4.7 Modified copolymers	41
1.4.8 Hand-mixing GIs	46
1.4.9 Testing methodology	47
1.4.10 The way forward?	48
<b>2. MATERIALS AND METHODS SUPPLEMENTAL MATERIAL</b>	<b>50</b>
2.1 Raw materials	50
2.1.1 Encapsulated GI restoratives	50

2.1.2	Hand-mixed GI restorative	52
2.2	GI restorative preparation	52
2.2.1	Encapsulated GI restoratives	52
2.2.2	Hand-mixed GI restorative	56
2.3	Mechanical testing protocols	58
2.3.1	Compressive fracture strength test	58
2.3.1.1	Specimen preparation	58
2.3.1.2	Compressive fracture strength testing procedure	62
2.3.2	Three-point flexure test	64
2.3.2.1	Specimen preparation	64
2.3.2.2	Three-point flexure testing procedure	67
2.3.3	Biaxial flexure strength	69
2.3.3.1	Specimen preparation	69
2.3.3.2	Biaxial flexure strength testing procedure	71
2.3.4	Hertzian Indentation test	73
2.3.4.1	Specimen preparation	73
2.3.4.1.1	Encapsulated GI restoratives	73
2.3.4.1.2	Hand-mixed GI restorative	75
2.3.4.2	Hertzian Indentation testing procedure	77
2.3.5	Fracture toughness test	79
2.3.5.1	Specimen preparation	79
2.3.5.1.1	Encapsulated GI restoratives	79
2.3.5.1.2	Hand-mixed GI restorative	84
2.3.5.2	Fracture toughness testing procedure	85
2.3.6	Fractography	87



2.3.6.1 Scanning electron microscope	89
2.3.6.2 Specimen preparation for fractography	89
2.3.6.3 Scanning electron microscopy procedure	90
2.3.7 Profilometry	91
2.3.7.1 Specimen preparation for profilometry	93
2.3.7.2 Profilometry procedure	93
2.3.8 Statistical analysis	94
2.3.8.1 Weibull analysis	96
<b>3. SELECTED MANUSCRIPTS</b>	<b>99</b>
3.1 Conventional glass-ionomer materials: A review of the developments in glass powder, polyacid liquid and the strategies of reinforcement	100
3.2 Hertzian indentation testing of glass-ionomer restoratives: A reliable and clinically relevant testing approach	117
3.3 Fracture toughness testing: A discriminatory mechanical testing performance indicator for glass-ionomer restoratives?	124
3.4 A discriminatory mechanical testing performance indicator protocol for hand-mixed glass-ionomer restoratives	135
<b>4. GENERAL DISCUSSION</b>	<b>147</b>
4.1 The need for a reinforced GI in restorative dentistry	147
4.2 International Organisation for Standardisation	153
4.3 A valid, reliable and discriminatory alternative mechanical testing methodology for encapsulated GIs	160
4.3.1 Hertzian Indentation test	162
4.3.2 Fracture toughness test	166

4.4 A discriminatory mechanical testing methodology for GI development	173
4.4.1 Compressive fracture strength test	174
4.4.2 Three-point flexure test	177
4.4.3 Biaxial flexure strength test	180
4.4.4 Hertzian Indentation test	183
4.4.5 Fracture toughness test	185
<b>5. CONCLUSIONS</b>	<b>188</b>
<b>6. RECOMMENDATIONS FOR FURTHER WORK</b>	<b>191</b>
<b>7. REFERENCES</b>	<b>193</b>
<b>APPENDIX</b>	<b>231</b>

## LIST OF FIGURES

- Figure 1.1** A two-dimensional (2D) schematic representation of silica illustrating the basic  $\text{SiO}_4$  tetrahedra structural units in (a) the glassy form where the basic  $\text{SiO}_4$  units are arranged in a non-periodic fashion lacking long-range order to give a random network and (b) the crystalline form where the basic  $\text{SiO}_4$  units are arranged in a regular lattice with short- and long-range order. Adapted from McMillan (1964). 5
- Figure 1.2** (a) A two-dimensional (2D) schematic representation of silica glass illustrating the basic  $\text{SiO}_4$  tetrahedra connected by bridging oxygens. The structure is shown in a simplified 2D form, where only three of the four oxygen ions surrounding each silicon ion are depicted. (b) The addition of network-modifying ions ( $\text{Na}^+$ ) results in a disruption of the glass network so that instead of a single bridging oxygen there are now four groups of two non-bridging oxygens. Adapted from McMillan (1964). 6
- Figure 1.3** A two-dimensional (2D) schematic representation of aluminosilicate glass illustrating the linked  $\text{SiO}_4$  and  $\text{AlO}_4$  tetrahedra connected by bridging oxygens. Due to the valency difference between  $\text{Si}^{4+}$  and  $\text{Al}^{3+}$ , one alkali metal cation ( $\text{M}^+$ ) per  $\text{AlO}_4$  tetrahedron must be present to ensure the electroneutrality of the glass network. Adapted from McMillan (1964). 7
- Figure 1.4** A schematic representation of hydrolysis of aluminium-oxygen-silicon bonds in an aluminosilicate glass network by the polyacid resulting in the release of metal cations for cross-linking with the polyacid. 12
- Figure 1.5** A schematic illustration of local charge balancing of aluminium and phosphorus cations forming a group of  $\text{AlPO}_7$ . The replacement of  $\text{Si}_2\text{O}_7$  groups in the glass network by  $\text{AlPO}_7$  groups provided an additional route to glass degradation by hydrolysis of the phosphorus-oxygen bonds in multi-component fluorophosphoaluminosilicate glasses. 12
- Figure 1.6** A schematic representation of an idealised model of a polymer chain confined in a tube of three-dimensional (3D) entanglements that gives rise to the entanglement theory. Adapted from Prentice (1985). 16

- Figure 1.7** A schematic representation of the ‘pull-out’ process in the formation of new surfaces during fracture where the polymer chain will be pulled out from the side of the fracture plane containing the shorter portion of the chain length. Adapted from Prentice (1985). 18
- Figure 1.8** The variation in (a) the mean compressive fracture strength (CFS) and (b) the mean elastic modulus for polyacrylic acid solutions of different molecular weights ranging from 5000 (PAA5) to 200,000 (PAA200) with increasing polyacrylic acid concentration highlighting a progressive increase in CFS and elastic modulus on increasing the polyacid concentration. On reaching an optimum polyacrylic acid concentration in solution for the individual polyacrylic acid molecular weights, the CFS and elastic moduli of the resultant conventional GIs were maximised. A further increase in the polyacid concentration of the different molecular weight polyacids resulted in a decrease in the CFS and elastic moduli. Adapted from Dowling and Fleming (2011a). 21
- Figure 1.9** The change in viscosity of the polyacrylic acid solutions of different molecular weights ranging from 5000 (PAA5) to 200,000 (PAA200) with increasing polyacrylic acid concentrations highlighting a progressive increase in viscosity with the increase in polyacrylic acid concentration for the polyacrylic acid molecular weights investigated. The increase in viscosity with increasing polyacrylic acid concentration was more distinct for the higher molecular weights investigated, namely 100,000 (PAA100) and 200,000 (PAA200). Adapted from Dowling and Fleming (2011a). 23
- Figure 1.10** The variation in the compressive fracture strength (CFS) (continuous line) and the elastic moduli (broken line) of GIs prepared with polyacrylic acid molecular weight mixtures containing 15,000 (P15) and 81,000 (P81) molecular weight polyacrylic acids at concentrations of 25, 35 and 45% with increasing P15:P81 blend ratios. A significant increase in CFS and elastic moduli for the molecular weight mixture at P15:P81 blend ratios of 70:30, 80:20 and 90:10 were highlighted when compared with the lower molecular weight control group (P15) for the three concentrations investigated. Adapted from Dowling and Fleming (2011b). 25

- Figure 1.11** The variation in viscosity of the polyacrylic acid solutions for a polyacrylic acid molecular weight mixture containing 15,000 (P15) and 81,000 (P81) molecular weight polyacrylic acids at concentrations of 25, 35 and 45%. A progressive decrease in the viscosity of the polyacrylic acid molecular weight mixture solution was highlighted as the blend ratio of the lower molecular weight polyacrylic acid (P15) to the higher molecular weight polyacrylic acid (P81) was increased for the three concentrations investigated. Adapted from Dowling and Fleming (2011b). 26
- Figure 2.1** Schematic representation of (a) the capsule design for Chemfil Rock highlighting the capsule plunger which was pressed to activate the capsule and (b) the capsule extruder used to facilitate extrusion of the mechanically mixed GI. 54
- Figure 2.2** Schematic representation of (a) the capsule design for Fuji IX<sub>GP</sub> Fast showing the capsule plunger which was pressed to partially activate the capsule and (b) the capsule applicator used for complete activation of the capsule by clicking the lever once and for extrusion of the GI mix following mechanical mixing. 55
- Figure 2.3** Schematic representation of (a) the capsule design for Ionofil Molar AC identifying the clamp located on the side of the capsule which was pressed using (b) the capsule activator. The capsule was placed into the capsule holder of the activator such that the clamp on the capsule faced the lever of the activator and following mechanical mixing the GI mix was extruded using (c) the capsule applicator. 56
- Figure 2.4** Schematic representation of the polytetrafluoroethylene (PTFE) split-mould assembly employed to manufacture cylindrical GI specimens for compressive fracture strength (CFS) testing. The two halves of the split-mould were aligned on top of the PTFE base using the locating pin and the PTFE wedges inserted to one side of the split-mould to ensure equal pressure was applied along the length of the split-mould. 59
- Figure 2.5** Schematic representation of the compressive fracture strength (CFS) testing apparatus identifying the application of a piece of wet filter paper to the compression loading platens. The cylindrical CFS specimens were placed vertically on the compression loading platen and a load applied along the long axis of the cylinder. 63

- Figure 2.6** Schematic representation of the rate of change of compressive strain as a function of compressive stress for a cylindrical GI specimen under compressive load identifying the linear elastic region, elastic limit and plastic zone prior to fracture. The compressive modulus was calculated from the slope of the initial linear segment of the stress-strain plot for each individual compressive fracture strength (CFS) specimen. 64
- Figure 2.7** Schematic representation of (a) the open-ended knife-edged polytetrafluoroethylene (PTFE) mould employed to manufacture bar-shaped three-point flexure specimens. The specimens were demoulded using (b) a customised stainless-steel demoulding device which was inserted into one end of the mould and gently pressed against the specimen end. Sliding the demoulding device along the length of mould facilitated specimen removal from the opposite end of the mould. 65
- Figure 2.8** Schematic representation of the three-point flexure test assembly highlighting a bar-shaped three-point flexure specimen resting on top of two point supports. Load was applied through the indenter in the central region of the bar-shaped specimen and the maximum load-to-failure recorded. 68
- Figure 2.9** Schematic representation of the polytetrafluoroethylene (PTFE) ring-mould employed to manufacture disc-shaped biaxial flexure strength (BFS) specimens identifying the internal diameter and thickness of the mould which produced disc-shaped specimens with the corresponding dimensions of  $13.0 \pm 0.1$  mm diameter and  $1.0 \pm 0.1$  mm thickness. 69
- Figure 2.10** Schematic representation of the biaxial flexure strength (BFS) testing apparatus highlighting a disc-shaped BFS specimen resting on top of a knife-edge annular ring support covered with a thin sheet of latex to assist uniform loading. The BFS specimens were loaded centrally using a 4 mm diameter stainless-steel ball indenter and the maximum load-to-failure recorded. 72
- Figure 2.11** Schematic representation of the polyetheretherketone (PEEK) ring-mould employed to manufacture disc-shaped Hertzian Indentation (HI) specimens identifying the internal diameter and thickness of the mould which produced disc-shaped specimens with the corresponding dimensions of  $10.0 \pm 0.1$  mm diameter and  $3.1 \pm 0.03$  mm thickness. 73

- Figure 2.12** Schematic representation of the demoulding apparatus used for the Hertzian Indentation (HI) specimens highlighting a ring-mould containing the disc-shaped HI specimen which was placed into a customised brass holder with a 12 mm diameter hole in the centre of the bottom surface. A customised 8 mm diameter brass plug was pressed against the specimen from the top which caused the specimen to ‘pop out’ from the ring-mould and drop through the hole in the bottom surface of the brass holder. 75
- Figure 2.13** Schematic representation of the Hertzian Indentation (HI) testing apparatus identifying the disc-shaped HI specimen resting on top of a nylon substrate which was constrained in a brass holder. The HI specimens were loaded from the top using a 20 mm diameter hard steel ball to simulate cusp contact. 78
- Figure 2.14** Schematic representation of the polytetrafluoroethylene (PTFE) lined brass split-mould assembly employed to manufacture single-edge notched (SEN) bend specimens for fracture toughness ( $K_{IC}$ ) testing highlighting (a) a PTFE lined brass split-mould with four screw holes located at the corners of the split-mould, two brass plugs and a scalpel blade secured in a brass blade holder. The split-mould and the brass plugs were assembled and secured onto (b) the PTFE lined brass base plate with multiple screws. 81
- Figure 2.15** Schematic representation of a single-edge notched (SEN) bend specimen resting on top of two point supports for fracture toughness ( $K_{IC}$ ) testing using a three-point flexure test assembly with the notched surface facing the point supports. Load was applied from the top through the indenter in the central region of the SEN bend specimen such that the notched surface of the specimen was placed under tension during loading. 86
- Figure 2.16** A profilometric trace extracted from the longitudinal scan (x-direction) of the fracture surfaces of two fracture fragments (left and right) of a single-edge notched (SEN) bend specimen. The length of the fracture surface on each fracture fragment measured in mm from the end of the scalpel blade impression (point 0) to the edge of the fracture fragment (point 1) for the left fracture fragment and from the edge of the fracture fragment (point 0) to the end of the scalpel blade impression (point 1) for the right fracture fragment. 94

<b>Appendix Figure 1</b>	A stress-strain plot of a cylindrical compressive fracture strength (CFS) specimen prepared with the manufacturer's recommended powder content (100%) highlighting a maximum stress of 120 MPa and a compressive strain of 0.07 mm/mm. The compressive modulus (CM) was calculated from the initial linear segment of the stress-strain graph.	231
<b>Appendix Figure 2</b>	A stress-strain plot of a cylindrical compressive fracture strength (CFS) specimen prepared with 20% of the manufacturer's recommended powder content highlighting a maximum stress of 22 MPa and a compressive strain of 0.16 mm/mm. The compressive modulus (CM) was calculated from the initial linear segment of the stress-strain graph.	231
<b>Appendix Figure 3</b>	A load-deflection plot of a bar-shaped three-point flexure strength (TFS) specimen prepared with the manufacturer's recommended powder content (100%) highlighting a maximum load of 8 N and a compressive extension of 0.09 mm. The three-point flexure modulus (TFM) was calculated from the initial linear segment of the load-deflection plot.	232
<b>Appendix Figure 4</b>	A load-deflection plot of a bar-shaped three-point flexure strength (TFS) specimen prepared with 20% of the manufacturer's recommended powder content highlighting a maximum load of 3 N and a compressive extension of 0.4 mm. The three-point flexure modulus (TFM) was calculated from the initial linear segment of the load-deflection plot.	232
<b>Appendix Figure 5</b>	A load-deflection plot of a disc-shaped biaxial flexure strength (BFS) specimen prepared with the manufacturer's recommended powder content (100%) highlighting a maximum load of 35 N and a compressive extension of 0.15 mm.	233
<b>Appendix Figure 6</b>	A load-deflection plot of a disc-shaped biaxial flexure strength (BFS) specimen prepared with 20% of the manufacturer's recommended powder content highlighting a maximum load of 6 N and a compressive extension of 0.16 mm.	233
<b>Appendix Figure 7</b>	A load-deflection plot of a disc-shaped Hertzian Indentation (HI) specimen prepared with the manufacturer's recommended powder content (100%) highlighting a maximum load of 800 N and a compressive extension of 0.19 mm.	234



<b>Appendix Figure 8</b>	A load-deflection plot of a disc-shaped Hertzian Indentation (HI) specimen prepared with 20% of the manufacturer's recommended powder content highlighting a maximum load of 400 N and a compressive extension of 0.27 mm.	234
<b>Appendix Figure 9</b>	A load-deflection plot of a single-edge notched (SEN) fracture toughness ( $K_{IC}$ ) specimen prepared with the manufacturer's recommended powder content (100%) highlighting a maximum load of 9 N and a compressive extension of 0.04 mm.	235
<b>Appendix Figure 10</b>	A load-deflection plot of a single-edge notched (SEN) fracture toughness ( $K_{IC}$ ) specimen prepared with 20% of the manufacturer's recommended powder content highlighting a maximum load of 6.5 N and a compressive extension of 0.13 mm.	235

## LIST OF TABLES

<b>Table 2.1</b>	The hand-mixed GI powder:liquid mixing ratios and the corresponding weight and volume percentages for each GI powder:liquid mixing ratio group investigated.	58
<b>Table 2.2</b>	The powder:liquid mixing ratio groups, weight percentages of the manufacturers recommended powder content and the corresponding weights of the GI powder and liquid employed for the preparation of the cylindrical compressive fracture strength (CFS) specimens.	61
<b>Table 2.3</b>	The powder:liquid mixing ratio groups, weight percentages of the manufacturers recommended powder content and the corresponding weights of the GI powder and liquid employed for the preparation of the bar-shaped three-point flexure specimens.	67
<b>Table 2.4</b>	The powder:liquid mixing ratio groups, weight percentages of the manufacturers recommended powder content and the corresponding weights of the GI powder and liquid employed for the preparation of the disc-shaped biaxial flexure strength (BFS) specimens.	71
<b>Table 2.5</b>	The powder:liquid mixing ratio groups, weight percentages of the manufacturers recommended powder content and the corresponding weights of the GI powder and liquid employed for the preparation of the disc-shaped Hertzian Indentation (HI) specimens.	77
<b>Table 2.6</b>	The powder:liquid mixing ratio groups, weight percentages of the manufacturers recommended powder content and the corresponding weights of the GI powder and liquid employed for the preparation of the single-edge notched (SEN) fracture toughness ( $K_{IC}$ ) specimens.	85

## 1. INTRODUCTION

### 1.1 HISTORICAL DEVELOPMENT OF GLASS-IONOMER MATERIALS

Glass-ionomers (GIs) were developed and patented (Wilson and Kent, 1969) in the late 1960's by Alan Wilson and co-workers at the Laboratory of the Government Chemist (LGC) in London to replace dental silicate cements. Dental silicate cements - then the primary material of choice for the restoration of anterior dentition, were inherently brittle, susceptible to acid erosion, failed to adhesively bond to sound tooth structure and raised concerns owing to increased pulpal sensitivity (Wilson and Batchelor, 1967a). A major impediment to the developmental progress of dental silicate cements was the lack of understanding of the setting chemistry (Wilson, 1996). The discovery by Wilson and Batchelor (1967b, 1968) that the dental silicate cement matrix was partially composed of aluminium and calcium phosphates led to the suggestion to replace phosphoric acid with a less aggressive organic chelating acid.

For this purpose, experimental cements were prepared by Wilson and co-workers by mixing series of acids, namely pyruvic, tartaric, tannic, fluoroboric, glycerophosphoric and tetraphosphoric acids, at concentrations of 35-50% in solution and polyacrylic acid at a concentration of 25% in solution with the aluminosilicate glass powder (Wilson, 1968). The resultant cements (formed from pyruvic, tartaric, tannic, fluoroboric, glycerophosphoric and tetraphosphoric acids in the concentrations investigated) demonstrated adequate handling and working characteristics but slow setting characteristics and poor hydrolytic stability which precluded clinical usage. However, the cement formed with the 25% polyacrylic acid solution highlighted a reduced susceptibility to hydrolytic disintegration but had 'little or no working time' (Wilson, 1996).

Wilson and Kent (1972) discovered that the reactivity of the glass was controlled by the alumina:silica ratio, whereby hydrolytically stable cements could be formed by employing novel glass formulations. The early cements formed from modified alumina:silica ratio glass formulations also had poor working and setting characteristics (Wilson and McLean, 1988a) and it was not until the 200<sup>th</sup> glass composition (G-200) - which was high in fluoride and calcium, that a usable dental cement was formed (Wilson, 1996). The cement was reported as a GI or aluminosilicate polyacrylate (ASPA) cement (Wilson and Kent, 1972). Despite the heightened anticipation for the clinical success of GIs, the first practical cement (ASPA-I) failed to impress John McLean, the clinical consultant who raised concerns regarding the poor setting characteristics and limited working time (Wilson, 1996). Delayed hardening of the earliest GIs exposed them to the deleterious effects of moisture contamination during clinical placement (Causton, 1981) and desiccation (Earl et al., 1989; Wilson, 1989) during the early stages of the setting reaction. In an attempt to improve the setting characteristics of GIs, Wilson et al. (1976) investigated the role of a third component, a chelating agent, in the setting reaction using citric acid, salicylic acid, acetylone, sequestric acid, polyglycol and tartaric acid. The results for tartaric acid were promising (Wilson et al., 1976) and proved to be 'effective beyond all expectations' (Wilson, 1996). Tartaric acid lengthened the working time (Wilson et al., 1976), shortened the setting time (Crisp and Wilson, 1976; Crisp et al., 1979), increased the compressive fracture strength (CFS) (Crisp et al., 1979) and increased the resistance to acid dissolution (Wilson, 1996).

A subsequent version of ASPA-I containing tartaric acid, the G-200 glass and polyacrylic acid (ASPA-II) showed favourable handling characteristics when used as a pit and fissure sealant (McLean and Wilson, 1974). Interestingly, the discovery of the role of tartaric acid in the setting reaction provided opportunities for the use of glasses other than G-200. However,

changes to the liquid component of ASPA-II were required due to gelation of the polyacrylic acid homopolymer (Crisp et al., 1975a) which prompted investigations into the use of a methanol containing modification (ASPA-III) and later a further variant containing a copolymer of acrylic and itaconic acids (ASPA-IV) (Crisp et al., 1976, 1980). Thereafter, the use of the acronym 'ASPA' as a generic term was abandoned and confined to coding experimental materials developed at the LGC (Wilson, 1996). ASPA-IV was the first commercial GI material, launched by the Amalgamated Dental Company (Dentsply DeTrey, Konstanz, Germany) as a hand-mixed GI cement in 1975 under the trade name 'ASPA' (Wilson, 1991). When five dental nurses and one dentist were asked to hand-mix the ASPA material in a clinical simulation study, Mount and Makinson (1978a) identified a wide range of powder:liquid mixing ratios below that specified by the manufacturer. On average, 85% (by weight) of the manufacturer's recommended powder content was incorporated by the operators, although powder contents as low as 42% (by weight) were identified (Mount and Makinson, 1978a). As a result of the difficulties in operators reproducing the manufacturer's powder:liquid mixing ratio in a clinical simulation, Dentsply DeTrey launched an encapsulated version of ASPA in 1978 (Mount and Makinson, 1978b) which eliminated operator induced variability in proportioning the powder and liquid constituents.

Today a wide variety of commercial hand-mixed and encapsulated GIs are available to the general dental practitioner for clinical use as luting agents, liners and bases for placement under amalgam restorations or the restoration of anterior and posterior dentition. GIs are routinely supplied in two presentational forms: as a separate glass powder and polyacid liquid (Wilson and Kent, 1972) or as a blend of glass powder and vacuum-dried polyacid which is mixed with distilled water or a solution of tartaric acid termed 'anhydrous' GIs (McLean et al., 1984; Prosser et al., 1984). The handling characteristics and mechanical properties of

commercial GI products have been optimised by the manufacturers through developments in the glass powder and polyacid liquid constituents used in the GI formulations.

## **1.2 DEVELOPMENTS IN THE GI POWDER**

GIs are composed of an ion leachable glass powder and a polyacid liquid which are mixed together using a predetermined powder:liquid mixing ratio to form a solid mass on setting. The GI powder is prepared from an aluminosilicate glass which serves as a source of ions for the cement forming reaction (Wilson and McLean, 1988b; Nicholson, 1998). The glass composition controls the setting rate of the cement forming reaction (Kent et al., 1979; Wilson and Nicholson, 1993) and the refractive index match to the polysalt matrix dictates the translucency of the set GI (Wilson and McLean, 1988c). The glass component is prepared by sintering mixtures of powdered silica ( $\text{SiO}_2$ ), alumina ( $\text{Al}_2\text{O}_3$ ), cryolite ( $\text{Na}_3\text{AlF}_6$ ), aluminium trifluoride ( $\text{AlF}_3$ ), fluorite ( $\text{CaF}_2$ ) and aluminium phosphate ( $\text{AlPO}_4$ ) at 1100-1500°C depending upon the chemical composition of the glass (Wilson and Nicholson, 1993). The glass melt is shock quenched in water, the resultant coarse glass frit is ground using a ball mill and sieved to form a powder with a maximum particle size of 45  $\mu\text{m}$  for GI restoratives and 15  $\mu\text{m}$  for GI luting cements (Wilson and Nicholson, 1993).

### **1.2.1 Glass structure**

The ability of a glass to form a usable cement when mixed with a polyacid is dictated by the alumina:silica ratio during glass formulation (Kent et al., 1979; Wilson and McLean, 1988c; Wilson and Nicholson, 1993; Wilson, 1996). The alumina:silica ratio defines the reactivity of the glass and serves as the rate controlling factor in the setting reaction (Kent et al., 1979; Wilson and McLean, 1988c; Wilson and Nicholson, 1993; Wilson, 1996). The influence of

the alumina:silica ratio on the reactivity of the glass may be explained by the random network model for glasses proposed by Zachariasen (1932). The random network model advocates that for oxide glass formation to occur, each oxygen ion must not be linked to more than two multivalent cations and that the oxygen polyhedra must be linked at the corners. The silica-oxygen tetrahedron ( $\text{SiO}_4$ ) serves as the basic structural unit, where the silicon cation ( $\text{Si}^{4+}$ ) resides in the interstices formed by four oxygen anions ( $\text{O}^{2-}$ ) to form the  $\text{SiO}_4$  tetrahedra which are linked at the corners to form chains. Silicate glasses exist in a form where they lack long-range order (Figure 1.1a) whereas crystalline silica is more ordered and has both short- and long-range order (Figure 1.1b).

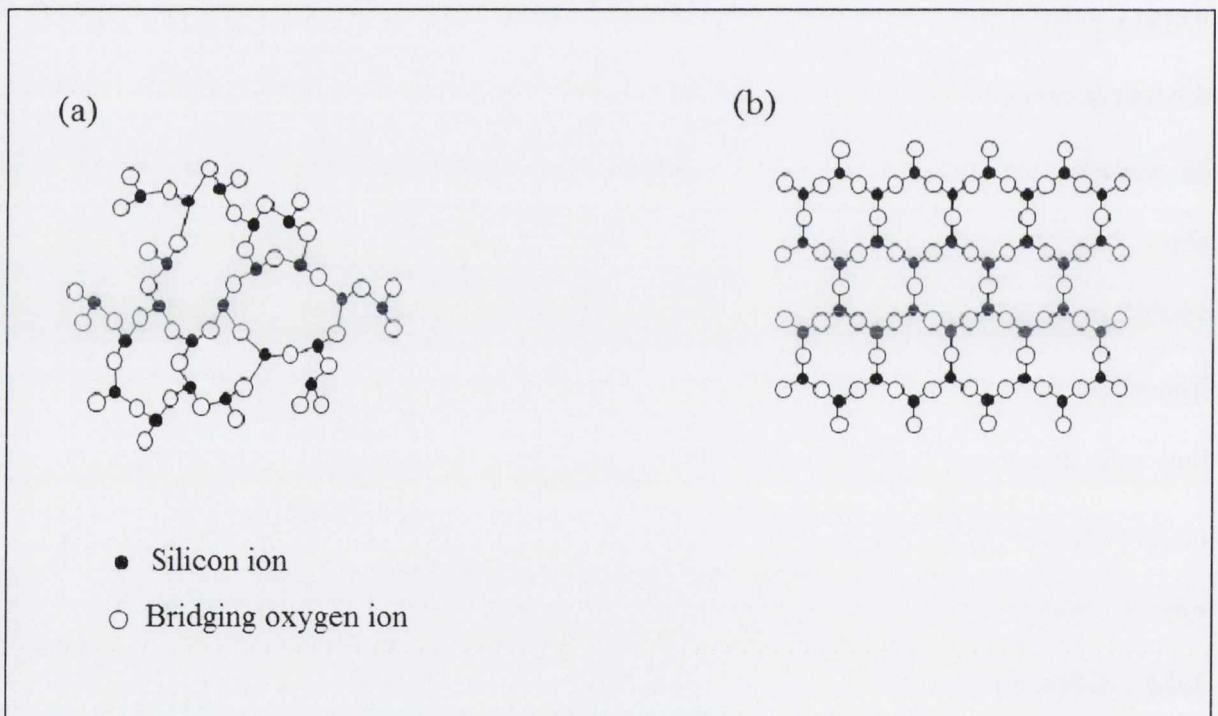


**Figure 1.1.** A two-dimensional (2D) schematic representation of silica illustrating the basic  $\text{SiO}_4$  tetrahedra structural units in (a) the glassy form where the basic  $\text{SiO}_4$  units are arranged in a non-periodic fashion lacking long-range order to give a random network and (b) the crystalline form where the basic  $\text{SiO}_4$  units are arranged in a regular lattice with short- and long-range order. Adapted from McMillan (1964).

Silicon is termed as the network-former constituting the backbone of the polymer which may be modified by the addition of randomly distributed alkali oxides ( $\text{CaO}$ ,  $\text{Na}_2\text{O}$ ) (Figure 1.2b).

The network connectivity is determined by the bridging oxygens which link the  $\text{SiO}_4$  tetrahedra and the non-bridging oxygens which do not (Darling and Hill, 1994). The network-modifiers ( $\text{Ca}^{2+}$ ,  $\text{Na}^+$ ) disrupt the network structure and reduce the network connectivity by reducing the number of bridging oxygens with a concomitant increase in non-bridging oxygens.

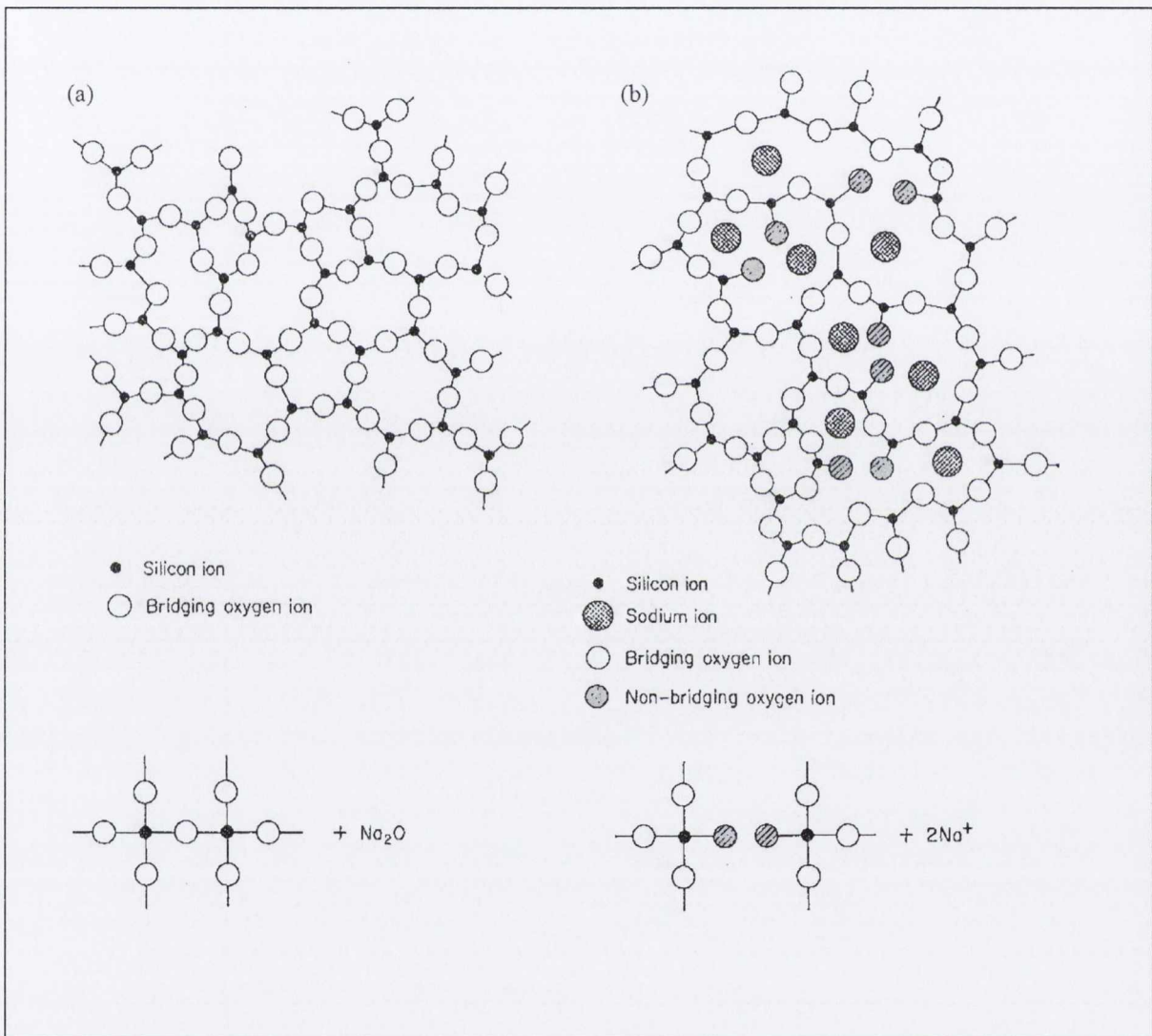


**Figure 1.2.** (a) A two-dimensional (2D) schematic representation of silica glass illustrating the basic  $\text{SiO}_4$  tetrahedra connected by bridging oxygens. The structure is shown in a simplified 2D form, where only three of the four oxygen ions surrounding each silicon ion are depicted. (b) The addition of network-modifying ions ( $\text{Na}^+$ ) results in a disruption of the glass network so that instead of a single bridging oxygen there are now four groups of two non-bridging oxygens. Adapted from McMillan (1964).



A simple silicate glass comprises a three-dimensional (3D) network of linked  $\text{SiO}_4$  tetrahedra with no charge which is resistant to acid attack owing to the electroneutrality of the glass network. For aluminosilicate glasses, the aluminium ion ( $\text{Al}^{3+}$ ) may exist as a network-former in four-fold coordination or as a network-modifier in six-fold coordination. In the four-fold coordination, the  $\text{Al}^{3+}$  is able to replace  $\text{Si}^{4+}$  in the glass network owing to similar ionic radii of  $\text{Al}^{3+}$  and  $\text{Si}^{4+}$ , such that the glass network then consists of linked  $\text{SiO}_4$  and  $\text{AlO}_4$  tetrahedra (McMillan, 1964) (Figure 1.3).

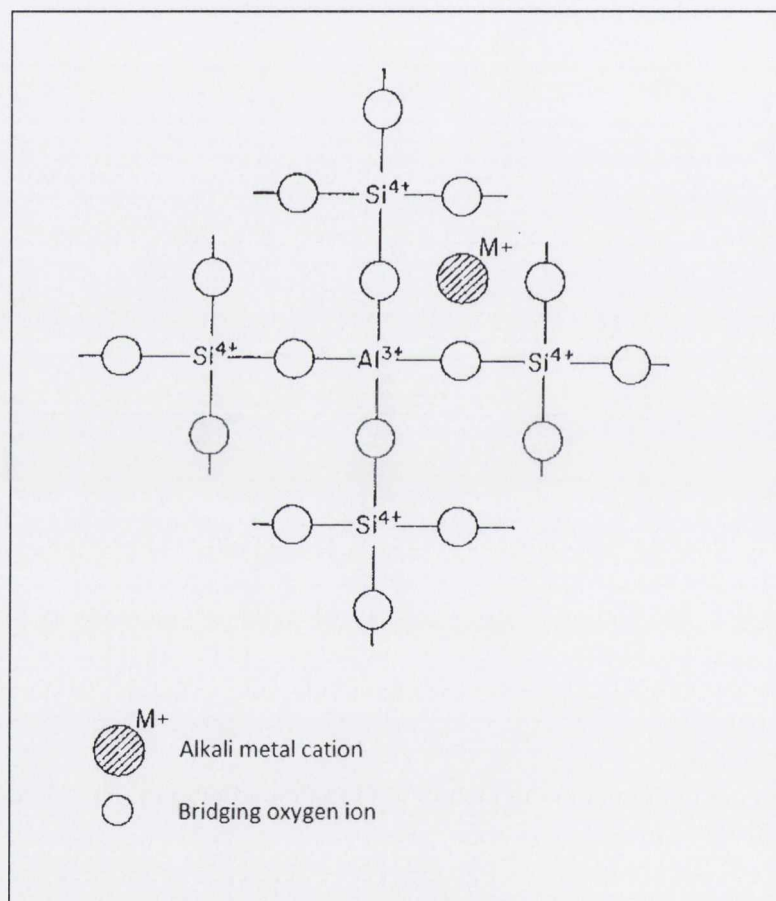


**Figure 1.3.** A two-dimensional (2D) schematic representation of aluminosilicate glass illustrating the linked  $\text{SiO}_4$  and  $\text{AlO}_4$  tetrahedra connected by bridging oxygens. Due to the valency difference between  $\text{Si}^{4+}$  and  $\text{Al}^{3+}$ , one alkali metal cation ( $\text{M}^+$ ) per  $\text{AlO}_4$  tetrahedron must be present to ensure the electroneutrality of the glass network. Adapted from McMillan (1964).

The replacement of  $\text{Si}^{4+}$  by  $\text{Al}^{3+}$  confers a negative charge to the glass network due to the valency difference between  $\text{Si}^{4+}$  and  $\text{Al}^{3+}$  (Kent et al., 1979; Nicholson, 1998). The negative charge of the glass network is balanced by the positive charge of the network-modifying cations ( $\text{Ca}^{2+}$ ,  $\text{Na}^+$ ) (Kent et al., 1979; Nicholson, 1998). If there are insufficient network-modifying cations ( $\text{Ca}^{2+}$ ,  $\text{Na}^+$ ), some of the  $\text{Al}^{3+}$  ions will take up a six-fold coordination to balance the charge of the glass network (Nicholson, 1998). Increasing the alumina:silica ratio increases the basicity of the glass network and at an alumina:silica ratio of 1:1 the glass network acquires sufficient negative charge to become susceptible to attack by hydrogen ions ( $\text{H}^+$ ) from the polyacid (Kent et al., 1979; Wilson and McLean, 1988c). The optimum alumina:silica ratio lies between 1:2 and 1:3 (by mass). An alumina:silica ratio of greater than 1:3 results in a prolonged setting time (6.5-18 mins) while an alumina:silica ratio of less than 1:2 results in a reduced setting time (2.5-5 mins) such that practical cements cannot be formed (Kent et al., 1979; Wilson and McLean, 1988c; Wilson and Nicholson, 1993).

### **1.2.2 Glass composition**

For the earliest experimental GI (ASPA-I), the 200<sup>th</sup> glass composition (G-200) ( $\text{SiO}_2\text{-Al}_2\text{O}_3\text{-AlF}_3\text{-CaF}_2\text{-NaF-AlPO}_4$ ) investigated by Wilson and Kent (1972) served as the powder component and was high in fluoride and calcium. G-200 was unique in that it was the only glass composition at the time of the development of GIs that was capable of forming a clinically usable GI when mixed with a 50% polyacrylic acid solution in the absence of a reaction controlling additive (Wilson, 1996). However, John McLean expressed concerns regarding the poor aesthetics and sluggish set when ASPA-I was employed clinically. The poor aesthetics were attributed to the poor translucency of G-200 owing to the high fluoride content which made the glass heavily opal (Wilson, 1996). The setting characteristics of ASPA-I were improved with the discovery of the role of tartaric acid as a reaction controlling

additive (Crisp and Wilson 1976; Wilson et al., 1976; Crisp et al., 1979) which prolonged the working time (Wilson et al., 1976) by inhibition of the initial set by preventing the formation of calcium polyacrylate (Nicholson et al., 1988), thereby allowing the GI to retain fluidity for an extended duration (Hill and Wilson, 1988). Tartaric acid also sharpened the final set through acceleration of the rate of formation of aluminium polyacrylate (Crisp and Wilson, 1976; Nicholson et al., 1988).

Following the discovery of the role of tartaric acid in the setting reaction (Crisp and Wilson, 1976; Wilson et al., 1976; Crisp et al., 1979), GI glass formulations were no longer restricted to the opal G-200, providing opportunities for the use of more translucent glasses to produce aesthetic GIs. Consequently, a large number of potential glass formulations (Kent et al., 1979; Wilson et al., 1980; Wilson and McLean, 1988c; Wilson and Nicholson, 1993) were identified for use as the powder constituent of GIs which were usually based on calcium aluminosilicates ( $\text{SiO}_2\text{-Al}_2\text{O}_3\text{-CaO}$ ) or calcium fluoroaluminosilicates ( $\text{SiO}_2\text{-Al}_2\text{O}_3\text{-CaF}_2$ ). The presence of fluoride in the glass system was advantageous as it lowered the fusion temperature by disrupting the glass network (Kent et al., 1979; Wilson and McLean, 1988c; Wood and Hill, 1991; de Barra and Hill, 2000) and allowed for the employment of a more economical fusion temperature when preparing glasses for commercial exploitation. The fluoride content in glasses increased the CFS (Kent et al., 1979), improved the translucency of the mixed GI (Wilson and McLean, 1988c; Wood and Hill, 1991) and apparently inhibited caries formation when placed clinically (Forsten, 1998; Mayanagi et al., 2014). In high fluoride containing glasses, fluorine is lost from the glass melt as silicon tetrafluoride ( $\text{SiF}_4$ ) and aluminium trifluoride ( $\text{AlF}_3$ ) which may hydrolyse to form hydrofluoric acid (HF),  $\text{SiO}_2$  and  $\text{Al}_2\text{O}_3$  (Wood and Hill, 1991). HF is corrosive towards furnace linings and crucibles, while the  $\text{SiO}_2$  and  $\text{Al}_2\text{O}_3$  form a crust on the surface of the glass which has to be removed

manually. The fluorine loss during glass manufacture resulted in variability in the pre- and post-sintered glass composition which changed the alumina:silica ratio in the glass. Wood and Hill (1991) highlighted that the loss of fluorine during glass manufacture was not accounted for in the wide range of high fluoride glasses reported by Kent et al. (1979) and Wilson et al. (1980) which led to difficulties in correlating the chemical composition of the glasses with the mechanical properties reported for the resultant GIs (Wood and Hill, 1991). The authors identified the addition of a basic oxide (CaO) to a fluoride containing aluminosilicate glass decreased fluorine loss from the glass melt and enabled the production of glasses with a more controlled composition following sintering (Wood and Hill, 1991).

Novel glass compositions based on aluminoborate glasses were trialled as an alternative to aluminosilicates (Neve et al., 1992a,b, 1993), although the rationale for studying borate glasses was unclear owing to the known solubility of borate species (Darling and Hill, 1994). The authors reported that the reactivity of aluminoborate glasses varied with alumina content and that the addition of 5% tartaric acid resulted in GI formulations with adequate setting characteristics and increased CFS and diametral tensile strength (DTS) values (Neve et al., 1992a,b, 1993). However, GIs formulated from aluminoborate glasses were hydrolytically unstable when compared with aluminosilicate glasses (Neve et al., 1992b). Darling and Hill (1994) reported zinc silicate glasses based on CaO-ZnO-SiO<sub>2</sub>, R<sub>2</sub>O-ZnO-SiO<sub>2</sub> and Al<sub>2</sub>O<sub>3</sub>-ZnO-SiO<sub>2</sub> glass systems. The zinc silicate glasses were prepared with increased amounts of zinc oxide and silica and minor amounts of the third oxide. The authors identified that hydrolytically stable GIs could be formed from the Al<sub>2</sub>O<sub>3</sub>-ZnO-SiO<sub>2</sub> but not the CaO-ZnO-SiO<sub>2</sub> and R<sub>2</sub>O-ZnO-SiO<sub>2</sub> glass systems (Darling and Hill, 1994). For the zinc silicate glasses, the cement forming ability was dictated by the network connectivity of the glass and not the alumina:silica ratio. Consequently, the zinc silicate glass reported (Darling and Hill, 1994)

had an alumina:silica ratio of 1:9 which had previously been proposed as being too low for GI cement formation (Wilson and Kent, 1969; Wilson and Nicholson, 1993). However, the maximum CFS value of 93 MPa reported for the zinc silicate glasses (Darling and Hill, 1994) was inadequate to meet the International Organisation for Standardisation (ISO) CFS requirement of 100 MPa (ISO 9917-1:2007). Aluminoborate (Neve et al., 1992a,b, 1993) and zinc silicate glasses (Darling and Hill, 1994) could therefore not be advocated as alternatives to the aluminosilicate glasses for the commercial exploitation as practical GIs.

The powder components of commercial GI products are composed of complex multi-component glasses. The G-388 glass composition was a multi-component translucent glass ( $\text{SiO}_2\text{-Al}_2\text{O}_3\text{-AlF}_3\text{-CaF}_2\text{-NaF-AlPO}_4$ ) used in the early commercial GIs and contained significant quantities of phosphorus, fluorine and alkali metals (Griffin and Hill, 1999). Commercial glasses also contained strontium, barium or lanthanum ions to impart radiopacity for increased detection and contrast with dental tissues and other restorative materials on dental radiographs (Smith, 1998). Strontium has been reported as an ideal candidate for the replacement of calcium in the glass structure due to their similar ionic radii, whereby strontium replaces calcium without disrupting the glass network or loss of translucency of the glass (Debb and Nicholson, 1999). Griffin and Hill (1999, 2000) investigated multi-component fluorophosphoaluminosilicate glasses ( $\text{SiO}_2\text{-Al}_2\text{O}_3\text{-CaO-P}_2\text{O}_5\text{-CaF}_2$ ) and highlighted that the reactivity of the multi-component glasses used in commercial GIs was not solely dictated by acid hydrolysis of the aluminium-oxygen-silicon bonds (Figure 1.4) but also by hydrolysis of the phosphorus-oxygen bonds (Figure 1.5). Phosphorus ions ( $\text{P}^{5+}$ ) occupied tetrahedral sites adjacent to  $\text{AlO}_4$  tetrahedra such that the excess positive charge on  $\text{P}^{5+}$  ions resulted in local charge compensation of the charge deficient  $\text{Al}^{3+}$  ions (Dupree et al., 1989; Kirkpatrick and Brow, 1995) (Figure 1.5). It was proposed that an additional route to

glass degradation by hydrolysis of the phosphorus-oxygen bonds was provided through the replacement of  $\text{Si}_2\text{O}_7$  groups by  $\text{AlPO}_7$  groups in the glass network (Griffin and Hill, 1999, 2000) (Figure 1.5).

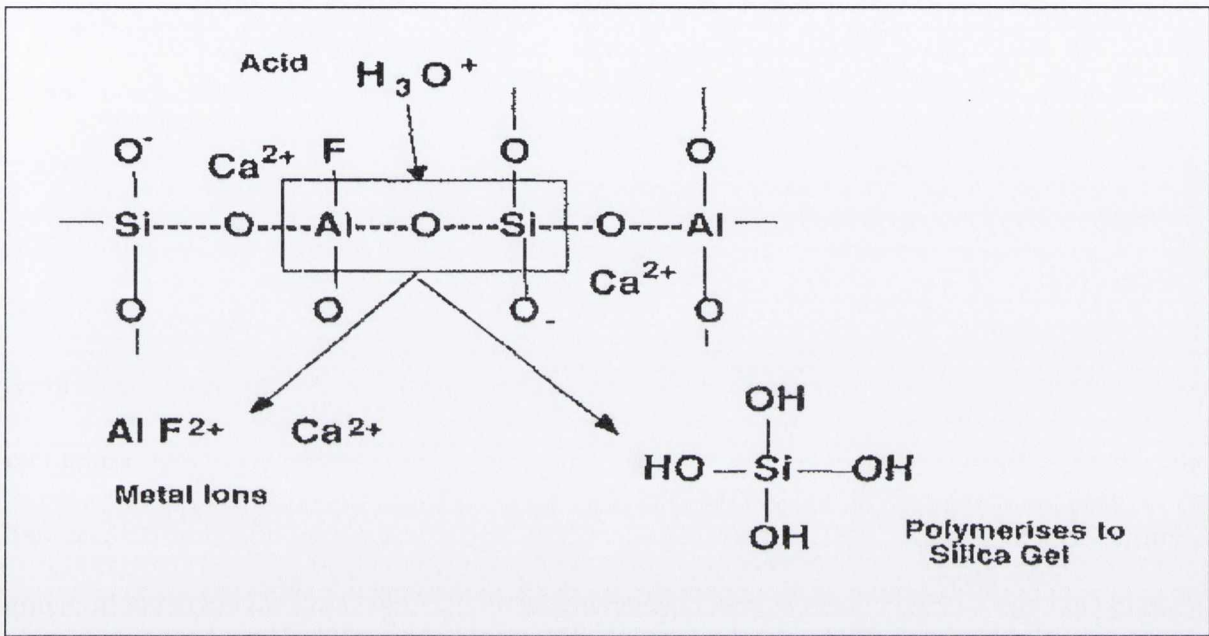


Figure 1.4. A schematic representation of hydrolysis of aluminium-oxygen-silicon bonds in an aluminosilicate glass network by the polyacid resulting in the release of metal cations for cross-linking with the polyacid.

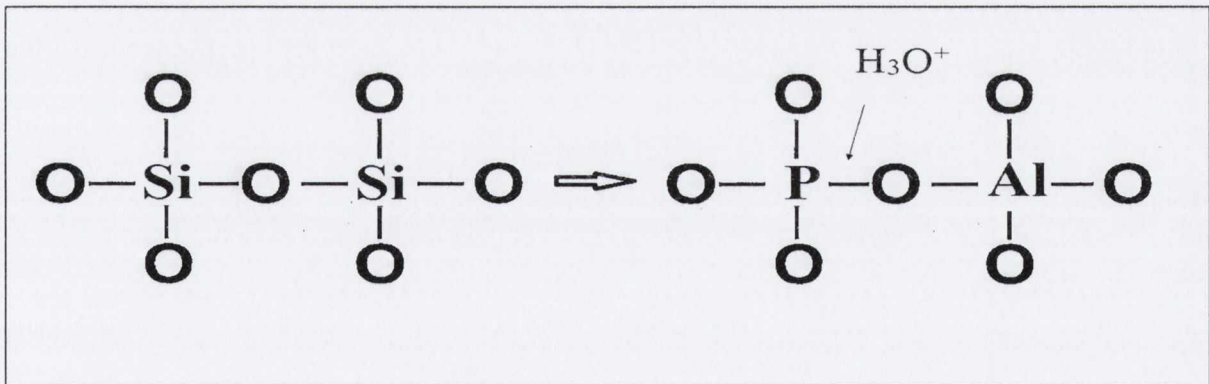


Figure 1.5. A schematic illustration of local charge balancing of aluminium and phosphorus cations forming a group of  $\text{AlPO}_7$ . The replacement of  $\text{Si}_2\text{O}_7$  groups in the glass network by  $\text{AlPO}_7$  groups provided an additional route to glass degradation by hydrolysis of the phosphorus-oxygen bonds in multi-component fluorophosphoaluminosilicate glasses.

Today commercially available GIs are supplied by numerous manufacturers and are composed of zinc containing (Chemfil Rock; Dentsply DeTrey), lanthanum containing (Ketac Molar; 3M ESPE, St. Paul, Minnesota, USA) or strontium containing (Fuji IX; GC Corporation, Tokyo, Japan and Ionofil Molar; Voco GmbH, Cuxhaven, Germany) calcium fluoroaluminosilicate glasses. The reactivity of a commercial GI glass powder with the corresponding GI liquid is determined by the chemical composition (Kent et al., 1979; Wilson and McLean 1988c), glass fusion temperature (Wilson and Nicholson, 1993), surface treatment through acid washing (Schmitt et al., 1983) and the powder particle size (Kaplan et al., 2004), however, these specific details are never routinely supplied by manufacturers. The glass variables (composition, fusion temperature, surface treatment, particle size) are tailored by each manufacturer for specific GI formulations. The liquid component in commercial GIs differ in acid constituent (homopolymers of acrylic acid and copolymers of acrylic and itaconic or maleic acids) with varying acid molecular weights and concentrations being routinely used. Modification of the setting time is controlled by the addition of tartaric acid at various concentrations. It is therefore imperative that a specific dental manufacturer's GI glass powder is only used with the appropriate GI liquid for that product to ensure an adequate chemical reaction between the constituents for optimum clinical performance.

### **1.3 DEVELOPMENTS IN THE GI LIQUID**

The liquid component of the earliest experimental GI (ASPA-I) was composed of an acrylic acid homopolymer solution (50% by mass) which had poor working and setting characteristics and was susceptible to gelation due to formation of intermolecular hydrogen bonds between the polymer chains (Crisp et al., 1975a). To improve the handling characteristics, tartaric acid (5% by mass) was added to the acrylic acid homopolymer (47.5%

by mass) to form ASPA-II (Crisp et al., 1975b) which improved the working and setting characteristics. Conversely, the tartaric acid modified GI liquid suffered from an inadequate shelf life which was limited to 10-30 weeks such that the gelation of the liquid component made it unfeasible for commercial exploitation (Crisp et al., 1975b). To reduce gelation, methanol (5% by mass) was added to the acrylic acid homopolymer (45.25% by mass) (ASPA-III) which reduced intermolecular hydrogen bond formation between the polymer chains and delayed gelation (Crisp et al., 1975a). Esterification of some of the carboxylic acid groups of the acrylic acid polymer chain by methanol also resulted in an extended setting time for the mixed cement (Crisp et al., 1975b). However, GIs prepared using the methanol containing liquid of ASPA-III discoloured when placed clinically (Wilson and McLean, 1988c) and further investigations were abandoned.

### **1.3.1 Acrylic acid and itaconic or maleic acid copolymers**

Crisp and Wilson (1977) suggested that copolymers of acrylic acid with other unsaturated carboxylic acids (itaconic acid and maleic acid) would reduce intermolecular hydrogen bonding owing to their reduced stereoregularity when compared with homopolymers of acrylic acid. The reduced intermolecular hydrogen bonding observed in these copolymers was attributed to a higher degree of cross-linking due to the presence of two carboxyl groups in the copolymer structures. The authors developed an aqueous solution of acrylic acid and itaconic acid (47.5% by mass) copolymers with tartaric acid (5%) which was used in ASPA-IV and resulted in a GI liquid solution that was resistant to gelation in solution (Crisp and Wilson, 1977; Crisp et al., 1980).

Consequently, the first commercially available GI (ASPA) contained the acrylic acid and itaconic acid copolymer formulation developed for ASPA-IV (Crisp et al., 1976).



Copolymers of acrylic acid and maleic acid have been reported in the liquid component of Chelon Fil (ESPE GmbH, Seefeld, Germany) (Williams and Billington, 1991; Nicholson and Abiden, 1997), Ketac Fil (ESPE GmbH) (Pearson and Atkinson, 1991; Williams and Billington, 1991; Khouw-Liu et al., 1999a,b) and Ketac Molar (ESPE GmbH) (Khouw-Liu et al., 1999a,b). Investigating the influence of long-term water storage of GIs on the CFS (Williams and Billington, 1991) and biaxial flexure strength (BFS) (Pearson and Atkinson, 1991), investigators (Williams and Billington, 1991; Pearson and Atkinson, 1991) identified GIs based on copolymers of acrylic acid (Chelon Fil and Ketac Fil) were more susceptible to strength decreases on aging (Williams and Billington, 1991; Pearson and Atkinson, 1991) compared with GIs based on homopolymers of acrylic acid (Chemfil II; Dentsply DeTrey and Opusfil W; Davis Schottlander and Davis, London, UK) owing to the greater susceptibility of the copolymers to hydrolysis. Nicholson and Abiden (1997) suggested the decrease in CFS of copolymer containing GIs, compared with GIs based on homopolymers on long-term water storage, was a consequence of the high cross-linking density of copolymers rather than hydrolysis (Pearson and Atkinson, 1991; Williams and Billington, 1991) which caused the GIs to become more brittle on aging (Nicholson and Abiden, 1997).

### **1.3.2 GIs as thermoplastic polymers**

Using dynamic mechanical thermal analysis, Hill et al. (1989) identified GIs as thermoplastic polymer composites by the presence of sharp loss peaks indicative of continually breaking and reforming ionic cross-links. Hill et al.'s (1989) observation was supported by Gonzalez (1984) who suggested a limited lifetime for ionic cross-links in polystyrene sulfonate ionomers. In the melt and glassy state, most polymers exist in the form of chain-like molecules oriented in a random coil configuration (Bucknall, 1973). During deformation and fracture, the chains must be stretched for chain scission to occur whereby the chains must be

securely held at the ends (Prentice, 1985; Hill et al., 1989; Wilson et al., 1989). Edwards (1967) proposed the entanglement theory where a polymer chain was viewed as being contained within a tube formed by the neighbouring chains as opposed to forming physical entanglement knots (Figure 1.6). Analysing the Brownian motion of a chain within the tube, de Gennes (1979) derived mathematical expressions for the rate of motion of the chain along its tube. It was proposed that the lateral movement of the chain was limited by the proximity of the neighbouring chain entanglements and longitudinal movement was restricted by the interactions of polar side groups between neighbouring chains (Hill et al., 1989; Wilson et al., 1989).

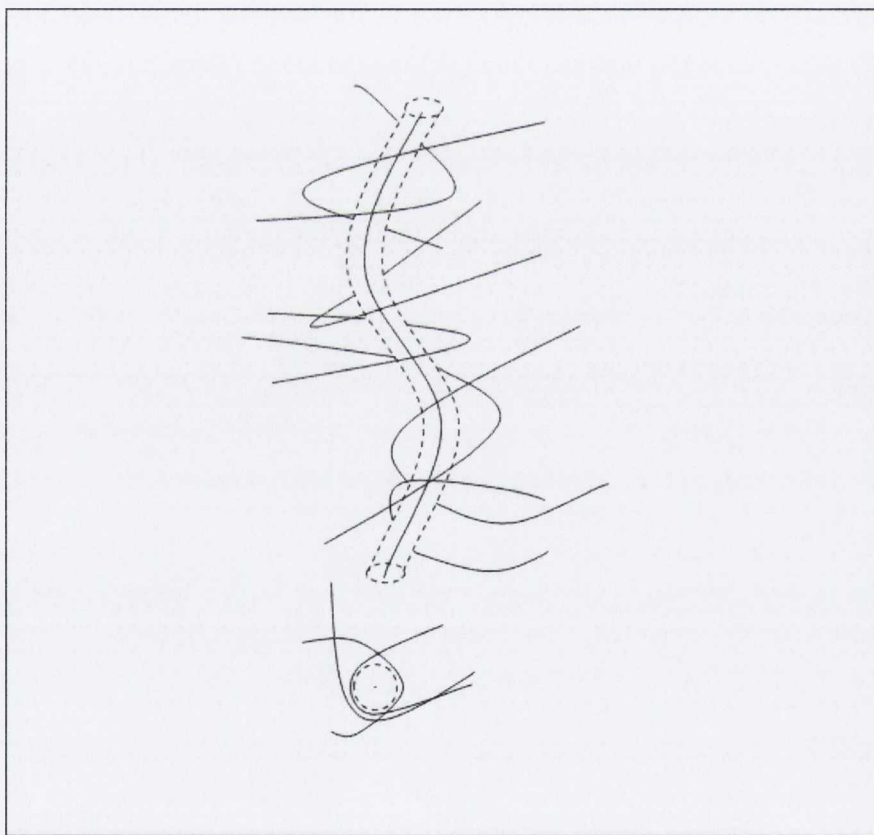


**Figure 1.6. A schematic representation of an idealised model of a polymer chain confined in a tube of three-dimensional (3D) entanglements that gives rise to the entanglement theory. Adapted from Prentice (1985).**

The polymer chains in an unstressed specimen are embedded in both sides of the fracture plane of a propagating crack (Prentice, 1985). As the crack propagates, the chain will be 'pulled out' from the side of the plane containing the shorter portion of the chain length (Prentice, 1985) (Figure 1.7). The surface energy per unit area of a fracture plane is proportional to the square of the length of the chain, such that a critical polymer chain length exists which corresponds to the critical molecular weight of the polymer ( $M_c$ ). At  $M_c$ , the stress required to pull-out the chain contained within a tube would be greater than the stress required to break the carbon-carbon bond of the polymer backbone (Prentice, 1985; Hill et al., 1989). Therefore, chain pull-out was proposed as the dominant failure mechanism below  $M_c$  while chain scission was the dominant failure mechanism above  $M_c$  (Hill et al., 1989; Wilson et al., 1989). Applying a simple power law viscous model for polyacrylic acid based on the analyses reported by Prentice (1985), Hill et al. (1989) proposed the  $M_c$  for an anhydrous polyacrylic acid to be approximately 100,000. The authors also proposed that a critical entanglement molecular weight ( $M_e$ ) existed below which the polymeric constituent in the resultant GI would fail to form entanglements (Hill et al., 1989). Hill et al. (1989) proposed the  $M_e$  for an anhydrous polyacrylic acid to range from 7,000-21,000.

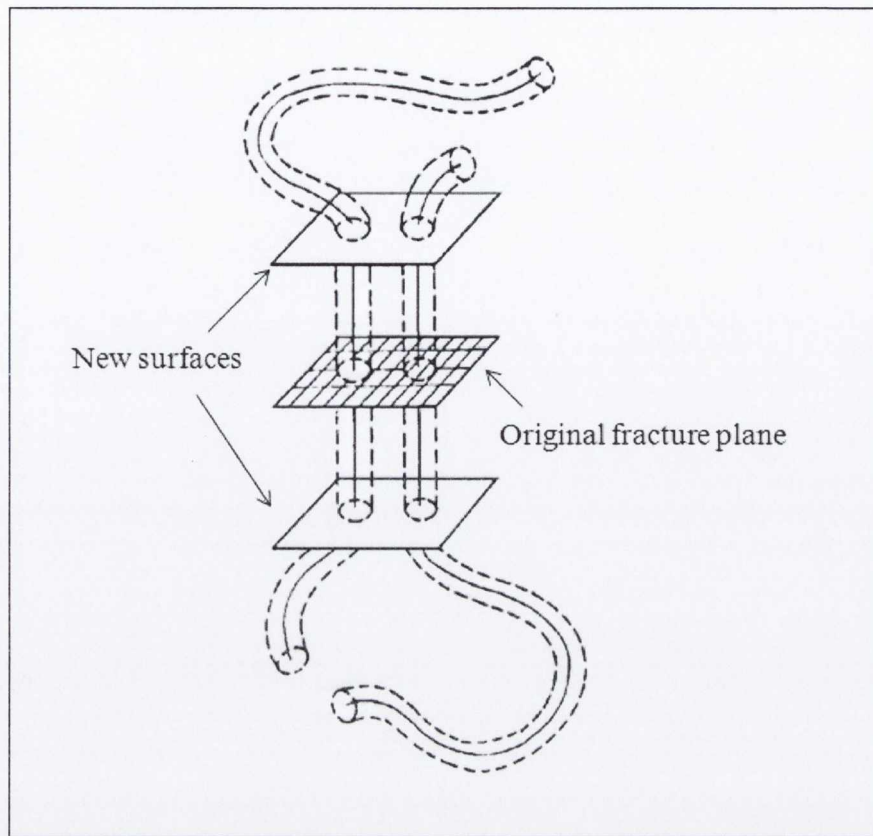


**Figure 1.7.** A schematic representation of the ‘pull-out’ process in the formation of new surfaces during fracture where the polymer chain will be pulled out from the side of the fracture plane containing the shorter portion of the chain length. Adapted from Prentice (1985).

### 1.3.3 Molecular weight and concentration of polyacrylic acid

A limited number of studies have reported the influence of polyacid concentration (Crisp et al., 1977; de Barra and Hill, 1998; Fennell and Hill, 2001a,b,c; Dowling and Fleming, 2011a) and molecular weight (Wilson et al., 1977; Prosser et al., 1986; Hill et al., 1989; Wilson et al., 1989; Griffin and Hill, 1998; Fennell and Hill, 2001a,b,c; Dowling and Fleming, 2011a,b) on the performance of GIs. Initial studies (Crisp et al., 1977; Wilson et al., 1977; Prosser et al. 1986) assessed the polyacrylic acid concentration and molecular weight simultaneously which makes interpretation of the results difficult. In addition, the authors manipulated the polyacid concentration and molecular weight groups with varying powder:liquid mixing ratios to maintain a workable consistency which further complicated interpretation of the

reported results (Crisp et al., 1977; Wilson et al., 1977). The reported strength data did, however, highlight a trend towards an increase in DTS (Crisp et al., 1977; Wilson et al., 1977), CFS (Crisp et al., 1977; Wilson et al., 1977) and three-point flexure strength (TFS) (Prosser et al., 1986) on increasing polyacid concentration and molecular weight.

Wilson et al. (1989) investigated increasing the polyacid molecular weight (11,500-1,080,000) of GIs prepared with a commercial GI glass powder on the setting rate, acid erosion rate, fracture toughness ( $K_{IC}$ ) and wear resistance. The authors highlighted the polymer chain length as a crucial parameter in the formulation of GIs and concluded that the higher the molecular weight of the polyacid, the better the GI performance (Wilson et al., 1989). Wilson et al.'s (1989) observations were supported by the findings of Hill et al. (1989), Griffin and Hill (1998) and Fennell and Hill (2001a), who reported a progressive increase in the  $K_{IC}$  (Hill et al., 1989) and CFS (Griffin and Hill, 1998; Fennell and Hill, 2001a) with increasing molecular weights - although the studies were limited to anhydrous GIs. For the anhydrous GIs, the polyacrylic acid was vacuum-dried and added to the GI glass powder prior to mixing with a tartaric acid solution. To initiate the setting reaction, the vacuum-dried polyacrylic acid was required to dissolve in the available water, thereby retarding the setting reaction and allowing for the use of polyacrylic acids with higher molecular weights (Hill et al., 1989; Wilson et al., 1989; Griffin and Hill, 1998; Fennell and Hill, 2001a).

The majority of commercially available GIs are routinely supplied as separate glass powder and polyacid liquid components where the polyacid is usually prepared by a free-radical polymerisation of the polymer in an aqueous solution at a concentration of 40-50% (Wilson and Nicholson, 1993). Attempts at improvements in the mechanical properties of GIs through

modification of the liquid component have included the development of copolymers of acrylic acid with itaconic acid (Crisp and Wilson, 1977; Crisp et al., 1980; Wilson and McLean, 1988c) or maleic acid (Schmitt et al., 1982; Pearson and Atkinson, 1991; Williams and Billington, 1991; Nicholson and Abiden, 1997; Khouw-Liu et al., 1999a,b), the use of high molecular weight polyacid solutions (Wilson et al., 1977; Dowling and Fleming, 2011a) and concentrations (Crisp et al., 1977; Dowling and Fleming, 2011a) and the use of polyacrylic acid molecular weight mixtures (Dowling and Fleming, 2011b). Dowling and Fleming (2011a) investigated polyacrylic acid liquid solutions of varying molecular weights (ranging from 5,000-200,000) over a range of concentrations (10-60%) which were hand-mixed with a commercial GI glass powder (Ionofil Molar) at the manufacturer's recommended powder:liquid mixing ratio (4:1 g:g). The authors identified an optimum polyacrylic acid concentration in solution for individual polyacrylic acid molecular weights where the CFS and elastic moduli of the resultant GIs were maximised and above which the CFS and elastic moduli decreased (Dowling and Fleming, 2011a) (Figure 1.8).

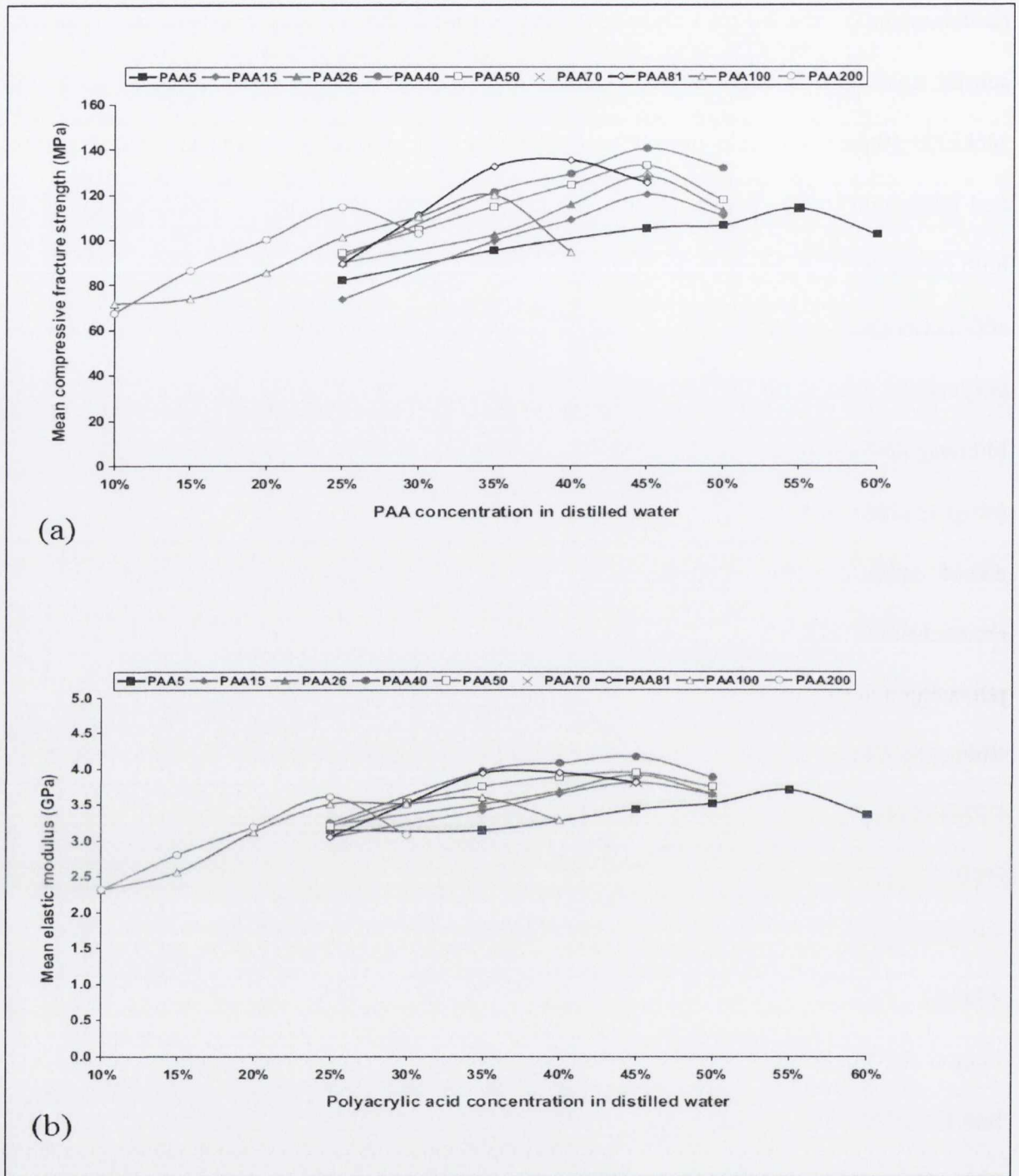
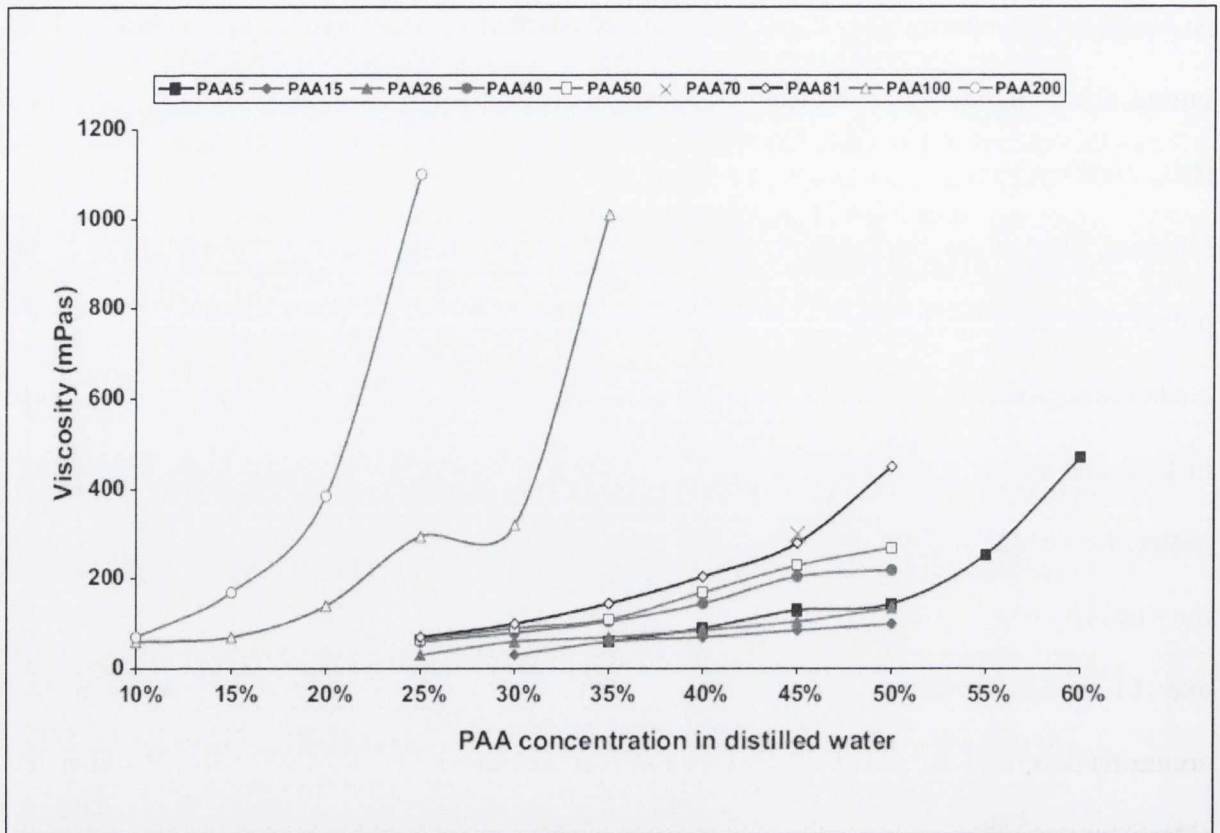


Figure 1.8. The variation in (a) the mean compressive fracture strength (CFS) and (b) the mean elastic modulus for polyacrylic acid solutions of different molecular weights ranging from 5000 (PAA5) to 200,000 (PAA200) with increasing polyacrylic acid concentration highlighting a progressive increase in CFS and elastic modulus on increasing the polyacid concentration. On reaching an optimum polyacrylic acid concentration in solution for the individual polyacrylic acid molecular weights, the CFS and elastic moduli of the resultant conventional GIs were maximised. A further increase in the polyacid concentration of the different molecular weight polyacids resulted in a decrease in the CFS and elastic moduli. Adapted from Dowling and Fleming (2011a).

At reduced polyacrylic acid concentrations, cross-linking between polymer chains during setting was hindered due to a greater distance between the polymer molecules (de Barra and Hill, 1998) resulting in a decreased CFS and elastic modulus for the GI (Dowling and Fleming, 2011a). At increased polyacrylic acid concentrations, the increased density of the polyacrylic acid chains resulted in increased cross-linking between the polyacid chains and chain entanglements (Hill et al., 1989; Wilson et al., 1989) leading to a progressive increase in CFS and elastic modulus (Dowling and Fleming, 2011a). However, the concentration and molecular weight of the polyacid solution employable was limited by the resultant increase in the viscosity of the polyacrylic acid solution (Crisp et al., 1977; Wilson et al., 1977; Dowling and Fleming, 2011a) (Figure 1.9) such that a balance exists between the polyacid concentration, molecular weight and viscosity to achieve an improved GI for practical use (Dowling and Fleming, 2011a).





**Figure 1.9.** The change in viscosity of the polyacrylic acid solutions of different molecular weights ranging from 5000 (PAA5) to 200,000 (PAA200) with increasing polyacrylic acid concentrations highlighting a progressive increase in viscosity with the increase in polyacrylic acid concentration for the polyacrylic acid molecular weights investigated. The increase in viscosity with increasing polyacrylic acid concentration was more distinct for the higher molecular weights investigated, namely 100,000 (PAA100) and 200,000 (PAA200). Adapted from Dowling and Fleming (2011a).

The increase in viscosity associated with increased concentration and molecular weight exacerbates the difficulties associated with hand-mixing for conventional polyacrylic acid solutions when compared with anhydrous GI formulations which employ water or weak tartaric acid solutions (Crisp et al., 1979; Hill et al., 1989). Consequently, Dowling and Fleming (2011a) proposed the  $M_c$  (80,000) and  $M_c$  (5,000) for polyacrylic acid solutions used for conventional GI formulations to be lower when compared with the  $M_c$  (100,000) and lower bound  $M_c$  (7,000) theoretically predicted by Hill et al. (1989) for GIs prepared using anhydrous polyacrylic acid. This observation (Dowling and Fleming, 2011a) confirmed Hill

et al.'s (1989) suggestion that the predicted  $M_c$  would decrease where there were 'strong intermolecular interactions' existing between the polymer chains.

Improvements in the CFS and elastic moduli of GIs were investigated using polyacrylic acid molecular weight mixtures comprising of polyacrylic acids with varying chain length distributions (Dowling and Fleming, 2011b). Vacuum-dried polyacrylic acid powders were used to prepare six polyacrylic acid molecular weight mixtures with different molecular weights (15,000, 25,700, 40,000 and 80,800) above  $M_c$  and  $M_c$  (Dowling and Fleming, 2011b). The powders were dry-blended at varying powder:powder blend ratios ranging from 90:10-10:90 (in 10:0 increments) and mixed with distilled water to prepare polyacrylic acid solutions at concentrations of 25, 35 and 45%. Replacing 10-30% of a lower molecular weight polyacrylic acid with a higher molecular weight polyacrylic acid produced GIs with significantly increased CFS and elastic moduli when compared with the lower molecular weight polyacrylic acid control group (Dowling and Fleming, 2011b) (Figure 1.10). However, no significant increase in CFS and elastic moduli were identified for GIs prepared from the polyacrylic acid molecular weight mixtures when compared with the highest molecular weight polyacrylic acid solutions investigated (40,000 and 80,800) (Dowling and Fleming, 2011b) (Figure 1.10). It was suggested that improvements in the CFS and elastic moduli of GIs could be achieved by optimising the powder:liquid mixing ratio in conjunction with the optimum polyacrylic acid concentration, polyacrylic acid molecular weight mixtures and blend ratios (Dowling and Fleming, 2011b).

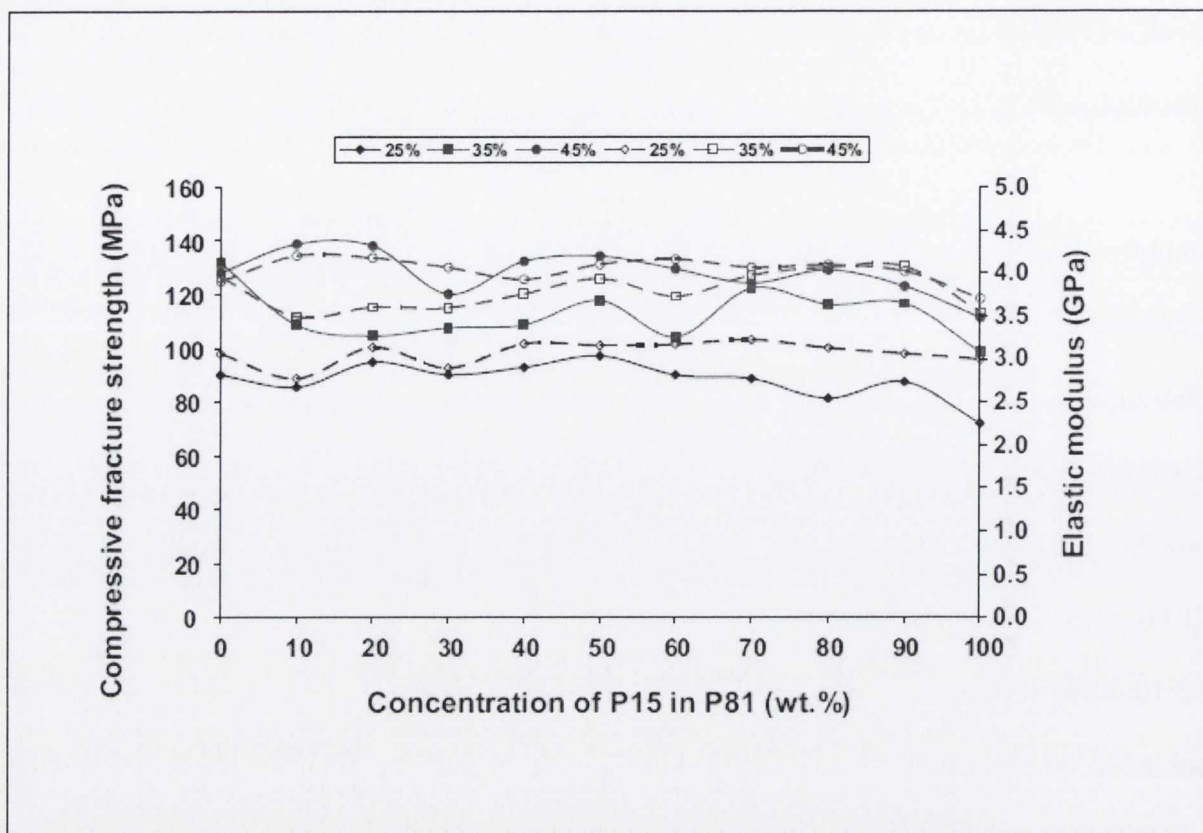


**Figure 1.10. The variation in the compressive fracture strength (CFS) (continuous line) and the elastic moduli (broken line) of GIs prepared with polyacrylic acid molecular weight mixtures containing 15,000 (P15) and 81,000 (P81) molecular weight polyacrylic acids at concentrations of 25, 35 and 45% with increasing P15:P81 blend ratios. A significant increase in CFS and elastic moduli for the molecular weight mixture at P15:P81 blend ratios of 70:30, 80:20 and 90:10 were highlighted when compared with the lower molecular weight control group (P15) for the three concentrations investigated. Adapted from Dowling and Fleming (2011b).**

For the polyacrylic acid molecular weight mixtures, a progressive increase in viscosity of the polyacrylic acid solutions was identified on increasing the average molecular weight of the solution (Dowling and Fleming, 2011b). Conversely, a significant reduction in the viscosity of the polyacrylic acid solutions was observed as the blend ratio of the lower molecular weight polyacrylic acid to the higher molecular weight polyacrylic acid was increased (Figure 1.11), although the mixing of two polyacrylic acids with varying molecular weight exacerbated variations in the viscosity of the polyacrylic acid molecular weight mixture solutions (Dowling and Fleming, 2011b).

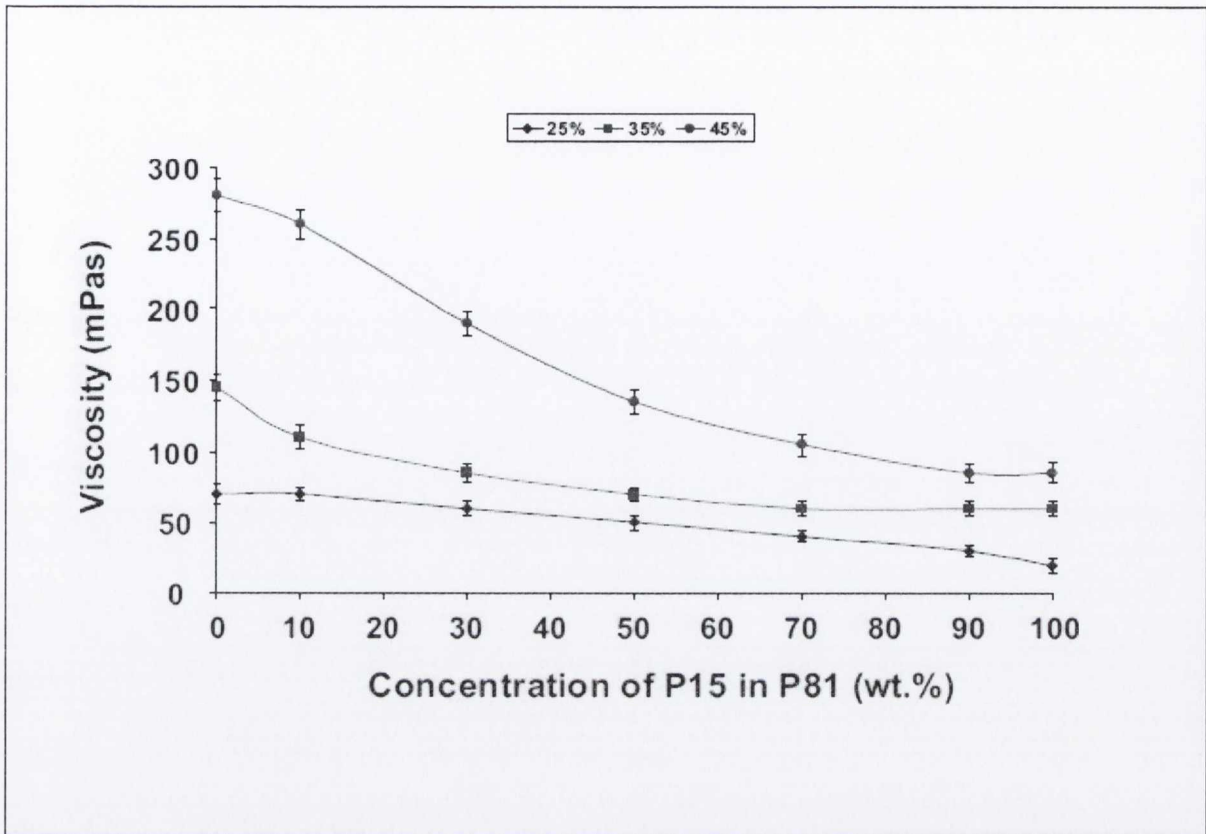


**Figure 1.11.** The variation in viscosity of the polyacrylic acid solutions for a polyacrylic acid molecular weight mixture containing 15,000 (P15) and 81,000 (P81) molecular weight polyacrylic acids at concentrations of 25, 35 and 45%. A progressive decrease in the viscosity of the polyacrylic acid molecular weight mixture solution was highlighted as the blend ratio of the lower molecular weight polyacrylic acid (P15) to the higher molecular weight polyacrylic acid (P81) was increased for the three concentrations investigated. Adapted from Dowling and Fleming (2011b).

Despite the optimisation of the GI liquid component, mixed GIs remain too weak to be ‘truly’ advocated for clinical use as posterior restoratives. Numerous attempts have been made to enhance the mechanical properties of GIs through reinforcement of the GI powder or liquid constituent with variously reported levels of success.

#### 1.4 STRATEGIES OF REINFORCEMENT PREVIOUSLY EMPLOYED FOR GIs

Since the introduction of ASPA to the dental market in the early 1970’s, the GI powder and liquid constituents have undergone significant changes in chemical make-up. As a result, the

range of clinical applications has expanded from luting cements to cavity liners or bases and restorative materials. The major advantage of GIs over dental amalgam and resin-based composites (RBCs) for the restoration of natural dentition is the ability of GIs to chemically bond to sound tooth structure (Wilson and McLean, 1988d; Van Meerbeek et al., 2003). In addition, fluoride release from GI restorations has been claimed to be therapeutic for prevention of secondary caries (Forsten, 1998; Mayanagi et al., 2014). Despite these clinical advantages, GIs cannot 'truly' be advocated for the restoration of posterior dentition due to the poor mechanical properties when compared with dental amalgam and RBCs. To improve the mechanical properties of GIs and enable their clinical use posteriorly, attempts have been made to reinforce the GI matrix through the addition of various filler types to the GI powder component. The fillers used included fibres (Sced and Wilson, 1980; Oldfield and Ellis, 1991; Kobayashi et al., 2000; Lohbauer et al., 2003), metallic powders (Sced and Wilson, 1980; Simmons, 1983, 1990; Miller et al., 1984; McLean and Gasser, 1985; El Mallakh et al., 1987; Walls et al., 1987; Nakajima et al., 1989; McLean, 1990; Kerby and Bleiholder, 1991; Williams et al., 1992; Elsaka et al., 2011; Dowling et al., 2014), hydroxyapatite powders (Nicholson et al., 1993; Lucas et al., 2003; Yap et al., 2002; Gu et al., 2005; Moshaverinia et al., 2008a), bioactive glass particles (Yli-Urpo et al., 2005) and montmorillonite clay additions (Dowling et al., 2006; Dowling and Fleming, 2007).

#### **1.4.1 Fibres**

Sced and Wilson (1980) investigated the influence of addition of carbon and alumina fibres to a commercial GI powder (Chembond; Dentsply DeTrey) on the flexural strength of bar-shaped GI specimens (25 mm length, 3 mm width, 3 mm thickness) prepared in accordance with the British standard (BS 5199:1975). The fibre lengths were >1000  $\mu\text{m}$  with fibre diameters ranging from 10-200  $\mu\text{m}$ . The reinforcing fibres were incorporated into the GI

powder at 25 vol%, hand-mixed with the appropriate GI liquid (Chembond) and compared with the hand-mixed Chembond control group. The authors reported an increase in the mean flexure strength value from 10 MPa for the GI control group (Chembond) to 53 MPa and 44 MPa for the GIs prepared with carbon and alumina fibre additions, respectively (Sced and Wilson, 1980).

Eleven years later, the addition of carbon fibres (250-1000  $\mu\text{m}$  length, 8  $\mu\text{m}$  diameter, ICI Ltd., Cheshire, UK) and alumina fibres (500  $\mu\text{m}$  length, 3  $\mu\text{m}$  diameter, ICI Ltd.) to experimental GI glass systems, namely MP-4 (Pilkington Bros., Lancashire, UK) and G-338 (LGC, London, UK) glasses was reported whereby the fibres were added to the GI glass powders at 0-20 vol% (in 2.5 vol% increments) (Oldfield and Ellis, 1991). Appropriate amounts of freeze-dried polyacrylic acid powder were added to the GI powder-fibre blend prior to mechanically mixing to obtain an 'even distribution' of powders (Oldfield and Ellis, 1991). The dry-blended powder was hand-mixed with water (powder:liquid mixing ratio not reported) and cylindrical bar-shaped specimens (4.5 mm diameter, length not reported) were prepared and tested following 24 h water storage using a four-point flexure test assembly. An increase in four-point flexural strength value for 5 vol% carbon fibres addition to MP-4 (45 MPa) and G-338 (30 MPa) glass powders was reported although the flexural strength values for the unreinforced GIs were not reported (Oldfield and Ellis, 1991). Alumina fibre incorporation was reported to increase the brittleness of the reinforced GIs (Oldfield and Ellis, 1991).

The addition of short glass fibres ( $\text{CaO-P}_2\text{O}_5\text{-SiO}_2\text{-Al}_2\text{O}_3$ ) of varying lengths (33.5-100.4  $\mu\text{m}$ ) and diameters (9.7-21.5  $\mu\text{m}$ ) to a commercial hand-mixed GI powder (HY Bond Glasionomer CX; Shofu Inc., Fukuine, Kyoto, Japan) was reported by Kobayashi et al. (2000). Short glass

fibre concentrations ranging from 0-100 wt% (in 20 wt% increments) were incorporated into the GI powder and the blended powder was hand-mixed with the appropriate GI liquid (HY Bond Glasionomer CX) at a powder:liquid mixing ratio of 2:1 g:g. Disc-shaped DTS specimens (6 mm diameter, 3 mm thickness: n=7) and bar-shaped TFS specimens (25 mm length, 6 mm width, 3 mm thickness: n=7) were prepared and tested following 24 h water storage. Increasing the short glass fibre wt% from 0-60% (in 20 wt% increments) resulted in an increase in the mean DTS value from 11 MPa (commercial GI) to 18 MPa (60 wt% short glass fibre addition) and mean TFS value from 8 MPa (commercial GI) to 35 MPa (60 wt% short glass fibre addition) (Kobayashi et al., 2000). Further short glass fibres addition (>60 wt%) resulted in a deterioration in the mean DTS and TFS values compared with the commercial GI formulation (Kobayashi et al., 2000).

The  $K_{IC}$  of a 10, 20 and 30 wt% glass fibre (GC Corporation) blended with a hand-mixed commercial GI powder (Fuji I; GC Corporation) was reported by Luksanasombool et al. (2002). The glass fibre diameters ranged from 20-100  $\mu\text{m}$  even-though the fibre lengths were not reported. The GI powder and glass fibres were hand-mixed with the Fuji I liquid at 1.8:1 g:g and single-edge notched (SEN) bend specimens (dimensions not reported) were prepared in accordance with the American Society for Testing and Materials (ASTM) International (ASTM 399:2009). The specimens were loaded in a three-point flexure test assembly following storage for 1 week in physiologically buffered saline (Luksanasombool et al., 2002). The authors identified a decrease in the  $K_{IC}$  value for Fuji I ( $0.48 \text{ MNm}^{-1.5}$ ) with increasing glass fibre addition to  $0.35 \text{ MNm}^{-1.5}$  at the 30 wt% blend which was attributed to increased porosity during glass fibres incorporation on blending (Luksanasombool et al., 2002).

SiO<sub>2</sub>-Al<sub>2</sub>O<sub>3</sub>-CaO-NaF-AlF<sub>3</sub>-Na<sub>3</sub>AlF<sub>6</sub> glass fibres addition ( $580 \pm 160 \mu\text{m}$  length,  $26 \mu\text{m}$  diameter) to a variety of experimental GI glass powders were also reported (Lohbauer et al., 2003). CFS specimens (6 mm height, 4 mm diameter: n=15) were prepared by hand-mixing powders prepared from a series of nine experimental glasses with a GI liquid (40-45 wt% polyacrylic acid with 8-10 wt% tartaric acid solution) to determine the optimum powder particle size (2.4-12.2  $\mu\text{m}$ ), glass surface treatment (acid washing and heat treatment), powder:liquid mixing ratio (1.5:1-2.8:1 g:g) and glass fibre fraction (20, 40, 60 vol%). Under the optimum conditions (2.4  $\mu\text{m}$  powder particle size, 7 h acid washing in 3% HCL glass surface treatment, 6 h heat treatment at 360°C, powder:liquid mixing ratio of 1.8:1 g:g, 20 vol% glass fibre fraction), bar-shaped specimens (25 mm length, 2 mm width, 2 mm thickness: n=15) were prepared and loaded in a four-point flexure assembly following 24 h water storage. The authors reported a significant increase in the four-point flexural strength values for the fibre reinforced GI ( $16 \pm 2 \text{ MPa}$ ) when compared with the unreinforced control ( $10 \pm 1 \text{ MPa}$ ) (Lohbauer et al., 2003).

With respect to fibre incorporation in GI powders, the aspect ratio (fibre length:diameter), chemical composition, reinforcing addition filler volume fraction, composition of the GI powder and liquid and the powder:liquid mixing ratios employed were markedly different for the studies reporting fibre reinforcement of GIs (Sced and Wilson, 1980; Oldfield and Ellis, 1991; Kobayashi et al., 2000; Lucksanasombool et al., 2002; Lohbauer et al., 2003), such that a direct comparison under controlled conditions was not possible.

#### **1.4.2 Metallic powders**

Researchers have investigated the influence of the addition of a range of metallic powders to GI powders, namely aluminium (Sced and Wilson, 1980), chromium (Sced and Wilson,



1980), nickel-aluminium alloy (Sced and Wilson, 1980), silver-tin alloy (Sced and Wilson, 1980; Simmons, 1983, 1990; Miller et al., 1984; El Mallakh et al., 1987; Nakajima et al., 1989; Williams et al., 1992), stainless-steel (Kerby and Bleiholder, 1991) and titanium dioxide powders (Elsaka et al., 2011; Dowling et al., 2014). In addition enhancement of mechanical properties of GIs with fused silver, gold or palladium has been investigated by dental researchers and manufacturers (McLean and Gasser, 1985; Walls et al., 1987; McLean, 1990; Williams et al., 1992).

Sced and Wilson (1980) reported a flexure strength value for Chembond of 10 MPa while the addition of aluminium (21 MPa), chromium (22 MPa), nickel-aluminium alloy (22 MPa) and silver-tin alloy (40 MPa) enhanced the flexure strength values of the metallic reinforced Chembond GI. No details of the wt% metallic additions were provided although the poor polishability and aesthetics of the silver-tin alloy reinforced GI restorations precluded their clinical usage (Wilson and Prosser, 1984; Wilson and Nicholson, 1993).

The addition of a spherical amalgam alloy powder (Lumi Alloy; GC Corporation) to Fuji II (GC Corporation) was proposed by Simmons (1983, 1990) and a variant was subsequently marketed as Miracle Mix in 1983 by the GC Corporation (Williams et al., 1992). Miller et al. (1984) investigated the CFS of cylindrical Miracle Mix specimens (12 mm height, 6 mm diameter) prepared at GI powder:spherical amalgam alloy powder ratios from 5:1-8:1 g:g at 1 and 24 h. An increase in mean CFS value of Miracle Mix at 1 h ( $104 \pm 7$  MPa) and 24 h ( $197 \pm 12$  MPa) was identified when compared with Fuji II (65 MPa and 151 MPa, respectively) (Miller et al., 1984). An increased 24 h mean CFS (148 MPa) and mean DTS (15 MPa) values for cylindrical Miracle Mix specimens (6 mm height, 3 mm diameter: n=5) compared with Fuji II (143 MPa and 12 MPa, respectively) was also reported (El Mallakh et al., 1987).

Interestingly, no difference in the 24 h mean CFS value ( $120 \pm 15$  MPa) for cylindrical Miracle Mix specimens (12 mm height, 6 mm diameter:  $n=4-10$ ) was identified compared with Fuji Ionomer II (GC Corporation) ( $120 \pm 10$  MPa) (Nakajima et al., 1989). However, an increase in the 24 h mean TFS value was evident for bar-shaped Miracle Mix specimens (25 mm length, 4 mm width, 2 mm thickness:  $n=4-10$ ) when compared with Fuji Ionomer II ( $25 \pm 3$  MPa and  $18 \pm 1$  MPa, respectively) (Nakajima et al., 1989). Cylindrical CFS (12 mm height, 6 mm diameter:  $n=6$ ), disc-shaped DTS (8 mm diameter, 4 mm thickness:  $n=6$ ), bar-shaped TFS (22 mm length, 2 mm width, 2 mm thickness:  $n=6$ ) and disc-shaped BFS specimens (15 mm diameter, 1 mm thickness:  $n=6$ ) of Miracle Mix and Fuji II were tested following 24 h water storage (Williams et al., 1992). No increase in the mean CFS and DTS values was identified but the mean TFS and BFS values of Miracle Mix ( $40 \pm 10$  MPa and  $32 \pm 10$  MPa, respectively) was increased when compared with Fuji II ( $36 \pm 3$  MPa and  $25 \pm 6$  MPa, respectively) (Williams et al., 1992). The increased TFS values for Miracle Mix containing the metal filler, when compared with the conventional GI (Fuji II) were attributed to the change in fracture mode from ductile failure (Miracle Mix) to brittle failure (Fuji II) (Nakajima et al., 1989). Although the addition of metal filler changed the fracture mode, it is unlikely that chemical interfacial bonding occurred between the metal filler and the GI matrix (Darvell, 2002) which would be required to produce a 'true' composite material with improved mechanical properties.

Experimental stainless-steel powder (mean particle size  $9 \mu\text{m}$ ) reinforced GIs were investigated and compared with Miracle Mix (Kerby and Bleiholder, 1991). The stainless-steel powder was acid etched, washed with water and methyl alcohol before blending with Fuji II at 17 vol%. Cylindrical CFS and DTS specimens (12 mm height, 6 mm diameter:  $n=10$ ) were prepared and tested following 24 h water storage. The mean CFS and DTS values

of Miracle Mix ( $169 \pm 10$  MPa and  $11 \pm 2$  MPa, respectively) were significantly reduced compared with the stainless-steel reinforced GI ( $268 \pm 15$  MPa and  $23 \pm 2$  MPa, respectively) (Kerby and Bleiholder, 1991). However, GIs prepared from Miracle Mix and the experimental stainless-steel reinforced powder were not tooth-coloured owing to the presence of alloy powder constituent.

The influence of 3, 5 and 7 wt% TiO<sub>2</sub> nano-powder (mean particle size 21 nm, Batch MKBC-4174, Sigma Aldrich) addition to Kavitan Plus (SpofaDental; Jičín, Czech Republic) was reported (Elsaka et al., 2011). Cylindrical CFS (6 mm height, 4 mm diameter: n=20), bar-shaped TFS (25 mm length, 2 mm width, 2 mm thickness: n=20) and knife-edge notch K<sub>IC</sub> (25 mm length, 5 mm width, 2.5 mm thickness with a reported 2.5 mm notch: n=20) specimens were prepared when the dry-blended powders were hand-mixed with the Kavitan Plus liquid at a powder:liquid mixing ratio of 2.7:1 g:g. Following 24 h water storage, a significant increase in mean CFS value from  $149 \pm 8$  MPa to  $176 \pm 8$  MPa, TFS value from  $14 \pm 3$  MPa to  $23 \pm 3$  MPa and K<sub>IC</sub> value from  $0.69 \pm 0.03$  MNm<sup>-1.5</sup> to  $1.29 \pm 0.05$  MNm<sup>-1.5</sup> were reported with 3 wt% TiO<sub>2</sub> nano-powder addition (Elsaka et al., 2011). More recently, Dowling et al. (2014) revisited the TiO<sub>2</sub> powder reinforcement strategy for GIs with the addition of 0.5 to 15 wt% of the same TiO<sub>2</sub> nano-powder employed previously (Elsaka et al., 2011) to Ionofil Molar which was subsequently mixed with a 40% polyacrylic acid liquid solution at a powder:liquid mixing ratio of 4:1 g:g (Dowling et al., 2014). Testing the cylindrical CFS specimens (6 mm height, 4 mm diameter: n=20) following 24 h water storage failed to identify any strengthening with the TiO<sub>2</sub> nano-powder inclusion groups (Dowling et al., 2014) which appear to cast doubt on the truly remarkable and almost unbelievable CFS, TFS and K<sub>IC</sub> data reported previously (Elsaka et al., 2011).

The sintering of a precious metal (silver, gold or palladium) with the GI glass constituent was proposed as an alternative approach to metal reinforcement of GIs and was marketed in 1986 by ESPE GmbH as glass-cermet cements under the trade names of Chelon Silver which was hand-mixed and Ketac Silver which was encapsulated (McLean and Gasser, 1985; McLean 1990). The cermet powders were prepared by mixing equal volumes of silver powder (mean particle size 3.5  $\mu\text{m}$ ) and a GI glass powder. The blended powders were compressed at 350 MPa to form metal-glass powder pellets which were sintered at 800°C and ground to fine powder. In an attempt to improve the aesthetics, 5 wt% of titanium dioxide was added and the blended powders were mixed with a 46% solution of acrylic, maleic and tartaric acids at powder:liquid mixing ratios of 4:1 g:g (Chelon Silver) and 4.5:1 g:g (Ketac Silver) (McLean and Gasser, 1985). Williams et al. (1992) compared a conventional hand-mixed GI (Chelon Fil) with Chelon Silver on CFS testing cylindrical specimens (12 mm height, 6 mm diameter: n=6), DTS testing disc-shaped specimens (8 mm diameter, 4 mm thickness: n=6), BFS testing disc-shaped specimens (15 mm diameter, 1 mm thickness: n=6) and TFS testing bar-shaped specimens (22 mm length, 2 mm width, 2 mm thickness: n=6) following 24 h water storage. A reduction in the mean CFS ( $137 \pm 17$  MPa), DTS ( $13 \pm 2$  MPa), BFS ( $45 \pm 4$  MPa) and TFS ( $29 \pm 4$  MPa) values was evident for the hand-mixed Chelon Silver when compared with the CFS ( $147 \pm 15$  MPa), DTS ( $19 \pm 3$  MPa), BFS ( $36 \pm 5$  MPa) and TFS ( $21 \pm 3$  MPa) values of its hand-mixed conventional GI counterpart (Chelon Fil). When bar-shaped TFS specimens (20 mm length, 2.5 mm width, 2.5 mm thickness: n=10) were tested following 1 week water storage, Walls et al. (1987) reported a reduction in both the TFS value from  $45 \pm 5$  MPa to  $29 \pm 7$  MPa and the three-point flexure modulus (TFM) value from  $13 \pm 2$  GPa to  $8 \pm 4$  GPa for Ketac Fil compared with Ketac Silver, namely the encapsulated products. In addition, the cermet materials were not tooth-coloured owing to the silver in the powder constituent (Sarkar et al., 1988) which caused discolouration of the cermet restored teeth

(Croll and Philips, 1986). The poor aesthetics of cermets limited their range of clinical applications to paediatric and domiciliary dental care. Kilpatrick et al. (1995) investigated the durability of Ketac Silver and Ketac Fil in a 2.5 year prospective clinical trial. Ketac Silver and Ketac Fil were used to restore 46 pairs of class II lesions in deciduous molars and when the restorations were assessed using the modified United States Public Health Services (USPHS) criteria, the failure rate for Ketac Silver (41%) was increased when compared with Ketac Fil (23%). In addition, the median survival time for Ketac Silver of 20.3 months was shorter than Ketac Fil (25.3 months) with increased marginal integrity and anatomic form deterioration for Ketac Silver restorations (Kilpatrick et al., 1995). Results from the clinical trial reported by Kilpatrick et al. (1995) provided sufficient evidence to preclude the clinical use of Ketac Silver as it failed to offer any clinical longevity advantage over the conventional GI (Ketac Fil).

### **1.4.3 Hydroxyapatite**

Hydroxyapatite is the primary mineral constituent of enamel and adhesively interacts with GIs (Skinner et al., 1986; Yoshida et al., 2001). The addition of finely divided hydroxyapatite (Bio-Gel HTP, Bio-Rad Laboratories, Richmond, California, USA) to two experimental glasses MP-4 ( $\text{Al}_2\text{O}_3\text{-SiO}_2\text{-CaO-Na}_2\text{O}$  at 35.0-28.0-26.0-11.0 wt%) and G-200D ( $\text{Al}_2\text{O}_3\text{-SiO}_2\text{-NaAlF}_6\text{-CaF}_2\text{-AlF}_3\text{-AlPO}_4$  at 16.6-29.0-5.0-34.3-5.3-9.9 wt%) was investigated (Nicholson et al., 1993). The hydroxyapatite was substituted at 2.5, 5, 10, 20, 25 wt% for MP-4 and 2.5, 5, 10, 20, 25, 30, 40, 50 wt% for G-200D glass powders and blends were hand-mixed with a 40% solution of polyacrylic acid (Versicol E7, Allied Colloids, Low Moor, Bradford, UK) at a powder:liquid mixing ratio of 2:1 g:g to prepare cylindrical specimens (12 mm height, 6 mm diameter) for CFS testing following 24 h storage. A progressive deterioration in mean CFS values from  $20 \pm 1$  MPa to  $8 \pm 1$  MPa for MP-4 and

from  $55 \pm 8$  MPa to  $26 \pm 2$  MPa for G-200D was evident with increasing hydroxyapatite content (Nicholson et al., 1993).

The influence of addition of hydroxyapatite powder (mean particle size  $17 \mu\text{m}$ ) to Fuji IX<sub>GP</sub> was investigated by Yap et al. (2002) by substituting 4, 12, 28 vol% hydroxyapatite for the GI powder in the powder compartment of the capsule. The powder mixture was mechanically mixed (HSMI, GC Corporation) at a powder:liquid mixing ratio of 3.6:1 g:g and cylindrical CFS (8 mm height, 4 mm diameter: n=5) and disc-shaped DTS specimens (6 mm diameter, 3 mm thickness: n=5) were prepared. Following water storage for 24 h and 1 week, no difference in mean CFS ( $142 \pm 31$  MPa and  $177 \pm 28$  MPa, respectively) or DTS ( $12 \pm 3$  MPa and  $14 \pm 3$  MPa, respectively) values for the 4 vol% hydroxyapatite reinforced GIs were observed when compared with the CFS ( $150 \pm 45$  MPa and  $162 \pm 37$  MPa, respectively) and DTS ( $12 \pm 2$  MPa and  $14 \pm 4$  MPa, respectively) values of the Fuji IX<sub>GP</sub> groups (Yap et al., 2002). Further incorporation of the hydroxyapatite powder (12 and 28 vol%) resulted in a marked deterioration in mean CFS and DTS values following 24 h and 1 week water storage (Yap et al., 2002).

Substitution of 4, 12, 28 and 40 vol% hydroxyapatite-zirconia powder for the GI powder constituent in Fuji IX<sub>GP</sub> capsules was assessed by Gu et al. (2005) by mechanically mixing the powder blend at a powder:liquid mixing ratio of 3.6:1 g:g to prepare cylindrical CFS (8 mm height, 4 mm diameter: n=5) and disc-shaped DTS (6 mm diameter, 3 mm thickness: n=5) specimens following 24 h water storage. The CFS and DTS of the 4 and 12 vol% hydroxyapatite-zirconia powder substituted GI identified no increase in the mean strength values when compared with the Fuji IX<sub>GP</sub> control group (Gu et al., 2005). A deterioration in

the mean CFS and DTS values was identified when the concentration of hydroxyapatite-zirconia powder substitution was increased to 28 and 40 vol% (Gu et al., 2005).

The influence of hydroxyapatite reinforcement of Fuji IX on the  $K_{IC}$  was investigated using SEN bend specimens (25 mm length, 5 mm width, 2.5 mm thickness with a reported 2.5 mm notch: n=24) by substituting 8 wt% of the Fuji IX powder with hydroxyapatite (particle size 5-20  $\mu\text{m}$ ) (Lucas et al., 2003). The GI-hydroxyapatite powder blend was hand-mixed at a powder:liquid mixing ratio of 3.6:1 g:g. Twelve specimens were tested at 15 mins and the remaining twelve were tested after 24 h water storage in a three-point flexure assembly. An increase in  $K_{IC}$  on hydroxyapatite substitution (8 wt%) at 15 min ( $0.56 \pm 0.10 \text{ MNm}^{-1.5}$ ) and 24 h ( $0.58 \pm 0.09 \text{ MNm}^{-1.5}$ ) was evident when compared with the Fuji IX control group ( $0.36 \pm 0.06 \text{ MNm}^{-1.5}$  and  $0.45 \pm 0.06 \text{ MNm}^{-1.5}$ , respectively) (Lucas et al., 2003).

Hydroxyapatite (5 wt%) and fluoroapatite (5 wt%) powder (particle size 100-200 nm) substitution to Fuji II followed by manual grinding using a mortar and pestle for 20 mins prior to hand-mixing at a powder:liquid mixing ratio of 2.7:1 g:g was also investigated (Moshaverinia et al., 2008a). CFS cylinders (6 mm height, 4 mm diameter: n=6), DTS discs (4 mm diameter, 2 mm thickness: n=6) and BFS discs (10 mm diameter, 1 mm thickness: n=6) were tested following 24 h and 1 week water storage. An increase in mean CFS ( $177 \pm 10 \text{ MPa}$  and  $179 \pm 12 \text{ MPa}$ ), DTS ( $16 \pm 4 \text{ MPa}$  and  $17 \pm 4 \text{ MPa}$ ) and BFS ( $26 \pm 6 \text{ MPa}$  and  $28 \pm 7 \text{ MPa}$ ) values for the hydroxyapatite and fluoroapatite substituted GIs, respectively was observed when compared with the CFS ( $160 \pm 12 \text{ MPa}$ ), DTS ( $12 \pm 3 \text{ MPa}$ ) and BFS ( $14 \pm 5 \text{ MPa}$ ) values of the Fuji II control group tested at 24 h. A further increase in CFS, DTS and BFS values was highlighted after 1 week water storage (Moshaverinia et al., 2008a).

#### 1.4.4 Bioactive glass particles

Bioactive glass particle (S53P4, Vivoxid Ltd., Turku, Finland) substitution of 10 wt% (mean particle size 20  $\mu\text{m}$ ) to Fuji II was investigated by Yli-Urpo et al. (2005) using a powder:liquid mixing ratio of 1.7:1 g:g, although the authors reported using 'level scoops' when determining the powder:liquid mixing ratio. Cylindrical CFS specimens (6 mm height, 4 mm diameter: n=6) were stored in water for 1, 3, 7, 14, 30 and 180 days. A deterioration in mean CFS value for the 10 wt% bioactive glass particle substituted GIs ( $95 \pm 20$  MPa to  $80 \pm 15$  MPa) was highlighted when compared with the Fuji II control group ( $120 \pm 20$  MPa to  $105 \pm 30$  MPa) on testing following 1 and 180 days water storage, respectively (Yli-Urpo et al., 2005).

#### 1.4.5 Montmorillonite clay

The addition of two montmorillonite clays, a pristine calcium montmorillonite clay (Ca-MMT) (Süd Chemie, Munich, Germany) and an organically modified 12-amino-dodecanoic acid montmorillonite clay (ADA-MMT) (Nanocor Inc., IL, USA) on the CFS of Chemfil Superior (Dentsply DeTrey) was investigated (Dowling et al., 2006). The montmorillonite clays were added to the GI powder at 0.5, 1.0, 1.5, 2.0 and 2.5 wt% and mixed at a powder:liquid mixing ratio of 7.4:1 g:ml to prepare cylindrical CFS specimens (6 mm height, 4 mm diameter: n=30) prior to testing following 24 h water storage (Dowling et al., 2006). A progressive deterioration in mean CFS values for the Chemfil Superior control ( $105 \pm 22$  MPa) occurred up to 2.5 wt% Ca-MMT clay addition but an increase in CFS values was observed when 0.5 wt% ( $133 \pm 10$  MPa) and 1.0 wt% ( $128 \pm 22$  MPa) of the ADA-MMT clay was added to Chemfil Superior. The mean CFS values decreased with further ADA-MMT clay addition (1.5-2.5 wt%) (Dowling et al., 2006).



Alternatively, to enhance the mechanical properties of GIs, investigators have also explored modifications of the GI liquid component to increase cross-linking between the polymer chains during the setting reaction. The GI liquid modifications include the formation of novel polyacids (Wilson and Ellis, 1989; Ellis et al., 1991) and the introduction of acrylic and itaconic or maleic acid copolymers containing flexible side chains of amino acids (Culbertson and Kao, 1994; Kao et al., 1996; Culbertson et al., 1999), N-vinylpyrrolidone (Xie et al., 1998; Culbertson, 2001, 2006; Yamazaki et al., 2005; Moshaverinia et al., 2008b) or N-vinylcaprolactam (Moshaverinia et al., 2009, 2010).

#### **1.4.6 Novel polyacids**

Despite the early investigations regarding the use of copolymers of acrylic and itaconic or maleic acids (Crisp and Wilson, 1977; Schmitt et al., 1982) and polyacids of increased molecular weights and concentrations (Wilson et al., 1977; Crisp et al., 1977; Dowling and Fleming., 2011a,b), little attention has been paid to the development of novel polyacids in the dental literature. It was not until the early 1990's when the use of polyvinylphosphonic acid (PVPA) as a novel and alternative GI liquid to polyacrylic acid was reported by Wilson and Ellis (1989) and Ellis et al. (1991). Calcium and aluminum cations ( $\text{Ca}^{2+}$  and  $\text{Al}^{3+}$ ) released from the GI glass powder were suggested to form stronger cross-links between the polyacid chains of PVPA than the cross-links formed between polyacrylic acid chains since unpolymerised dibasic phosphonic acids were stronger acids than unpolymerised acrylic acid (Wilson and Ellis, 1989). These stronger cross-links were expected to result in the formation of GIs with improved mechanical properties when compared with conventional GIs based on polyacrylic acid (Wilson and Ellis, 1989). The PVPA containing GIs were also suggested to undergo a faster maturation owing to the increased reactivity of PVPA (Ellis et al., 1991), thereby reducing the susceptibility of PVPA containing GIs to the deleterious effects of

moisture contamination (Causton, 1981) and desiccation (Earl et al., 1989; Wilson, 1989) during the initial stages of the setting reaction. However, the more reactive PVPA could not be used as a direct replacement for polyacrylic acid due to the setting time (45 s) when compared with conventional GIs (180-240 s) (Wilson and Ellis, 1989). Deactivation of the reactive glasses by heat treatment and the use of a reaction controlling additive (10 wt% aminotrismethylenephosphonic acid) in the PVPA liquid was necessary to ensure adequate working characteristics for practical clinical usage (Ellis et al., 1991). Modification of PVPA with 10% zinc fluoride at the preparation stage was proposed to improve the mean CFS of the resultant GIs (Akinmade and Braybrook, 1995). Cylindrical CFS specimens (12 mm height, 6 mm diameter: n=6) were prepared by hand-mixing a 10% zinc fluoride modified PVPA solution and an unmodified PVPA solution with an experimental glass powder. Following 24 h water storage, an increase in the mean CFS value from  $121 \pm 14$  MPa for the GI specimens prepared with the unmodified PVPA solution to  $147 \pm 10$  MPa for the 10% zinc fluoride modified PVPA solution was reported, suggesting reinforcement of the GI was achievable (Akinmade and Braybrook, 1995). Employing the same solutions as Akinmade and Braybrook (1995) but a different experimental glass powder, testing cylindrical CFS specimens (12 mm height, 6 mm diameter: n=6) followed by water storage for 1, 7, 30 and 90 days also showed reinforcement (Anstice and Nicholson, 1995). Following 1 and 90 day water storage, the CFS values of the GIs prepared with the unmodified PVPA solution were markedly reduced ( $84 \pm 15$  MPa to  $112 \pm 9$  MPa) compared with the 10% zinc fluoride modified PVPA solution ( $158 \pm 15$  MPa to  $226 \pm 35$  MPa) (Anstice and Nicholson, 1995).

The concept of PVPA containing GIs was explored by one dental manufacturer (Associated Dental Products Ltd., Kemdent Works, Wiltshire, UK) in the form of 'Diamond Carve'. Diamond Carve was reported to contain a strontium aluminosilicate glass, freeze-dried

copolymer of PVPA and acrylic acid as the powder component which was manipulated with an aqueous solution of polyacrylic acid and tartaric acid at a powder:liquid mixing ratio of 4:1 g:g (Product specification). On testing disc-shaped BFS specimens (10 mm diameter, 1 mm thickness: n=6) following 24 h water storage, no improvement in the mean BFS value of Diamond Carve was achieved ( $36.5 \pm 2.9$  MPa) compared with the commercial GI restoratives tested (HiFi; Shofu Inc.,  $40.4 \pm 6.7$  MPa and Ketac Molar,  $44.7 \pm 6.0$  MPa) (Khouw-Liu et al., 1999b). No clinical study of Diamond Carve is available in the dental literature owing to the poor mechanical performance compared with the commercial GI investigated.

#### **1.4.7 Modified copolymers**

Wilson and McLean (1988b) highlighted that during the setting reaction of GIs not all of the carboxyl groups on the polymer backbone of the polyacid were converted to metal carboxylates by the  $\text{Ca}^{2+}$  and  $\text{Al}^{3+}$  ions released from the glass powder. The close attachment of the pendant carboxyl groups to the polymer backbone in the polyacrylic acid homopolymers and copolymers of acrylic and itaconic or maleic acids was proposed to cause steric hindrance which would prevent the conversion of some of the carboxyl groups on the polymer backbone to metal carboxylate complexes (salt bridges) by the  $\text{Ca}^{2+}$  and  $\text{Al}^{3+}$  ions (Kao et al., 1996). It was proposed that the introduction of a flexible spacer to link the pendant functional carboxyl groups with the polymer backbone would prevent steric hindrance and allow greater mobility of the pendant carboxyl groups to react with the  $\text{Ca}^{2+}$  and  $\text{Al}^{3+}$  ions to form the metal cation salt bridges (Culbertson and Kao, 1994; Kao et al., 1996; Culbertson, 2001). As a result, amino acid monomers (N-acryloylglutamic acid, N-methacryloylglutamic acid) (Culbertson and Kao, 1994; Kao et al., 1996; Culbertson et al., 1999), N-vinylpyrrolidone (Xie et al., 1998; Yamazaki et al., 2005; Moshaverinia et al.,

2008b) and N-vinylcaprolactam (Moshaverinia et al., 2009, 2010) were investigated as flexible spacers in acrylic acid and itaconic acid (Culbertson and Kao, 1994; Kao et al., 1996; Xie et al., 1998; Culbertson et al., 1999; Moshaverinia et al., 2008b, 2009, 2010) or acrylic acid and maleic acid copolymers (Yamazaki et al., 2005).

N-acryloylglutamic acid was used to modify acrylic acid and itaconic acid copolymer solutions at acrylic acid:itaconic acid:N-acryloylglutamic acid molar ratios of 10:1:1 and 10:1:4 (Kao et al., 1996). The modified copolymer solutions were hand-mixed with Fuji II powder at a powder:liquid mixing ratio of 2.7:1 g:g to prepare cylindrical CFS and DTS specimens (12 mm height, 6 mm diameter: n=10), bar-shaped TFS specimens (25 mm length, 3 mm width, 3 mm thickness: n=10) and SEN compact tension  $K_{IC}$  specimens (6.6 mm length, 6.3 mm width, 1.7 mm thickness: n=10) following 24 h and 1 week water storage (Kao et al., 1996). GIs prepared with the 10:1:1 and 10:1:4 acrylic acid:itaconic acid:N-acryloylglutamic acid molar ratio solutions were compared with Fuji II control group tested at 24 h. The Fuji II control mean CFS ( $168 \pm 11$  MPa), DTS ( $13 \pm 2$  MPa), TFS ( $9 \pm 2$  MPa) and  $K_{IC}$  ( $0.20 \pm 0.04$  MNm<sup>-1.5</sup>) values were increased for the acid molar ratio modified solutions with mean CFS ( $195 \pm 11$  MPa and  $212 \pm 9$  MPa), DTS ( $22 \pm 2$  MPa and  $20 \pm 3$  MPa), TFS ( $38 \pm 4$  MPa and  $34 \pm 3$  MPa) and  $K_{IC}$  ( $0.37 \pm 0.02$  MNm<sup>-1.5</sup> and  $0.39 \pm 0.05$  MNm<sup>-1.5</sup>) values reported, respectively. A further increase in CFS, DTS, TFS and  $K_{IC}$  values of GIs prepared with the N-acryloylglutamic acid modified solutions was identified following 1 week water storage (Kao et al., 1996). However, the N-acryloylglutamic acid product yield was reported to be too low for commercial exploration (Culbertson et al., 1999). N-methacryloylglutamic acid produced a 70% increased yield compared with N-acryloylglutamic acid and was therefore proposed for the modification of acrylic acid and itaconic acid copolymers at an acrylic acid:itaconic acid:N-methacryloylglutamic acid molar

ratio of 7:3:3 (Culbertson et al., 1999; Culbertson, 2006). Cylindrical CFS (12 mm height, 6 mm diameter) and bar-shaped TFS specimens (25 mm length, 3 mm width, 3 mm thickness) were prepared by hand-mixing the modified copolymer solution with Fuji II powder (Culbertson et al., 1999). Following 1 week water storage, the CFS ( $185 \pm 9$  MPa) and TFS ( $15 \pm 1$  MPa) values of the Fuji II specimens were markedly reduced compared with the CFS ( $224 \pm 8$  MPa) and TFS ( $35 \pm 7$  MPa) values of GIs prepared from the N-methacryloylglutamic acid modified acrylic acid and itaconic acid copolymer solution (Culbertson et al., 1999).

Acrylic acid and itaconic acid copolymer solutions were modified using N-vinylpyrrolidone as a flexible spacer in the copolymer backbone at an acrylic acid:itaconic acid:N-vinylpyrrolidone molar ratio of 7:1:3 (Xie et al., 1998). The modified solutions were hand-mixed with Ketac Molar powder at a powder:liquid mixing ratio of 3.1:1 g:g to prepare bar-shaped TFS specimens (25 mm length, 2 mm width, 2 mm thickness: n=6) which were tested following 1 week water storage. N-vinylpyrrolidone modification of the acrylic acid and itaconic acid copolymer solutions highlighted a decreased mean TFS value for the Ketac Molar specimens ( $17 \pm 1$  MPa) compared with the GI specimens prepared with the N-vinylpyrrolidone modified solution ( $31 \pm 3$  MPa) (Xie et al., 1998). Acrylic acid and maleic acid copolymer solutions were modified with N-vinylpyrrolidone at acrylic acid:maleic acid:N-vinylpyrrolidone molar ratios of 8:1:1, 7:3:1, 6:4:2 and 5:5:3 (Yamazaki et al., 2005). Cylindrical CFS (6 mm height, 4 mm diameter: n=6-10), disc-shaped DTS (4 mm diameter, 2 mm thickness: n=6-10) and bar-shaped TFS (20 mm length, 2 mm width, 2 mm thickness: n=6) specimens were prepared by hand-mixing the N-vinylpyrrolidone modified acrylic acid and maleic acid copolymer solutions with Fuji IX powder at a powder:liquid mixing ratio of 3.6:1 g:g. When the CFS and DTS values of the N-vinylpyrrolidone modified molar ratio

groups (8:1:1, 7:3:1, 6:4:2 and 5:5:3) were examined and compared with the Fuji IX control group ( $273 \pm 16$  MPa and  $21 \pm 2$  MPa, respectively), no increase in mean CFS ( $277 \pm 31$  MPa,  $252 \pm 27$  MPa,  $206 \pm 33$  MPa and  $167 \pm 9$  MPa) and DTS ( $22 \pm 3$  MPa,  $19 \pm 2$  MPa,  $16 \pm 1$  MPa and  $12 \pm 2$  MPa) values were identified (Yamazaki et al., 2005), although an increase in mean TFS ( $46 \pm 7$  MPa,  $41 \pm 12$  MPa and  $40 \pm 7$  MPa) values was highlighted for the 8:1:1, 7:3:1 and 6:4:2 molar ratio groups compared with Fuji IX ( $32 \pm 11$  MPa) (Yamazaki et al., 2005).

It was proposed that altering the monomeric sequence in N-vinylpyrrolidone modified copolymers from acrylic acid:itaconic acid:N-vinylpyrrolidone to acrylic acid:N-vinylpyrrolidone:itaconic acid would allow for greater mobility of the side chains leading to enhanced ionic bond formation (Moshaverinia et al., 2008b). Acrylic acid and itaconic acid copolymer solutions were modified using N-vinylpyrrolidone at an acrylic acid:N-vinylpyrrolidone:itaconic acid molar ratio of 8:1:1 (Moshaverinia et al., 2008b). The N-vinylpyrrolidone modified solutions were hand-mixed with Fuji II powder at a powder:liquid mixing ratio of 2.7:1 g:g to prepare cylindrical CFS (6 mm height, 4 mm diameter: n=6), disc-shaped DTS (4 mm diameter, 2 mm thickness: n=6) and disc-shaped BFS (10 mm diameter, 1 mm thickness: n=6) specimens. Following 24 h water storage, a decrease in the mean CFS ( $161 \pm 12$  MPa), DTS ( $12 \pm 2$  MPa) and BFS ( $15 \pm 2$  MPa) values for Fuji II specimens were identified compared with the mean CFS ( $167 \pm 10$  MPa), DTS ( $17 \pm 3$  MPa) and BFS ( $29 \pm 3$  MPa) values of GI specimens prepared with the N-vinylpyrrolidone modified copolymer solution (Moshaverinia et al., 2008b).

N-vinylcaprolactam is a chemical analogue of N-vinylpyrrolidone with increased biocompatibility (Vihola et al., 2002; Moshaverinia et al., 2009) and was investigated for

modification of acrylic acid and itaconic acid copolymer solutions at an acrylic acid:itaconic acid:N-vinylcaprolactam molar ratio of 8:1:1 (Moshaverinia et al., 2009, 2010). The modified copolymer solutions were hand-mixed with Fuji IX powder at a powder:liquid mixing ratio of 3.6:1 g:g to prepare cylindrical CFS (6 mm height, 4 mm diameter: n=6), disc-shaped DTS (4 mm diameter, 2 mm thickness: n=6), disc-shaped BFS (10 mm diameter, 1 mm thickness: n=6), bar-shaped TFS (20 mm length, 2 mm width, 2 mm thickness: n=7) and SEN compact tension disc-shaped  $K_{IC}$  specimens (8 mm diameter, 2 mm thickness). Following water storage for 24 h and 1 week, the mean CFS ( $236 \pm 41$  MPa and  $248 \pm 36$  MPa), DTS ( $20 \pm 11$  MPa and  $24 \pm 10$  MPa), BFS ( $41 \pm 10$  MPa and  $43 \pm 12$  MPa), TFS ( $38 \pm 6$  MPa and  $45 \pm 6$  MPa) and  $K_{IC}$  ( $0.43 \pm 0.08$  MNm<sup>-1.5</sup> and  $0.47 \pm 0.09$  MNm<sup>-1.5</sup>) values of the Fuji IX control group were markedly reduced compared with the mean CFS ( $303 \pm 33$  MPa and  $319 \pm 34$  MPa), DTS ( $38 \pm 11$  MPa and  $44 \pm 8$  MPa), BFS ( $82 \pm 13$  MPa and  $85 \pm 13$  MPa), TFS ( $52 \pm 6$  MPa and  $58 \pm 6$  MPa) and  $K_{IC}$  ( $0.58 \pm 0.09$  MNm<sup>-1.5</sup> and  $0.67 \pm 0.2$  MNm<sup>-1.5</sup>) values for the GI specimens prepared with the N-vinylcaprolactam modified copolymer solutions (Moshaverinia et al., 2009, 2010).

With respect to the type of the flexible spacer chosen to link the pendant functional carboxyl groups with the polymer backbone, the copolymer:spacer molar ratio, the monomeric sequence, the chemical composition of the GI powder and the GI powder:liquid mixing ratio employed were markedly different for the studies reporting modification of the copolymer solutions (Culbertson and Kao, 1994; Kao et al., 1996; Xie et al., 1998; Culbertson et al., 1999; Yamazaki et al., 2005; Moshaverinia et al., 2008b, 2009, 2010), such that a direct comparison between the studies was not possible. Despite the claimed improvements in CFS, DTS, TFS, BFS and  $K_{IC}$  for GIs prepared with the modified copolymer solutions, commercial

exploration of GIs with these GI liquid modifications was not identified in the dental literature suggesting problems with the systems.

A review of the reinforcement strategies investigated for GIs does not leave the reader with any great deal of optimism. Despite the variously reported attempts to reinforce GIs, the reinforcement strategies could not produce GIs with mechanical properties close to dental amalgam or RBCs. Examination of the mixing and testing conditions reported by researchers investigating the reinforcement strategies for GIs revealed a wide variation in the mixing and testing conditions employed. For the GI reinforcement strategies investigated in the dental literature, the majority of investigators employed hand-mixing of GIs with the exception of two studies (Yap et al., 2002; Gu et al., 2005) that substituted a portion of the GI powder from encapsulated Fuji IX<sub>GP</sub> with hydroxyapatite, prior to mechanical mixing at 3.6:1 g:g. The use of encapsulated GIs when investigating a reinforcement strategy ignored the influence of the initial viscosity of the GI mix which may have not been optimised for the hydroxyapatite substituted powder, thereby failing to provide adequate information on the reinforcement strategy to the investigator.

#### **1.4.8 Hand-mixing GIs**

For hand-mixed GIs, the relative proportions of powder and liquid constituent required to produce the manufacturer's recommended powder:liquid mixing ratio are routinely dispensed using the measuring systems provided by the manufacturer, namely powder scoops and liquid dropper bottles, respectively (Mount, 1994). The volume of powder dispensed using a scoop can vary depending on the powder packing density (Billington et al., 1990; Fleming et al., 2003) while the volume of a drop of liquid dispensed depends on the angulation that the dropper bottle is held at and the pressure applied to squeeze out the drop (Eames et al., 1977).



Hand-mixed GIs tested in the laboratory are therefore exposed to variations in the powder:liquid mixing ratios produced owing to the non-standardised nature of the product delivery systems. Discrepancies in the accurate determination of the GI powder and liquid constituents are evident in the dental literature in the reporting of the reinforcement strategies for GIs. Investigators have employed the scoop and dropper bottle provided by the manufacturer (Yli-Urpo et al., 2005) although the majority of investigators (Sced and Wilson, 1980; Simmons, 1983; Miller et al., 1984; McLean and Gasser, 1985; Walls et al., 1987; El Mallakh et al., 1987; Nakajima et al., 1989; Kerby and Bleiholder, 1991; Williams et al., 1992; Culbertson and Kao, 1994; Kao et al., 1996; Xie et al., 1998; Culbertson et al., 1999; Kobayashi et al., 2000; Lucas et al., 2003; Yamazaki et al., 2005; Moshaverinia et al., 2008a,b, 2009, 2010) failed to provide adequate information on the powder and liquid measurement systems employed. Therefore, it remains uncertain as to whether the investigators used the non-standardised powder scoops and liquid dropper bottles provided by the manufacturer or a weighing balance for accurate dispensation of the GI powder and liquid constituents. The production of the optimum powder:liquid mixing ratio could have only been ensured by the use of a weighing balance.

#### **1.4.9 Testing methodology**

The CFS test was identified as the most commonly employed testing methodology when investigating GI reinforcement by powder additive substitution (Miller et al., 1984; El Mallakh et al., 1987; Walls et al., 1987; Nakajima et al., 1989; Kerby and Bleiholder, 1991; Williams et al., 1992; Nicholson et al., 1993; Yap et al., 2002; Gu et al., 2005; Yli-Urpo et al., 2005; Dowling et al., 2006, 2014; Moshaverinia et al., 2008a; Elsaka et al., 2011) or liquid modification (Culbertson and Kao, 1994; Kao et al., 1996; Culbertson et al., 1999; Yamazaki et al., 2005; Moshaverinia et al., 2008b, 2009, 2010). Other less commonly

employed mechanical testing methodologies included the DTS (Kerby and Bleiholder, 1991; Williams et al., 1992; Kao et al., 1996; Kobayashi et al., 2000; Yamazaki et al., 2005; Moshaverinia et al., 2008a,b, 2009), TFS (Sced and Wilson, 1980; Walls et al., 1987; Nakajima et al., 1989; Culbertson and Kao, 1994; Kao et al., 1996; Xie et al., 1998; Kobayashi et al., 2000; Yamazaki et al., 2005; Moshaverinia et al., 2010; Elsaka et al., 2011), BFS (Moshaverinia et al., 2008a,b, 2009) and  $K_{IC}$  (Kao et al., 1996; Lucas et al., 2003; Moshaverinia et al., 2010) protocols. Investigators have suggested that loading during masticatory function results in stressing patterns analogous to compression during CFS testing (Yettram et al., 1976) such that a high CFS was advocated to tolerate the masticatory forces routinely encountered in the mouth (White and Yu, 1993). Therefore, ISO 9917-1:2007 specifies the CFS test as the strength test of choice for evaluating GIs, although the poor control over the mixing and testing conditions identified in the studies employing the CFS testing methodology prevented a valid comparison between the studies.

#### **1.4.10 The way forward**

A realisation of the need for a definitive study to identify a valid (Darvell, 1990) and reliable (McCabe et al., 1990) mechanical testing protocol for GIs was championed by Fleming et al. (2012) in a study entitled, 'The crushing truth about glass-ionomer restoratives: exposing the standard of the standard'. In a follow-up study entitled 'Improving the standard of the standard for glass-ionomers: an alternative to the compressive fracture strength test for consideration?', CFS, TFS and BFS testing protocols were investigated under standardised ISO 9917-1:2007 conditions (padding material (filter paper), loading rate (1 mm/min), environment (wet), storage time (24 h)) using groups of 40 specimens (Dowling et al., 2012). To eliminate dispensing errors with the powder and liquid constituents (Billington et al., 1990; Fleming et al., 2003) and to standardise the mixing regime, three encapsulated

commercial GI restoratives were investigated (Dowling et al., 2012). Interestingly, the TFS and BFS testing methodologies failed to discriminate between the encapsulated GI products, despite the GI products being supplied by different manufacturers with different glass compositions, liquid compositions and powder:liquid mixing ratios while differences in CFS values were evident. One significant oversight in these two studies (Dowling et al., 2012; Fleming et al., 2012) was the employment of encapsulated GI restoratives. If one was charged with the task of delivering a novel reinforced GI restorative, the initial and fundamental step would involve the determination of the optimum powder:liquid mixing ratio by hand-mixing the GI liquid with varying GI powder contents and performing preliminary mechanical tests. Resistance to compressive, tensile and shear forces under loading during mastication is provided by the reinforcing glass filler component rather than the weaker polyacrylate matrix (Xie et al., 2000) such that maximising the glass filler powder particles in the set GI will ensure optimum resistance to fracture in service (Brune and Smith, 1982; Wilson and McLean, 1988b; Hatton and Brook, 1992; Xie et al., 2000). Therefore, a deterioration in the mechanical properties would be expected on reducing the powder content from the optimum value specified by the manufacturer. The mechanical testing protocol of choice when investigating novel reinforced GI restoratives would be required to be discriminatory between the different powder:liquid mixing ratios employed by identifying a linear deterioration in the property being measured when the powder content is reduced from the optimum value - something that could not be elucidated from the encapsulated GI restoratives used previously (Dowling et al., 2012; Fleming et al., 2012). The aim of the current investigation was therefore to identify a valid, reliable and discriminatory mechanical testing methodology to act as a performance indicator for GIs.

## 2. MATERIALS AND METHODS SUPPLEMENTAL MATERIAL

### 2.1 RAW MATERIALS

#### 2.1.1 Encapsulated GI restoratives

Three encapsulated posterior GI restoratives, namely Chemfil Rock, Fuji IX<sub>GP</sub> Fast and Ionofil Molar AC were investigated.

##### Chemfil Rock

The encapsulated posterior GI restorative Chemfil Rock (Lot 1109004048, 1208000039, shade A3) was supplied by Dentsply DeTrey (Konstanz, Germany). Each Chemfil Rock capsule was suggested by the manufacturer to contain 0.442 g of a zinc calcium fluorophosphoaluminosilicate glass powder, however, the relative proportions of the glass elements were not reported. The glass powder was also reported to contain pigments of iron oxide and titanium dioxide in addition to polycarboxylic acid, although the relative proportions of the pigments and polycarboxylic acid in the powder were not stated (Product specification). The liquid component in each Chemfil Rock capsule was detailed to consist of 0.12 ml of polycarboxylic and tartaric acids (Product specification). The relative proportions, molecular weight and concentration of the polycarboxylic and tartaric acids in solution were not disclosed by the manufacturer. The powder:liquid mixing ratio maintained in each Chemfil Rock capsule was stated by the manufacturer to be 3.7:1 g:ml. It was also claimed by the manufacturer that 0.1 ml of the GI restorative mix was dispensable from each capsule after mechanical mixing.

### Fuji IX<sub>GP</sub> Fast

Fuji IX<sub>GP</sub> Fast capsules (Lot 1011181, 1305171, shade A2) were supplied by GC Europe (Leuven, Belgium). The powder component in each Fuji IX<sub>GP</sub> Fast capsule was reported by the manufacturer to consist of 0.4 g of a strontium fluoroaluminosilicate glass (Product specification). The relative proportions of the glass constituents were not detailed by the manufacturer. It was stated by the manufacturer that the liquid solution in each Fuji IX<sub>GP</sub> Fast capsule contained 0.09 ml of polyacrylic acid but the molecular weight and concentration of the polyacrylic acid were not disclosed by the manufacturer (Product specification). The Fuji IX<sub>GP</sub> Fast capsules were suggested by the manufacturer to have a powder:liquid mixing ratio of 4.4:1 g:ml. In addition, the manufacturer claimed that a minimum of 0.14 ml of the GI mix was extrudable from each Fuji IX<sub>GP</sub> Fast capsule after mechanical mixing.

### Ionofil Molar AC

Ionofil Molar AC (Lot 1105302, 1228502, shade A3) was supplied by Voco GmbH (Cuxhaven, Germany). According to the manufacturer, the powder component in each Ionofil Molar AC capsule consisted of 0.43 g of a strontium fluoroaluminosilicate glass, although the proportions of the glass constituents were not disclosed. In addition, the GI powder was stated by the manufacturer to contain pigments, polyacrylic acid and tartaric acid (Product specification). The manufacturer did not disclose the relative proportions of the glass, pigments, polyacrylic acid and tartaric acid in the powder. The liquid element of Ionofil Molar AC was stated by the manufacturer to consist of 0.125 g of polyacrylic acid, although the manufacturer failed to report the molecular weight and concentration of the polyacrylic acid in solution (Product specification). The powder:liquid mixing ratio reported by the manufacturer for each Ionofil Molar AC capsule was 3.4:1 g:g. The manufacturer highlighted

that each Ionofil Molar AC capsule dispensed 0.15 ml of the GI restorative mix after mechanical mixing.

### **2.1.2 Hand-mixed GI restorative**

The hand-mixed GI restorative used was Ionofil Molar which was supplied by Voco GmbH in the form of two separate components, a powder (Lot V50335, shade A2) and a liquid (Lot V50375). The manufacturer claimed that the powder consisted of a strontium fluoroaluminosilicate glass, although the proportions of the glass elements were not disclosed. The powder was also reported by the manufacturer to contain pigments, polyacrylic acid and tartaric acid (Product specification). However, the relative proportions of the glass, pigments, polyacrylic acid and tartaric acid in the powder were not provided. The hand-mixed liquid was stated by the manufacturer to be composed of an aqueous solution of polyacrylic acid (Product specification). The molecular weight and concentration of the polyacrylic acid in solution were not divulged by the manufacturer. The optimum powder:liquid mixing ratio recommended by the manufacturer for the hand-mixed Ionofil Molar was 4:1 g:g.

## **2.2 GI RESTORATIVE PREPARATION**

All GI restorative preparation was performed in a temperature ( $21 \pm 1^\circ\text{C}$ ) and humidity controlled laboratory.

### **2.2.1 Encapsulated GI restoratives**

For the encapsulated GI restoratives investigated, the powder and liquid components were contained within individual compartments of the respective capsules and separated by a

membrane. To initiate the setting reaction, it was necessary to rupture the membrane separating the GI powder and liquid constituents prior to mechanical mixing which allowed contact between the GI powder and liquid in a process called ‘activation’ of the GI capsule. Each encapsulated GI product required a different activation procedure but prior to activation, each GI capsule was mandated to be tapped against a hard surface of the laboratory bench to loosen the powder within the capsule.

### Chemfil Rock

The Chemfil Rock capsules were activated by vertically holding the capsule against the laboratory bench with the capsule nozzle facing upwards, followed by manually pressing the plunger to the maximum allowable depth (Figure 2.1a). Pushing the capsule plunger into the body of the capsule resulted in the displacement of the liquid component into the powder chamber of the capsule. Following activation, the Chemfil Rock capsules were placed into the holder of a Capmix mechanical mixing machine (3M ESPE). The capsules were vibratory mixed at a mixing speed of 4300 oscillations per minute which was within the range of the mixing speed specified by the manufacturer (4000-4500 oscillations per minute) for Chemfil Rock (Product specification). In line with the manufacturer’s instructions, Chemfil Rock capsules were mechanically mixed for 15 s (Product specification) and following mixing, the capsules were placed in a ‘capsule extruder’ (Capsule Extruder 2; Dentsply DeTrey) to facilitate extrusion of the GI mix (Figure 2.1b).

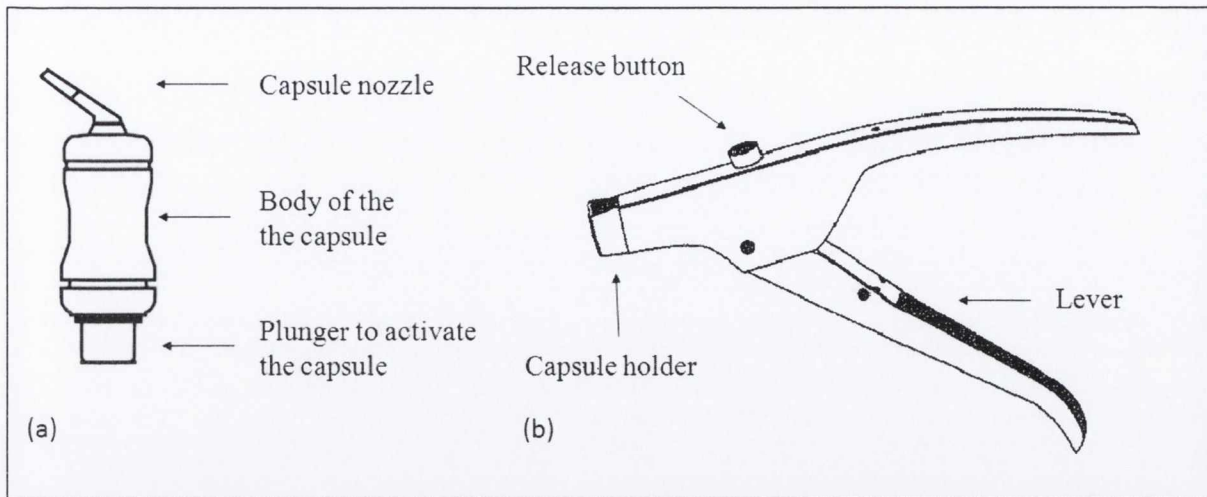


**Figure 2.1. Schematic representation of (a) the capsule design for Chemfil Rock highlighting the capsule plunger which was pressed to activate the capsule and (b) the capsule extruder used to facilitate extrusion of the mechanically mixed GI.**

#### Fuji IX<sub>GP</sub> Fast

For the Fuji IX<sub>GP</sub> Fast capsules, activation was achieved by pushing the plunger until it was level with the main body of the capsule (Figure 2.2a), followed by placing the capsule onto a ‘capsule applicator’ (Capsule Applicator II; GC Corporation) and clicking the trigger once (Figure 2.2b). As a result of the trigger click, the liquid was transferred into the powder compartment of the capsule. The activated capsule was then removed from the capsule applicator and placed into the holder of the Capmix mechanical mixing machine. Following the manufacturer’s instructions, the Fuji IX<sub>GP</sub> Fast capsules were vibratory mixed at 4300 oscillations per minute for 10 s (Product specification). Following mixing, the Fuji IX<sub>GP</sub> Fast capsules were remounted onto the capsule applicator and the trigger clicked twice to facilitate dispensation of the GI mix (Figure 2.2b).



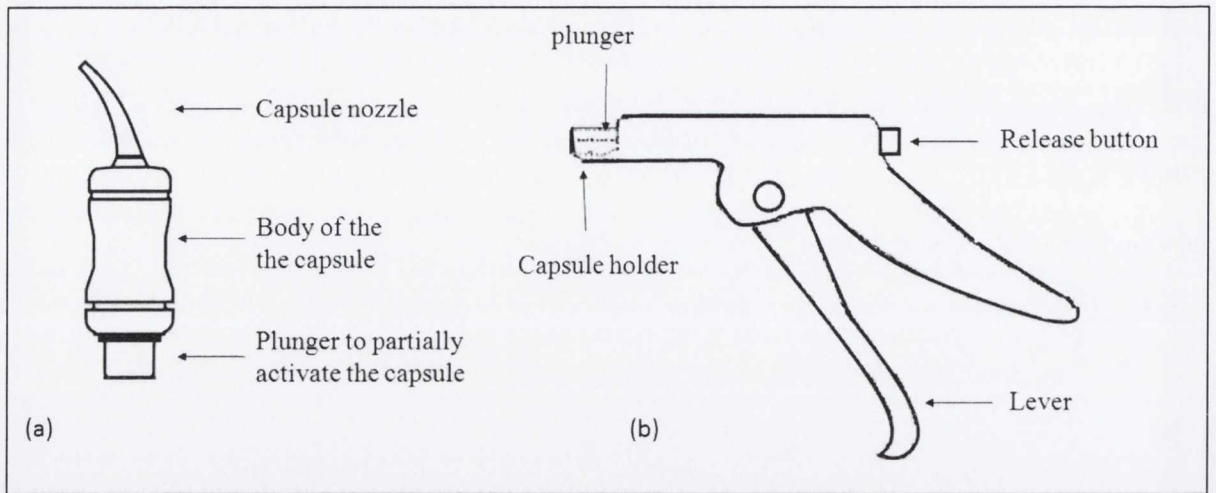


**Figure 2.2. Schematic representation of (a) the capsule design for Fuji IX<sub>GP</sub> Fast showing the capsule plunger which was pressed to partially activate the capsule and (b) the capsule applicator used for complete activation of the capsule by clicking the lever once and for extrusion of the GI mix following mechanical mixing.**

#### Ionofil Molar AC

The Ionofil Molar AC capsules were activated by placing the capsule in a ‘capsule activator’ (AC Activator; Voco GmbH) which was a purpose-designed device for activation of Ionofil Molar AC capsules (Figure 2.3a). The capsule activator consisted of a capsule holder attached to a metal base, a lever placed adjacent to the capsule holder and a metal pin fixed to the metal base to limit the movement of the lever (Figure 2.3b). The capsules were placed into the capsule holder of the activator with the nozzle of the capsule facing upwards and a clamp on the side of the capsule facing the activator lever which was compressed until it touched the metal stop for 2 s (Figure 2.3b). The compression of the lever against the clamp on the capsule pushed the liquid from a sachet placed underneath the clamp into the powder chamber of the capsule. The activated capsules were removed from the activator and placed into the holder of the Capmix mechanical mixing machine. According to the manufacturer’s instructions, Ionofil Molar AC capsules were vibratory mixed for 10 s at a mixing speed of 4300 oscillations per minute which was within the range of that recommended by the manufacturer (4000-4500 oscillations per minute) (Product specification). Following mixing,

the capsules were removed from the Capmix mechanical mixer and placed into a ‘capsule applicator’ (Applicator-AC type 1; Voco GmbH) (Figure 2.3c). Prior to extrusion of the GI mix, the Ionofil Molar AC capsules required ‘opening’ of the capsule by twisting the capsule cap a half turn (Figure 2.3a).

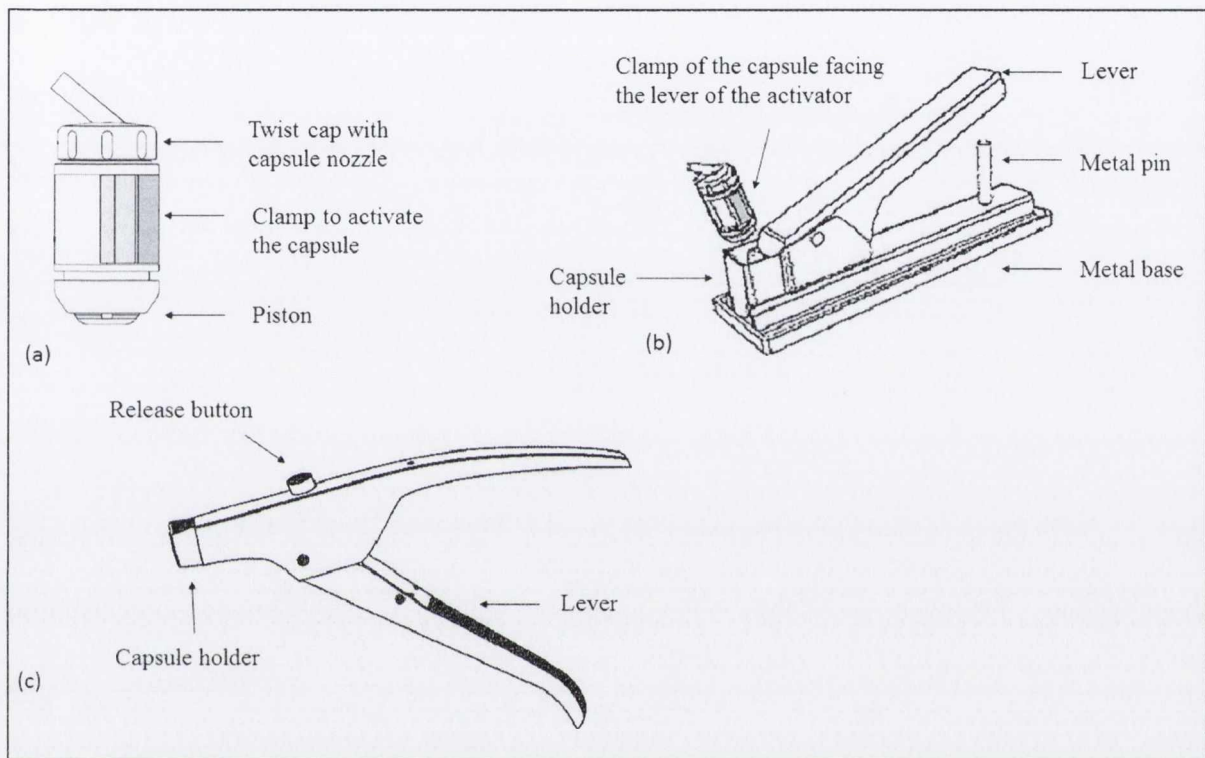


**Figure 2.3. Schematic representation of (a) the capsule design for Ionofil Molar AC identifying the clamp located on the side of the capsule which was pressed using (b) the capsule activator. The capsule was placed into the capsule holder of the activator such that the clamp on the capsule faced the lever of the activator and following mechanical mixing the GI mix was extruded using (c) the capsule applicator.**

### 2.2.2 Hand-mixed GI restorative

For the hand-mixed Ionofil Molar GI restorative, the manufacturer’s recommended powder:liquid mixing ratio (4:1 g:g) was the control group for all experimentation. In line with the manufacturer’s instructions, the powder container was shaken well to fluff the GI powder prior to dispensation. A weighing boat was placed on an electronic precision balance accurate to 0.001 g (Sartorius Expert, Sartorius AG, Goettingen, Germany) and the scale was

set to zero prior to dispensation of the GI powder. The appropriate amount of the GI powder was weighed onto the weigh boat which was then removed from the balance. A glass mixing slab was placed on the balance which was tared to reset the scale to zero and the appropriate amount of the GI liquid was dispensed onto one end of the glass slab using an adjustable 200  $\mu\text{l}$  pipette (Gilson, Middleton, WI, USA). The glass slab was subsequently removed from the balance and the GI powder was transferred from the weigh boat to the other end of the glass slab. The GI powder was divided into two approximately equal halves and a stainless-steel mixing spatula was used to incorporate the first half of the GI powder into all of the GI liquid within 20 s. In accordance with the manufacturer's instructions, the second half of the GI powder was then introduced into the GI mix and manipulated for an additional 20 s to ensure a total mixing time of 40 s.

Hand-mixed GIs were prepared with reduced powder content from that recommended by the manufacturer for a constant weight of liquid to simulate the distribution of powder:liquid mixing ratios routinely employed clinically and beyond (Mount and Makinson, 1978a; Billington et al., 1990). The GI powder content for each powder:liquid mixing ratio group investigated was reduced in 10% increments (by weight) for a constant weight of liquid, to a minimum of 20% of the manufacturer's powder:liquid mixing ratio. To identify the corresponding reduction in the volume of the GI powder in each powder:liquid mixing ratio group investigated, the GI powder volume percentages were calculated using Equation 2.1.

$$V = \frac{m}{\rho}$$

Equation 2.1

where  $V$ ,  $m$ , and  $\rho$  are the volume, mass and density of the GI powder, respectively. The powder:liquid mixing ratio groups investigated in the current study were plotted and

discussed in terms of weight percentage groups for comparison purposes with the GI studies identified in the dental literature (Mount and Makinson, 1978a; Billington et al., 1990; Fleming et al., 2003; Dowling and Fleming, 2008, 2009). The hand-mixed GI powder:liquid mixing ratio groups and the corresponding GI powder (wt% and vol%) for each group investigated are highlighted in Table 2.1. The hand-mixed GI powder and liquid components for the varying powder:liquid mixing ratio groups investigated (n=9) were dispensed and mixed in accordance with the manufacturer's instructions.

**Table 2.1. The hand-mixed GI powder:liquid mixing ratios and the corresponding weight and volume percentages for each GI powder:liquid mixing ratio group investigated.**

<b>Powder:liquid mixing ratio (g:g)</b>	<b>Weight% of the manufacturer's recommended powder content</b>	<b>Volume% of the manufacturer's recommended powder content</b>
4:1	100	64
3.6:1	90	62
3.2:1	80	59
2.8:1	70	56
2.4:1	60	52
2:1	50	47
1.6:1	40	42
1.2:1	30	35
0.8:1	20	26

## **2.3 MECHANICAL TESTING PROTOCOLS**

### **2.3.1 COMPRESSIVE FRACTURE STRENGTH TEST**

#### **2.3.1.1 Specimen Preparation**

The hand-mixed GI restorative cylindrical specimens ( $6.0 \pm 0.1$  mm height and  $4.0 \pm 0.1$  mm diameter) were prepared for CFS testing in accordance with ISO 9917-1:2007 (ISO 9917-1:2007) using a polytetrafluoroethylene (PTFE) split-mould assembly. The PTFE split-mould

assembly consisted of a PTFE split-mould resting on a PTFE base, a 4 mm diameter locating pin and two PTFE sliding wedges (Figure 2.4).

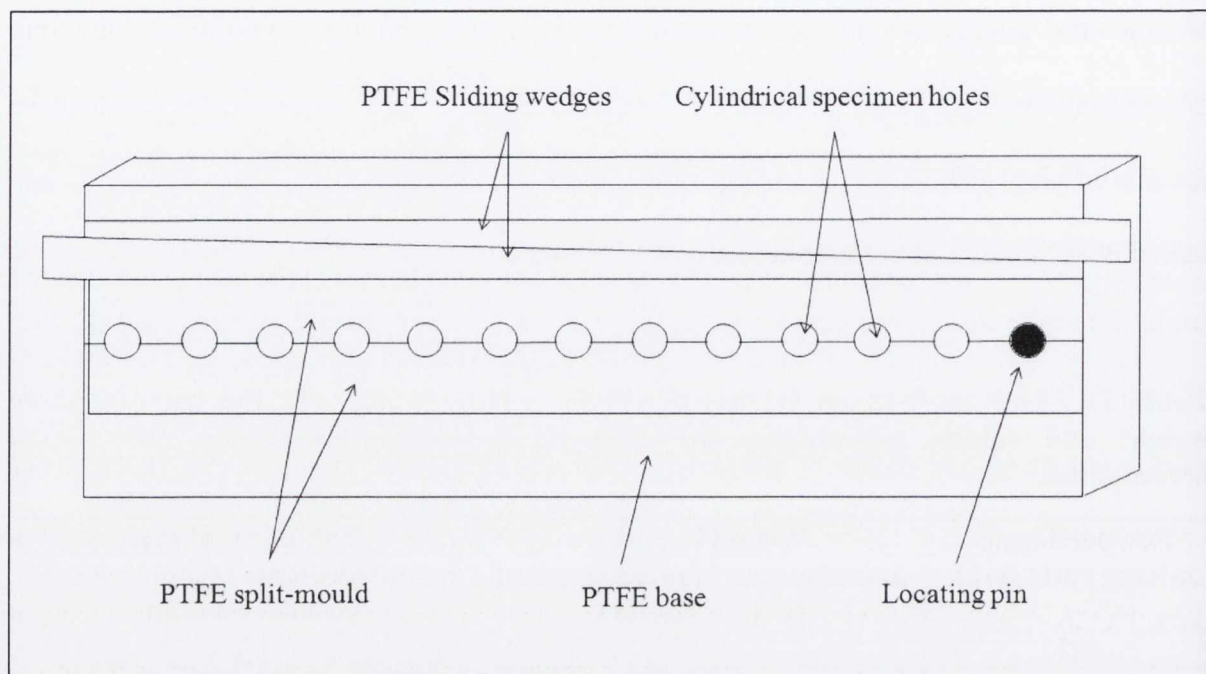


**Figure 2.4. Schematic representation of the polytetrafluoroethylene (PTFE) split-mould assembly employed to manufacture cylindrical GI specimens for compressive fracture strength (CFS) testing. The two halves of the split-mould were aligned on top of the PTFE base using the locating pin and the PTFE wedges inserted to one side of the split-mould to ensure equal pressure was applied along the length of the split-mould.**

The PTFE base was covered with an acetate strip to prevent specimen adhesion to the base of the mould. The two halves of the split-mould were assembled onto the acetate covered base and aligned by inserting the locating pin into the first hole of the split-mould. When the two halves of the split-mould were assembled, the split-mould was capable of holding twelve cylindrical specimens (Figure 2.4). Following alignment of the split-mould, the PTFE wedges were fitted to one side of the split-mould to ensure equal pressure was applied along the length of the split-mould (Figure 2.4).

To prepare the CFS specimens, the hand-mixed GI was transferred to the split-mould within 60 s of the completion of mixing using the stainless-steel mixing spatula. To minimise the introduction of air bubbles into the specimens, the largest convenient portion of the mixed GI was conveyed to one side of an individual hole in the split-mould and allowed to flow into the mould (Fleming et al., 1999). Each hole in the split-mould was filled sequentially from the side of the locating pin towards the opposite side of the split-mould. The filled holes in the split-mould were covered with an acetate strip and a 1 kg mass applied on top using a glass slab. The split-mould assembly was clamped using a G-clamp such that equal pressure was applied to the split-mould to ensure parallelism of specimen ends for uniform specimen contact with the loading platens of the testing apparatus (Lloyd and Mitchell, 1984). Following clamping, the split-mould assembly was transferred to a water-bath maintained at  $37 \pm 1^\circ\text{C}$  for 1 h. The specimen fabrication procedure was repeated to prepare two batches of four specimens at each specimen preparation interval.

Following 1 h conditioning in the water-bath, the split-mould assembly was removed and the clamps opened. The split-mould was disassembled by removing the sliding wedges, whereby disassembly of the split-mould resulted in demoulding of the cylindrical specimens which were visually inspected for defects such as pores and chipped edges. Specimens that were free of defects on visual inspection were numbered in accordance with the sequence of manufacture. The residual flash was removed through hand-lapping using P600 silicon carbide abrasive paper (Buehler, Lake Bluff, IL, USA) under water lubrication. The cylindrical specimens were stored in glass containers filled with 50 ml of distilled water and transferred to an incubator (Climate Cabinet, Firlabo, Meyzieu, France) maintained at  $37 \pm 1^\circ\text{C}$  for an additional 23 h prior to testing.

A sufficient quantity of the GI restorative was hand-mixed to prepare four CFS specimens from one GI mix. The preparation of four CFS specimens from one GI mix at the manufacturer's recommended powder:liquid mixing ratio (4:1 g:g) required hand-mixing 0.6 g of the GI powder with a corresponding 0.15 g of the GI liquid. To prepare the powder:liquid mixing ratio groups with 90, 80, 70, 60, 50, 40, 30 and 20% of the manufacturer's recommended powder content, the powder content was reduced from 0.6 g to 0.54, 0.48, 0.42, 0.36, 0.3, 0.24, 0.18 and 0.12 g, respectively, for the 0.15 g of GI liquid (Table 2.2).

**Table 2.2. The powder:liquid mixing ratio groups, weight percentages of the manufacturer's recommended powder content and the corresponding weights of the GI powder and liquid employed for the preparation of the cylindrical compressive fracture strength (CFS) specimens.**

<b>Powder:liquid mixing ratio (g:g)</b>	<b>Weight% of the manufacturer's recommended powder content</b>	<b>Weight of powder:weight of liquid (g:g) for CFS specimen preparation</b>
4:1	100	0.6:0.15
3.6:1	90	0.54:0.15
3.2:1	80	0.48:0.15
2.8:1	70	0.42:0.15
2.4:1	60	0.36:0.15
2:1	50	0.3:0.15
1.6:1	40	0.24:0.15
1.2:1	30	0.18:0.15
0.8:1	20	0.12:0.15

### 2.3.1.2 Compressive fracture strength testing procedure

Following 23 h water storage, the CFS specimens were removed from the glass container and the mean diameter of each cylindrical specimen was determined from three points along the long axis of the specimen using a digital micrometer screw gauge reading to 1  $\mu\text{m}$  (Mitutoyo, Kawasaki, Japan). In accordance with ISO 9917-1:2007, a piece of filter paper (Whatman No. 1, Whatman International Ltd., Maidstone, England) was applied to the loading platens of the universal testing machine (Instron Model 5565, High Wycombe, England) prior to testing to accommodate for non-parallel specimen ends. In addition, the filter paper was soaked in water prior to application to the loading platens to ensure a wet testing environment (ISO 9917-1:2007). The cylindrical specimens were placed vertically on the loading platen of the testing apparatus on top of the wet filter paper and a compressive load was applied to the long axis of the specimens at a loading rate of 1 mm/min (Figure 2.5). ISO 9917-1:2007 advocates the use of compressive loading rates ranging from 0.45 mm/min to 1.05 mm/min, however, to allow for comparisons with Dowling et al.'s (2012) study who investigated the CFS of encapsulated GI restoratives under controlled conditions, the cylindrical specimens were loaded at the same loading rate (1 mm/min) employed by Dowling et al. (2012). The maximum load-to-failure was recorded and the CFS calculated for each cylindrical specimen using Equation 2.2 (ISO 9917-1:2007).

$$CFS = \frac{4P}{\pi d^2}$$

Equation 2.2

where  $P$  was the load-to-failure (N) and  $d$  the mean specimen diameter (mm).



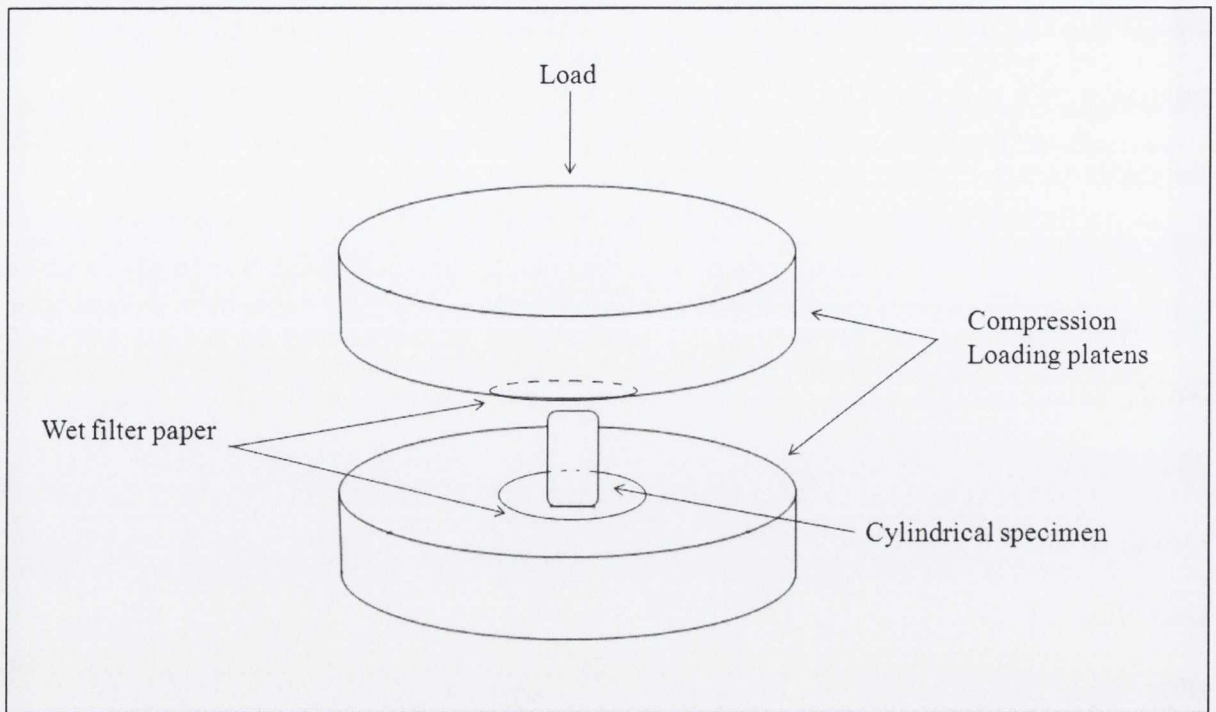


**Figure 2.5. Schematic representation of the compressive fracture strength (CFS) testing apparatus identifying the application of a piece of wet filter paper to the compression loading platens. The cylindrical CFS specimens were placed vertically on the compression loading platen and a load applied along the long axis of the cylinder.**

Strength is not an intrinsic material property such that the height and diameter of the cylindrical specimen influence the maximum load-to-failure which in turn influences the CFS value recorded. Cylindrical specimens with increased specimen dimensions have an increased probability of containing crack initiating defects which would reduce the CFS value recorded (Ritter, 1995). The compressive modulus (CM) is an intrinsic material property which is independent of specimen dimensions and is calculated from the initial linear segment of the stress-strain plot generated for cylindrical specimens loaded under compression. In the dental literature, the CM value was identified to be more sensitive to highlighting the influence of powder content variations for hand-mixed GI restoratives when compared with the CFS value (Dowling and Fleming, 2008, 2009). Therefore, the CM was determined for each cylindrical specimen by calculating the slope of the initial linear segment of the stress-strain plot (Figure 2.6).

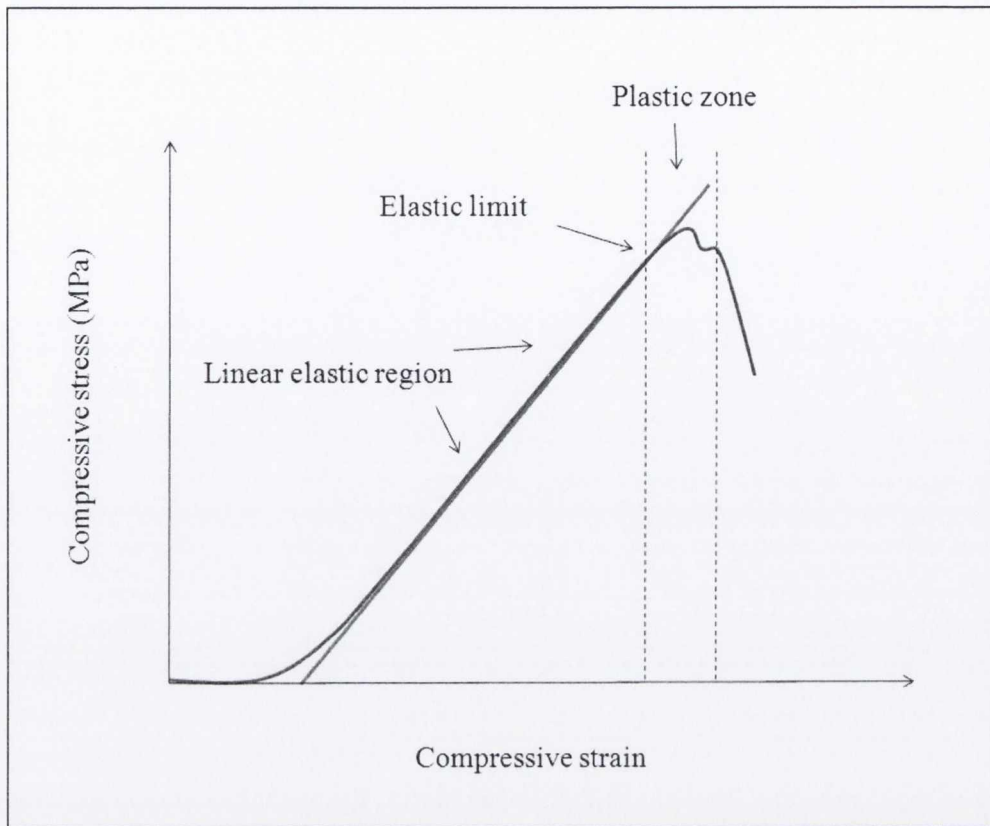


**Figure 2.6.** Schematic representation of the rate of change of compressive strain as a function of compressive stress for a cylindrical GI specimen under compressive load identifying the linear elastic region, elastic limit and plastic zone prior to fracture. The compressive modulus was calculated from the slope of the initial linear segment of the stress-strain plot for each individual compressive fracture strength (CFS) specimen.

### 2.3.2 THREE-POINT FLEXURE TEST

#### 2.3.2.1 Specimen Preparation

The hand-mixed GI restorative bar-shaped specimens ( $25.0 \pm 0.1$  mm length,  $2.0 \pm 0.1$  mm width and  $2.0 \pm 0.1$  mm thickness) were prepared for TFS testing using open-ended knife-edged PTFE moulds (Dowling et al., 2012) (Figure 2.7a). The hand-mixed GI was transferred to the PTFE mould within 60 s of completion of mixing and condensed along the length of the mould using the stainless-steel mixing spatula. The open-ended design of the PTFE mould facilitated flow of the hand-mixed GI into the mould, thereby minimising air entrapment (Musanje et al., 2001).

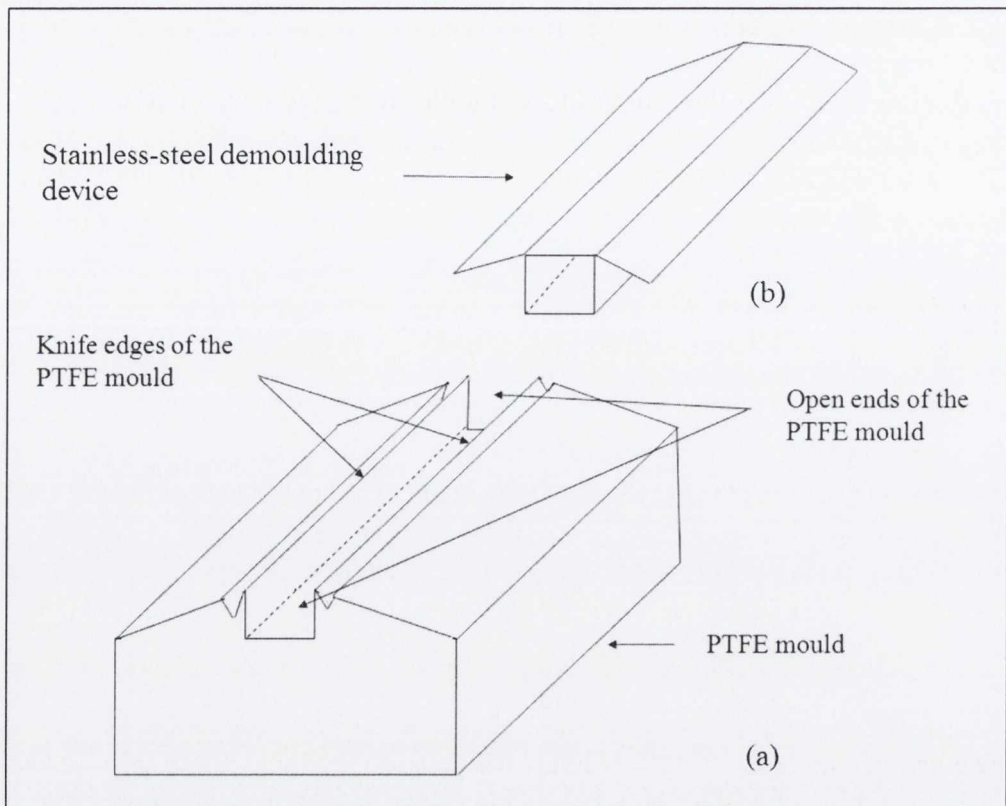


**Figure 2.7. Schematic representation of (a) the open-ended knife-edged polytetrafluoroethylene (PTFE) mould employed to manufacture bar-shaped three-point flexure specimens. The specimens were demoulded using (b) a customised stainless-steel demoulding device which was inserted into one end of the mould and gently pressed against the specimen end. Sliding the demoulding device along the length of mould facilitated specimen removal from the opposite end of the mould.**

The filled mould was covered with an acetate strip and a 1 kg mass applied to the top surface using a glass slab to ensure consistent packing of the hand-mixed GI into the mould. To ensure equal pressure was applied along the length of the mould, the filled mould was clamped using a G-clamp and the clamped assembly was transferred to the water-bath maintained at  $37 \pm 1^\circ\text{C}$  for 1 h. Individual batches of four specimens were prepared at each specimen preparation interval by repeating the specimen fabrication procedure.

Following 1 h conditioning, the clamped PTFE moulds were removed from the water-bath, the clamps opened and the bar-shaped specimens demoulded using a customised stainless-steel demoulding device (Figure 2.7b). The demoulding device was inserted into one end of

the open-ended PTFE mould and gently pressed against the specimen end, such that sliding the demoulding device along the length of the mould instigated specimen removal from the opposite end of the open-ended PTFE mould (Figure 2.7a). The knife-edge design of the PTFE mould facilitated separation of the flash produced from surplus material overflow (Musanje et al., 2001). Any remaining excess flash was removed through hand-lapping on the P600 silicon carbide abrasive paper using water as a lubricant. The bar-shaped specimens were visually inspected for defects or porosity inclusions and the specimens without visible defects were numbered in accordance with the sequence of manufacture, placed into 50 ml of distilled water and transferred to the incubator maintained at  $37 \pm 1^\circ\text{C}$  for 23 h.

To produce an adequate amount of the GI mix for the preparation of one bar-shaped specimen at the manufacturer's recommended powder:liquid mixing ratio (4:1 g:g), 0.3 g of the GI powder and a corresponding 0.075 g of the GI liquid were required. To prepare the powder:liquid mixing ratio groups with 90, 80, 70, 60, 50, 40, 30 and 20% powder content, the manufacturer's recommended powder content was reduced from 0.3 g to 0.27, 0.24, 0.21, 0.18, 0.15, 0.12, 0.09 and 0.06 g, respectively, for the 0.075 g of GI liquid (Table 2.3).

**Table 2.3.** The powder:liquid mixing ratio groups, weight percentages of the manufacturer’s recommended powder content and the corresponding weights of the GI powder and liquid employed for the preparation of the bar-shaped three-point flexure specimens.

<b>Powder:liquid mixing ratio (g:g)</b>	<b>Weight% of the manufacturer’s recommended powder content</b>	<b>Weight of powder:weight of liquid (g:g) for TFS specimen preparation</b>
4:1	100	0.3:0.075
3.6:1	90	0.27:0.075
3.2:1	80	0.24:0.075
2.8:1	70	0.21:0.075
2.4:1	60	0.18:0.075
2:1	50	0.15:0.075
1.6:1	40	0.12:0.075
1.2:1	30	0.09:0.075
0.8:1	20	0.06:0.075

### **2.3.2.2 Three-point flexure testing procedure**

The bar-shaped specimens were loaded in a standard three-point flexure test assembly using the universal testing machine (ISO 4049:2000). The three-point flexure test assembly consisted of a central loading indenter and two point supports separated by a loading span of 20 mm (Figure 2.8). The bar-shaped specimens were placed horizontally on the two point supports and positioned in the centre of the test jig (Figure 2.8).

Load was applied through the indenter to the centre of the bar-shaped specimen at a crosshead speed of 1 mm/min and the maximum load-to-failure was recorded. Following fracture, the width and thickness of the two fracture fragments were measured at the fracture surface using the micrometer screw gauge and the TFS of each bar-shaped specimen was calculated using Equation 2.3 (ISO 4049:2000).

$$TFS = \frac{3PL}{2bh^2}$$

Equation 2.3

where  $P$  was the load-to-failure (N),  $L$  the span between the two point supports (20 mm),  $b$  the specimen width (mm) and  $h$  the specimen thickness (mm).

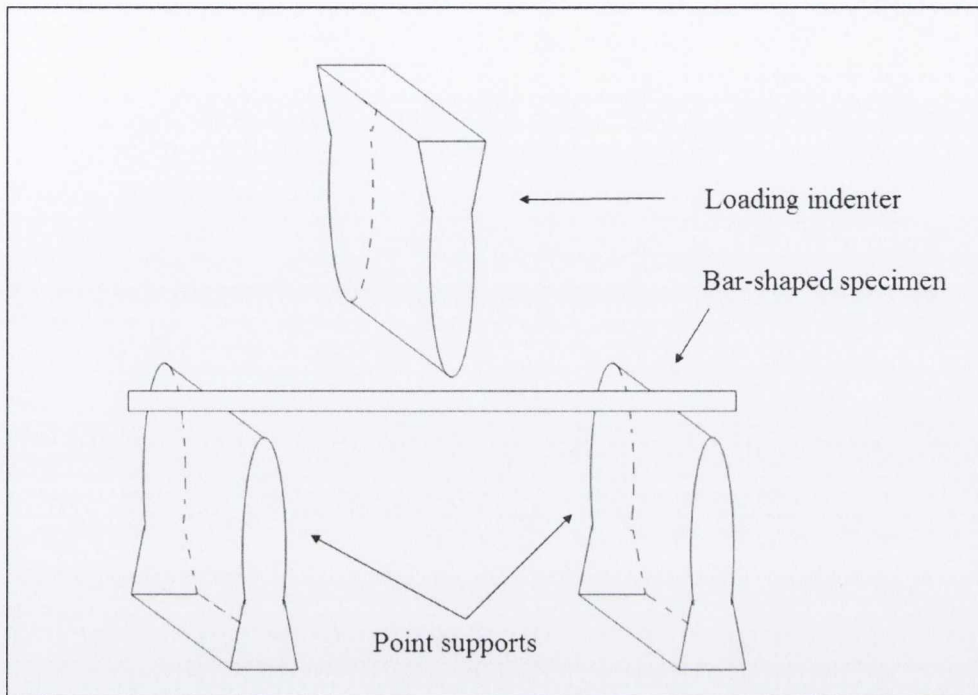


**Figure 2.8. Schematic representation of the three-point flexure test assembly highlighting a bar-shaped three-point flexure specimen resting on top of two point supports. Load was applied through the indenter in the central region of the bar-shaped specimen and the maximum load-to-failure recorded.**

The three-point flexure modulus (TFM) is an intrinsic material property capable of reproducing the internal structure of the material and any association with the neighbouring atoms (Braem, 1999). The TFM information is contained within the load-to-failure and specimen deflection data of bar-shaped specimens loaded in a three-point flexure test assembly and has been highlighted in the dental literature to be more sensitive to powder content variations for a hand-mixed GI restorative when compared with the TFS (Bonifacio et al., 2013). Therefore, the TFM was calculated for each bar-shaped specimen following loading in a three-point flexure test assembly using Equation 2.4 (ISO 4049:2000).

$$TFM = \left( \frac{\Delta P}{\Delta D} \right) \frac{L^3}{4bh^3}$$

Equation 2.4

where  $\Delta P/\Delta D$  was the gradient of the steepest linear portion of the load-deflection curve generated for each bar-shaped specimen.

### 2.3.3 BIAXIAL FLEXURE STRENGTH TEST

#### 2.3.3.1 Specimen Preparation

Disc-shaped specimens ( $13.0 \pm 0.1$  mm diameter and  $1.0 \pm 0.1$  mm thickness) for BFS testing were prepared from the hand-mixed GI restorative using PTFE ring-moulds ( $23.0 \pm 0.1$  mm outer diameter and  $13.0 \pm 0.1$  mm inner diameter) (Dowling et al., 2012) (Figure 2.9).

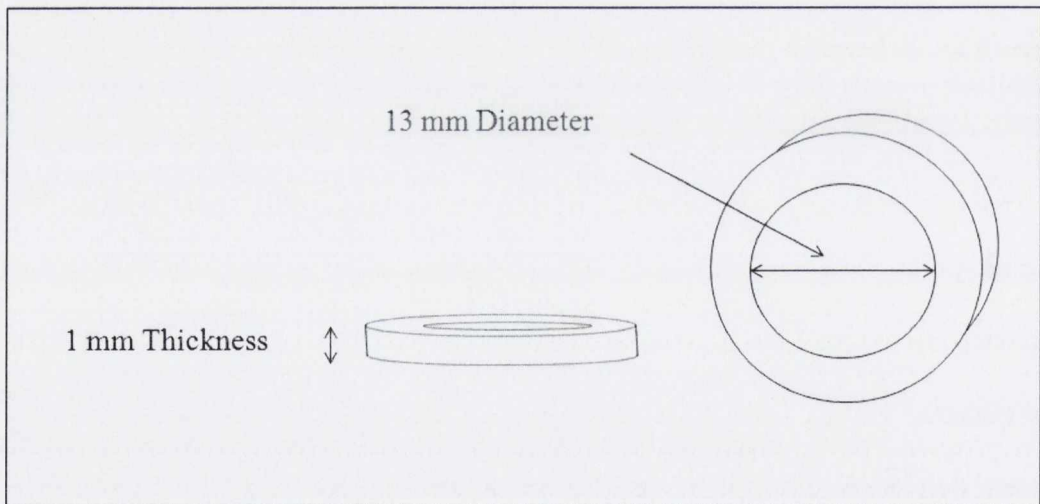


**Figure 2.9. Schematic representation of the polytetrafluoroethylene (PTFE) ring-mould employed to manufacture disc-shaped biaxial flexure strength (BFS) specimens identifying the internal diameter and thickness of the mould which produced disc-shaped specimens with the corresponding dimensions of  $13.0 \pm 0.1$  mm diameter and  $1.0 \pm 0.1$  mm thickness.**

A ring-mould was placed on top of a glass slab and to prevent specimen adhesion the glass slab was covered with an acetate strip. To minimise air bubble incorporation, the hand-mixed

GI restorative was transferred to the centre of the ring-mould using the stainless-steel mixing spatula within 60 s of the completion of mixing (Fleming et al., 1999). The filled mould was covered with a second acetate strip and a 1 kg mass applied to facilitate even spread of the GI mix throughout the mould. Parallelism of the specimen surfaces was ensured by securing the filled mould between glass slabs using a G-clamp. Following clamping, the mould assembly was transferred to the water-bath maintained at  $37 \pm 1^\circ\text{C}$  for 1 h. At each specimen preparation interval, batches of four specimens were prepared by repeating the specimen fabrication procedure.

The clamped assembly was removed following 1 h conditioning in the water-bath and the specimens carefully demoulded by applying light finger pressure against the edges of the disc-shaped specimen. The retrieved specimens were visually inspected for defects and the specimens without defects were numbered, placed in 50 ml of distilled water and stored in the incubator maintained at  $37 \pm 1^\circ\text{C}$  for 23 h prior to testing.

The preparation of one disc-shaped BFS specimen at the manufacturer's recommended powder:liquid mixing ratio (4:1 g:g) involved hand-mixing 0.3 g of the GI powder and a corresponding 0.075 g of the GI liquid. Powder:liquid mixing ratio groups with 90, 80, 70, 60, 50, 40, 30 and 20% of the manufacturer's recommended powder content (100%) were prepared by reducing the recommended powder content from 0.3 g to 0.27, 0.24, 0.21, 0.18, 0.15, 0.12, 0.09 and 0.06 g, respectively, for the 0.075 g of GI liquid (Table 2.4).



**Table 2.4. The powder:liquid mixing ratio groups, weight percentages of the manufacturer's recommended powder content and the corresponding weights of the GI powder and liquid employed for the preparation of the disc-shaped biaxial flexure strength (BFS) specimens.**

<b>Powder:liquid mixing ratio (g:g)</b>	<b>Weight% of the manufacturer's recommended powder content</b>	<b>Weight of powder:weight of liquid (g:g) for BFS specimen preparation</b>
4:1	100	0.3:0.075
3.6:1	90	0.27:0.075
3.2:1	80	0.24:0.075
2.8:1	70	0.21:0.075
2.4:1	60	0.18:0.075
2:1	50	0.15:0.075
1.6:1	40	0.12:0.075
1.2:1	30	0.09:0.075
0.8:1	20	0.06:0.075

### **2.3.3.2 Biaxial flexure strength testing procedure**

Following incubation of the disc-shaped specimens in distilled water for 23 h, the BFS was determined using a ball-on-ring test configuration (de With and Wageman, 1989) in the universal testing machine (Figure 2.10). The ball-on-ring test configuration consisted of a 4 mm diameter stainless-steel ball indenter and a 10 mm diameter knife-edge annular ring support. To minimise the influence of support friction on the recorded BFS (Morell, 2007), a 0.2 mm thickness latex sheet was placed on top of the annular ring support prior to testing which compensated for small lateral displacements of the disc-shaped specimens during loading (Bhamra et al., 2002). The disc-shaped BFS specimens were placed on top of the latex covered annular ring support and loaded centrally using the ball indenter at a crosshead speed of 1 mm/min.

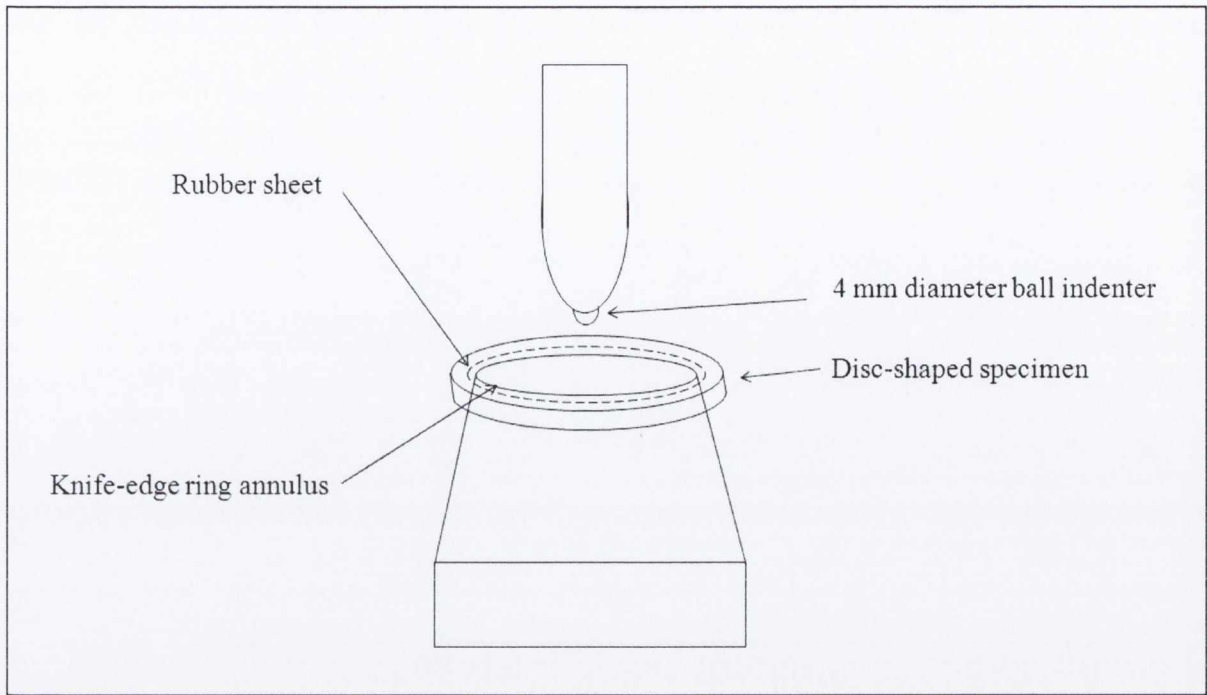


**Figure 2.10. Schematic representation of the biaxial flexure strength (BFS) testing apparatus highlighting a disc-shaped BFS specimen resting on top of a knife-edge annular ring support covered with a thin sheet of latex to assist uniform loading. The BFS specimens were loaded centrally using a 4 mm diameter stainless-steel ball indenter and the maximum load-to-failure recorded.**

Following testing, the thickness of the fracture fragments was measured using the micrometer screw gauge and the BFS was calculated using Equation 2.5 (Timoshenko and Woinowsky-Krieger, 1959).

$$BFS = \frac{P}{h^2} \left\{ (1 + \nu) \left[ 0.485 \ln \left( \frac{a}{h} \right) + 0.52 \right] + 0.48 \right\} \quad \text{Equation 2.5}$$

where  $P$  was the load-to-failure (N),  $h$  the mean thickness of the fracture fragments (mm),  $\nu$  the Poisson's ratio of the GI restorative (0.3) (Akinmade and Nicholson, 1995) and  $a$  was the radius of the knife-edge ring annulus (5 mm). To determine the amount of deflection of the BFS specimens on loading, the compressive extension was recorded from the initial linear

portion of the load-deflection plot to the maximum load-to-failure for each individual BFS specimen.

### 2.3.4 HERTZIAN INDENTATION TEST

#### 2.3.4.1 Specimen preparation

##### 2.3.4.1.1 Encapsulated GI restoratives

Disc-shaped GI restorative specimens ( $10.0 \pm 0.1$  mm diameter and  $3.1 \pm 0.03$  mm thickness) for HI testing were prepared using polyetheretherketone (PEEK) ring-moulds ( $20.0 \pm 0.1$  mm outer diameter and  $10.0 \pm 0.1$  mm inner diameter) (Figure 2.11).

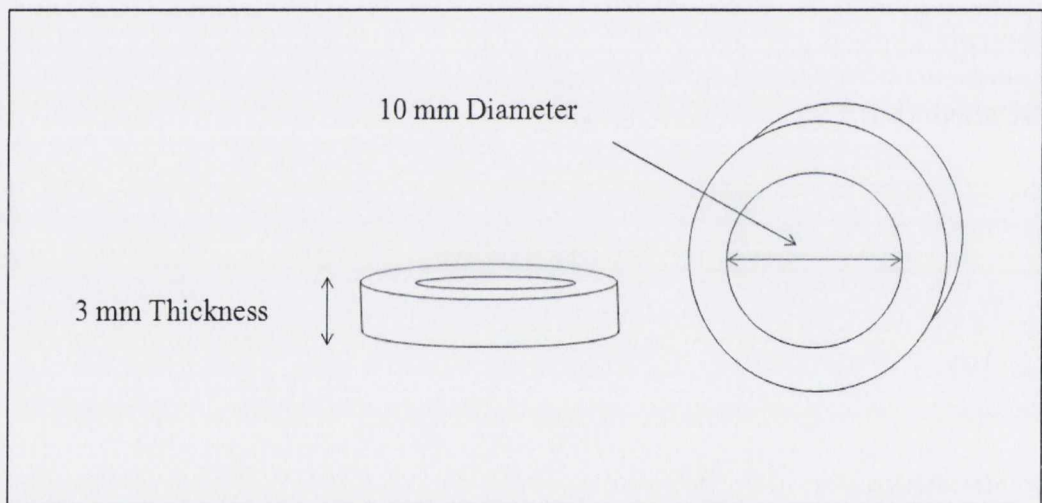


**Figure 2.11. Schematic representation of the polyetheretherketone (PEEK) ring-mould employed to manufacture disc-shaped Hertzian Indentation (HI) specimens identifying the internal diameter and thickness of the mould which produced disc-shaped specimens with the corresponding dimensions of  $10.0 \pm 0.1$  mm diameter and  $3.1 \pm 0.03$  mm thickness.**

A mould was placed on top of a glass slab which was covered with an acetate strip to prevent adhesion to the glass slab. To prepare one HI disc-shaped specimen, the mixed contents from two capsules of each encapsulated GI investigated was required. Therefore, the second capsule was tapped and activated while the first capsule was being mechanically mixed. To

reduce the likelihood of air bubble incorporation, the GI restorative was extruded until the GI mix was visible in the capsule nozzle prior to the application of the mixed GI into the ring-mould. The mixed GI from the first capsule was transferred to the ring-mould within 10 s of the completion of mechanical mixing by placing the capsule nozzle in contact with the acetate covered glass slab in the centre of the ring-mould and slowly extruding the mixed GI to provide laminar flow, thereby further minimising air bubble incorporation (Fleming et al., 1999). The mixed contents from the second capsule were added on top of the first GI increment within 10 s of the completion of mechanical mixing and the filled ring-mould was covered with a second acetate strip. A 1 kg mass was applied to the top surface of the filled ring-mould using a glass slab to spread the mix evenly in the ring-mould. The filled ring-mould was clamped between the glass slabs using a G-clamp to ensure parallelism of the specimen surfaces and the clamped assembly was transferred to the water-bath maintained at  $37 \pm 1^\circ\text{C}$  for 1 h. The specimen fabrication procedure was repeated to prepare individual batches of four specimens at each specimen preparation interval.

After 1 h, the clamped assembly was removed from the water-bath and the clamps were opened. The specimens were demoulded by placing the ring-mould containing the disc-shaped specimen into a customised brass holder which had a 12 mm diameter hole in the centre of the bottom surface (Figure 2.12). A customised 8 mm diameter brass plug was pressed against the specimen on the upper surface which caused the specimen to 'pop out' from the ring-mould and drop through the hole in the bottom surface of the brass holder (Figure 2.12).

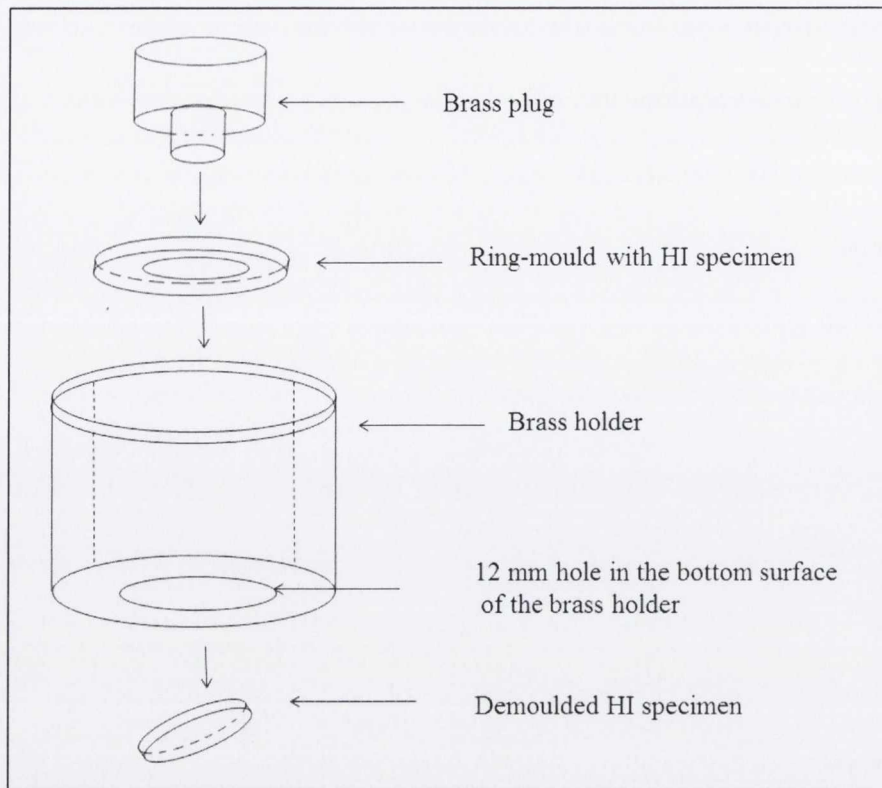


**Figure 2.12. Schematic representation of the demoulding apparatus used for the Hertzian Indentation (HI) specimens highlighting a ring-mould containing the disc-shaped HI specimen which was placed into a customised brass holder with a 12 mm diameter hole in the centre of the bottom surface. A customised 8 mm diameter brass plug was pressed against the specimen from the top which caused the specimen to ‘pop out’ from the ring-mould and drop through the hole in the bottom surface of the brass holder.**

Any excess residual flash was carefully removed through hand-lapping on P600 silicon carbide abrasive paper using water as a lubricant. The specimens were inspected for visible defects such as pores and chipped edges and those containing defects were discarded. The demoulded defect free specimens were numbered on the top surface in the sequence of manufacture, stored in glass containers filled with 50 ml of distilled water and transferred to an incubator maintained at  $37 \pm 1^\circ\text{C}$  for an additional 23 h prior to testing.

#### **2.3.4.1.2 Hand-mixed GI restorative**

HI specimens ( $10.0 \pm 0.1$  mm diameter and  $3.1 \pm 0.03$  mm thickness discs) were prepared from the hand-mixed GI using the PEEK ring-moulds (Figure 2.11). A ring-mould was

placed on top of a glass slab and to prevent adhesion of the specimen to the glass slab, the glass slab was covered with an acetate strip. A sufficient quantity of the GI was hand-mixed at one time to prepare one HI specimen. To minimise the incorporation of air bubbles, the largest convenient portion of the GI mix was placed into the centre of the ring-mould within 60 s of the completion of mixing using the stainless-steel mixing spatula and the filled mould was covered with acetate. A 1 kg mass was placed on top to evenly spread the GI in the ring-mould which was clamped between the glass slabs to ensure surface parallelism and the clamped assembly was transferred to the water-bath maintained at  $37 \pm 1^\circ\text{C}$  for 1 h. The specimen preparation procedure was repeated to prepare one batch of four hand-mixed HI specimens. The clamped assembly was removed from the water bath 1 h after the commencement of hand-mixing and the specimens were demoulded using the customised specimen demoulding apparatus (Figure 2.12). The residual flash was removed by hand-lapping using P600 silicon carbide abrasive paper under water lubrication, the specimens visually inspected for defects and defect free specimens were numbered from the top surface in accordance with the manufacturing sequence prior to storage for 23 h in 50 ml of distilled water at  $37 \pm 1^\circ\text{C}$  in the incubator prior to testing.

At the manufacturer's recommended powder:liquid mixing ratio (4:1 g:g), 0.5 g of the GI powder and a corresponding 0.125 g of the GI liquid element were required to produce a sufficient amount of the GI mix for the preparation of one HI specimen. The powder:liquid mixing ratio groups containing powder contents reduced from that specified by the manufacturer (100%) to 90, 80, 70, 60, 50, 40, 30 and 20% were prepared by reducing the weight of the GI powder from 0.5 g to 0.45, 0.4, 0.35, 0.3, 0.25, 0.2, 0.15 and 0.1 g, respectively, for the 0.125 g of GI liquid (Table 2.5).

**Table 2.5. The powder:liquid mixing ratio groups, weight percentages of the manufacturer's recommended powder content and the corresponding weights of the GI powder and liquid employed for the preparation of the disc-shaped Hertzian Indentation (HI) specimens.**

<b>Powder:liquid mixing ratio (g:g)</b>	<b>Weight% of the manufacturer's recommended powder content</b>	<b>Weight of powder:weight of liquid (g:g) for HI specimen preparation</b>
4:1	100	0.5:0.125
3.6:1	90	0.45:0.125
3.2:1	80	0.4:0.125
2.8:1	70	0.35:0.125
2.4:1	60	0.3:0.125
2:1	50	0.25:0.125
1.6:1	40	0.2:0.125
1.2:1	30	0.15:0.125
0.8:1	20	0.1:0.125

#### **2.3.4.2 Hertzian Indentation testing procedure**

Following 23 h water storage, the encapsulated and hand-mixed GI specimens were removed from the distilled water and tested using a HI testing apparatus which consisted of a brass holder with a hollow cavity of 10.5 mm diameter and 6.5 mm height (Figure 2.13). To simulate the clinical scenario for GI restoratives, the cavity in the brass holder was filled with a 10 mm diameter and 5 mm thick disc of a dentine analogue substrate material (Wang and Darvell, 2007) which was reported by the manufacturer to be composed of a 30% glass fiber reinforced polyamide (nylon-6,6). The polyamide substrate was selected as a dentine analogue material as it was stated by the manufacturer (Goodfellow Cambridge, Huntingdon, England) to have an elastic modulus value of 10-11 GPa (Product specification) which was within the range of that reported for dentine at 11-18 GPa (Marshall et al., 1997). The disc-shaped GI specimens were placed on top of the dentine analogue which was constrained in the brass holder and the HI testing assembly was centrally aligned on a compression loading platen using a customised ring-shaped central alignment device (Figure 2.13). To simulate cusp contact, the HI specimens were loaded from the top through a 20 mm diameter hard

steel ball indenter at a crosshead speed of 1 mm/min using the universal testing machine (Figure 2.13). The maximum load-to-failure was recorded when a 20% drop in the peak compressive load value was detected by the load cell. After failure, the load-deflection plot for each specimen was used to calculate the compressive extension from the initial linear portion of the load-deflection plot to the maximum load-to-failure. Following testing under HI, the number of fracture fragments was recorded for each individual specimen and the thickness of each fracture fragment was measured using the digital micrometer screw gauge.

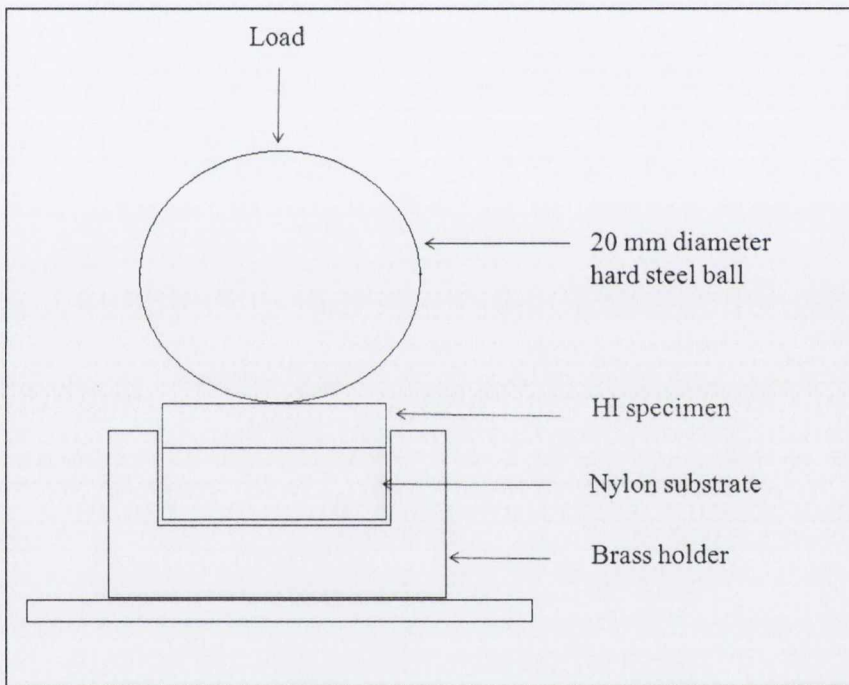


**Figure 2.13. Schematic representation of the Hertzian Indentation (HI) testing apparatus identifying the disc-shaped HI specimen resting on top of a nylon substrate which was constrained in a brass holder. The HI specimens were loaded from the top using a 20 mm diameter hard steel ball to simulate cusp contact.**



## **2.3.5 FRACTURE TOUGHNESS TEST**

### **2.3.5.1 Specimen preparation**

#### **2.3.5.1.1 Encapsulated GI restoratives**

No specific standard exists detailing the specimen preparation and testing condition requirements for the accurate determination of  $K_{IC}$  of GIs. In the absence of a specific standard, the majority of investigators (Lloyd and Mitchell, 1984; Lloyd and Adamson, 1987; Mathis and Ferracane, 1989; Beatty and Pidaparti, 1993; Pidaparti and Beatty, 1995; Kao et al., 1996; Miyazaki et al., 1996; Lucas et al., 2003; Elsaka et al., 2011; Ilie et al., 2012) reporting the  $K_{IC}$  of GIs have employed the techniques described by the ASTM International (ASTM 399:2009) and ISO standards (ISO 12737:2010) for the  $K_{IC}$  testing of metallic materials which prescribe the use of SEN bend or SEN compact tension specimens. Owing to similarities of brittle fracture of GIs to dental ceramics, the ASTM International standard test method for determination of  $K_{IC}$  of advanced ceramics (ASTM C1421:2010) appears to be more relevant when investigating the  $K_{IC}$  of GIs. ASTM C1421:2010 prescribes the use of either SEN pre-cracked beam, surface cracked beam or chevron notched beam geometries, however, no publications employing ASTM C1421:2010 could be identified in the literature on  $K_{IC}$  testing of GIs.

In the dental literature, the  $K_{IC}$  of GIs has also been reported using rectangular double torsion (Goldman, 1985; Hill et al., 1989; Wilson et al., 1989), cylindrical chevron notched (Mitchell et al., 1999) and ring-shaped  $K_{IC}$  specimens (Mitsuhashi et al, 2003). Using RBCs, the specimen preparation technique and specimen alignment requirements during loading for the accurate determination of  $K_{IC}$  were identified to be 'less demanding' for the SEN bend and SEN compact tension specimens when compared with the rectangular double torsion and

cylindrical chevron notched specimens (Fujishima and Ferracane, 1996). In addition, control of substantial deviation of crack propagation from within the groove created for double torsion specimens (Truong et al., 1990; Fujishima and Ferracane, 1996) and from the plane of the notch for chevron notched specimens (Fujishima and Ferracane, 1996) was difficult to achieve. These problems would be exacerbated for GIs which are known to be more brittle when compared with RBCs (Goldman, 1985). Therefore, the  $K_{IC}$  of GIs was determined using the SEN bend specimen geometry in the current investigation to ensure reproducibility of test results achieved.

The encapsulated GI restorative SEN bend specimens ( $35.0 \pm 0.1$  mm length,  $6.0 \pm 0.1$  mm width and  $3.0 \pm 0.1$  mm thickness) were prepared for  $K_{IC}$  testing using a PTFE lined brass split-mould assembly (Lloyd and Mitchell, 1984) (Figure 2.14). The split-mould assembly consisted of a PTFE lined brass split-mould (Figure 2.14a), two brass plugs (Figure 2.14a), a straight-edge surgical scalpel blade (Type 10A, Swann-Morton Ltd., Sheffield, UK) secured in a brass blade holder (Figure 2.14a) and a PTFE lined brass base plate (Figure 2.14b).

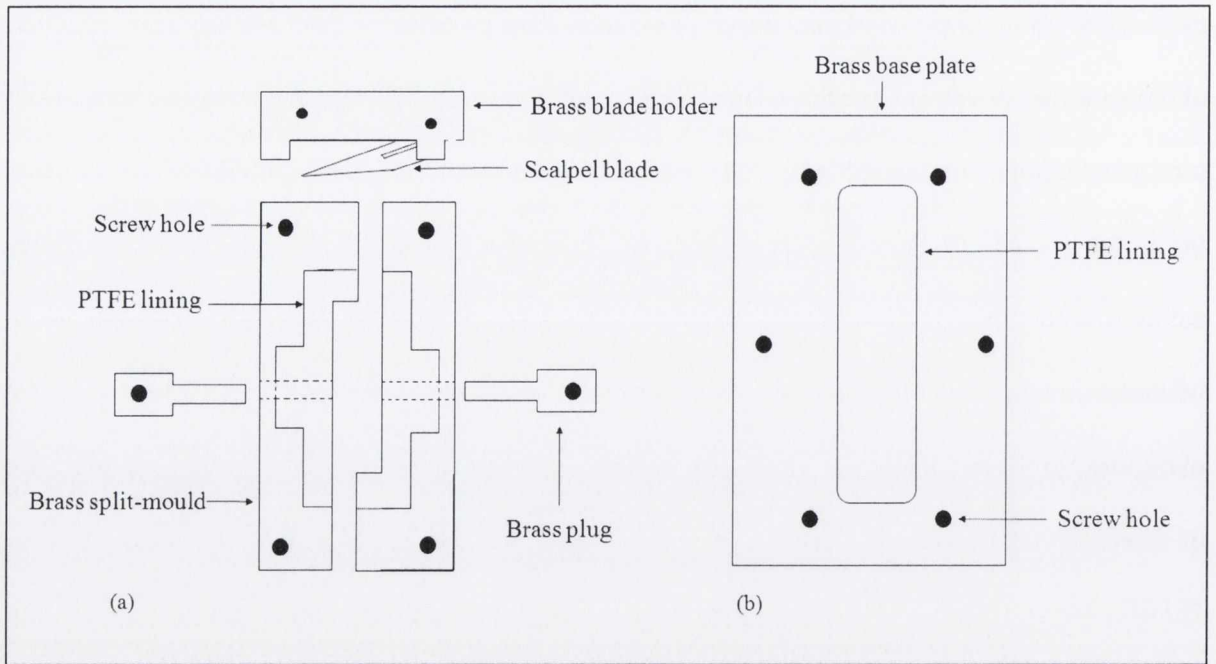


**Figure 2.14. Schematic representation of the polytetrafluoroethylene (PTFE) lined brass split-mould assembly employed to manufacture single-edge notched (SEN) bend specimens for fracture toughness ( $K_{IC}$ ) testing highlighting (a) a PTFE lined brass split-mould with four screw holes located at the corners of the split-mould, two brass plugs and a scalpel blade secured in a brass blade holder. The split-mould and the brass plugs were assembled and secured onto (b) the PTFE lined brass base plate with multiple screws.**

To avoid specimen adhesion, the split-mould was designed and constructed with PTFE on the surfaces in contact with the material which were supported with brass to provide mould rigidity (Figure 2.14a). Prior to specimen manufacture, the PTFE lined surfaces of the split-mould (Figure 2.14a) were covered with two layers of transparent adhesive tape (Sellotape, Henkel Ltd., Winsford, Cheshire, UK) to further prevent specimen adhesion to the mould. In addition, the adhesive tape facilitated specimen removal such that peeling the tape from the top surface of the mould applied a uniform force to the specimen and prevented premature fracture through the transmission of direct and localised forces on the specimen during demoulding. To prevent specimen adhesion to the base of the split-mould, a single layer of the adhesive tape was also applied to the PTFE surface of the brass base plate (Figure 2.14b).

Following application of the adhesive tape, the two parts of the split-mould were joined together using two screws, each of which extended through the entire width of one part of the split-mould and approximately half the width of the second part. The joined split-mould was secured to the PTFE lined brass base plate by inserting four screws into the screw holes located at each corner of the split-mould (Figure 2.14a). Two brass plugs were inserted into channels located at mid-length on each part of the split-mould and were secured to the base plate with two screws (Figure 2.14a). Positioning of the two brass plugs into the channels on each side of the split-mould created a narrow close fitting slot for the insertion of the scalpel blade (Figure 2.14a). The depth of penetration of the scalpel blade on insertion into the slot created by the brass plugs was limited by two stops located on the brass blade holder which ensured penetration of the scalpel blade to approximately half the width of the specimen (Lloyd and Iannetta, 1982) (Figure 2.14a).

For Chemfil Rock and Fuji IX<sub>GP</sub> Fast encapsulated GIs, the mixed contents from five capsules were required for the fabrication of a single SEN bend specimen, although for Ionofil Molar AC four capsules provided a sufficient quantity of mixed GI for the preparation of a single SEN bend specimen. To ensure consistent specimen manufacture and minimise transfer time between the mixed capsules, assistance from a second operator was acquired. While the mixed content from a GI capsule was being transferred to the mould by the first operator, the second operator activated and mixed the following GI capsules, thereby simulating 'four-handed dentistry' (Paul, 1983). To minimise air inclusion, the GI restorative was extruded until the GI mix was visible in the capsule nozzle prior to the application of the mixed GI into the split-mould. The capsule nozzle was placed in contact with the PTFE lined base plate at mid-length of the split-mould and the mixed GI slowly extruded to provide laminar flow, thereby further minimising air entrapment (Fleming et al., 1999). The mixed

contents from two GI capsules were transferred to the centre of the mould within 10 s of the completion of mechanical mixing. A sharp notch was formed in the specimen by inserting the scalpel blade into the close fitting slot located at mid-length of the split-mould which penetrated to approximately half the width of the freshly mixed GI placed in the centre of the split-mould (Figure 2.14a). The mixed contents from the remaining GI capsules were then transferred within 10 s of the completion of mechanical mixing to the lateral aspects of the mould and the filled mould was covered with two strips of acetate, one placed adjacent to each side of the scalpel blade. To ensure adequate packing of the GI into the mould, pressure was applied to the top surface using a 1 kg mass and the mould assembly was transferred to the incubator maintained at  $37 \pm 1^\circ\text{C}$  and 100% relative humidity for 1 h. A single SEN bend specimen was prepared at each specimen preparation interval.

Following 1 h conditioning, the split-mould assembly was retrieved from the incubator and the scalpel blade carefully removed. The split-mould was separated from the base plate by removing the screws that were used to secure the split-mould and the brass plugs to the base plate. Following detachment from the base plate, the split-mould was disassembled by removing the screws that were used to unite the two parts of the split-mould. The SEN bend specimen was carefully demoulded by peeling the adhesive tape from the top surface of the split-mould which created a tab that could be lifted, thereby ensuring that a uniform force was applied to the specimen to prevent premature fracture during demoulding. Any residual flash was removed through hand-lapping using the P600 silicon carbide abrasive paper under water lubrication. The specimens were visually inspected for defects or pores and those containing visible defects were discarded. The specimens without defects were numbered, stored in 50 ml of distilled water and maintained at  $37 \pm 1^\circ\text{C}$  for 23 h prior to testing.

### 2.3.5.1.2 Hand-mixed GI restorative

The hand-mixed GI restorative SEN bend specimens ( $35.0 \pm 0.1$  mm length,  $6.0 \pm 0.1$  mm width and  $3.0 \pm 0.1$  mm thickness) were prepared for  $K_{IC}$  testing using the bespoke PTFE lined brass split-mould assembly (Figure 2.14). The PTFE surfaces of the split-mould (Figure 2.14a) and the brass base plate (Figure 2.14b) were covered with the transparent adhesive tape to prevent specimen adhesion and facilitate specimen removal. A sufficient amount of the hand-mixed GI was manipulated at one time to fabricate a single SEN bend specimen. To minimise the introduction of air bubbles in the specimen, the hand-mixed GI was transferred to the split-mould in three increments whereby one increment was placed at the centre of the split-mould and two at the lateral aspects of the split-mould. A sharp notch was formed in the specimen by inserting the scalpel blade into the slot located at mid-length of the split-mould which penetrated to approximately half the width of the hand-mixed GI increment placed in the centre of the split-mould (Figure 2.14a). The filled split-mould was covered with acetate and a 1 kg mass applied to ensure consistent packing of the GI into the mould which was then transferred to the incubator maintained at  $37 \pm 1^\circ\text{C}$  and 100% relative humidity for 1 h. Following incubation for 1 h, the scalpel blade was removed from the split-mould assembly and the split-mould disassembled by removing the multiple screws on the split-mould and the brass plugs. Following disassembly of the split-mould, the adhesive tape was peeled from the top surface of the split-mould to create a tab which was raised to demould the specimen by applying a uniform force and preventing premature fracture during demoulding. The P600 silicon carbide abrasive paper was used to remove any residual flash through hand-lapping using water as a lubricant. The specimens containing defects or pores on visual inspection were discarded and those without defects were numbered, stored in 50 ml of distilled water and maintained at  $37 \pm 1^\circ\text{C}$  for 23 h prior to testing.

To produce an adequate amount of the GI mix for the preparation of a single SEN bend specimen for  $K_{IC}$  testing at the manufacturer's recommended powder:liquid mixing ratio (4:1 g:g), 1.2 g of the GI powder and a corresponding 0.3 g of the GI liquid were required. To prepare the powder:liquid mixing ratio groups with 90, 80, 70, 60, 50, 40, 30 and 20% powder content, the manufacturer's recommended powder content was reduced from 1.2 g to 1.08, 0.96, 0.84, 0.72, 0.6, 0.48, 0.36 and 0.24 g, respectively, for the 0.3 g of GI liquid (Table 2.6).

**Table 2.6. The powder:liquid mixing ratio groups, weight percentages of the manufacturer's recommended powder content and the corresponding weights of the GI powder and liquid employed for the preparation of the single-edge notched (SEN) bend specimens for fracture toughness ( $K_{IC}$ ) testing.**

<b>Powder:liquid mixing ratio (g:g)</b>	<b>Weight% of the manufacturer's recommended powder content</b>	<b>Weight of powder:weight of liquid (g:g) for <math>K_{IC}</math> specimen preparation</b>
4:1	100	1.2:0.3
3.6:1	90	1.08:0.3
3.2:1	80	0.96: 0.3
2.8:1	70	0.84: 0.3
2.4:1	60	0.72: 0.3
2:1	50	0.6: 0.3
1.6:1	40	0.48: 0.3
1.2:1	30	0.36: 0.3
0.8:1	20	0.24: 0.3

### **2.3.5.2 Fracture toughness testing procedure**

Following 23 h water storage, the SEN bend specimens were removed from the glass container and loaded in a standard three-point flexure test assembly using the universal testing machine (ISO 12737:2010). The SEN bend specimens were placed horizontally on top of two point supports with the notched surface facing the point supports such that the notched surface of the SEN bend specimens was placed under tension during loading (Figure 2.15).

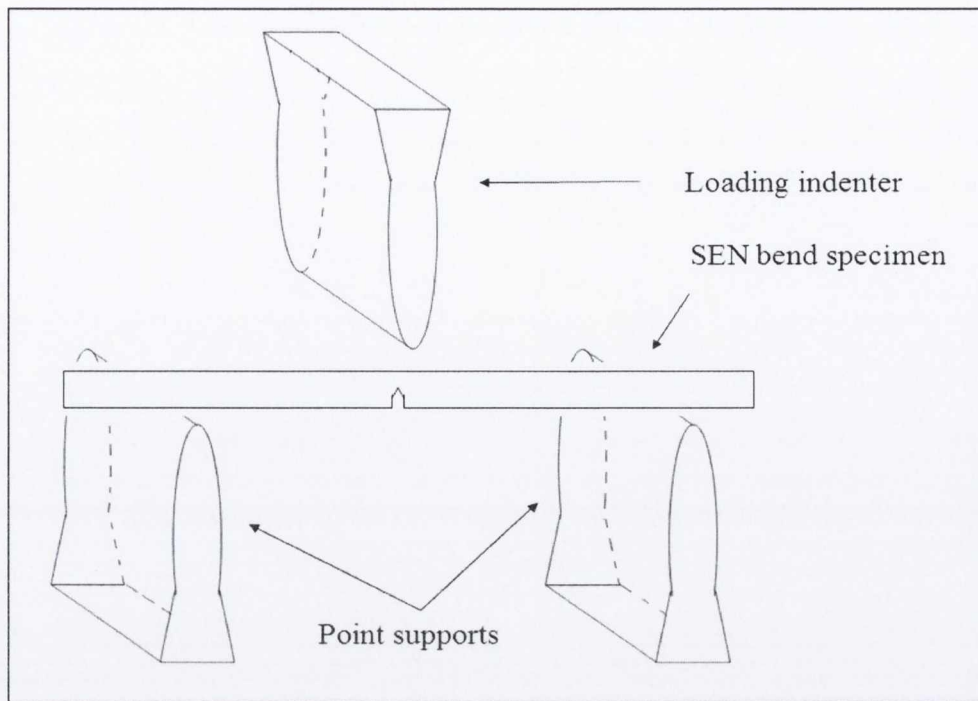


**Figure 2.15. Schematic representation of a single-edge notched (SEN) bend specimen resting on top of two point supports for fracture toughness ( $K_{IC}$ ) testing using a three-point flexure test assembly with the notched surface facing the point supports. Load was applied from the top through the indenter in the central region of the SEN bend specimen such that the notched surface of the specimen was placed under tension during loading.**

Load was applied through the indenter to the centre of the SEN bend specimen at a crosshead speed of 0.1 mm/min and the maximum load-to-failure recorded. Following fracture, the specimen width and thickness were measured using the micrometer screw gauge. To ensure reproducible measurements of the crack length for each SEN bend specimen, the fracture surface of each fracture fragment was scanned using a contact profilometer (Talysurf CLI 2000, Taylor-Hobson Precision, Leicester, England). The crack length was determined by measuring the distance below the notch at mid-thickness and quarter-thickness points on each fracture surface scan. Following measurement of the specimen width, thickness and crack length, the  $K_{IC}$  was calculated for each SEN bend specimen using Equation 2.6 (ISO 12737:2010).



$$K_{IC} = \frac{PL}{BW^{3/2}} f(a/W) \quad \text{Equation 2.6}$$

where  $P$  was the load-to-failure (N),  $L$  the span length (20 mm),  $B$  the specimen thickness,  $W$  the specimen width,  $a$  the crack length and  $f(a/W)$  a geometrical function dependant on  $a/W$  which was calculated using Equation 2.7 (ISO 12737:2010).

$$f(a/W) = \frac{3(a/W)^{1/2} [1.99 - (a/W)(1 - a/W) \{2.15 - 3.93(a/W) + 2.7(a/W)^2\}]}{2(1 + 2a/W)(1 - a/W)^{3/2}}$$

Equation 2.7

### 2.3.6 FRACTOGRAPHY

Fractography is the examination of fracture surfaces which display features resulting from the interaction of a propagating crack with the microstructure of the material and is routinely performed using optical or scanning electron microscopy (SEM). The fracture of restorative dental materials can be traced back to the fracture initiation site or the ‘fracture origin’ which provides an indication of the failure mode (Mecholsky et al., 1974; Mecholsky, 1995; Scherrer et al., 2006). The analysis of the fracture surface topography includes the size and location of the fracture initiating crack, the crack path and the failure mode (Quinn, 2007). For brittle materials such as glass, four distinct regions can be identified on a fracture surface which expand radially from the fracture origin site and are indicative of the evolution of the crack. These include the mirror region (adjacent to the fracture origin site), the mist, the hackle and the macroscopic crack branching regions (Mecholsky et al., 1974; Kelly et al., 1990; Quinn, 2007). Once a crack becomes unstable it grows rapidly, leaving behind a smooth region namely the mirror which is representative of the region where the crack has

insufficient energy for secondary crack formation. A rougher mist region lies adjacent to the mirror region which results from the crack front attaining sufficient energy for secondary crack nucleation, although there is insufficient energy for secondary crack propagation. The hackle represents the region where the system has gained sufficient energy for the propagation of the secondary cracks and on attaining further energy the secondary cracks can branch macroscopically to form the crack branching region (Mecholsky et al., 1974; Kelly et al., 1990; Quinn, 2007).

In the dental literature, fractography has been used to determine the fracture origin and failure mode in clinically fractured dental ceramic restorations (Kelly et al., 1990; Thompson et al., 1994; Quinn et al., 2005; Scherrer et al., 2006; Oilo and Gjerdet, 2013) and in anatomic crown shaped specimens fractured using the *in vitro* 'crunch the crown' test in an attempt to establish the clinical relevance of laboratory testing (Kelly, 1999; Kelly et al., 2012). For specimens loaded using the crunch the crown test, the failure mode involves indenter contact damage and does not replicate the failure mechanism of sub surface radial cracking routinely observed on fractographic analysis of clinically failed restorations (Kelly, 1999; Kelly et al., 2012). To identify an appropriate method to reproduce the failure mode occurring in service, the HI test was explored which simulated cusp contact by applying load through a spherical indenter to a flat mono-, bi- or tri-layered specimen surface (Lawn et al., 2001, 2002). The HI test was identified to replicate the clinically relevant failure mode of sub surface radial cracking for dental ceramics when employed using a range of testing conditions evident on fractographic analysis of the fractured specimens (Lawn et al., 2001, 2002). Fractographic analysis of the fracture surfaces of disc-shaped dental amalgam (Wang and Darvell, 2007, 2008, 2010), RBC (Wang and Darvell, 2008), and GI specimens (Wang and Darvell, 2007, 2008, 2012) tested under HI revealed that for a range of specimen thicknesses, fracture

occurred through the clinically relevant failure mode of radial cracking from the surface under tension (Kelly, 1999), suggesting that the HI test could be extended from dental ceramics to dental amalgam, RBCs and GIs (Wang and Darvell, 2007, 2008, 2009, 2010, 2012). To identify and compare the fracture origin and failure mode of the GI restorative disc-shaped HI specimens tested in the current investigation with those reported in the dental literature (Wang and Darvell, 2007, 2008, 2009, 2012), fractographic analysis of the fracture surfaces of selected specimens was performed using a scanning electron microscope (Zeiss Ultra Plus Field Emission SEM, Carl Zeiss, Jena, Germany).

#### **2.3.6.1 Scanning electron microscope**

A scanning electron microscope consists of a tungsten filament gun as an electron source to produce an electron cloud which is confined and focused into an electron beam by metal apertures and magnetic condenser lenses. The incident electron beam scans the surface of the specimen and drives different forms of emission from the scanned surface as secondary or back-scattered electrons which are collected by an electron detector to form an SEM image (Watt, 1997). Secondary electrons are emitted by atoms near the surface of a specimen when the electrons have gained sufficient energy to escape the specimen surface while back-scattered electrons are the electrons that have re-emerged from the specimen after undergoing elastic scattering (Seiler, 1983). The form of electrons chosen to create the desired SEM images is dependent upon the type of specimen surfaces and specimen materials being viewed under the SEM (Watt, 1997).

#### **2.3.6.2 Specimen preparation for fractography**

Since electrons from the incident electron beam are electrically charged, the specimen surfaces viewed under the microscope are required to be conductive to disperse this charge

(Watt, 1997). Electrically insulating specimens such as GIs fail to dissipate the incident electrons and do not provide a pathway for the removal of electrons produced by the electron source which causes the specimen surface to become charged and decreases the quality and resolution of the image (Watt, 1997). To prevent accumulation of electrostatic charge at the fracture surfaces, the fracture surfaces of the GI restorative HI specimens were sputter-coated using gold in a vacuum evaporator (Emscope SC 500, Quorum Technologies Ltd., Kent, England). Following application of the metal coating on the fracture surfaces, the fracture fragments were mounted vertically on aluminium stubs using a conductive carbon cement (Leit-C conductive carbon cement, SPI Supplies, West Chester, PA, USA) which further facilitated the removal of excess electrons from the specimen surfaces and enhanced the image quality.

### **2.3.6.3 Scanning electron microscopy procedure**

Observation of fracture surfaces in the secondary electron mode provides fully illuminated images of the surface topography due to the superior spatial resolution of the secondary electron images when compared with images produced in the back-scattered electron mode (Thompson et al., 1994). Therefore, the microscope was used in secondary electron mode under high vacuum ( $1 \times 10^{-6}$  Pa) where the operating voltage, electron beam current and spot size were kept constant at 5 kV,  $10^{-9}$  A and 11 nm, respectively for all HI specimens viewed. Multiple images of cracks on the fracture surfaces of the specimens were recorded at progressively increasing magnifications from 22 to 100x. The loaded surface of the fracture fragment was positioned at the top of the scanning electron micrograph to provide a consistent frame of reference to distinguish between the top initiated cone cracking from the surface under compression and the bottom initiated radial cracking from the surface under

tension. The fracture origin and crack path on each fracture surface image was identified and the failure mode determined.

### **2.3.7 PROFILOMETRY**

A surface profile results from the intersection of the surface by a specified plane. Profilometry is a two-dimensional (2D) measurement technique used to identify the characteristics of a surface profile by scanning the surface along a fixed trajectory while measuring the point by point variation in height and may be performed using a non-contact or contact profilometer. For non-contact profilometry, the surface is scanned and characterised using optical techniques such as laser triangulation, confocal microscopy or low coherence interferometry. Indications for non-contact profilometry include surfaces that are susceptible to surface contact damage and where the reflective properties are compatible with the selected optical scanning method. Contact profilometry employs a sharp stylus tip to record the vertical deflection when placed in physical contact with a surface under examination and is indicated for scanning transparent or hard surfaces. In addition to the means of recording the point by point variation in height of the surface, namely an optical instrument (non-contact) or a stylus tip (contact), a profilometer consists of a transducer to convert the vertical movements of the optical instrument or the stylus tip into electrical signals which are automated through a computer connected to the profilometer to form a 2D image of the profilometric trace. Incremental scanning of profilometric traces along the fixed trajectory allows for reconstitution and conversion of the profilometric traces into a three-dimensional (3D) image using an analysis software package provided by the manufacturer for further analyses.

In the dental literature, profilometry has been employed to determine the surface characteristics of dental enamel (Heurich et al., 2010), RBCs (Whitehead et al., 1996; Kakaboura et al., 2007), dental ceramics (Whitehead et al., 1999; Addison et al., 2007; Isgro et al., 2010, 2011) or soda lime glass (Hooi et al., 2013, 2014) and to investigate the volumetric wear of dental restoratives (Peters et al., 1999; Dowling et al., 2007; Theocharopoulos et al., 2010). In the current investigation, it was considered useful to extend the application of contact profilometry to the determination of the crack length of SEN bend  $K_{IC}$  specimens following scanning of the fracture surfaces. Fracture surface scans provide the possibility to create reproducible reference points on the fracture surface scans for the accurate and consistent measurements of crack length. According to the standards for the  $K_{IC}$  testing of metallic materials (ASTM 399:2009; ISO 12737:2010), the crack length must be determined accurately for a reliable estimation of the  $K_{IC}$ . In the dental literature on  $K_{IC}$  testing of GIs using SEN bend specimens, the determination of the crack length has been reported using a travelling microscope (Lloyd and Mitchell, 1984; Lloyd and Adamson, 1987) or an optical microscope (Ilie et al., 2012) although images of the crack length were never supplied. In addition, reproducibility of the crack length measurements using microscopy would not be guaranteed owing to possible inter- and/or intra-operator variability. The majority of investigators reporting the  $K_{IC}$  of SEN bend GI specimens, however, failed to report the methodology employed to accurately determine the crack length, thereby assuming the crack length to be half of the specimen width (Beatty and Pidaparti, 1993; Pidaparti and Beatty, 1995; Miyazaki et al., 1996; Lucas et al., 2003; Elsaka et al., 2011). To ensure accurate crack length measurements and reliable determination of  $K_{IC}$  of the GI restoratives investigated, the fracture surfaces of the fracture fragments from all SEN bend specimens tested were scanned in the current investigation using the Talysurf CLI 2000 contact profilometer.

### **2.3.7.1 Specimen preparation for Profilometry**

To ensure consistent profilometric scanning of a specimen surface, the specimen must be securely held on a stable workpiece. The fracture fragments of the SEN bend specimens scanned in the current investigation were secured onto a stable platform which consisted of a cell culture plate mounted on a rectangular stainless-steel plate. Each well in the cell culture plate was filled with a putty silicone impression material (VPS Hydro Putty, Henry Schein Inc., Melville, NY, USA), following kneading of equal volumes of the base and catalyst putty material until the mixed material was uniform and streak-free in colour. The two fracture fragments were inserted vertically into the centre of the filled well such that the fracture surfaces were mounted adjacent to each other and the impression material was allowed to set following initial adjustment of the fracture fragments. Care was taken to avoid contact with the fracture surfaces during mounting of the fracture fragments to minimise contamination of the fracture surfaces which could interfere with the scanning process.

### **2.3.7.2 Profilometry procedure**

The profilometric analysis was performed by longitudinally scanning the fracture surfaces of the fracture fragments across a rectangular area of  $10 \text{ mm}^2$  (5 mm length and 1 mm width on each fracture fragment) using an induction gauge conisphere diamond stylus tip of  $2 \text{ }\mu\text{m}$  radius at a measurement velocity of 2 mm/s. To determine the start and end points of the fracture surface, each scan included a section of the scalpel blade impression and the total length of the fracture surface (Figure 2.16). The scan resolution was 42 nm (z-direction) following scanning for 1001 points (x-direction) and 101 traces (y-direction) using a step size of  $10 \text{ }\mu\text{m}$  (x and y direction). Following scanning, the TalyMap analysis software package (Taylor-Hobson Precision, Leicester, UK) was used to generate a detailed 3D profile representation of the fracture surfaces. The length of the fracture surface was recorded as the

distance in mm from the end of the scalpel blade impression to the lower edge of the fracture fragment (Figure 2.16). The mean length was determined by extracting and averaging three longitudinal traces from each fracture surface scan, one at mid-thickness and two at quarter-thickness points, such that the difference between any two of the three measurements did not exceed 10% of the mean value (ISO 12737:2010). The crack length was determined by subtracting the length of the fracture surface from the specimen width which was recorded using the micrometer screw gauge.

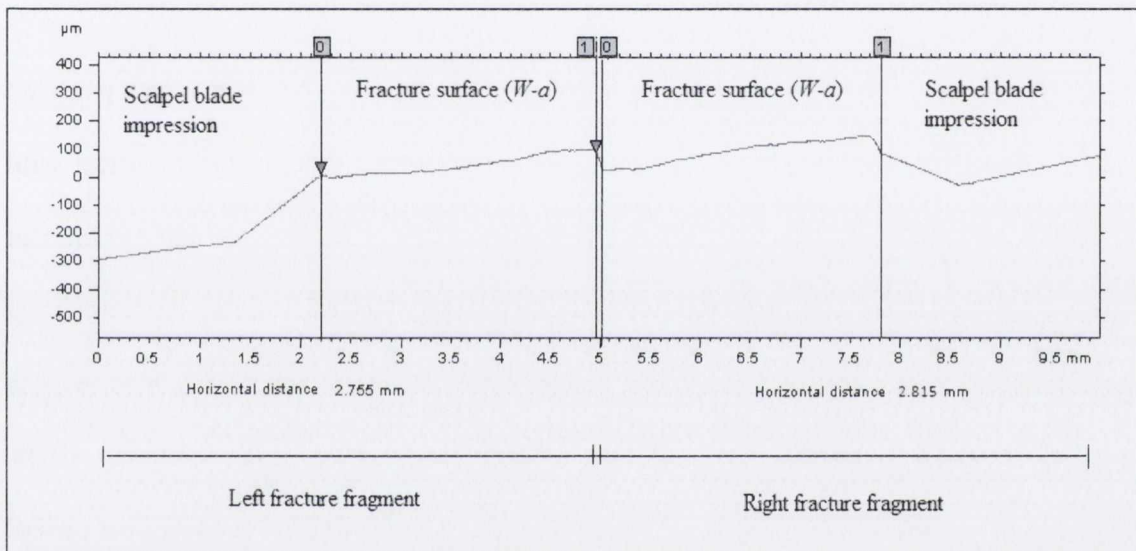


**Figure 2.16.** A profilometric trace extracted from the longitudinal scan (x-direction) of the fracture surfaces of two fracture fragments (left and right) of a single-edge notched (SEN) bend specimen. The length of the fracture surface on each fracture fragment measured in mm from the end of the scalpel blade impression (point 0) to the edge of the fracture fragment (point 1) for the left fracture fragment and from the edge of the fracture fragment (point 0) to the end of the scalpel blade impression (point 1) for the right fracture fragment.

### 2.3.8 STATISTICAL ANALYSIS

In the dental literature, groups of  $\geq 10$  GI specimens are routinely employed by investigators, although data obtained with this sample size does not provide reliable results (McCabe and Carrick, 1986). In general, more reliable results are obtained by increasing the sample size,



thereby increasing the power of the study (Swinscow, 1996). The variability of the data, the effect size and the sample size employed in a study should be justified for the data to be meaningful (Hannigan and Lynch, 2013). GIs are brittle materials and a distribution of strength data is inevitable (Ritter, 1995), owing to the likelihood of pore inclusion during restorative mixing or placement into the mould (Fleming et al., 2003; Fleming and Zala, 2003). Consequently, the reported standard deviations in the mean strength data for GI restoratives are routinely 15% or less (Fleming et al., 2003, 2012; Fleming and Zala, 2003; Dowling and Fleming, 2008, 2009; Dowling et al., 2012).

A precedent exists for CFS, TFS and BFS data for specimens prepared with the encapsulated GI restoratives used in the current investigation, namely Chemfil Rock, Fuji IX<sub>GP</sub> Fast and Ionofil Molar AC (Dowling et al., 2012). To determine the sample size for the current investigation, any precedent strength data may be employed. The CFS data was considered for reasons of relevance to the prescribed standard for GIs (ISO 9917-1:2007), which demonstrated standard deviations of 13.5 MPa, 16.4 MPa and 14.3 MPa, equivalent to 10%, 12% and 11% of the mean CFS values for Chemfil Rock (130.1 MPa), Fuji IX<sub>GP</sub> Fast (136.2 MPa) and Ionofil Molar AC (124.6 MPa), respectively (Dowling et al., 2012). Based on the reported precedent data, the sample size  $n$  in the current investigation was determined using Equation 2.8 (Swinscow, 1996).

$$n = 16 \frac{\sigma^2}{d^2} \quad \text{Equation 2.8}$$

where  $\sigma$  was the standard deviation conservatively assumed to be 20 MPa and  $d$  was the effect size specified to be 15% of the mean CFS which resulted in a sample size of  $n=17$ ,  $n=15$ ,  $n=18$  for Chemfil Rock, Fuji IX<sub>GP</sub> Fast and Ionofil Molar AC, respectively. Therefore,

a sample size of  $n=20$  was employed in the current investigation for all GI products investigated to exceed the minimum sample size required for the identification of significant differences between groups in the mechanical property being investigated.

The strength data (CFS, TFS, BFS), HI load-to-failure data and  $K_{IC}$  data were statistically analysed using IBM SPSS Statistics V22.0 (SPSS Inc., Chicago, IL, USA). The Shapiro-Wilk test was used to assess the normality of the data sets with a critical alpha value of 0.05. The homogeneity of variance of the data was determined using the Levene's test of homogeneity. One-way analyses of variance (ANOVA) with Tukey's post hoc tests were conducted at a significance level of  $p<0.05$  to test for differences between group means. Regression analyses were performed at a significance value of  $p<0.05$  to check for trends within the encapsulated and hand-mixed GI data sets regarding batch and specimen number. Additionally, for the hand-mixed GI powder:liquid mixing ratio groups, regression analyses were employed ( $p<0.05$ ) to determine significant trends within the data sets as powder content was reduced. The mean data (CFS, TFS, BFS, HI and  $K_{IC}$ ) was plotted and fitted with linear regression curves where linearisation was identified at an  $R^2$ -value of 0.95 (Lipson and Sheth, 1973). The coefficient of variation (CoV) namely the standard deviation divided by the group mean is a useful measure of reproducibility of the data sets and was assessed for each test methodology (CFS, TFS, BFS, HI and  $K_{IC}$ ) for the encapsulated and hand-mixed GI powder:liquid mixing ratios investigated.

#### **2.3.8.1 Weibull analysis**

To assess the probability with which failure occurs within a material at a given level of applied load, Weibull (1951) derived an equation which described a distribution for strength data. The Weibull distribution is based on the concept of the failure of the weakest link, such

that the Weibull equation assumes that the most critical flaw in a specimen is responsible for failure. The basic form of the Weibull distribution is presented in Equation 2.9.

$$P_f = 1 - \exp\left[-\left(\frac{\sigma - \sigma_u}{\sigma_0}\right)^m\right] \quad \text{Equation 2.9}$$

where  $\sigma$  is the applied stress at failure,  $\sigma_u$  the threshold stress,  $\sigma_0$  the normalising or scaling constant,  $m$  the Weibull modulus and  $P_f$  the probability of failure. The threshold stress ( $\sigma_u$ ) is the stress at which the failure probability approaches zero and for brittle materials such as GIs, there is always a finite probability that a critical flaw may be present in the material under investigation before it is stressed, therefore,  $\sigma_u$  can be assumed to be zero. The Weibull modulus ( $m$ ) was given physical meaning by Trustrum and Jayatilaka (1979) as characterising the brittleness of a material such that a higher value of  $m$  highlights a closer grouping of the data as  $m$  is indicative of the flaw size distribution (Zeng et al., 1996). The probability of failure ( $P_f$ ) varies from zero to one and is presented in Equation 2.10.

$$P_f = \left(\frac{n}{N+1}\right) \quad \text{Equation 2.10}$$

where  $N$  is the total number of specimens and  $n$  is the ranking number of the specimen attained on ranking all specimens in an ascending order. Consequently, Equation 2.9 can be reduced to

$$P_s = 1 - P_f = 1 - \left(1 - \exp\left[-\left(\frac{\sigma}{\sigma_0}\right)^m\right]\right) \quad \text{Equation 2.11}$$

where  $P_s$  is the probability of survival. Equation 2.11 can be simplified by using natural logarithms to the form  $y=mx+c$  as shown in Equation 2.12.

$$\ln \ln \left( \frac{1}{P_s} \right) = m \ln(\sigma) - m \ln(\sigma_0) \quad \text{Equation 2.12}$$

In the current investigation, the strength data (CFS, TFS, BFS) was ranked in ascending order and the reliability of the data sets was assessed by performing a Weibull analysis (Weibull, 1951) using Equation 2.11. The strength data was graphically displayed by plotting  $\ln \ln(1/P_s)$  against  $m \ln(\sigma)$  such that the slope of the regression line superimposed on the data points corresponded to the Weibull modulus ( $m$ ). In addition, the  $R^2$ -value provided information regarding the defect population with an  $R^2 \geq 0.95$  representative of a uni-modal defect distribution and  $R^2 < 0.95$  indicative of a multi-modal defect distribution (Lipson and Sheth, 1973). The 95% confidence intervals (CI) of the Weibull moduli were calculated for each data set investigated and differences were considered to be significant when the confidence intervals failed to overlap (Thoman et al., 1969).

### **3. SELECTED MANUSCRIPTS**

The current investigation is presented as a series of manuscripts which have been published (Manuscripts 3.2 and 3.4) or are currently in press for publication (Manuscript 3.1 and 3.3) in relevant peer-reviewed dental journals, namely 'Journal of Dentistry' (Manuscripts 3.1 and 3.2) and 'Dental Materials' (Manuscripts 3.3 and 3.4). The manuscripts are therefore presented in the style and format appropriate for each respective journal and comprehensively summarised to describe the sequence of work in the context of the overall investigation.

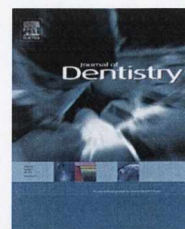
### **3.1 CONVENTIONAL GLASS-IONOMER MATERIALS: A REVIEW OF THE DEVELOPMENTS IN THE GLASS POWDER, POLYACID LIQUID AND THE STRATEGIES OF REINFORCEMENT.**

MS Baig, GJP Fleming (2015). Conventional glass-ionomer materials: a review of the developments in the glass powder, polyacid liquid and the strategies of reinforcement. *Journal of Dentistry*, Article in press.

GI restoratives are currently the only class of restorative materials that chemically bond to vital tooth structure (Wilson and McLean, 1988d) and thereby eliminate the need for excessive cavity preparation which makes the material unique in the area of restorative dentistry. Improvements in the mechanical properties of GIs would be desirable in the dental field. The current manuscript reviewed the dental literature aiming to highlight all developments in GI powder and liquid constituents since their inception and adoption into the dental field in the early 1970's. This review further aimed to highlight the various reinforcement strategies employed in the dental literature to improve the mechanical properties of GIs with their corresponding levels of success or failure. In the context of the overall investigation, the mixing and testing conditions employed by investigators for each GI reinforcement strategy were critically reviewed and all experimental short-comings were highlighted. The GI dental literature is replete with studies failing to report the mixing and testing conditions employed and with many failing to follow the specifications prescribed in ISO 9917-1:2007 for CFS testing of GIs which has not been highlighted previously in the dental literature. The need for a discriminatory testing methodology when investigating novel GIs was highlighted. The employment of a non-discriminatory testing methodology by researchers investigating GI reinforcement strategies would not positively add to the current literature and confidence in their research work would be low.

Available online at [www.sciencedirect.com](http://www.sciencedirect.com)

ScienceDirect

journal homepage: [www.intl.elsevierhealth.com/journals/jden](http://www.intl.elsevierhealth.com/journals/jden)

## Review

# Conventional glass-ionomer materials: A review of the developments in glass powder, polyacid liquid and the strategies of reinforcement



Mirza Shahzad Baig, Garry J.P. Fleming\*

Materials Science Unit, Dublin Dental University Hospital, Trinity College Dublin, Dublin 2, Ireland

## ARTICLE INFO

## Article history:

Received 4 March 2015

Received in revised form

1 April 2015

Accepted 2 April 2015

## Keywords:

Glass-ionomer restorative

Glass powder

Polyacid liquid

Reinforcement

Mechanical testing protocol

ISO 9917:2007

## ABSTRACT

**Objectives:** The development of glass-ionomers (GIs) from the earliest experimental GI formulations to the modern day commercially available GIs was reviewed. The aim of the review was to identify the developments in the glass powder and polyacid liquid constituents of GIs since their inception in the late 1960s.

**Data:** The glass powder has undergone major changes from the earliest GI powder formulation (G200) in an effort to enhance the reactivity with the polyacid liquid. The GI liquids have also been optimised by the manufacturers in terms of polyacid composition, molecular weight and concentration to improve the handling characteristics. Despite these developments in the glass powder and polyacid liquid constituents, GIs cannot 'truly' be advocated for the restoration of posterior dentition due to the poor mechanical properties when compared with dental amalgam and resin-based composites (RBCs).

**Sources:** Various attempts to improve the mechanical properties of GIs through substitution of reinforcing fillers to the GI powder or modification of the GI liquid were identified in the dental literature. Despite the claimed improvements in mechanical properties of the modified GIs, a wide variation in mixing and testing conditions was identified which prevented a valid assessment of the reported reinforcement strategies. When investigating a GI reinforcement strategy it is crucial that the mixing and testing conditions are standardised to allow a valid comparison between studies.

**Study selection:** The dental literature reporting the earliest experimental GIs to modern day commercially available GIs (1969–2015) was reviewed. In addition, full-text publications and abstracts published in English reporting various GI reinforcement strategies were included.

**Conclusion:** Nevertheless, major improvements in GI formulations through a reinforcement strategy have yet to be made to enable clinical usage of GIs for the restoration of posterior dentition.

**Clinical Significance:** GIs chemically are inherently weak but bond to sound tooth structure without the need for preconditioning or removal of sound tooth structure such that improvements in the mechanical properties of GIs would be desirable. Although advances have been made through different GI glass powder and polyacid liquid formulations over the past 40 years, further improvements in the mechanical properties of the current GIs are required to be indicated for the restoration of posterior dentition. The literature is replete with reports on GI reinforcement, however, improved reporting and control of mixing and testing conditions are required for a valid assessment of the reinforcement strategies.

© 2015 Elsevier Ltd. All rights reserved.

\* Corresponding author at: Materials Science Unit, Dublin Dental University Hospital, Trinity College Dublin, Dublin, Ireland. Tel.: +353 1 612 7371; fax: +353 1 612 7297.

E-mail address: [garry.fleming@dental.tcd.ie](mailto:garry.fleming@dental.tcd.ie) (Garry J.P. Fleming).

<http://dx.doi.org/10.1016/j.jdent.2015.04.004>

0300-5712/© 2015 Elsevier Ltd. All rights reserved.

## 1. Historical development of glass-ionomers

Glass-ionomers (GIs) were developed and patented<sup>1</sup> in the late 1960s by Alan Wilson and co-workers at the Laboratory of the Government Chemist (LGC) in London to replace dental silicate cements. Dental silicate cements – then the primary material of choice for the restoration of anterior dentition – were inherently brittle, susceptible to acid erosion, failed to adhesively bond to sound tooth structure and raised concerns owing to increased pulpal sensitivity.<sup>2</sup> A major impediment to the developmental progress of dental silicate cements was the lack of understanding of the setting chemistry.<sup>3</sup> The discovery by Wilson and Batchelor<sup>4,5</sup> that the dental silicate cement matrix was partially composed of aluminium and calcium phosphates led to the suggestion to replace phosphoric acid with a less aggressive organic chelating acid.

For this purpose, experimental cements were prepared by Wilson and co-workers by mixing series of pyruvic, tartaric, tannic, fluoroboric, glycerophosphoric and tetraphosphoric acids, at concentrations of 35–50% in solution and polyacrylic acid at a concentration of 25% in solution with the aluminosilicate glass powder.<sup>6</sup> The resultant cements (formed from pyruvic, tartaric, tannic, fluoroboric, glycerophosphoric and tetraphosphoric acids in the concentrations investigated) demonstrated adequate handling and working characteristics but slow setting characteristics and poor hydrolytic stability which precluded clinical usage. However, the cement formed with the 25% polyacrylic acid solution<sup>6</sup> highlighted a reduced susceptibility to hydrolytic disintegration but had 'little or no working time'.<sup>3</sup>

Wilson and Kent<sup>7</sup> discovered that the reactivity of the glass was controlled by the alumina:silica ratio, whereby hydrolytically stable cements could be formed by employing novel glass formulations. The early cements formed from modified alumina:silica ratio glass formulations also had poor working and setting characteristics<sup>8</sup> and it was not until the 200th glass composition (G-200) – which was high in fluoride and calcium – that a usable dental cement was formed.<sup>3</sup> The cement was reported<sup>7</sup> as a GI or aluminosilicate polyacrylate (ASPA) cement. Despite the heightened anticipation for the clinical success of GIs, the first practical cement (ASPA-I) failed to impress John McLean, the clinical consultant who raised concerns regarding the poor setting characteristics and limited working time.<sup>3</sup> Delayed hardening of the earliest GIs exposed them to the deleterious effects of moisture contamination during clinical placement<sup>9</sup> and desiccation<sup>10,11</sup> during the early stages of the setting reaction. In an attempt to improve the setting characteristics of GIs, Wilson et al.<sup>12</sup> investigated the role of a third component, a chelating agent, in the setting reaction using citric acid, salicylic acid, acetylone, sequestric acid, polyglycol and tartaric acid. The results for tartaric acid were promising<sup>12</sup> and proved to be 'effective beyond all expectations'.<sup>3</sup> Tartaric acid lengthened the working time,<sup>12</sup> shortened the setting time,<sup>13,14</sup> increased the compressive fracture strength (CFS)<sup>14</sup> and increased the resistance to acid dissolution.<sup>3</sup>

A subsequent version of ASPA-I containing tartaric acid, the G-200 glass and polyacrylic acid (ASPA-II) showed favourable handling characteristics when used as a pit and

fissure sealant.<sup>15</sup> Interestingly, the discovery of the role of tartaric acid in the setting reaction provided opportunities for the use of glasses other than G-200. However, changes to the liquid component of ASPA-II were required due to gelation of the polyacrylic acid homopolymer<sup>16</sup> which prompted investigations into the use of a methanol containing modification (ASPA-III) and later a further variant containing a copolymer of acrylic and itaconic acids (ASPA-IV).<sup>17,18</sup> Thereafter, the use of the acronym 'ASPA' as a generic term was abandoned and confined to coding experimental materials developed at the LGC.<sup>3</sup> ASPA-IV was the first commercial GI material, launched by the Amalgamated Dental Company (Dentsply DeTrey, Konstanz, Germany) as a hand-mixed GI cement in 1975 under the trade name 'ASPA'.<sup>19</sup> When five dental nurses and one dentist were asked to hand-mix the ASPA material in a clinical simulation study, Mount and Makinson<sup>20</sup> identified a wide range of powder:liquid mixing ratios below that specified by the manufacturer. On average, 85% (by weight) of the manufacturers recommended powder content was incorporated by the operators, although powder contents as low as 42% (by weight) were identified.<sup>20</sup> As a result of the difficulties in operators reproducing the manufacturers powder:liquid mixing ratio in a clinical simulation, Dentsply DeTrey launched an encapsulated version of ASPA in 1978<sup>21</sup> which eliminated operator induced variability in proportioning the powder and liquid constituents.

Today a wide variety of commercial hand-mixed and encapsulated GIs are available to the general dental practitioner for clinical use as luting agents, liners and bases for placement under amalgam restorations or the restoration of anterior and posterior dentition. GIs are routinely supplied in two presentational forms: as a separate glass powder and polyacid liquid<sup>7</sup> or as a blend of glass powder and vacuum-dried polyacid which is mixed with distilled water or a solution of tartaric acid termed 'anhydrous' GIs.<sup>22,23</sup> The handling characteristics and mechanical properties of commercial GI products have been optimised by the manufacturers through developments in the glass powder and polyacid liquid constituents used in the GI formulations.

## 2. Developments in GI powder

GIs are composed of an ion leachable glass powder and a polyacid liquid which are mixed together using a predetermined powder:liquid mixing ratio to form a solid mass on setting. The GI powder is prepared from an aluminosilicate glass which serves as a source of ions for the cement forming reaction.<sup>24,25</sup> The glass composition controls the setting rate of the cement forming reaction<sup>26,27</sup> and the refractive index match to the polysalt matrix dictates the translucency of the set GI.<sup>28</sup> The glass component is prepared by sintering mixtures of powdered silica (SiO<sub>2</sub>), alumina (Al<sub>2</sub>O<sub>3</sub>), cryolite (Na<sub>3</sub>AlF<sub>6</sub>), aluminium trifluoride (AlF<sub>3</sub>), fluorite (CaF<sub>2</sub>) and aluminium phosphate (AlPO<sub>4</sub>) at 1100–1500 °C depending upon the chemical composition of the glass.<sup>27</sup> The glass melt is shock quenched in water, the resultant coarse glass frit is ground using a ball mill and sieved to form a powder with a maximum particle size of 45 µm for GI restoratives and 15 µm for GI luting cements.<sup>27</sup>



## 2.1. Glass composition

For the earliest experimental GI (ASPA-I), the 200th glass composition (G-200) ( $\text{SiO}_2\text{-Al}_2\text{O}_3\text{-AlF}_3\text{-CaF}_2\text{-NaF-AlPO}_4$ ) investigated by Wilson and Kent<sup>7</sup> served as the powder component and was high in fluoride and calcium. G-200 was unique in that it was the only glass composition at the time of the development of GIs that was capable of forming a clinically usable GI when mixed with a 50% polyacrylic acid solution in the absence of a reaction controlling additive.<sup>3</sup> However, John McLean expressed concerns regarding the poor aesthetics and sluggish set when ASPA-I was employed clinically. The poor aesthetics were attributed to the poor translucency of G-200 owing to the high fluoride content which made the glass heavily opal.<sup>3</sup> The setting characteristics of ASPA-I were improved with the discovery of the role of tartaric acid as a reaction controlling additive<sup>12–14</sup> which prolonged the working time<sup>12</sup> by inhibition of the initial set by preventing the formation of calcium polyacrylate,<sup>29</sup> thereby allowing the GI to retain fluidity for an extended duration.<sup>30</sup> Tartaric acid was also reported to sharpen the final set through acceleration of the rate of formation of aluminium polyacrylate.<sup>13,29</sup>

Following the discovery of the role of tartaric acid in the setting reaction,<sup>12–14</sup> GI glass formulations were no longer restricted to the opal G-200, providing opportunities for the use of more translucent glasses to produce aesthetic GIs. Consequently, a large number of potential glass formulations<sup>26–28,31</sup> were identified for use as the powder component of GIs which were usually based on calcium aluminosilicates ( $\text{SiO}_2\text{-Al}_2\text{O}_3\text{-CaO}$ ) or calcium fluoroaluminosilicates ( $\text{SiO}_2\text{-Al}_2\text{O}_3\text{-CaF}_2$ ). The presence of fluoride in the glass system was advantageous as it lowered the fusion temperature by disrupting the glass network<sup>26,28,32,33</sup> and allowed for the employment of a more economical fusion temperature when preparing glasses for commercial exploitation. The fluoride content in glasses increased the CFS,<sup>26</sup> improved the translucency of the mixed GI<sup>28,32</sup> and apparently inhibited caries formation when placed clinically.<sup>34,35</sup> In high fluoride containing glasses, fluorine is lost from the glass melt as silicon tetrafluoride ( $\text{SiF}_4$ ) and aluminium trifluoride ( $\text{AlF}_3$ ) which may hydrolyse to form hydrofluoric acid (HF),  $\text{SiO}_2$  and  $\text{Al}_2\text{O}_3$ .<sup>32</sup> HF is corrosive towards furnace linings and crucibles, while the  $\text{SiO}_2$  and  $\text{Al}_2\text{O}_3$  form a crust on the surface of the glass which has to be removed manually. The fluorine loss during glass manufacture resulted in variability in the pre- and post-sintered glass composition which changed the alumina:silica ratio in the glass. Wood and Hill<sup>32</sup> highlighted that the loss of fluorine during glass manufacture was not accounted for in the wide range of high fluoride glasses reported by Kent et al.<sup>26</sup> and Wilson et al.<sup>31</sup> which led to difficulties in correlating the chemical composition of the glasses with the mechanical properties reported for the resultant GIs.<sup>32</sup> The authors identified the addition of a basic oxide (CaO) to a fluoride containing aluminosilicate glass decreased fluorine loss from the glass melt and enabled the production of glasses with a more controlled composition following sintering.<sup>32</sup>

Novel glass compositions based on aluminoborate glasses were trialled as an alternative to aluminosilicates,<sup>36–38</sup> although the rationale for studying borate glasses was unclear owing to the known solubility of borate species.<sup>39</sup> The authors

reported that the reactivity of aluminoborate glasses varied with alumina content and the addition of 5% tartaric acid resulted in GI formulations with adequate setting characteristics and increased CFS and diametral tensile strength (DTS) values.<sup>36–38</sup> However, GIs formulated from aluminoborate glasses were hydrolytically unstable when compared with aluminosilicate glasses.<sup>37</sup> Darling and Hill<sup>39</sup> reported zinc silicate glasses based on  $\text{CaO-ZnO-SiO}_2$ ,  $\text{R}_2\text{O-ZnO-SiO}_2$  and  $\text{Al}_2\text{O}_3\text{-ZnO-SiO}_2$  glass systems. The zinc silicate glasses were prepared with increased amounts of zinc oxide and silica and minor amounts of the third oxide. The authors identified that hydrolytically stable GIs could be formed from the  $\text{Al}_2\text{O}_3\text{-ZnO-SiO}_2$  but not the  $\text{CaO-ZnO-SiO}_2$  and  $\text{R}_2\text{O-ZnO-SiO}_2$  glass systems.<sup>39</sup> For the zinc silicate glasses, the cement forming ability was dictated by the network connectivity of the glass and not the alumina:silica ratio. Consequently, the zinc silicate glass reported<sup>39</sup> had an alumina:silica ratio of 1:9 which had previously been proposed as being too low for GI cement formation.<sup>1,27</sup> However, the maximum CFS value of 93 MPa reported for the zinc silicate glasses<sup>39</sup> was inadequate for the International Organisation for Standardisation (ISO) CFS requirement of 100 MPa.<sup>40</sup> Aluminoborate<sup>36–38</sup> and zinc silicate glasses<sup>39</sup> could therefore not be advocated as alternatives to the aluminosilicate glasses for the commercial exploitation as practical GIs. The powder components of commercial GI products are composed of complex multi-component glasses. The G-388 glass composition was a multi-component translucent glass ( $\text{SiO}_2\text{-Al}_2\text{O}_3\text{-AlF}_3\text{-CaF}_2\text{-NaF-AlPO}_4$ ) used in the early commercial GIs and contained significant quantities of phosphorus, fluorine and alkali metals.<sup>41</sup> Commercial glasses also contained strontium, barium or lanthanum ions to impart radiopacity for increased detection and contrast with dental tissues and other restorative materials on dental radiographs.<sup>42</sup> Strontium has been reported as an ideal candidate for the replacement of calcium in the glass structure due to a similar ionic radius, whereby strontium replaces calcium without disrupting the glass network or loss of translucency of the glass.<sup>43</sup> Griffin and Hill<sup>41,44</sup> investigated multi-component fluorophosphoaluminosilicate glasses ( $\text{SiO}_2\text{-Al}_2\text{O}_3\text{-CaO-P}_2\text{O}_5\text{-CaF}_2$ ) and highlighted that the reactivity of the multi-component glasses used in commercial GIs was not solely dictated by acid hydrolysis of the aluminium-oxygen-silicon bonds but also by hydrolysis of the phosphorus-oxygen bonds.

Today commercially available GIs are supplied by numerous manufacturers and are composed of zinc containing (Chemfil Rock; Dentsply DeTrey),<sup>45</sup> lanthanum containing (Ketac Molar; 3M ESPE, St. Paul, MN, USA)<sup>46</sup> or strontium containing (Fuji IX; GC Corporation, Tokyo, Japan and Ionofil Molar; Voco GmbH, Cuxhaven, Germany)<sup>47,48</sup> calcium fluoroaluminosilicate glasses. The reactivity of a commercial GI glass powder with the corresponding GI liquid is determined by the chemical composition,<sup>26,28</sup> glass fusion temperature,<sup>27</sup> surface treatment through acid washing<sup>49</sup> and the powder particle size,<sup>50</sup> however, these specific details are never routinely supplied by manufacturers. The glass variables (composition, fusion temperature, surface treatment, particle size) are tailored by each manufacturer for specific GI formulations. The liquid component in commercial GIs differs in acid constituent (homopolymers of acrylic acid and

copolymers of acrylic and itaconic or maleic acids) with varying acid molecular weights and concentrations being routinely used. Modification of the setting time is controlled by the addition of tartaric acid at various concentrations. It is therefore imperative that a specific dental manufacturer's GI glass powder is only used with the appropriate GI liquid for that product to ensure an adequate chemical reaction between the constituents for optimum clinical performance.

### 3. Developments in GI liquid

The liquid component of the earliest experimental GI (ASPA-I) was composed of an acrylic acid homopolymer solution (50% by mass)<sup>16</sup> which had poor working and setting characteristics and was susceptible to gelation due to formation of intermolecular hydrogen bonds between the polymer chains.<sup>16</sup> To improve the handling characteristics, tartaric acid (5% by mass) was added to the acrylic acid homopolymer (47.5% by mass) to form ASPA-II<sup>51</sup> which improved the working and setting characteristics. Conversely, the tartaric acid modified GI liquid suffered from an inadequate shelf life which was limited to 10–30 weeks<sup>51</sup> such that the gelation of the liquid component made it unfeasible for commercial exploitation.<sup>51</sup> To reduce gelation, methanol (5% by mass) was added to the acrylic acid homopolymer (45.25% by mass) (ASPA-III) which reduced intermolecular hydrogen bond formation between the polymer chains and delayed gelation.<sup>16</sup> Esterification of some of the carboxylic acid groups of the acrylic acid polymer chain by methanol also resulted in an extended setting time for the mixed cement.<sup>51</sup> However, GIs prepared using the methanol containing liquid of ASPA-III discoloured when placed clinically<sup>28</sup> and further investigations were abandoned.

#### 3.1. Acrylic acid and itaconic or maleic acid copolymers

Crisp and Wilson<sup>52</sup> suggested that copolymers of acrylic acid with other unsaturated carboxylic acids (itaconic acid and maleic acid) would reduce intermolecular hydrogen bonding owing to their reduced stereoregularity when compared with homopolymers of acrylic acid. The reduced intermolecular hydrogen bonding observed in these copolymers was attributed to a higher degree of cross-linking due to the presence of two carboxyl groups in the copolymer structures. The authors developed an aqueous solution of acrylic acid and itaconic acid (47.5% by mass) copolymers with tartaric acid (5%) which was used in ASPA-IV and resulted in a GI liquid solution that was resistant to gelation in solution.<sup>18,52</sup>

Consequently, the first commercially available GI (ASPA) contained the acrylic acid and itaconic acid copolymer formulation developed for ASPA-IV.<sup>17</sup> Copolymers of acrylic acid and maleic acid have been reported in the liquid component of Chelon Fil (ESPE GmbH, Seefeld, Germany),<sup>53,54</sup> Ketac Fil (ESPE GmbH)<sup>53,55–57</sup> and Ketac Molar (ESPE GmbH).<sup>56,57</sup> Investigating the influence of long term water storage of GIs on the CFS<sup>53</sup> and biaxial flexure strength (BFS),<sup>55</sup> investigators<sup>53,55</sup> identified GIs based on copolymers of acrylic acid (Chelon Fil and Ketac Fil) were more susceptible to strength decreases on ageing compared with GIs based on homopolymers of acrylic acid (Chemfil II; Dentsply DeTrey and

Opusfil W; Davis Schottlander and Davis, London, UK) owing to the greater susceptibility of the copolymers to hydrolysis. Nicholson and Abiden<sup>54</sup> suggested the decrease in CFS of the copolymer containing GIs, compared with GIs based on homopolymers on long term water storage, was a consequence of the high cross-linking density of copolymers rather than hydrolysis<sup>53,55</sup> which caused the GIs to become more brittle on ageing.<sup>54</sup>

#### 3.2. GIs as thermoplastic polymers

Using dynamic mechanical thermal analysis, Hill et al.<sup>58</sup> identified GIs as thermoplastic polymer composites by the presence of sharp loss peaks indicative of continually breaking and reforming ionic cross-links. Hill et al.'s<sup>58</sup> observation was supported by Gonzalez<sup>59</sup> who suggested a limited lifetime for ionic cross-links in polystyrene sulfonate ionomers. In the melt and glassy state, most polymers exist in the form of chain-like molecules oriented in a random coil configuration.<sup>60</sup> During deformation and fracture, the chains must be stretched for chain scission to occur whereby the chains must be securely held at the ends.<sup>58,61,62</sup> Edwards<sup>63</sup> proposed the entanglement theory where a polymer chain was viewed as being contained within a tube formed by the neighbouring chains as opposed to forming physical entanglement knots (Fig. 1). Analysing the Brownian motion of a chain within the tube, de Gennes<sup>64</sup> derived mathematical expressions for the rate of motion of the chain along its tube. It was proposed that the lateral movement of the chain was limited by the proximity of the neighbouring chain entanglements and longitudinal movement was restricted by the interactions of

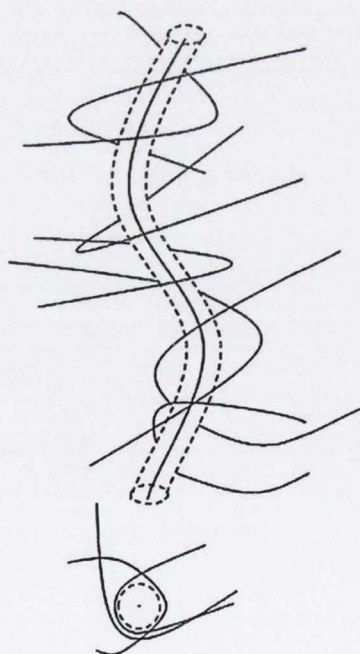


**Fig. 1 – A schematic representation of an idealised model of a polymer chain confined in a tube of three-dimensional entanglements that gives rise to the entanglement theory. Adapted from Prentice.<sup>61</sup>**

polar side groups between neighbouring chains.<sup>58,62</sup> The motion of a polymer chain within a tube of entanglements resembles that of a snake, such that the model became known as the reptation model. The entanglement theory or the reptation model has been successfully applied to polymer diffusion, viscosity and fracture. The application of the reptation model to the fracture of GIs may be considered inquisitive, however, the fracture of GIs is essentially fracture of the polymer matrix phase suggesting the reptation model to be pertinent to the GI system.

The polymer chains in an unstressed specimen are embedded in both sides of the fracture plane of a propagating crack.<sup>61</sup> As the crack propagates, the chain will be 'pulled out' from the side of the plane containing the shorter portion of the chain length<sup>61</sup> (Fig. 2). The surface energy per unit area of a fracture plane is proportional to the square of the length of the chain, such that a critical polymer chain length exists which corresponds to the critical molecular weight of the polymer ( $M_c$ ). At  $M_c$ , the stress required to pull-out the chain contained within a tube would be greater than the stress required to break the carbon-carbon bond of the polymer backbone.<sup>58,61</sup> Therefore, chain pull-out was proposed as the dominant failure mechanism below  $M_c$  while chain scission was the dominant failure mechanism above  $M_c$ .<sup>58,62</sup> Applying a simple power law viscous model for polyacrylic acid based on the analyses reported by Prentice,<sup>61</sup> Hill et al.<sup>58</sup> proposed the  $M_c$  for an anhydrous polyacrylic acid to be approximately 100,000. The authors also proposed that a critical entanglement molecular weight ( $M_e$ ) existed below which the polymeric constituent in the resultant GI would fail to form

entanglements.<sup>58</sup> Hill et al.<sup>58</sup> proposed the  $M_e$  for an anhydrous polyacrylic acid to range from 7000 to 21,000.

### 3.3. Molecular weight and concentration of polyacrylic acid

A limited number of studies have reported the influence of polyacid concentration<sup>65–70</sup> and molecular weight<sup>58,62,67–74</sup> on the performance of GIs. Initial studies<sup>65,71,72</sup> assessed the polyacrylic acid concentration and molecular weight simultaneously which makes interpretation of the results difficult. In addition, the authors manipulated the polyacid concentration and molecular weight groups with varying powder:liquid mixing ratios to maintain a workable consistency which further complicated interpretation of the reported results.<sup>65,71</sup> The reported strength data did, however, highlight a trend towards an increase in DTS,<sup>65,71</sup> CFS<sup>65,71</sup> and three-point flexure strength (TFS)<sup>72</sup> on increasing polyacid concentration and molecular weight.

Wilson et al.<sup>62</sup> investigated increasing the polyacid molecular weight (11,500–1,080,000) of GIs prepared with a commercial GI glass powder on the setting rate, acid erosion rate, fracture toughness ( $K_{IC}$ ) and wear resistance. The authors highlighted the polymer chain length as a crucial parameter in the formulation of GIs and concluded that the higher the molecular weight of the polyacid, the better the GI performance.<sup>62</sup> Wilson et al.'s<sup>62</sup> observations were supported by the findings of Hill et al.,<sup>58</sup> Griffin and Hill<sup>73</sup> and Fennell and Hill,<sup>67</sup> who reported a progressive increase in the  $K_{IC}$ <sup>58</sup> and CFS<sup>67,73</sup> with increasing molecular weights – although the studies were limited to anhydrous GIs. For the anhydrous GIs, the polyacrylic acid was vacuum-dried and added to the GI glass powder prior to mixing with a tartaric acid solution. To initiate the setting reaction, the vacuum-dried polyacrylic acid was required to dissolve in the available water, thereby retarding the setting reaction and allowing for the use of polyacrylic acids with higher molecular weights.<sup>58,62,67,73</sup>

The majority of commercially available GIs are routinely supplied as separate glass powder and polyacid liquid components where the polyacid is usually prepared by a free-radical polymerisation of the polymer in an aqueous solution at a concentration of 40–50%.<sup>27</sup> Attempts at improvements in the mechanical properties of GIs through modification of the liquid component have included the development of copolymers of acrylic acid with itaconic acid<sup>18,28,52,75</sup> or maleic acid,<sup>53–57,76</sup> the use of high molecular weight polyacid solutions<sup>70,71</sup> and concentrations<sup>65,70</sup> and the use of polyacrylic acid molecular weight mixtures.<sup>74</sup> Dowling and Fleming<sup>70</sup> investigated polyacrylic acid liquid solutions of varying molecular weights (ranging from 5000 to 200,000) over a range of concentrations (10–60%) which were hand-mixed with a commercial GI glass powder (Ionofil Molar) at the manufacturers recommended powder:liquid mixing ratio (4:1 g:g). The authors identified an optimum polyacrylic acid concentration in solution for individual polyacrylic acid molecular weights where the CFS and elastic moduli of the resultant GIs were maximised and above which the CFS and elastic moduli decreased.<sup>70</sup> At reduced polyacrylic acid concentrations, cross-linking between polymer chains during setting was hindered due to a greater distance between the

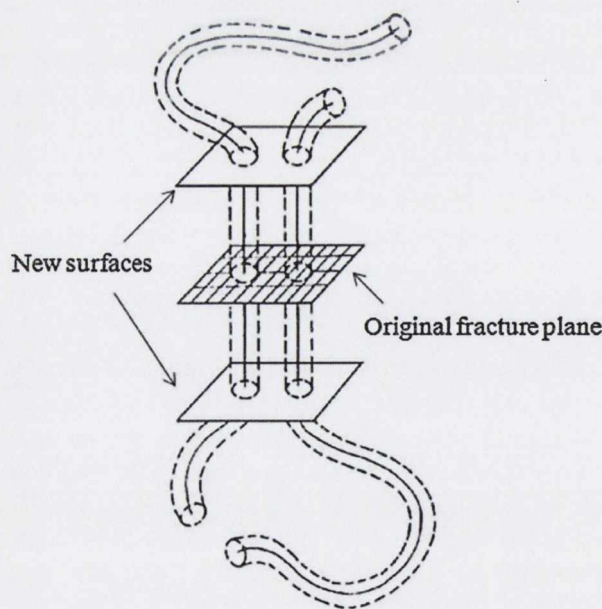


**Fig. 2 – A schematic representation of the 'pull-out' process in the formation of new surfaces during fracture, where the polymer chain will be pulled out from the side of the fracture plane containing the shorter portion of the chain length.**

Adapted from Prentice.<sup>61</sup>

polymer molecules<sup>66</sup> resulting in a decreased CFS and elastic modulus for the GI.<sup>70</sup> At increased polyacrylic acid concentrations, the increased density of the polyacrylic acid chains resulted in increased cross-linking between the polyacid chains and chain entanglements<sup>58,62</sup> leading to a progressive increase in CFS and elastic modulus.<sup>70</sup> However, the concentration and molecular weight of the polyacid solution employable were limited by the resultant increase in the viscosity of the polyacrylic acid solution<sup>65,70,71</sup> such that a balance existed between the polyacid concentration, molecular weight and viscosity to achieve an improved GI for practical use.<sup>70</sup> The increase in viscosity associated with increased concentration and molecular weight exacerbates the difficulties associated with hand-mixing for conventional polyacrylic acid solutions when compared with anhydrous GI formulations which employ water or weak tartaric acid solutions.<sup>14,58</sup> Consequently, Dowling and Fleming<sup>70</sup> proposed the  $M_c$  (80,000) and  $M_e$  (5000) for polyacrylic acid solutions used for conventional GI formulations to be lower when compared with the  $M_c$  (100,000) and lower bound  $M_e$  (7000) theoretically predicted by Hill et al.<sup>58</sup> for GIs prepared using anhydrous polyacrylic acid. This observation<sup>70</sup> confirmed Hill et al.'s<sup>58</sup> suggestion that the predicted  $M_c$  would decrease where there were 'strong intermolecular interactions' existing between the polymer chains.

Despite the optimisation of the GI liquid component, mixed GIs remain too weak to be 'truly' advocated for clinical use as posterior restoratives. Numerous attempts have been made to enhance the mechanical properties of GIs through reinforcement of the GI powder or liquid constituent with variously reported levels of success.

#### 4. Strategies of reinforcement

Since the introduction of ASPA to the dental market in the early 1970s, the GI powder and liquid constituents have undergone significant changes in chemical make-up. As a result, the range of clinical applications has expanded from luting cements to cavity liners or bases and restorative materials. The major advantage of GIs over dental amalgam and resin-based composites (RBCs) for the restoration of natural dentition is the ability of GIs to chemically bond to sound tooth structure.<sup>77,78</sup> In addition, fluoride release from GI restorations has been claimed to be therapeutic for prevention of secondary caries.<sup>34,35</sup> Despite these clinical advantages, GIs cannot 'truly' be advocated for the restoration of posterior dentition due to the poor mechanical properties when compared with dental amalgam and RBCs. To improve the mechanical properties of GIs and enable their clinical use posteriorly, attempts have been made to reinforce the GI matrix through the addition of various filler types to the GI powder component. The fillers used included fibres,<sup>79–83</sup> metallic powders,<sup>79,84–95</sup> hydroxyapatite powders,<sup>96–100</sup> bioactive glass particles<sup>101</sup> and montmorillonite clay additions.<sup>102,103</sup>

##### 4.1. Fibres

Sced and Wilson<sup>79</sup> investigated the addition of carbon and alumina fibres to a commercial GI powder (Chembond;

Dentsply DeTrey) on the flexural strength of bar-shaped GI specimens (25 mm length, 3 mm width, 3 mm thickness) prepared in accordance with the British Standard.<sup>104</sup> The fibre lengths were >1000  $\mu\text{m}$  with fibre diameters ranging from 10 to 200  $\mu\text{m}$ . The reinforcing fibres were incorporated into the GI powder at 25 vol%, hand-mixed with the appropriate GI liquid (Chembond) and compared with the hand-mixed Chembond control group. The authors reported an increase in the mean flexure strength value from 10 MPa for the GI control group (Chembond) to 53 MPa and 44 MPa for the GIs prepared with carbon and alumina fibre additions, respectively.<sup>79</sup>

Eleven years later, the addition of carbon fibres (250–1000  $\mu\text{m}$  length, 8  $\mu\text{m}$  diameter, ICI Ltd., Cheshire, UK) and alumina fibres (500  $\mu\text{m}$  length, 3  $\mu\text{m}$  diameter, ICI Ltd.) to experimental GI glass systems, namely MP-4 (Pilkington Bros., Lancashire, UK) and G-338 (LGC, London, UK) glasses was reported<sup>80</sup> whereby the fibres were added to the GI glass powders at 0–20 vol% (in 2.5 vol% increments). Appropriate amounts of freeze-dried polyacrylic acid powder were added to the GI powder-fibre blend prior to mechanically mixing to obtain an 'even distribution' of powders.<sup>80</sup> The dry-blended powder was hand-mixed with water (powder:liquid mixing ratio not reported) and cylindrical bar-shaped specimens (4.5 mm diameter, length not reported) were prepared and tested following 24 h water storage using a four-point flexure test assembly. An increase in four-point flexural strength value for 5 vol% carbon fibres addition to MP-4 (45 MPa) and G-338 (30 MPa) glass powders was reported although the flexural strength values for the unreinforced GIs were not reported.<sup>80</sup> Alumina fibre incorporation was reported to increase the brittleness of the reinforced GIs.<sup>80</sup>

The addition of short glass fibres ( $\text{CaO-P}_2\text{O}_5\text{-SiO}_2\text{-Al}_2\text{O}_3$ ) of varying lengths (33.5–100.4  $\mu\text{m}$ ) and diameters (9.7–21.5  $\mu\text{m}$ ) to a commercial hand-mixed GI powder (HY Bond Glasionomer CX; Shofu Inc., Fukuine, Kyoto, Japan) was reported by Kobayashi et al.<sup>81</sup> Short glass fibre concentrations ranging from 0 to 100 wt% (in 20 wt% increments) were incorporated into the GI powder and the blended powder was hand-mixed with the appropriate GI liquid (HY Bond Glasionomer CX) at a powder:liquid mixing ratio of 2:1 g/g. Disc-shaped DTS specimens (6 mm diameter, 3 mm thickness:  $n = 7$ ) and bar-shaped TFS specimens (25 mm length, 6 mm width, 3 mm thickness:  $n = 7$ ) were prepared and tested following 24 h water storage. Increasing the short glass fibre wt% from 0 to 60% (in 20 wt% increments) resulted in an increase in the mean DTS value from 11 MPa (commercial GI) to 18 MPa (60 wt% short glass fibre addition) and mean TFS value from 8 MPa (commercial GI) to 35 MPa (60 wt% short glass fibre addition). Further short glass fibres addition (>60 wt%) resulted in a deterioration in the mean DTS and TFS values compared with the commercial GI formulation.

The  $K_{IC}$  of a 10, 20 and 30 wt% glass fibre (GC Corporation) blended with a hand-mixed commercial GI powder (Fuji I; GC Corporation) was reported by Lucksanasombool et al.<sup>82</sup> The glass fibre diameters ranged from 20 to 100  $\mu\text{m}$  even-though the fibre lengths were not reported. The GI powder and glass fibres were hand-mixed with the Fuji I liquid at 1.8:1 g/g and single-edge notched (SEN) bend specimens (dimensions not reported) were prepared in accordance with the American Society for Testing and Materials (ASTM) 399.<sup>105</sup> The specimens

were loaded in a three-point flexure test assembly following storage for 1 week in physiologically buffered saline.<sup>83</sup> The authors identified a decrease in the  $K_{IC}$  value for Fuji I ( $0.48 \text{ MN m}^{-1.5}$ ) with increasing glass fibre addition to  $0.35 \text{ MN m}^{-1.5}$  at the 30 wt% blend which was attributed to increased porosity during glass fibres incorporation on blending.<sup>82</sup>

$\text{SiO}_2\text{-Al}_2\text{O}_3\text{-CaO-NaF-AlF}_3\text{-Na}_3\text{AlF}_6$  glass fibres addition ( $580 \pm 160 \mu\text{m}$  length,  $26 \mu\text{m}$  diameter) to a variety of experimental GI glass powders were also reported.<sup>83</sup> CFS specimens (6 mm height, 4 mm diameter:  $n = 15$ ) were prepared by hand-mixing powders prepared from a series of nine experimental glasses with a GI liquid (40–45 wt% polyacrylic acid with 8–10 wt% tartaric acid solution) to determine the optimum powder particle size ( $2.4\text{--}12.2 \mu\text{m}$ ), glass surface treatment (acid washing and heat treatment), powder:liquid mixing ratio (1.5:1–2.8:1 g:g) and glass fibre fraction (20, 40, 60 vol%). Under the optimum conditions ( $2.4 \mu\text{m}$  powder particle size, 7 h acid washing in 3% HCL glass surface treatment, 6 h heat treatment at  $360^\circ\text{C}$ , powder:liquid mixing ratio of 1.8:1 g:g, 20 vol% glass fibre fraction), bar-shaped specimens (25 mm length, 2 mm width, 2 mm thickness:  $n = 15$ ) were prepared and loaded in a four-point flexure assembly following 24 h water storage. The authors reported a significant increase in the four-point flexural strength values for the fibre reinforced GI ( $16 \pm 2 \text{ MPa}$ ) when compared with the unreinforced control ( $10 \pm 1 \text{ MPa}$ ).<sup>83</sup>

With respect to fibre incorporation in GI powders, the aspect ratio (fibre length:diameter), chemical composition, reinforcing addition filler volume fraction, composition of the GI powder and liquid and the powder:liquid mixing ratios employed were markedly different for the studies reporting fibre reinforcement of GIs,<sup>79–83</sup> such that a direct comparison under controlled conditions was not possible.

#### 4.2. Metallic powders

Researchers have investigated the influence of the addition of a range of metallic powders (aluminium,<sup>79</sup> chromium,<sup>79</sup> nickel–aluminium alloy,<sup>79</sup> silver–tin alloy,<sup>79,84–86,90–92</sup> stainless-steel [93]) and titanium dioxide<sup>94,95</sup> to GI powders. In addition, enhancement of the mechanical properties of GIs with fused silver, gold or palladium has been investigated by dental researchers and manufacturers.<sup>87–89,92</sup>

Sced and Wilson<sup>79</sup> reported a flexure strength value for Chembond of 10 MPa while the addition of aluminium (21 MPa), chromium (22 MPa), nickel–aluminium alloy (22 MPa) and silver–tin alloy (40 MPa) enhanced the flexure strength values of the metallic reinforced Chembond GI. No details of the wt% metallic additions were provided although the poor polishability and aesthetics of the silver–tin alloy reinforced GI restorations precluded their clinical usage.<sup>27,106</sup>

The addition of a spherical amalgam alloy powder (Lumi Alloy; GC Corporation) to Fuji II (GC Corporation) was proposed by Simmons<sup>84,85</sup> and a variant was subsequently marketed as Miracle Mix in 1983 by the GC Corporation.<sup>92</sup> Miller et al.<sup>86</sup> investigated the CFS of cylindrical Miracle Mix specimens (12 mm height, 6 mm diameter) prepared at GI powder:spherical amalgam alloy powder ratios from 5:1 to 8:1 g:g at 1 and 24 h. An increase in mean CFS value of Miracle Mix at 1 h ( $104 \pm 7 \text{ MPa}$ ) and 24 h ( $197 \pm 12 \text{ MPa}$ ) was identified when

compared with Fuji II (65 MPa and 151 MPa, respectively).<sup>86</sup> An increased 24 h mean CFS (148 MPa) and mean DTS (15 MPa) values for cylindrical Miracle Mix specimens (6 mm height, 3 mm diameter:  $n = 5$ ) compared with Fuji II (143 MPa and 12 MPa, respectively) were also reported.<sup>90</sup> Interestingly, no difference in the 24 h mean CFS value ( $120 \pm 15 \text{ MPa}$ ) for cylindrical Miracle Mix specimens (12 mm height, 6 mm diameter:  $n = 4\text{--}10$ ) was identified compared with Fuji Ionomer II (GC Corporation) ( $120 \pm 10 \text{ MPa}$ ).<sup>91</sup> However, an increase in the 24 h mean TFS value was evident for bar-shaped Miracle Mix specimens (25 mm length, 4 mm width, 2 mm thickness:  $n = 4\text{--}10$ ) when compared with Fuji Ionomer II ( $25 \pm 3 \text{ MPa}$  and  $18 \pm 1 \text{ MPa}$ , respectively).<sup>91</sup> Cylindrical CFS (12 mm height, 6 mm diameter:  $n = 6$ ), disc-shaped DTS (8 mm diameter, 4 mm thickness:  $n = 6$ ), bar-shaped TFS (22 mm length, 2 mm width, 2 mm thickness:  $n = 6$ ) and disc-shaped BFS specimens (15 mm diameter, 1 mm thickness:  $n = 6$ ) of Miracle Mix and Fuji II were tested following 24 h water storage.<sup>92</sup> No increase in the mean CFS and DTS values was identified but the mean TFS and BFS values of Miracle Mix ( $40 \pm 10 \text{ MPa}$  and  $32 \pm 10 \text{ MPa}$ , respectively) were increased when compared with Fuji II ( $36 \pm 3 \text{ MPa}$  and  $25 \pm 6 \text{ MPa}$ , respectively).<sup>92</sup> The increased TFS values for Miracle Mix containing the metal filler, when compared with the conventional GI (Fuji II) were attributed to the change in fracture mode from ductile failure (Miracle Mix) to brittle failure (Fuji II).<sup>91</sup> Although the addition of metal filler changed the fracture mode, it is unlikely that chemical interfacial bonding occurred between the metal filler and the GI matrix<sup>107</sup> which would be required to produce a 'true' composite material with improved mechanical properties.

Experimental stainless-steel powder (mean particle size  $9 \mu\text{m}$ ) reinforced GIs were investigated and compared with Miracle Mix.<sup>93</sup> The stainless-steel powder was acid etched, washed with water and methyl alcohol before blending with Fuji II at 17 vol%. Cylindrical CFS and DTS specimens (12 mm height, 6 mm diameter:  $n = 10$ ) were prepared and tested following 24 h water storage. The mean CFS and DTS values of Miracle Mix ( $169 \pm 10 \text{ MPa}$  and  $11 \pm 2 \text{ MPa}$ , respectively) were significantly reduced compared with the stainless-steel reinforced GI ( $268 \pm 15 \text{ MPa}$  and  $23 \pm 2 \text{ MPa}$ , respectively).<sup>93</sup> However, GIs prepared from Miracle Mix and the experimental stainless-steel reinforced powder were not tooth-coloured owing to the presence of alloy powder constituent.

The influence of 3, 5 and 7 wt%  $\text{TiO}_2$  nano-powder (mean particle size 21 nm, Batch MKBC-4174, Sigma Aldrich) addition to Kavitan Plus (SpofaDental; Jičín, Czech Republic) was reported.<sup>94</sup> Cylindrical CFS (6 mm height, 4 mm diameter:  $n = 20$ ), bar-shaped TFS (25 mm length, 2 mm width, 2 mm thickness:  $n = 20$ ) and knife-edge notch  $K_{IC}$  (25 mm length, 5 mm width, 2.5 mm thickness with a reported 2.5 mm notch:  $n = 20$ ) specimens were prepared when the dry-blended powders were hand-mixed with the Kavitan Plus liquid at a powder:liquid mixing ratio of 2.7:1 g:g. Following 24 h water storage, a significant increase in mean CFS value from  $149 \pm 8 \text{ MPa}$  to  $176 \pm 8 \text{ MPa}$ , TFS value from  $14 \pm 3 \text{ MPa}$  to  $23 \pm 3 \text{ MPa}$  and  $K_{IC}$  value from  $0.69 \pm 0.03 \text{ MN m}^{-1.5}$  to  $1.29 \pm 0.05 \text{ MN m}^{-1.5}$  were reported with 3 wt%  $\text{TiO}_2$  nano-powder addition.<sup>94</sup> More recently, Dowling et al.<sup>95</sup> revisited the  $\text{TiO}_2$  powder reinforcement strategy for GIs with the addition of 0.5 to 15 wt% of the same  $\text{TiO}_2$  nano-powder employed

previously<sup>94</sup> to Ionofil Molar which was subsequently mixed with a 40% polyacrylic acid liquid solution at a powder:liquid mixing ratio of 4:1 g:g.<sup>95</sup> Testing the cylindrical CFS specimens (6 mm height, 4 mm diameter:  $n = 20$ ) following 24 h water storage failed to identify any strengthening with the TiO<sub>2</sub> nano-powder inclusion groups which appear to cast doubt on the truly remarkable and almost unbelievable CFS, TFS and K<sub>IC</sub> data reported previously.<sup>94</sup>

The sintering of a precious metal (silver, gold or palladium) with the GI glass constituent was proposed as an alternative approach to metal reinforcement of GIs and was marketed in 1986 by ESPE GmbH as glass-cermet cements under the trade names of Chelon Silver which was hand-mixed and Ketac Silver which was encapsulated.<sup>87,88</sup> The cermet powders were prepared by mixing equal volumes of silver powder (mean particle size 3.5 μm) and a GI glass powder. The blended powders were compressed at 350 MPa to form metal-glass powder pellets which were sintered at 800 °C and ground to fine powder. In an attempt to improve the aesthetics, 5 wt% of titanium dioxide was added and the blended powders were mixed with a 46% solution of acrylic, maleic and tartaric acids at powder:liquid mixing ratios of 4:1 g:g (Chelon Silver) and 4.5:1 g:g (Ketac Silver).<sup>87</sup> Williams et al.<sup>92</sup> compared a conventional hand-mixed GI (Chelon Fil) with Chelon Silver on CFS testing cylindrical specimens (12 mm height, 6 mm diameter:  $n = 6$ ), DTS testing disc-shaped specimens (8 mm diameter, 4 mm thickness:  $n = 6$ ), BFS testing disc-shaped specimens (15 mm diameter, 1 mm thickness:  $n = 6$ ) and TFS testing bar-shaped specimens (22 mm length, 2 mm width, 2 mm thickness:  $n = 6$ ) following 24 h water storage. A reduction in the mean CFS (137 ± 17 MPa), DTS (13 ± 2 MPa), BFS (45 ± 4 MPa) and TFS (29 ± 4 MPa) values was evident for the hand-mixed Chelon Silver when compared with the CFS (147 ± 15 MPa), DTS (19 ± 3 MPa), BFS (36 ± 5 MPa) and TFS (21 ± 3 MPa) values of its hand-mixed conventional GI counterpart (Chelon Fil).<sup>92</sup> When bar-shaped TFS specimens (20 mm length, 2.5 mm width, 2.5 mm thickness:  $n = 10$ ) were tested following 1 week water storage, Walls et al.<sup>89</sup> reported a reduction in both the TFS value from 45 ± 5 MPa to 29 ± 7 MPa and the three-point flexure modulus (TFM) value from 13 ± 2 GPa to 8 ± 4 GPa for Ketac Fil compared with Ketac Silver, namely the encapsulated products. In addition, the cermet materials were not tooth-coloured owing to the silver in the powder constituent<sup>108</sup> which caused discolouration of the cermet restored teeth.<sup>109</sup> The poor aesthetics of cermets limited their range of clinical applications to paediatric and domiciliary dental care.

#### 4.3. Hydroxyapatite

Hydroxyapatite is the primary mineral constituent of enamel and adhesively interacts with GIs.<sup>110,111</sup> The addition of finely divided hydroxyapatite (Bio-Gel HTP, Bio-Rad Laboratories, Richmond, CA, USA) to two experimental glasses MP-4 (Al<sub>2</sub>O<sub>3</sub>-SiO<sub>2</sub>-CaO-Na<sub>2</sub>O at 35.0–28.0–26.0–11.0 wt%) and G-200D (Al<sub>2</sub>O<sub>3</sub>-SiO<sub>2</sub>-NaAlF<sub>6</sub>-CaF<sub>2</sub>-AlF<sub>3</sub>-AlPO<sub>4</sub> at 16.6–29.0–5.0–34.3–5.3–9.9 wt%) was investigated.<sup>96</sup> The hydroxyapatite was substituted at 2.5, 5, 10, 20, 25 wt% for MP-4 and 2.5, 5, 10, 20, 25, 30, 40, 50 wt% for G-200D glass powders and blends were hand-mixed with a 40% solution of polyacrylic acid (Versicol E7, Allied Colloids, Low Moor, Bradford, UK) at a

powder:liquid mixing ratio of 2:1 g:g to prepare cylindrical specimens (12 mm height, 6 mm diameter) for CFS testing following 24 h storage. A progressive deterioration in mean CFS values from 20 ± 1 MPa to 8 ± 1 MPa for MP-4 and from 55 ± 8 MPa to 26 ± 2 MPa for G-200D was evident with increasing hydroxyapatite content.<sup>96</sup>

The influence of addition of hydroxyapatite powder (mean particle size 17 μm) to Fuji IX<sub>GP</sub> was investigated by Yap et al.<sup>97</sup> by substituting 4, 12, 28 vol% hydroxyapatite for the GI powder in the powder compartment of the capsule. The powder mixture was mechanically mixed (HSMI, GC Corporation) at a powder:liquid mixing ratio of 3.6:1 g:g and cylindrical CFS (8 mm height, 4 mm diameter:  $n = 5$ ) and disc-shaped DTS specimens (6 mm diameter, 3 mm thickness:  $n = 5$ ) were prepared. Following water storage for 24 h and 1 week, no difference in mean CFS (142 ± 31 MPa and 177 ± 28 MPa, respectively) or DTS (12 ± 3 MPa and 14 ± 3 MPa, respectively) values for the 4 vol% hydroxyapatite reinforced GIs were observed when compared with the CFS (150 ± 45 MPa and 162 ± 37 MPa, respectively) and DTS (12 ± 2 MPa and 14 ± 4 MPa, respectively) values of the Fuji IX<sub>GP</sub> groups.<sup>97</sup> Further incorporation of the hydroxyapatite powder (12 and 28 vol%) resulted in a marked deterioration in mean CFS and DTS values following 24 h and 1 week water storage.<sup>97</sup>

Substitution of 4, 12, 28 and 40 vol% hydroxyapatite-zirconia powder for the GI powder constituent in Fuji IX<sub>GP</sub> capsules was assessed by Gu et al.<sup>98</sup> by mechanically mixing the powder blend at a powder:liquid mixing ratio of 3.6:1 g:g to prepare cylindrical CFS (8 mm height, 4 mm diameter:  $n = 5$ ) and disc-shaped DTS (6 mm diameter, 3 mm thickness:  $n = 5$ ) specimens following 24 h water storage. The CFS and DTS of the 4 and 12 vol% hydroxyapatite-zirconia powder substituted GI identified no increase in the mean strength values when compared with the Fuji IX<sub>GP</sub> control group.<sup>98</sup> A deterioration in the mean CFS and DTS values was identified when the concentration of hydroxyapatite-zirconia powder substitution was increased to 28 and 40 vol%.<sup>98</sup>

The influence of hydroxyapatite reinforcement of Fuji IX on the K<sub>IC</sub> was investigated using SEN bend specimens (25 mm length, 5 mm width, 2.5 mm thickness with a reported 2.5 mm notch:  $n = 24$ ) by substituting 8 wt% of the Fuji IX powder with hydroxyapatite (particle size 5–20 μm).<sup>99</sup> The GI-hydroxyapatite powder blend was hand-mixed at a powder:liquid mixing ratio of 3.6:1 g:g. Twelve specimens were tested at 15 min and the remaining 12 were tested following 24 h water storage in a three-point flexure assembly. An increase in K<sub>IC</sub> values on hydroxyapatite substitution (8 wt%) at 15 min (0.56 ± 0.10 MN m<sup>-1.5</sup>) and 24 h (0.58 ± 0.09 MN m<sup>-1.5</sup>) was evident when compared with the Fuji IX control group (0.36 ± 0.06 MN m<sup>-1.5</sup> and 0.45 ± 0.06 MN m<sup>-1.5</sup>, respectively).<sup>99</sup>

Hydroxyapatite (5 wt%) and fluoroapatite (5 wt%) powder (particle size 100–200 nm) substitution to Fuji II followed by manual grinding using a mortar and pestle for 20 min prior to hand-mixing at a powder:liquid mixing ratio of 2.7:1 g:g was also investigated.<sup>100</sup> CFS cylinders (6 mm height, 4 mm diameter:  $n = 6$ ), DTS discs (4 mm diameter, 2 mm thickness:  $n = 6$ ) and BFS discs (10 mm diameter, 1 mm thickness:  $n = 6$ ) were tested following 24 h and 1 week water storage. An increase in mean CFS (177 ± 10 MPa and 179 ± 12 MPa), DTS (16 ± 4 MPa and 17 ± 4 MPa) and BFS (26 ± 6 MPa and

28 ± 7 MPa) values for the hydroxyapatite and fluoroapatite substituted GIs, respectively was observed when compared with the CFS (160 ± 12 MPa), DTS (12 ± 3 MPa) and BFS (14 ± 5 MPa) values of the Fuji II control group tested at 24 h. A further increase in CFS, DTS and BFS values was highlighted following 1 week water storage.<sup>100</sup>

#### 4.4. Bioactive glass particles

Bioactive glass particle (S53P4, Vivoxid Ltd., Turku, Finland) substitution of 10 wt% (mean particle size 20 µm) to Fuji II was investigated by Yli-Urpo et al.<sup>101</sup> using a powder:liquid mixing ratio of 1.7:1 g:g, although the authors reported using 'level scoops' when determining the powder:liquid mixing ratio. Cylindrical CFS specimens (6 mm height, 4 mm diameter: n = 6) were stored in water for 1, 3, 7, 14, 30 and 180 days. A deterioration in mean CFS value for the 10 wt% bioactive glass particle substituted GIs (95 ± 20 MPa to 80 ± 15 MPa) was highlighted when compared with the Fuji II control group (120 ± 20 MPa to 105 ± 30 MPa) on testing following 1 and 180 days water storage, respectively.<sup>101</sup>

#### 4.5. Montmorillonite clay

Dowling et al.<sup>102</sup> investigated the addition of two montmorillonite clays, a pristine calcium montmorillonite clay (Ca-MMT) (Süd Chemie, Munich, Germany) and an organically modified 12-amino-dodecanoic acid montmorillonite clay (ADA-MMT) (Nanocor Inc., IL, USA) on the CFS of Chemfil Superior (Dentsply DeTrey). The montmorillonite clays were added to the GI powder at 0.5, 1.0, 1.5, 2.0 and 2.5 wt% and mixed at a powder:liquid mixing ratio of 7.4:1 g:mL to prepare cylindrical CFS specimens (6 mm height, 4 mm diameter: n = 30) prior to testing following 24 h water storage.<sup>102</sup> A progressive deterioration in mean CFS values for the Chemfil Superior control (105 ± 22 MPa) occurred up to 2.5 wt% Ca-MMT clay addition but an increase in CFS values was observed when 0.5 wt% (133 ± 10 MPa) and 1.0 wt% (128 ± 22 MPa) of the ADA-MMT clay were added to Chemfil Superior. The mean CFS values decreased with further ADA-MMT clay addition (1.5–2.5 wt%).<sup>102</sup>

Alternatively, to enhance the mechanical properties of GIs, investigators have also explored modifications of the GI liquid component to increase cross-linking between the polymer chains during the setting reaction. The GI liquid modifications include the formation of novel polyacids<sup>112,113</sup> and the introduction of acrylic and itaconic or maleic acid copolymers containing flexible side chains of amino acids,<sup>114–116</sup> N-vinylpyrrolidone<sup>117–121</sup> or N-vinylcaprolactam.<sup>122,123</sup>

#### 4.6. Novel polyacids

Despite the early investigations regarding the use of copolymers of acrylic and itaconic or maleic acids<sup>18,28,52–57,75,76</sup> and polyacids of increased molecular weights and concentrations,<sup>65,70,71,74</sup> little attention has been paid to the development of novel polyacids in the dental literature. It was not until the early 1990s when the use of polyvinylphosphonic acid (PVPA) as a novel and alternative GI liquid to polyacrylic acid was reported by Wilson and Ellis<sup>112</sup> and Ellis et al.<sup>113</sup> Calcium and aluminium cations (Ca<sup>2+</sup> and Al<sup>3+</sup>) released from

the GI glass powder were suggested to form stronger cross-links between the polyacid chains of PVPA than the cross-links formed between polyacrylic acid chains since unpolymerised dibasic phosphonic acids were stronger acids (pK<sub>a</sub> 2 and 8) than unpolymerised acrylic acid (pK<sub>a</sub> 4.25).<sup>112</sup> These stronger cross-links were expected to result in the formation of GIs with improved mechanical properties when compared with conventional GIs based on polyacrylic acid.<sup>112</sup> The PVPA containing GIs were also proposed to undergo a faster maturation owing to the increased reactivity of PVPA,<sup>113</sup> thereby reducing the susceptibility of PVPA containing GIs to the deleterious effects of moisture contamination<sup>9</sup> and desiccation<sup>10,11</sup> during the initial stages of the setting reaction. However, the more reactive PVPA could not be used as a direct replacement for polyacrylic acid due to the setting time (45 s) when compared with conventional GIs (180–240 s).<sup>112</sup> Deactivation of the reactive glasses by heat treatment and the use of a reaction controlling additive (10 wt% aminotrimethylenephosphonic acid) in the PVPA liquid were necessary to ensure adequate working characteristics for practical clinical usage.<sup>113</sup> Modification of PVPA with 10% zinc fluoride at the preparation stage was proposed to improve the mean CFS of the resultant GIs.<sup>124</sup> Cylindrical CFS specimens (12 mm height, 6 mm diameter: n = 6) were prepared by hand-mixing a 10% zinc fluoride modified PVPA solution and an unmodified PVPA solution with an experimental glass powder. Following 24 h water storage, an increase in the mean CFS value from 121 ± 14 MPa for the GI specimens prepared with the unmodified PVPA solution to 147 ± 10 MPa for the 10% zinc fluoride modified PVPA solution was reported, suggesting reinforcement of the GI was achievable.<sup>124</sup> Employing the same solutions as Akinmade and Braybrook<sup>124</sup> but a different experimental glass powder, testing cylindrical CFS specimens (12 mm height, 6 mm diameter: n = 6) followed by water storage for 1, 7, 30 and 90 days also showed reinforcement.<sup>125</sup> Following 1 and 90 days water storage, the CFS values of the GIs prepared with the unmodified PVPA solution were markedly reduced (84 ± 15 MPa to 112 ± 9 MPa) compared with the 10% zinc fluoride modified PVPA solution (158 ± 15 MPa to 226 ± 35 MPa).<sup>125</sup>

The concept of PVPA containing GIs was explored by one dental manufacturer (Associated Dental Products Ltd., Kempton Works, Wiltshire, UK) in the form of 'Diamond Carve'. Diamond Carve was reported to contain a strontium aluminosilicate glass, freeze-dried copolymer of PVPA and acrylic acid as the powder component which was manipulated with an aqueous solution of polyacrylic acid and tartaric acid at a powder:liquid mixing ratio of 4:1 g:g.<sup>126</sup> On testing disc-shaped BFS specimens (10 mm diameter, 1 mm thickness: n = 6) following 24 h water storage, no improvement in the mean BFS value of Diamond Carve was achieved (36.5 ± 2.9 MPa) compared with the commercial GI restoratives tested (HiFi; Shofu Inc., 40.4 ± 6.7 MPa and Ketac Molar, 44.7 ± 6.0 MPa).<sup>56,57</sup> No clinical study of Diamond Carve is available in the dental literature owing to the poor mechanical performance compared with the commercial GI investigated.

#### 4.7. Modified copolymers

Wilson and McLean<sup>24</sup> highlighted that during the setting reaction of GIs not all of the carboxyl groups on the polymer

backbone of the polyacid were converted to metal carboxylates by the  $\text{Ca}^{2+}$  and  $\text{Al}^{3+}$  ions released from the glass powder. The close attachment of the pendant carboxyl groups to the polymer backbone in the polyacrylic acid homopolymers and copolymers of acrylic and itaconic or maleic acids was proposed to cause steric hindrance which would prevent the conversion of some of the carboxyl groups on the polymer backbone to metal carboxylate complexes (salt bridges) by the  $\text{Ca}^{2+}$  and  $\text{Al}^{3+}$  ions.<sup>115</sup>

*N*-acryloylglutamic acid was used to modify acrylic acid and itaconic acid copolymer solutions at acrylic acid:itaconic acid:*N*-acryloylglutamic acid molar ratios of 10:1:1 and 10:1:4.<sup>115</sup> The modified copolymer solutions were hand-mixed with Fuji II powder at a powder:liquid mixing ratio of 2.7:1 g:g to prepare cylindrical CFS and DTS specimens (12 mm height, 6 mm diameter:  $n = 10$ ), bar-shaped TFS specimens (25 mm length, 3 mm width, 3 mm thickness:  $n = 10$ ) and SEN compact tension  $K_{IC}$  specimens (6.6 mm length, 6.3 mm width, 1.7 mm thickness:  $n = 10$ ) following 24 h and 1 week water storage.<sup>115</sup> GIs prepared with the 10:1:1 and 10:1:4 acrylic acid:itaconic acid:*N*-acryloylglutamic acid molar ratio solutions were compared with Fuji II control group tested at 24 h. The Fuji II control mean CFS (168  $\pm$  11 MPa), DTS (13  $\pm$  2 MPa), TFS (9  $\pm$  2 MPa) and  $K_{IC}$  (0.20  $\pm$  0.04 MN m<sup>-1.5</sup>) values were increased for the acid molar ratio modified solutions with mean CFS (195  $\pm$  11 MPa and 212  $\pm$  9 MPa), DTS (22  $\pm$  2 MPa and 20  $\pm$  3 MPa), TFS (38  $\pm$  4 MPa and 34  $\pm$  3 MPa) and  $K_{IC}$  (0.37  $\pm$  0.02 MN m<sup>-1.5</sup> and 0.39  $\pm$  0.05 MN m<sup>-1.5</sup>) values reported, respectively. A further increase in CFS, DTS, TFS and  $K_{IC}$  values of GIs prepared with the *N*-acryloylglutamic acid modified solutions was identified following 1 week water storage.<sup>115</sup> However, the *N*-acryloylglutamic acid product yield was reported to be too low for commercial exploration.<sup>116</sup> *N*-methacryloylglutamic acid produced a 70% increased yield compared with *N*-acryloylglutamic acid and was therefore proposed for the modification of acrylic acid and itaconic acid copolymers at an acrylic acid:itaconic acid:*N*-methacryloylglutamic acid molar ratio of 7:3:3.<sup>116,119</sup> Cylindrical CFS (12 mm height, 6 mm diameter) and bar-shaped TFS specimens (25 mm length, 3 mm width, 3 mm thickness) were prepared by hand-mixing the modified copolymer solution with Fuji II powder.<sup>116</sup> Following 1 week water storage, the CFS (185  $\pm$  9 MPa) and TFS (15  $\pm$  1 MPa) values of the Fuji II specimens were markedly reduced compared with the CFS (224  $\pm$  8 MPa) and TFS (35  $\pm$  7 MPa) values of GIs prepared from the *N*-methacryloylglutamic acid modified acrylic acid and itaconic acid copolymer solution.<sup>116</sup>

Acrylic acid and itaconic acid copolymer solutions were modified using *N*-vinylpyrrolidone as a flexible spacer in the copolymer backbone at an acrylic acid:itaconic acid:*N*-vinylpyrrolidone molar ratio of 7:1:3.<sup>117</sup> The modified solutions were hand-mixed with Ketac Molar powder at a powder:liquid mixing ratio of 3.1:1 g:g to prepare bar-shaped TFS specimens (25 mm length, 2 mm width, 2 mm thickness:  $n = 6$ ) which were tested following 1 week water storage. *N*-vinylpyrrolidone modification of the acrylic acid and itaconic acid copolymer solutions highlighted a decreased mean TFS value for the Ketac Molar specimens (17  $\pm$  1 MPa) compared with the GI specimens prepared with the *N*-vinylpyrrolidone modified solution (31  $\pm$  3 MPa).<sup>117</sup> Acrylic acid and maleic acid copolymer solutions were modified with *N*-vinylpyrrolidone at acrylic

acid:maleic acid:*N*-vinylpyrrolidone molar ratios of 8:1:1, 7:3:1, 6:4:2 and 5:5:3.<sup>120</sup> Cylindrical CFS (6 mm height, 4 mm diameter:  $n = 6-10$ ), disc-shaped DTS (4 mm diameter, 2 mm thickness:  $n = 6-10$ ) and bar-shaped TFS (20 mm length, 2 mm width, 2 mm thickness:  $n = 6$ ) specimens were prepared by hand-mixing the *N*-vinylpyrrolidone modified acrylic acid and maleic acid copolymer solutions with Fuji IX powder at a powder:liquid mixing ratio of 3.6:1 g:g. When the CFS and DTS values of the *N*-vinylpyrrolidone modified molar ratio groups (8:1:1, 7:3:1, 6:4:2 and 5:5:3) were examined and compared with the Fuji IX control group (273  $\pm$  16 MPa and 21  $\pm$  2 MPa, respectively), no increase in the mean CFS (277  $\pm$  31 MPa, 252  $\pm$  27 MPa, 206  $\pm$  33 MPa and 167  $\pm$  9 MPa) and DTS (22  $\pm$  3 MPa, 19  $\pm$  2 MPa, 16  $\pm$  1 MPa and 12  $\pm$  2 MPa) values were identified,<sup>120</sup> although an increase in the mean TFS (46  $\pm$  7 MPa, 41  $\pm$  12 MPa and 40  $\pm$  7 MPa) values was highlighted for the 8:1:1, 7:3:1 and 6:4:2 molar ratio groups when compared with Fuji IX (32  $\pm$  11 MPa).<sup>120</sup>

It was proposed that altering the monomeric sequence in *N*-vinylpyrrolidone modified copolymers from acrylic acid:itaconic acid:*N*-vinylpyrrolidone to acrylic acid:*N*-vinylpyrrolidone:itaconic acid would allow for greater mobility of the side chains leading to enhanced ionic bond formation.<sup>121</sup> Acrylic acid and itaconic acid copolymer solutions were modified using *N*-vinylpyrrolidone at an acrylic acid:*N*-vinylpyrrolidone:itaconic acid molar ratio of 8:1:1.<sup>121</sup> The *N*-vinylpyrrolidone modified solutions were hand-mixed with Fuji II powder at a powder:liquid mixing ratio of 2.7:1 g:g to prepare cylindrical CFS (6 mm height, 4 mm diameter:  $n = 6$ ), disc-shaped DTS (4 mm diameter, 2 mm thickness:  $n = 6$ ) and disc-shaped BFS (10 mm diameter, 1 mm thickness:  $n = 6$ ) specimens. Following 24 h water storage, a decrease in the mean CFS (161  $\pm$  12 MPa), DTS (12  $\pm$  2 MPa) and BFS (15  $\pm$  2 MPa) values for Fuji II specimens was identified compared with the mean CFS (167  $\pm$  10 MPa), DTS (17  $\pm$  3 MPa) and BFS (29  $\pm$  3 MPa) values of GI specimens prepared with the *N*-vinylpyrrolidone modified copolymer solution.<sup>121</sup>

*N*-vinylcaprolactam is a chemical analogue of *N*-vinylpyrrolidone with increased biocompatibility<sup>122,127</sup> and was investigated for modification of acrylic acid and itaconic acid copolymer solutions at an acrylic acid:itaconic acid:*N*-vinylcaprolactam molar ratio of 8:1:1.<sup>122,123</sup> The modified copolymer solutions were hand-mixed with Fuji IX powder at a powder:liquid mixing ratio of 3.6:1 g:g to prepare cylindrical CFS (6 mm height, 4 mm diameter:  $n = 6$ ), disc-shaped DTS (4 mm diameter, 2 mm thickness:  $n = 6$ ), disc-shaped BFS (10 mm diameter, 1 mm thickness:  $n = 6$ ), bar-shaped TFS (20 mm length, 2 mm width, 2 mm thickness:  $n = 7$ ) and SEN compact tension disc-shaped  $K_{IC}$  specimens (8 mm diameter, 2 mm thickness). Following water storage for 24 h and 1 week, the mean CFS (236  $\pm$  41 MPa and 248  $\pm$  36 MPa), DTS (20  $\pm$  11 MPa and 24  $\pm$  10 MPa), BFS (41  $\pm$  10 MPa and 43  $\pm$  12 MPa), TFS (38  $\pm$  6 MPa and 45  $\pm$  6 MPa) and  $K_{IC}$  (0.43  $\pm$  0.08 MN m<sup>-1.5</sup> and 0.47  $\pm$  0.09 MN m<sup>-1.5</sup>) values of the Fuji IX control group were markedly reduced compared with the mean CFS (303  $\pm$  33 MPa and 319  $\pm$  34 MPa), DTS (38  $\pm$  11 MPa and 44  $\pm$  8 MPa), BFS (82  $\pm$  13 MPa and 85  $\pm$  13 MPa), TFS (52  $\pm$  6 MPa and 58  $\pm$  6 MPa) and  $K_{IC}$  (0.58  $\pm$  0.09 MN m<sup>-1.5</sup> and 0.67  $\pm$  0.2 MN m<sup>-1.5</sup>) values for the GI specimens prepared with the *N*-vinylcaprolactam modified copolymer solutions.<sup>122,123</sup>



With respect to the type of the flexible spacer chosen to link the pendant functional carboxyl groups with the polymer backbone, the copolymer:spacer molar ratio, the monomeric sequence, the chemical composition of the GI powder and the GI powder:liquid mixing ratio employed were markedly different for the studies reporting modification of the copolymer solutions,<sup>114–117,120–123</sup> such that a direct comparison between the studies was not possible. Despite the claimed improvements in CFS, DTS, TFS, BFS and  $K_{IC}$  for GIs prepared with the modified copolymer solutions, commercial exploration of GIs with these GI liquid modifications was not identified in the dental literature suggesting problems with the systems.

A review of the reinforcement strategies investigated for GIs does not leave the reader with any great deal of optimism. Despite the variously reported attempts to reinforce GIs, the reinforcement strategies could not produce GIs with mechanical properties close to dental amalgam or RBCs. Examination of the mixing and testing conditions reported by researchers investigating the reinforcement strategies for GIs revealed a wide variation in the mixing and testing conditions employed. For the GI reinforcement strategies investigated in the dental literature, the majority of investigators employed hand-mixing of GIs with the exception of two studies<sup>97,98</sup> that substituted a portion of the GI powder from encapsulated Fuji IX<sub>GP</sub> with hydroxyapatite, prior to mechanical mixing at 3.6:1 g:g. The use of encapsulated GIs ignored the influence of the initial viscosity of the GI mix which may have not been optimised for the hydroxyapatite substituted powder, thereby failing to provide adequate information on the reinforcement strategy to the investigator.

#### 4.8. Hand-mixing GIs

For hand-mixed GIs, the relative proportions of powder and liquid constituent required to produce the manufacturers recommended powder:liquid mixing ratio are routinely dispensed using the measuring systems provided by the manufacturer, namely powder scoops and liquid dropper bottles, respectively.<sup>128</sup> The volume of powder dispensed using a scoop can vary depending on the powder packing density<sup>129,130</sup> while the volume of a drop of liquid dispensed depends on the angulation the dropper bottle is held and the pressure applied to squeeze out the drop.<sup>131</sup> Hand-mixed GIs tested in the laboratory are therefore exposed to variations in the powder:liquid mixing ratios produced owing to the non-standardised nature of the product delivery systems. Discrepancies in the accurate determination of the GI powder and liquid constituents are evident in the dental literature in the reporting of the reinforcement strategies for GIs. Investigators have employed the scoop and dropper bottle provided by the manufacturer<sup>101</sup> although the majority of investigators<sup>79–100,112–123</sup> failed to provide adequate information on the powder and liquid measurement systems employed. Therefore, it remains uncertain as to whether the investigators used the non-standardised powder scoops and liquid dropper bottles provided by the manufacturer or a weighing balance for accurate dispensation of the GI powder and liquid constituents. The production of the optimum powder:liquid mixing ratio could have only been ensured by the use of a weighing balance.

#### 4.9. Testing methodology

The CFS test was identified as the most commonly employed testing methodology when investigating GI reinforcement by powder additive substitution<sup>86,89–98,100–102</sup> or liquid modification.<sup>114–116,120–122</sup> Investigators have suggested that loading during masticatory function results in stressing patterns analogous to compression during CFS testing<sup>132</sup> such that a high CFS was advocated to tolerate the masticatory forces routinely encountered in the mouth.<sup>133</sup> Other less commonly employed mechanical testing methodologies included the DTS,<sup>81,92,93,100,115,120–122</sup> TFS,<sup>79,81,89,91,94,114,115,117,120,123</sup> BFS<sup>100,121,122</sup> and  $K_{IC}$ <sup>99,115,123</sup> protocols.

#### 4.10. International Organisation for Standardisation

Guidance for the evaluation of dental materials is provided for by the ISO to ensure the reproducibility of test results, under standard conditions, between different test centres. The CFS testing protocol is the only strength test specified for inclusion in ISO 9917-1:2007 – the international standard for powder/liquid acid–base cements and restoratives.<sup>40</sup> Non-parallel specimen ends can cause localised stress concentrations and premature failure during loading of CFS specimens.<sup>133,134</sup> To accommodate for non-parallel specimen ends, a layer of a padding material is often placed between the cylindrical specimen ends and the loading platens of the testing apparatus. Interestingly, the use of a padding material has been reported to influence the CFS values determined<sup>135</sup> but ISO 9917:2007 prescribes the use of a padding material (filter paper) to accommodate for non-parallel specimen ends which may be a deficiency in the standard.<sup>40</sup>

Loading CFS specimens in a wet environment is more clinically relevant accommodating for environmental assisted crack growth.<sup>136</sup> In addition, GI specimens are susceptible to desiccation<sup>10,11</sup> such that testing in a dry environment would produce markedly reduced CFS values. To prevent desiccation and resultant cracking of the GI specimens, ISO 9917:2007 advocates the placement of a wet filter paper between the CFS specimen and the loading platens of the testing apparatus with the use of a freshly wet piece of filter paper recommended for each individual specimen tested. The lack of information detailed in studies investigating GIs in the dental literature regarding the provision of a wet testing environment during testing make it impossible to interpret the findings between different studies despite specification in the standard.<sup>40</sup>

The time that GI specimens are stored in distilled water ( $37 \pm 1^\circ\text{C}$ ) influences the resultant CFS value due to GI maturation<sup>17,53</sup> following the initial stages of the setting reaction. GIs are reported to undergo a post-set hardening phase which continues for 24 h following the initial stages of the setting reaction and prior to the subsequent maturation stage which can continue over a period of several months.<sup>24</sup> Therefore, ISO 9917:2007 stipulate the CFS of GI specimens should be determined following conditioning in a mould for 1 h and water storage for  $23 \pm 0.5$  h, to ensure the completion of the post-set hardening phase. However, in the dental literature, CFS testing of GI specimens was routinely performed following 24 h<sup>86,89–98,100–102,114,121</sup> or 1 week water storage.<sup>97,101,115,116,120–122</sup> It is evident that prolonged water

storage (1 week) would increase the CFS values reported owing to the continuous maturation of GIs on setting<sup>17,53</sup> such that a comparison between studies where CFS testing was performed following different water storage time intervals is of little use to the dental research community.

The CFS of brittle materials such as GI restoratives is influenced by the rate of compressive loading where an increase in the CFS value occurs with increasing loading rate owing to the reduced time available for environmental assisted crack growth.<sup>137,138</sup> The compressive loading rate advocated in ISO 9917:2007 for CFS testing of GI specimens is  $0.75 \pm 0.30$  mm/min. The CFS loading rates identified for studies reporting GI reinforcement strategies were 0.5 mm/min<sup>86,91,94,100,114–118,120–122</sup> and 1 mm/min,<sup>89,92,93,95–98,101,102</sup> while El Mallakh et al.<sup>90</sup> failed to report the loading rate employed. Although the compressive loading rates employed by the researchers<sup>86,89,91–98,101,102,114–118,120–122</sup> were within the range recommended in ISO 9917-1:2007 (0.45–1.05 mm/min), a direct comparison between individual studies is not possible owing to the differences in the time available for environmental assisted crack growth to occur on loading to failure.<sup>137,138</sup> Therefore, to avoid confusion and allow direct comparisons between studies, it is proposed that a standard loading rate for CFS testing of GIs must be specified in ISO 9917-1:2007 rather than the loading rate range provided for in the standard.<sup>40</sup>

The CFS testing protocol in ISO 9917-1:2007 advocates testing cylindrical GI specimens ( $6.0 \pm 0.1$  mm height and  $4.0 \pm 0.1$  mm diameter). Strength is not an intrinsic material property such that the height and diameter of the cylindrical specimen influence the maximum load-to-failure which in turn influences the CFS value recorded. In theory, a larger specimen has an increased likelihood of containing crack initiating defects which would reduce the CFS value recorded.<sup>139</sup> Despite the cylindrical specimen dimensions of  $6.0 \pm 0.1$  mm height and  $4.0 \pm 0.1$  mm diameter being specified by inclusion in ISO 9917-1:2007, a wide variation in specimen dimensions was identified in studies pertaining to GI reinforcement strategies. These include studies employing specimen dimensions of 6 mm height and 3 mm diameter,<sup>90</sup> 6 mm height and 4 mm diameter,<sup>94,95,100–102,120–122</sup> 6 mm height and 5 mm diameter,<sup>89</sup> 8 mm height and 4 mm diameter<sup>97,98</sup> and 12 mm height and 6 mm diameter.<sup>86,91–93,96–98,114–116</sup> When testing the CFS of GI specimens, the wide variation in the specimen dimensions employed by dental researchers prevents any direct comparison between studies which is a further embarrassment to the review process in the dental literature.

GIs are brittle dental materials, such that a distribution in the strength data is inevitable.<sup>139</sup> ISO 9917-1:2007 suggests following CFS testing five cylindrical specimens, if four of the five CFS values are  $>100$  MPa then the GI restorative will pass the CFS criteria. If three or more of the five CFS values recorded are  $<100$  MPa, the GI restorative will fail the CFS criteria specified in ISO 9917-1:2007. If three specimens have a CFS value of  $>100$  MPa, an additional five specimens are tested and to pass the criteria specified in ISO 9917-1:2007, all additional five CFS values have to be  $>100$  MPa.<sup>40</sup> The pass/fail criteria specified in ISO 9917-1:2007 for the evaluation of the CFS of GIs was highlighted to be unsafe as it misidentified operative

variability.<sup>140</sup> A statistical approach using a minimum of 20 specimens therefore must be employed for meaningful interpretation of the CFS data sets,<sup>140,141</sup> although sample number data sets of 20 specimens are rarely employed by dental researchers investigating GI materials or reinforcement strategies.

#### 4.11. The way forward?

A realisation of the need for a definitive study to identify a valid<sup>135</sup> and reliable<sup>142</sup> mechanical testing protocol for GIs was championed by Fleming et al.<sup>140</sup> in a study entitled, 'The crushing truth about glass ionomer restoratives: exposing the standard of the standard'. In a follow-up study entitled 'Improving the standard of the standard for glass ionomers: an alternative to the compressive fracture strength test for consideration?', CFS, TFS and BFS testing protocols were investigated under standardised ISO 9917-1:2007 conditions (padding material (filter paper), loading rate (1 mm/min), environment (wet), storage time (24 h)) using groups of 40 specimens.<sup>143</sup> To eliminate dispensing errors with the powder and liquid constituents<sup>129,130</sup> and to standardise the mixing regime, three encapsulated commercial GI restoratives were investigated.<sup>143</sup> Interestingly, the TFS and BFS testing methodologies failed to discriminate between the encapsulated GI products, despite the GI products being supplied by different manufacturers with different glass compositions, liquid compositions and powder:liquid mixing ratios while differences in CFS values were evident. One significant oversight in these two studies<sup>140,143</sup> was the employment of encapsulated GI restoratives. If one was charged with the task of delivering a novel reinforced GI restorative, the initial and fundamental step would involve the determination of the optimum powder:liquid mixing ratio by hand-mixing the GI liquid with varying GI powder contents and performing preliminary mechanical tests. Resistance to compressive, tensile and shear forces under loading during mastication is provided by the reinforcing glass filler component rather than the weaker polyacrylate matrix<sup>144</sup> such that maximising the glass filler powder particles in the set GI will ensure optimum resistance to fracture in service.<sup>23,144–146</sup> Therefore, a deterioration in the mechanical properties would be expected on reducing the powder content from the optimum value specified by the manufacturer. The mechanical testing protocol of choice when investigating novel reinforced GI restoratives would therefore be required to be discriminatory between the different powder:liquid mixing ratios employed by identifying a linear deterioration in the property being investigated when the powder content is reduced from the optimum value<sup>147</sup> – something that could not be elucidated from the encapsulated GI restoratives used previously.<sup>140,143</sup>

## 5. Conclusion

In conclusion, the extensive literature available on GIs extending from the earliest to modern day commercially available materials was reviewed with the aim of highlighting the major developments in the GI powder and liquid components. The GI glass powder has undergone significant

changes from the earliest formulation (G-200) in an effort to enhance the reactivity with the GI liquid. The GI liquids have also been optimised by the manufacturers in terms of polyacid composition, molecular weight and concentration to improve the handling characteristics. Attempts to improve the mechanical properties of GIs through substitution of reinforcing fillers to the GI powder or modification of the GI liquid were also reviewed. A wide variation in mixing and testing conditions prevented a valid assessment of the reported reinforcement strategies. When investigating a GI reinforcement strategy it is imperative that the mixing and testing conditions are standardised to allow a valid comparison between studies. Nevertheless, major improvements through a reinforcement strategy have yet to be made to enable clinical usage of GIs for the restoration of posterior dentition.

#### REFERENCES

- Wilson AD, Kent BE. Surgical cement. *British Patent* 1969;1,316,129.
- Wilson AD, Batchelor RF. Dental silicate cements I. The chemistry of erosion. *Journal of Dental Research* 1967;46:1078–85.
- Wilson AD. A hard decade's work: steps in the invention of the glass-ionomer cement. *Journal of Dental Research* 1996;75:1723–7.
- Wilson AD, Batchelor RF. Dental silicate cements II. Preparation and durability. *Journal of Dental Research* 1967;46:1425–32.
- Wilson AD, Batchelor RF. Dental silicate cements III. Environment and durability. *Journal of Dental Research* 1968;47:115–20.
- Wilson AD. Dental silicate cements IV. Alternative liquid cement formers. *Journal of Dental Research* 1968;47:1133–6.
- Wilson AD, Kent BE. A new translucent cement for dentistry. The glass ionomer cement. *British Dental Journal* 1972;132:133–5.
- Wilson AD, McLean JW. Scientific and clinical development. In: Wilson AD, McLean JW, editors. *Glass-ionomer cement*. Chapter 1. Chicago, IL: Quintessence Publishing Co., Inc.; 1988. p. 13–20.
- Causton BE. The physico-mechanical consequences of exposing glass-ionomer cements to water during setting. *Biomaterials* 1981;2:112–5.
- Wilson AD. Developments in glass-ionomer cements. *International Journal of Prosthodontics* 1989;2:438–46.
- Earl MSA, Mount GJ, Hume WR. The effect of varnishes and other surface treatments on water movement across the glass-ionomer cement surface. *Australian Dental Journal* 1989;34:326–9.
- Wilson AD, Crisp S, Ferner AJ. Reactions in glass-ionomer cements IV. Effect of chelating comonomers on setting behaviour. *Journal of Dental Research* 1976;55:489–95.
- Crisp S, Wilson AD. Reactions in glass ionomer cements V. Effect of incorporating tartaric acid in the cement liquid. *Journal of Dental Research* 1976;55:1023–31.
- Crisp S, Lewis BG, Wilson AD. Characterisation of glass ionomer cements 5. The effect of the tartaric acid concentration in the liquid component. *Journal of Dentistry* 1979;7:304–12.
- McLean JW, Wilson AD. Fissure sealing and filling with an adhesive glass-ionomer cement. *British Dental Journal* 1974;136:269–76.
- Crisp S, Lewis BG, Wilson AD. Gelation of polyacrylic acid aqueous solutions and the measurement of viscosity. *Journal of Dental Research* 1975;54:1173–5.
- Crisp S, Lewis BG, Wilson AD. Characterisation of glass-ionomer cements 1. Long term hardness and compressive strength. *Journal of Dentistry* 1976;4:162–6.
- Crisp S, Kent BE, Lewis BG, Ferner AJ, Wilson AD. Glass-ionomer cement formulations II. The synthesis of novel polycarboxylic acids. *Journal of Dental Research* 1980;59:1055–63.
- Wilson AD. Glass-ionomer cements – origins, development and future. *Clinical Materials* 1991;7:275–82.
- Mount GJ, Makinson OF. Clinical characteristics of a glass-ionomer cement. *British Dental Journal* 1978;145:67–71.
- Mount GJ, Makinson OF. Letter to the editor. *British Dental Journal* 1978;145:125.
- Prosser HJ, Powis DR, Brant P, Wilson AD. Characterisation of glass-ionomer cements 7. The physical properties of current materials. *Journal of Dentistry* 1984;12:231–40.
- McLean JW, Wilson AD, Prosser HJ. Development and use of water-hardening glass-ionomer luting cements. *Journal of Prosthetic Dentistry* 1984;52:175–81.
- Wilson AD, McLean JW. The setting reaction and its clinical consequences. In: Wilson AD, McLean JW, editors. *Glass-ionomer cement*. Chapter 3. Chicago, IL: Quintessence Publishing Co., Inc.; 1988. p. 43–56.
- Nicholson JW. Chemistry of glass-ionomer cements: a review. *Biomaterials* 1998;19:485–94.
- Kent BE, Lewis BG, Wilson AD. Glass-ionomer cement formulations I. The preparation of novel fluoroaluminosilicate glasses high in fluorine. *Journal of Dental Research* 1979;58:1607–19.
- Wilson AD, Nicholson JW. Polyalkenoate cements. In: Wilson AD, Nicholson JW, editors. *Acid-base cements: their biomedical and industrial applications*. Chapter 5. Cambridge University Press; 1993. p. 90–196.
- Wilson AD, McLean JW. Composition. In: Wilson AD, McLean JW, editors. *Glass-ionomer cement*. Chapter 2. Chicago, IL: Quintessence Publishing Co., Inc.; 1988. p. 21–42.
- Nicholson JW, Brookman PJ, Lacy OM, Wilson AD. Fourier transform infrared spectroscopic study of the role of tartaric acid in glass-ionomer dental cements. *Journal of Dental Research* 1988;67:1451–4.
- Hill RG, Wilson AD. A rheological study of the role of additives on the setting of glass-ionomer cements. *Journal of Dental Research* 1988;67:1446–50.
- Wilson AD, Crisp S, Prosser HJ, Lewis BG, Merson SA. Aluminosilicate glasses for polyelectrolyte cements. *Industrial and Engineering Chemistry Product Research and Development* 1980;19:263–70.
- Wood D, Hill R. Structure–property relationship in ionomer glasses. *Clinical Materials* 1991;7:301–12.
- de Barra E, Hill RG. Influence of glass composition on the properties of glass polyalkenoate cements. Part III. Influence of fluorite content. *Biomaterials* 2000;21:563–9.
- Forsten L. Fluoride release and uptake by glass-ionomers and related materials and its clinical effect. *Biomaterials* 1998;19:503–8.
- Mayanagi G, Igarashi K, Washio J, Domon-Tawaraya H, Takahashi N. Effect of fluoride-releasing restorative materials on bacteria-induced pH fall at the bacteria–material interface: an in vitro model study. *Journal of Dentistry* 2014;42:15–20.
- Neve AD, Piddock V, Combe EC. Development of novel dental cements I. Formulation of aluminoborate glasses. *Clinical Materials* 1992;9:7–12.
- Neve AD, Piddock V, Combe ED. Development of novel dental cements II. Cement properties. *Clinical Materials* 1992;9:13–20.

38. Neve AD, Piddock V, Combe ED. The effect of glass heat treatment on the properties of a novel polyalkenoate cement. *Clinical Materials* 1993;12:113–6.
39. Darling M, Hill R. Novel polyalkenoate (glass-ionomer) dental cements based on zinc silicate glasses. *Biomaterials* 1994;15:299–306.
40. International Organisation for Standardisation ISO 9917-1:2007. Dentistry – water-based cements Part 1. Powder/liquid acid-base cements.
41. Griffin SG, Hill RG. Influence of glass composition on the properties of glass polyalkenoate cements. Part I. Influence of aluminium to silicon ratio. *Biomaterials* 1999;20:1579–86.
42. Smith DC. Development of glass-ionomer cement systems. *Biomaterials* 1998;19:467–78.
43. Debb S, Nicholson JW. The effect of strontium oxide in glass-ionomer cements. *Journal of Materials Science: Materials in Medicine* 1999;10:471–4.
44. Griffin SG, Hill RG. Influence of glass composition on the properties of glass polyalkenoate cements. Part II. Influence of phosphate content. *Biomaterials* 2000;21:399–403.
45. Product specification for Chemfil Rock. Dentsply DeTrey, Konstanz, Germany.
46. Product specification for Ketac Molar. 3M ESPE, St. Paul, Minnesota, USA.
47. Product specification for Fuji IX. GC Europe, Leuven, Belgium.
48. Product specification for Ionofil Molar. Voco GmbH, Cuxhaven, Germany.
49. Schmitt W, Purrmann R, Jochum P, Gasser O. Calcium depleted aluminium fluorosilicate glass powder for use in dental or bone cements. *US Patent* 1983;4,376,835.
50. Kaplan AE, Williams J, Billington RW, Braden M. Effects of variation in particle size on biaxial flexural strength of two conventional glass-ionomer cements. *Journal of Oral Rehabilitation* 2004;31:373–8.
51. Crisp S, Ferner AJ, Lewis BG, Wilson AD. Properties of improved glass-ionomer cement formulations. *Journal of Dentistry* 1975;3:125–30.
52. Crisp S, Wilson AD. Cements comprising acrylic and itaconic acid copolymers and fluoroaluminosilicate glass powder. *US Patent* 1977;1,532,954.
53. Williams JA, Billington RW. Changes in compressive strength of glass-ionomer restorative materials with respect to time periods of 24 h to 4 months. *Journal of Oral Rehabilitation* 1991;18:163–8.
54. Nicholson JW, Abiden F. Changes in compressive strength on ageing in glass polyalkenoate (glass-ionomer) cements prepared from acrylic/maleic acid copolymers. *Biomaterials* 1997;18:59–62.
55. Pearson GJ, Atkinson AS. Long-term flexural strength of glass-ionomer cements. *Biomaterials* 1991;12:658–60.
56. Khouw-Liu VHW, Anstice HM, Pearson GJ. An *in vitro* investigation of polyvinylphosphonic acid based cement with four conventional glass-ionomer cements. Part 2: maturation in relation to surface hardness. *Journal of Dentistry* 1999;27:359–65.
57. Khouw-Liu VHW, Anstice HM, Pearson GJ. An *in vitro* investigation of polyvinylphosphonic acid based cement with four conventional glass-ionomer cements. Part 1: flexural strength and fluoride release. *Journal of Dentistry* 1999;27:351–7.
58. Hill RG, Wilson AD, Warrens CP. The influence of polyacrylic acid molecular weight on the fracture toughness of glass-ionomer cements. *Journal of Materials Science* 1989;24:363–71.
59. Gonzalez AE. Viscoelasticity of ionomer gels. 2. The elastic moduli. *Polymer* 1984;25:1469–74.
60. Bucknall CB. In: Haward RN, editor. *The physics of glassy polymers*. London: Applied Science Publishers; 1973 p. 363–412.
61. Prentice P. The influence of molecular weight on the fracture of thermoplastic glassy polymers. *Journal of Materials Science* 1985;20:1445–54.
62. Wilson AD, Hill RG, Warrens CP, Lewis BG. The influence of polyacid molecular weight on some properties of glass-ionomer cements. *Journal of Dental Research* 1989;68:89–94.
63. Edwards SF. Statistical mechanics of polymerized material. *Proceedings of the Physical Society of London* 1967;92:9–16.
64. de Gennes PG. In: de Gennes PG, editor. *Scaling concepts in polymer physics*. Ithaca, NY: Cornell University Press; 1979. p. 219–44.
65. Crisp S, Lewis BG, Wilson AD. Characterisation of glass-ionomer cements 3. Effect of polyacid concentration on the physical properties. *Journal of Dentistry* 1977;5:51–6.
66. de Barra E, Hill RG. Influence of polyacrylic acid content on the fracture behaviour of glass polyalkenoate cements. *Journal of Materials Science* 1998;33:5487–97.
67. Fennell B, Hill RG. The influence of polyacrylic acid molar mass and concentration on the properties of polyalkenoate cements. Part I: compressive strength. *Journal of Materials Science* 2001;36:5193–202.
68. Fennell B, Hill RG. The influence of polyacrylic acid molar mass and concentration on the properties of polyalkenoate cements. Part II: Young's modulus and flexural strength. *Journal of Materials Science* 2001;36:5177–83.
69. Fennell B, Hill RG. The influence of polyacrylic acid molar mass and concentration on the properties of polyalkenoate cements. Part III: fracture toughness and toughness. *Journal of Materials Science* 2001;36:5185–92.
70. Dowling AH, Fleming GJP. The influence of polyacrylic acid number average molecular weight and concentration in solution on the compressive fracture strength and modulus of a glass-ionomer restorative. *Dental Materials* 2011;27:535–43.
71. Wilson AD, Crisp S, Abel G. Characterisation of glass-ionomer cements 4. Effect of molecular weight on physical properties. *Journal of Dentistry* 1977;5:117–20.
72. Prosser HJ, Powis DR, Wilson AD. Glass-ionomer cements of improved flexural strength. *Journal of Dental Research* 1986;65:146–8.
73. Griffin S, Hill RG. Influence of poly(acrylic acid) molar mass on the fracture properties of glass polyalkenoate cements. *Journal of Materials Science* 1998;33:5383–96.
74. Dowling AH, Fleming GJP. Can polyacrylic acid molecular weight mixtures improve the compressive fracture strength and elastic modulus of a glass-ionomer restorative? *Dental Materials* 2011;27:1170–9.
75. Crisp S, Wilson AD. Polycarboxylate cements. *British Patent* 1977;1,484,454.
76. Schmitt W, Purrmann R, Jochum P, Gasser O. Mixing component for dental glass-ionomer cements. *US Patent* 1982;4,360,605.
77. Wilson AD, McLean JW. Adhesion. In: Wilson AD, McLean JW, editors. *Glass-ionomer cement*. Chicago, IL: Quintessence Publishing Co., Inc.; 1988. p. 83–99.
78. Van Meerbeek B, De Munck J, Yoshida Y, Inoue S, Vargas M, Vijay P. Buonocore memorial lecture. Adhesion to enamel and dentin: current status and future challenges. *Operative Dentistry* 2003;28:215–35.
79. Sced I, Wilson AD. Polycarboxylic acid hardenable compositions. *British Patent* 1980;2,028,855A.
80. Oldfield CWB, Ellis B. Fibrous reinforcement of glass-ionomer cements. *Clinical Materials* 1991;7:313–23.
81. Kobayashi M, Kon M, Miyai K, Asaoka K. Strengthening of glass-ionomer cement by compounding short fibres with CaO–P<sub>2</sub>O<sub>5</sub>–SiO<sub>2</sub>–Al<sub>2</sub>O<sub>3</sub> glass. *Biomaterials* 2000;21:2051–8.
82. Lucksanasomboon P, Higgs WAJ, Higgs RJED, Swain MV. Toughness of glass fibres reinforced glass-ionomer cements. *Journal of Materials Science* 2002;37:101–8.

83. Lohbauer U, Walker J, Nikolaenko S, Werner J, Clare A, Petschelt A, Greil P. Reactive fibre reinforced glass-ionomer cements. *Biomaterials* 2003;24:2901–7.
84. Simmons JJ. The miracle mixture: glass-ionomer and alloy powder. *Texas Dental Journal* 1983;100:6–12.
85. Simmon JJ. Silver-alloy powder and glass-ionomer cement. *Journal of the American Dental Association* 1990;120:49–52.
86. Miller D, Marker VA, Okabe T, Simmons JJ. Formulation and evaluation of dental amalgam alloy added to glass-ionomer. *Journal of Dental Research* 1984;63. Special Issue B231 (Abstract 545).
87. McLean JW, Gasser O. Glass-cermet cements. *Quintessence International* 1985;16:333–43.
88. McLean JW. Cermet cements. *Journal of the American Dental Association* 1990;120:43–7.
89. Walls AWG, Adamson J, McCabe JF, Murray JJ. The properties of glass polyalkenoate (ionomer) cement incorporating sintered metallic particles. *Dental Materials* 1987;3:113–6.
90. El Mallakh B, Sarkar NK, Kamar A. Does metal incorporation improve glass-ionomer properties? *Journal of Dental Research* 1987;66. Special Issue B113 (Abstract 50).
91. Nakajima H, Hashimoto H, Marker VA, Hanaoka K, Miyakuni S, Teranaka T, Iwamoto T, Okabe T. Static and dynamic mechanical properties of glass-ionomers. *Journal of Dental Research* 1989;68. Special Issue B273 (Abstract 735).
92. Williams JA, Billington RW, Pearson GJ. The comparative strengths of commercial glass-ionomer cements with and without metal additions. *British Dental Journal* 1992;172: 279–82.
93. Kerby RE, Bleiholder RF. Physical properties of stainless-steel and silver-reinforced glass-ionomer cements. *Journal of Dental Research* 1991;70:1358–61.
94. El-saka SE, Hamouda IM, Swain MV. Titanium dioxide nanoparticles addition to a conventional glass-ionomer restorative: Influence on physical and antibacterial properties. *Journal of Dentistry* 2011;39:589–98.
95. Dowling AH, Schmitt WS, Fleming GJP. Modification of titanium dioxide particles to reinforce glass-ionomer restoratives. *Dental Materials* 2014;30S:e159–60.
96. Nicholson JW, Hawkins SJ, Smith JE. The incorporation of hydroxyapatite into glass-polyalkenoate ('glass-ionomer') cements: a preliminary study. *Journal of Materials Science: Materials in Medicine* 1993;4:418–21.
97. Yap AUJ, Pek YS, Kumar RA, Cheang P, Khor KA. Experimental studies on a new bioactive material: HAIonomer cements. *Biomaterials* 2002;23:955–62.
98. Gu Y, Yap AUJ, Cheang C, Khor KA. Effects of incorporation of HA/ZrO<sub>2</sub> into glass-ionomer cement (GIC). *Biomaterials* 2005;26:713–20.
99. Lucas ME, Arita K, Nishino M. Toughness, bonding and fluoride-release properties of hydroxyapatite-added glass ionomer cement. *Biomaterials* 2003;24:3787–94.
100. Moshaverinia A, Ansari S, Moshaverinia M, Roohpour N, Darr J, Rehman I. Effects of incorporation of hydroxyapatite and fluoroapatite nanobioceramics into conventional glass-ionomer cements (GIC). *Acta Biomaterialia* 2008;4: 432–40.
101. Yli-Urpo H, Lassila LVJ, Narhi T, Vallittu PK. Compressive strength and surface characterisation of glass-ionomer cements modified by particles of bioactive glass. *Dental Materials* 2005;21:201–9.
102. Dowling AH, Stamboulis A, Fleming GJP. The influence of montmorillonite clay reinforcement on the performance of a glass ionomer restorative. *Journal of Dentistry* 2006;34: 802–10.
103. Dowling AH, Fleming GJP. The impact of montmorillonite clay addition on the in vitro wear resistance of a glass-ionomer restorative. *Journal of Dentistry* 2007;35:309–17.
104. British Standards BS 5199:1975. Specification for resin-based dental filling materials.
105. American Society for Testing and Materials ASTM E399:2009. Standard test method for linear-elastic plane strain fracture toughness  $K_{IC}$  of metallic materials.
106. Wilson AD, Prosser HJ. A survey of inorganic and polyelectrolyte cements. *British Dental Journal* 1984;157: 449–54.
107. Darvell BW. Cements and liners. In: Darvell BW, editor. *Materials science for dentistry. Chapter 9*. Hong Kong: Darvell BW; 2002. p. 190–221.
108. Sarkar NK, El Mallakh B, Graves R. Silver release from metal-reinforced glass ionomers. *Dental Materials* 1988;4:103–4.
109. Croll TP, Philips RW. Glass-ionomer silver cermet restorations for primary teeth. *Quintessence International* 1986;17:607–15.
110. Skinner JC, Prosser HJ, Scott RP, Wilson AD. Adhesion of carboxylate cements to hydroxyapatite. *Biomaterials* 1986;7:438–40.
111. Yoshida Y, Van Meerbeck B, Nakayama Y, Yoshioka M, Snauwaert J, Abe Y, Lambrechts P, Vanherle G, Okazaki O. Adhesion to and decalcification of hydroxyapatite by carboxylic acids. *Journal of Dental Research* 2001;80:1565–9.
112. Wilson AD, Ellis J. Polyvinylphosphonic acid and metal oxide or cermet or glass-ionomer cement. *British Patent* 1989;2,219,289A.
113. Ellis J, Anstice M, Wilson AD. The glass polyphosphonate cement: a novel glass-ionomer cement based on polyvinylphosphonic acid. *Clinical Materials* 1991;7:341–6.
114. Culbertson BM, Kao EC. Water soluble polymers containing amino acid residues for dental restoratives. *US Patent* 1994;5,369,142.
115. Kao EC, Culbertson BM, Xie D. Preparation of glass-ionomer cement using N-acryloyl-substituted amino acid monomers: evaluation of physical properties. *Dental Materials* 1996;12:44–51.
116. Culbertson BM, Xie D, Thakur A. New matrix resins for glass polyalkenoates or glass-ionomers with pendant amino acid residues. *Journal of Macromolecular Science – Pure and Applied Chemistry* 1999;A36:681–96.
117. Xie D, Culbertson BM, Johnstone W. Improved flexural strength of N-vinylpyrrolidone modified acrylic acid copolymers for glass-ionomers. *Journal of Macromolecular Science – Pure and Applied Chemistry* 1998;A35:1615–29.
118. Culbertson BM. Glass-ionomer dental restoratives. *Progress in Polymer Science* 2001;26:577–604.
119. Culbertson BM. New polymeric materials for use in glass-ionomer cements. *Journal of Dentistry* 2006;34:556–65.
120. Yamazaki T, Brantley W, Culbertson B, Seghi R, Schricker S. The measure of wear in N-vinylpyrrolidone (NVP) modified glass-ionomer cements. *Polymers for Advanced Technology* 2005;16:113–6.
121. Moshaverinia A, Ansari S, Movasaghi Z, Billington RW, Darr JA, Rehman IU. Modification of conventional glass-ionomer cements with N-vinylpyrrolidone containing polyacids, nano-hydroxy and fluoroapatite to improve mechanical properties. *Dental Materials* 2008;24:1381–90.
122. Moshaverinia A, Roohpour N, Darr JA, Rehman IU. Synthesis and characterisation of a novel N-vinylcaprolactam-containing acrylic acid terpolymer for applications in glass-ionomer dental cements. *Acta Biomaterialia* 2009;5:2101–8.
123. Moshaverinia A, Brantley WA, Chee WWL, Roohpour N, Ansari S, Zheng F, Heshmati RH, Darr JA, Schricker SR, Rehman IU. Measure of microhardness, fracture toughness and flexural strength of N-vinylcaprolactam (NVC)-containing glass-ionomer dental cements. *Dental Materials* 2010;26:1137–43.

124. Akinmade AO, Braybrook HJ. Dental Cement. US Patent 1992;5,411,584.
125. Anstice HM, Nicholson JW. Investigation of the post-hardening reaction in glass-ionomer cements on polyvinylphosphonic acid. *Journal of Materials Science: Materials in Medicine* 1995;6:420–5.
126. Product specification for Diamond Carve. Associated Dental Products Ltd., Wiltshire, UK.
127. Vihola H, Laukkanen A, Hirvonen J, Tenhu H. Binding and release of drugs into and from thermosensitive poly(N-vinylcaprolactam) nanoparticles. *European Journal of Pharmaceutical Sciences* 2002;16:69–74.
128. Mount GJ. Description of glass-ionomer cements. In: Mount GJ, editor. *An atlas of glass-ionomer cements: a clinician's guide. Chapter 1*. London: Martin Dunitz; 1994. p. 1–24.
129. Billington RW, Williams JA, Pearson GJ. Variation in powder/liquid ratio of restorative glass-ionomer cement used in dental practice. *British Dental Journal* 1990;169:164–7.
130. Fleming GJP, Farooq AA, Barralet JE. Influence of powder/liquid mixing ratio on the performance of a restorative glass-ionomer dental cement. *Biomaterials* 2003;24:4173–9.
131. Eames WB, Monroe SD, Roan JD, O'Neal SJ. Proportioning and mixing of cements: a comparison of working times. *Operative Dentistry* 1977;2:97–104.
132. Yettram AL, Wright KW, Pickard HM. Finite element stress analysis of the crowns of normal and restored teeth. *Journal of Dental Research* 1976;55:1004–11.
133. White SN, Yu Z. Compressive and diametral tensile strengths of current adhesive luting agents. *Journal of Prosthetic Dentistry* 1993;69:568–72.
134. Lloyd CH, Mitchell L. The fracture toughness of tooth coloured restorative materials. *Journal of Oral Rehabilitation* 1984;11:257–72.
135. Darvell BW. Uniaxial compression tests and the validity of indirect tensile strength. *Journal of Materials Science* 1990;25:757–80.
136. Anusavice KJ, Lee RB. Effect of firing temperature and water exposure on crack propagation in unglazed porcelain. *Journal of Dental Research* 1989;68:1075–81.
137. Li ZC, White SN. Mechanical properties of dental luting cements. *Journal of Prosthetic Dentistry* 1999;81:597–609.
138. Higgs WAJ, Lucksanasombol P, Higgs RJED, Swain MV. Comparison of the material properties of PMMA and glass-ionomer based cements for use in orthopaedic surgery. *Journal of Materials Science: Materials in Medicine* 2001;12:453–60.
139. Ritter JE. Predicting lifetimes of materials and materials structures. *Dental Materials* 1995;11:142–6.
140. Fleming GJP, Dowling AH, Addison O. The crushing truth about glass ionomer restoratives: exposing the standard of the standard. *Journal of Dentistry* 2012;40:181–8.
141. McCabe JF, Carrick TE. A statistical approach to the mechanical testing of dental materials. *Dental Materials* 1986;2:139–42.
142. McCabe JF, Watts DC, Wilson HJ, Worthington HV. An investigation of test-house variability in the mechanical testing of dental materials. *Journal of Dentistry* 1990;18:90–7.
143. Dowling AH, Fleming GJP, McGinley EL, Addison O. Improving the standard of the standard for glass ionomers: an alternative to the compressive fracture strength test for consideration? *Journal of Dentistry* 2012;40:189–201.
144. Xie D, Brantley WA, Culbertson BM, Wang G. Mechanical properties and microstructures of glass-ionomer cements. *Dental Materials* 2000;16:129–38.
145. Brune D, Smith D. Microstructure and strength properties of silicate and glass ionomer cements. *Acta Odontologica Scandinavica* 1982;40:389–96.
146. Hatton PV, Brook IM. Characterisation of the ultrastructure of glass-ionomer (poly-alkenoate) cement. *British Dental Journal* 1992;173:275–7.
147. Baig MS, Dowling AH, Cao X, Fleming GJP. A discriminatory mechanical testing performance indicator protocol for hand-mixed glass-ionomer restoratives. *Dental Materials* 2015;31:273–83.

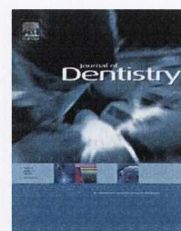
### **3.2 HERTZIAN INDENTATION TESTING OF GLASS-IONOMER RESTORATIVES: A RELIABLE AND CLINICALLY RELEVANT TESTING APPROACH.**

MS Baig, AH Dowling, GJP Fleming (2013). Hertzian indentation testing of glass-ionomer restoratives: a reliable and clinically relevant testing approach. *Journal of Dentistry*, 41:968-973.

The wide variation in mixing and testing conditions identified for studies pertaining to GI reinforcement strategies produced an impossibility for comparison between studies (Manuscript 3.1). Previously, the TFS and BFS testing protocols were highlighted as valid and reliable alternative mechanical testing methodologies to the CFS test when performed under standardised mixing and testing conditions, although the TFS and BFS tests failed to discriminate between encapsulated GI products despite the marked compositional and powder content variations, while differences in CFS values were evident (Dowling et al., 2012). The current study examined the validity, reliability and discriminatory ability of the HI testing methodology for encapsulated GIs. The hypothesis investigated was that the HI test would be the most clinically relevant testing methodology as occlusal loading contacts were simulated for HI specimens which were tested while resting on a dentine analogue substrate material. To enable a comparison with the previous study which examined the CFS, TFS and BFS tests under standardised mixing and testing conditions (Dowling et al., 2012), the same encapsulated GI products were used which eliminated product variability between the studies. To verify the fracture origin and failure mode of the GI specimens tested under HI, the fracture surfaces of the specimens were examined using a scanning electron microscope.

Available online at [www.sciencedirect.com](http://www.sciencedirect.com)

SciVerse ScienceDirect

journal homepage: [www.intl.elsevierhealth.com/journals/jden](http://www.intl.elsevierhealth.com/journals/jden)

## Hertzian indentation testing of glass-ionomer restoratives: A reliable and clinically relevant testing approach

Mirza Shahzad Baig\*, Adam H. Dowling, Garry J.P. Fleming

Materials Science Unit, Division of Oral Biosciences, Dublin Dental University Hospital, Lincoln Place, Trinity College Dublin, Dublin 2, Ireland

### ARTICLE INFO

#### Article history:

Received 18 February 2013

Received in revised form

5 April 2013

Accepted 6 April 2013

#### Keywords:

Glass-ionomer restorative

Hertzian indentation testing

Failure mode

Test validity

Test reliability

### ABSTRACT

**Objectives:** To investigate the load to failure of encapsulated posterior glass-ionomer (GI) restoratives tested under Hertzian indentation and to explore the validity and reproducibility of the test results achieved for consideration of inclusion as an ISO testing protocol.

**Methods:** Groups of 20 disc-shaped specimens ( $10.0 \pm 0.1$  mm diameter,  $3.10 \pm 0.03$  mm thickness) were prepared (in batches of four) from three encapsulated posterior GI restoratives. Discs were tested while resting freely on a dentine analogue material at 24 h under Hertzian indentation at a rate of 1 mm/min delivered through a 20 mm diameter hard steel ball. The failure mode and fracture origin of the GI specimens was assessed by fractography. Statistical analyses of the load to failure data were conducted using SPSS software ( $p < 0.05$ ) with the normality and homogeneity of variance of the load to failure data assessed using the Shapiro–Wilk and Levene's test, respectively. Data was also analysed using regression analyses to identify trends within the load to failure data sets.

**Results:** The load to failure data for the GI restorative groups investigated were normally distributed ( $p > 0.05$ ), homogenous ( $p > 0.05$ ) and not significantly influenced by batch ( $p > 0.780$ ) or specimen number ( $p > 0.447$ ) although significant differences ( $p < 0.05$ ) between the GI restorative materials were evident. Fractographic analysis identified smooth fracture surfaces parallel to the loading axis where the failure mode was bottom initiated radial cracking. The mean coefficient of variation (CoV) for the GI restorative load to failure data sets achieved using Hertzian indentation testing was 7%.

**Significance:** The failure mode and fracture origin of the GI restoratives tested using Hertzian indentation is representative of the clinical situation in vivo. The reliability of the load to failure data sets produced were improved compared with routinely employed mechanical testing approaches suggesting the possibility of inclusion as an ISO testing protocol.

© 2013 Elsevier Ltd. All rights reserved.

## 1. Introduction

A glass-ionomer (GI) material consists of a basic ion leachable glass powder and an acidic polymeric liquid which are mixed using a predetermined power to liquid mixing ratio to form a

solid on setting.<sup>1</sup> The major advantages of GI restoratives in the restoration of natural dentition is that they adhesively bond to sound tooth structure<sup>2–4</sup> without the need for the removal of sound tooth structure (micromechanical retention) or preconditioning the cavity for chemical adhesion (etching, priming and conditioning) as is required with dental

\* Corresponding author at: Materials Science Unit, Division of Oral Biosciences, Dublin Dental School & Hospital, Trinity College Dublin, Dublin, Ireland. Tel.: +353 1 612 7371; fax: +353 1 612 7297.

E-mail address: [mirzashahzad.baig@dental.tcd.ie](mailto:mirzashahzad.baig@dental.tcd.ie) (M.S. Baig).

0300-5712/\$ – see front matter © 2013 Elsevier Ltd. All rights reserved.

<http://dx.doi.org/10.1016/j.jdent.2013.04.004>



amalgams or resin-based composites (RBCs), respectively. The major disadvantage of using GIs to restore posterior dentition is their poor mechanical properties, namely compressive fracture strength (CFS),<sup>5,6</sup> three-point flexure strength (TFS),<sup>7</sup> biaxial flexure strength (BFS),<sup>8</sup> flexural modulus,<sup>9</sup> wear resistance<sup>10,11</sup> and fracture toughness<sup>7,12</sup> when compared with dental amalgam and RBC restoratives. The mechanical properties are further reduced when the powder to liquid mixing ratios routinely used in clinical practice are employed<sup>13</sup> and as a result, encapsulated GI restoratives were developed which offered a controlled powder to liquid mixing ratio and therefore eliminated operator induced variability.<sup>14</sup>

In the dental literature, strength is the most frequently reported mechanical test for GIs and although ISO 9917-1<sup>15</sup> specifies CFS as the strength test of choice, there are questions regarding the reliability<sup>16</sup> and validity<sup>17</sup> of the test results from CFS protocols.<sup>18</sup> Using encapsulated GI restorative materials, Dowling et al.<sup>19</sup> compared the three most popular GI strength tests (CFS, TFS and BFS) to experimentally determine the most reliable and valid strength testing methodology in an effort to replace CFS testing protocols from ISO 9917-1.<sup>15</sup> Dowling et al.<sup>19</sup> identified both BFS and TFS tests to be equally valid strength testing methodologies as the specimens failed under tensile stresses. However, the authors could not statistically differentiate between the reliability of the testing protocols with the coefficient of variation (CoV) of the TFS and BFS data reported as 12% (0.116) and 11% (0.109), respectively.<sup>19</sup> BFS was advocated over TFS for reasons of clinical relevance of specimen dimensions in conjunction with an increased simplicity of specimen fabrication.<sup>19</sup>

It is essential for any mechanical test used to evaluate the performance of dental restorative materials to demonstrate a failure mode which is representative of the clinical scenario *in vivo*.<sup>20,21</sup> The Hertzian indentation test involves applying a load through a spherical indenter against a flat specimen surface until failure occurs and has been employed to test dental ceramics,<sup>22–28</sup> dental amalgams,<sup>29–33</sup> RBCs<sup>30</sup> and GI restoratives.<sup>29,30,34,35</sup> The Hertzian indentation test simulates the loading conditions experienced by dental restorations under occlusal loading where opposing tooth contacts are simulated.<sup>20,23,29</sup> As a result, the aim of the current study was to investigate the load-bearing capacity of three commercially available encapsulated posterior GI restorative materials under Hertzian indentation and to explore the validity and reproducibility of test results achieved. The hypothesis proposed was that the Hertzian indentation test would be the most reliable mechanical test for posterior GI restorative materials, compared with CFS, TFS and BFS testing protocols, in terms of the reproducibility of test results achieved.

## 2. Materials and methods

Three encapsulated posterior GI restoratives, Chemfil Rock (Dentsply DeTrey, Konstanz, Germany; LOT 1109004048, shade A3), Fuji IX<sub>CP</sub> Fast Capsule (GC Europe, Leuven, Belgium; LOT 1011181, shade A2) and Ionofil Molar AC (Voco GmbH, Cuxhaven, Germany; LOT 1105302, shade A3) were tested under Hertzian indentation. Specimen preparation was performed in a temperature ( $21 \pm 1^\circ\text{C}$ ) and humidity

( $50 \pm 5\%$ ) controlled laboratory. Ring-moulds ( $10.0 \pm 0.1$  mm internal diameter,  $3.10 \pm 0.03$  mm thickness) were used to prepare 20 disc-shaped specimens, in five batches of four specimens, for each of the three encapsulated GI restoratives. To randomise specimen manufacture, each specimen batch was assigned a number (from 1 to 15) and numbers were randomly drawn prior to specimen manufacture to determine the GI restorative to be used. The time and day of manufacture for each specimen batch was recorded with randomisation of specimen manufacture performed<sup>19</sup> to prevent operator fatigue<sup>18</sup> and operator experience<sup>36</sup> influencing the results.

The ring-mould was placed on a glass slab covered with an acetate strip. Prior to activation, the encapsulated GI capsules were tapped to 'fluff' the powder, activated and mixed in accordance with the manufacturers' instructions.<sup>37–39</sup> Chemfil Rock capsule activation was achieved by manually pressing the capsule plunger, Fuji IX capsules were activated using a 'capsule applicator' (Capsule Applicator II, GC Corporation, Tokyo, Japan) and Ionofil Molar capsules were activated using a 'capsule activator' (AC Activator, Voco GmbH, Cuxhaven, Germany) for 2 s. Immediately after activation, the capsules were vibratory mixed at 4300 oscillations per minute<sup>40</sup> using a Capmix (3 M ESPE, Seefeld, Germany) mechanical mixing machine. In accordance with the manufacturers' instructions Chemfil Rock was mechanically mixed for 15 s with Fuji IX and Ionofil Molar mechanically mixed for 10 s.<sup>37–39</sup>

Immediately after mixing, the capsules were placed into the appropriate applicator and the GI restorative was extruded slowly to provide laminar flow<sup>14</sup> into the centre of the ring-mould, thereby minimising air bubble incorporation.<sup>41</sup> The contents of two GI restorative capsules were required to prepare a single specimen. While the GI restorative in the first capsule was being mixed, the second capsule was activated prior to mechanical mixing. Once the content of the capsules was transferred to the centre of the ring-mould, the mould was covered with another acetate strip and a 1 kg glass slab was applied to extrude the surplus material. The mould assembly was clamped between the glass slabs to ensure the top and bottom surfaces of the specimen were parallel with equal pressure applied to the specimens<sup>17</sup> and placed in a water bath maintained at  $37 \pm 1^\circ\text{C}$  for 1 h. The specimen fabrication procedure was repeated until one batch of four specimens was prepared.

After 1 h the clamps were removed, the specimens demoulded using a custom made jig and the top surfaces of the specimens numbered from 1 to 4, in accordance with the manufacturing sequence. The specimens were then stored in 50 ml of distilled water at  $37 \pm 1^\circ\text{C}$  for an additional 23 h. The specimens were removed from the distilled water 24 h after the commencement of mixing and the excess moisture on the specimens was blotted dry using an absorbent tissue prior to Hertzian indentation testing.

### 2.1. Hertzian indentation testing

The Hertzian indentation test was conducted using a universal tensile testing machine (Instron Model 5565, High Wycombe, England) such that the load was applied through a 20 mm diameter hard steel ball at a crosshead speed of 1 mm/min. A 30% glass fibre reinforced polyamide nylon 6,6

substrate (Goodfellow Cambridge, Huntingdon, England), 10 mm diameter and 5 mm thickness, was constrained in a brass holder and the GI restorative specimen was placed 'resting freely' on top of the polyamide substrate. The top surface of the specimen was placed in contact with the steel ball and aligned centrally using a customised device. The load to failure was recorded when the load cell detected a 20% drop in the peak compressive load value and the maximum load to failure value recorded was indicative of specimen failure. The thickness of each fractured fragment was measured using a digital micrometers screw gauge reading to 1  $\mu\text{m}$  (Mitutoyo, Kawasaki, Japan) and the fracture fragments were initially viewed under a stereomicroscope (Nikon Instruments Inc, USA).

## 2.2. Fractography

After testing under Hertzian indentation, selected GI specimens were gold sputtered in a vacuum evaporator (Emscope SC 500; Quorum Technologies Ltd., Kent, England) and observed at magnifications of 22x under a Scanning Electron Microscope (SEM) (Zeiss Ultra Plus Field Emission SEM; Carl Zeiss, Jena, Germany) to confirm the fracture origin and the failure mode. The fracture fragments were mounted vertically on SEM stubs using carbon cement (Leit-C conductive carbon cement; SPI Supplies, West Chester, PA, USA). The SEM was used in back-scattered electron mode under high vacuum ( $1 \times 10^{-6}$  Pa) at an operating voltage of 5 kV.

## 2.3. Statistical analyses

Statistical analyses of the load to failure data, namely one-way analyses of variance (ANOVA) with Tukey's post hoc tests, were conducted using SPSS software 12.0.1 (SPSS Inc., Chicago, IL, USA) at a significance value of  $p = 0.05$ . The normality of the load to failure data in each GI restorative group was assessed using the Shapiro–Wilk test ( $p < 0.05$ ). The Levene's test of homogeneity was used to determine the homogeneity of variance of the load to failure data. To check if there were trends within the load to failure data sets, in terms of batch and specimen number, six regression analyses ( $p < 0.05$ ) were conducted - two for each GI restorative material.

## 3. Results

When tested under Hertzian indentation, the 20 Chemfil Rock specimens had a mean load to failure value and associated standard deviation of  $1201 \pm 108$  N, with values ranging from 980 to 1387 N and a CoV of 9% (0.089). The load to failure values for the Fuji IX specimens ranged from 928 to 1116 N with a mean load to failure of  $1038 \pm 55$  N and a CoV of 5% (0.052). The mean load to failure and associated standard deviation recorded for Ionofil Molar specimens was  $1072 \pm 79$  N, ranging from 842 to 1182 N with a CoV of 7% (0.073) (Table 1). The thickness of all specimens of the GI restoratives under investigation was within a tolerance of 2% at  $3.14 \pm 0.07$  mm.

The Shapiro–Wilk test identified that the load to failure data for the GI restorative groups investigated were normally distributed ( $p > 0.05$ ) while the Levene's test of homogeneity

of variance identified the load to failure data for all GI restoratives under investigation to be homogenous ( $p > 0.05$ ). The regression analyses showed the load to failure data for the three GI restorative materials investigated were not significantly influenced by batch ( $p > 0.780$ ) or specimen number ( $p > 0.447$ ). The one-way ANOVA of the load to failure data highlighted significant differences ( $p < 0.05$ ) between the three encapsulated posterior GI restoratives. Tukey's post hoc tests identified significant increases in the load to failure data for Chemfil Rock compared with Fuji IX ( $p < 0.0001$ ) and Ionofil Molar ( $p < 0.0001$ ). No significant difference in the load to failure was noted between Fuji IX and Ionofil Molar ( $p = 0.402$ ) specimens using the Tukey's post hoc test.

On visual inspection, a consistent failure mode and fracture pattern was observed for all GI restorative specimens which resulted in the dissection of the specimens into two to five fracture fragments. However, the majority of the 20 specimens of each of the three GI restoratives, Chemfil Rock (17), Fuji IX (14) and Ionofil Molar (18), fractured into four fragments (Table 1). The fracture fragments had smooth fracture surfaces showing that the fracture surfaces were parallel to the loading axis, thereby presenting as a regular fracture pattern. No irregular fracture pattern was observed in any of the 60 specimens tested and examined from the three encapsulated posterior GI restorative materials investigated.

## 3.1. Fractography

Fractographic analysis identified bottom-initiated radial cracking generated from the dentine analogue/GI specimen interface as the primary failure mode for all GI specimens observed under the SEM (Fig. 1). The fractographic findings were consistent with the macroscopic observations showing smooth fracture surfaces.

## 4. Discussion

Clinically, GI restoratives fail in tension from a crack initiation site at or adjacent to the dentine/restoration interface.<sup>42</sup> Historically, it has been suggested that clinical failure is manifest from the stresses generated occlusally by masticatory forces which are predominantly compressive in nature,<sup>43</sup> albeit masticatory forces are always a sum of compressive, tensile and shear forces depending on the angle, inclination and loading direction of the opposing tooth. Therefore, to produce valid and clinically relevant experimental results, specimens tested in a laboratory simulation should fracture in a manner that is representative of the clinical failure mode in vivo.<sup>20,21</sup> In the CFS test, failure occurs due to crushing and 'some unresolved combination of tension and shear' stresses<sup>17</sup> which has resulted in considerable discussions over the last two decades to replace the CFS test from the ISO testing armamentarium.<sup>16,17</sup> TFS test specimens fail in tension<sup>44</sup> but the specimen dimensions are not representative of the size of GI restoratives when they are employed clinically. The BFS test specimens have a surface area to volume ratio similar to that of medium sized GI restorations<sup>45</sup> and the test specimens fail in tension.<sup>46</sup> However, loading a GI restorative on a ring support ignores the influence of the supporting dentine

**Table 1 – The mean load to failure ± standard deviation (SD) and coefficient of variation (CoV) for the three encapsulated GI restoratives. The number in parenthesis beside each load to failure value indicates the number of fracture fragments for that tested specimen.**

Specimen number	Chemfil Rock	Fuji IX <sub>GP</sub> Fast Capsule	Ionofil Molar AC
1	1382 (4)	1036 (4)	1096 (4)
2	1036 (4)	1050 (4)	1050 (4)
3	1171 (4)	1055 (4)	1100 (4)
4	1300 (4)	949 (4)	1149 (4)
Mean ± SD	1222 ± 151	1022 ± 50	1099 ± 40
CoV	0.124	0.048	0.037
5	1175 (4)	1093 (4)	842 (4)
6	1245 (4)	1052 (3)	1034 (4)
7	1036 (2)	1071 (3)	1013 (4)
8	1172 (4)	984 (4)	1139 (3)
Mean ± SD	1157 ± 87	1050 ± 47	1006 ± 123
CoV	0.075	0.044	0.122
9	1178 (4)	1067 (4)	1029 (4)
10	1234 (4)	1040 (4)	1109 (4)
11	1263 (4)	1050 (4)	1130 (4)
12	1159 (3)	959 (4)	1180 (5)
Mean ± SD	1208 ± 49	1029 ± 48	1112 ± 63
CoV	0.040	0.046	0.056
13	1206 (4)	1042 (3)	1036 (4)
14	1265 (4)	1073 (4)	1081 (4)
15	1255 (4)	928 (3)	1027 (4)
16	1097 (4)	1081 (3)	959 (4)
Mean ± SD	1206 ± 77	1031 ± 71	1026 ± 50
CoV	0.063	0.068	0.048
17	1304 (4)	945 (4)	1103 (4)
18	1174 (5)	1116 (4)	1080 (4)
19	1387 (4)	1082 (4)	1182 (4)
20	980 (4)	1086 (3)	1106 (4)
Mean ± SD	1212 ± 177	1057 ± 76	1118 ± 45
CoV	0.146	0.072	0.039
Total mean ± SD	1201 ± 108	1038 ± 55	1072 ± 79
Mean CoV	0.089	0.052	0.073

substructure<sup>20</sup> while loading with a 4 mm diameter ball indenter fails to match the occlusal contact surface of an opposing tooth cusp<sup>20</sup> which further limits the clinical applicability of the BFS testing methodology.

The bi-layered Hertzian indentation system used to test the encapsulated GI restoratives involved applying a load through a 20 mm diameter hard steel spherical indenter to a flat GI restorative specimen surface until failure occurred. Therefore, the Hertzian indentation test simulated the loading conditions experienced by GI restorations under occlusal loading.<sup>29,30,34,35</sup> Additionally, the Hertzian indentation test involved testing the specimens which ‘rest’ freely on top of a glass fibre reinforced nylon substrate. The substrate had an elastic modulus (10–11 GPa)<sup>47</sup> similar to that of dentine (11–18 GPa)<sup>48</sup> such that the failure occurred from tensile initiated radial cracking at the dentine analogue/GI restoration interface (Fig. 1).<sup>29,30,34,35</sup> The elastic modulus mismatch between the GI restorative specimen and the nylon substrate material resulted in the creation of a tensile stress at the substrate/specimen interface on loading,<sup>35</sup> leading to the initiation of radial cracks at the specimen undersurface which propagated

upwards through the specimen. The fracture mode and failure origin were confirmed by fractography. These observations are in agreement with the findings of Wang and Darvell<sup>29,30,34,35</sup> – the other researchers to have employed Hertzian indentation testing methodology to GI restoratives. Wang and Darvell observed a regular fracture pattern with bottom initiated radial cracking as the principle failure mode for GI restorative disc-shaped specimens of thicknesses varying from 0.4 to 3.6 mm.<sup>29</sup> In the present study, all specimens had a regular fracture pattern with smooth fracture surfaces indicating that radial cracking was the dominant failure mode (Fig. 1). Wang and Darvell identified some evidence of cone cracking only when the GI specimen thickness was increased from 4 to 7 mm.<sup>29</sup> The specimen thickness used in the current study (3.14 ± 0.07 mm) was consistent with the bottom initiated radial cracking and regular fracture pattern observed by Wang and Darvell<sup>29,30,34,35</sup> which is representative of the clinical failure mode for GI restoratives in vivo,<sup>42</sup> thereby confirming the validity of the Hertzian indentation testing protocol.

The reliability of the Hertzian indentation testing protocol employed in the current study was assessed by the

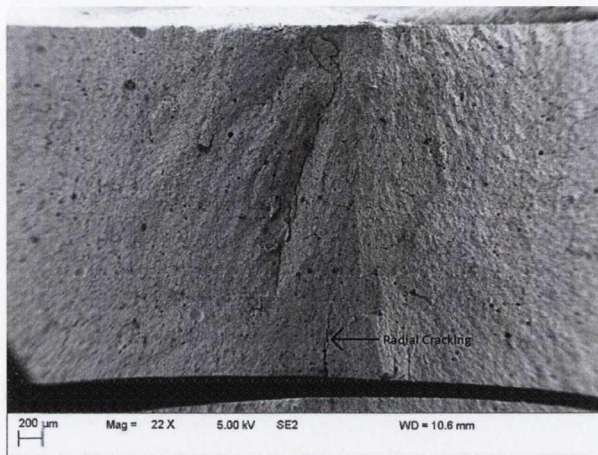


**Fig. 1 – Scanning electron micrograph of the fracture surface of an encapsulated GI restorative showing radial cracking.**

determination of the CoV, namely the ratio of the standard deviation to the mean load to failure values for the 20 specimens of each GI restorative investigated. The CoV identified the extent of the variability in the data sets in relation to the mean and is considered a useful measure of reliability, with a lower value of CoV indicative of a more reliable data set. The CoV for the data sets of Chemfil Rock, Fuji IX and Ionofil Molar were 9% (0.089), 5% (0.052) and 7% (0.073), respectively, with a mean CoV of 7% (0.071) for the three GI restorative data sets (60 specimens) investigated. The mean CoV of 7% for the GI restorative data sets achieved using Hertzian indentation testing was significantly reduced compared with the mean CoVs observed for the TFS (12%) and BFS (11%) when data sets for the same encapsulated GI restoratives were investigated previously.<sup>19</sup> This confirms the increased reproducibility of data sets generated by the Hertzian indentation testing protocol. The reduced CoV in the data recorded using the Hertzian indentation test could be due to a number of factors. The specimen preparation technique employed to manufacture the disc-shaped specimens is simple and does not require the operator to have a skill beyond that required of a dentist.<sup>32</sup> The testing protocol is easy to perform with the specimen placed on top of the substrate constrained in a brass holder and aligned with the help of a centralising device, thereby minimising any critical alignment concerns. The use of encapsulated GI restoratives minimised operator induced variability on mixing and only five specimen batches were prepared each day which minimised the potential for operator fatigue.<sup>18</sup>

## 5. Conclusion

The reliability of the load to failure data sets of the GI restoratives recorded using Hertzian indentation testing were significantly improved compared with the mechanical testing approaches routinely employed in the dental literature. The fracture origin and failure mode using Hertzian indentation is

representative of the clinical situation in vivo suggesting the possibility of inclusion as an ISO testing protocol.

## Acknowledgement

The authors would like to thank Dr. Heath Bagshaw for his assistance with the fractography.

## REFERENCES

1. Wilson AD, Kent BE. A new translucent cement for dentistry. The glass ionomer cement. *British Dental Journal* 1972;132:133–5.
2. Wilson AD, McLean JW. Adhesion. In: Wilson AD, editor. *Glass-ionomer cement*. Chicago, IL: Quintessence Publishing Co., Inc.; 1988. p. 83–99.
3. Zhi QH, Lo EC, Lin HC. Randomized clinical trial on effectiveness of silver diamine fluoride and glass ionomer in arresting dentine caries in preschool children. *Journal of Dentistry* 2012;40:962–7.
4. Taha NA, Palamara JE, Messer HH. Assessment of laminate technique using glass ionomer and resin composite for restoration of root filled teeth. *Journal of Dentistry* 2012;40:617–23.
5. Cho GC, Kaneko LM, Donovan TE, White SN. Diametral and compressive strength of dental core materials. *Journal of Prosthetic Dentistry* 1999;82:272–6.
6. Elsaka SE, Hamouda IM, Swain MV. Titanium dioxide nanoparticles addition to a conventional glass-ionomer restorative: influence on physical and antibacterial properties. *Journal of Dentistry* 2011;39:589–98.
7. Bapna MS, Gadia CM, Drummond JL. Effects of aging and cyclic loading on the mechanical properties of glass ionomer cements. *European Journal of Oral Science* 2002;110:330–4.
8. Frankel N, Pearson GJ, Labella R. Long-term strength of aesthetic restoratives. *Journal of Oral Rehabilitation* 1998;25:89–93.
9. Meyer JM, Cattani-Lorente MA, Dupuis V. Compomers: between glass-ionomer cements and composites. *Biomaterials* 1998;19:529–39.
10. Zanata RL, Magalhães AC, Lauris JR, Atta MT, Wang L, Navarro MF. Microhardness and chemical analysis of high-viscous glass-ionomer cement after 10 years of clinical service as ART restorations. *Journal of Dentistry* 2011;39:834–40.
11. Pelka M, Ebert J, Schneider H, Krämer N, Petschelt A. Comparison of two- and three-body wear of glass-ionomers and composites. *European Journal of Oral Science* 1996;104:132–7.
12. Lloyd CH, Mitchell L. The fracture toughness of tooth coloured restorative materials. *Journal of Oral Rehabilitation* 1984;11:257–72.
13. Billington RW, Williams JA, Pearson GJ. Variation in powder/liquid ratio of restorative glass ionomer dental cement used in dental practice. *British Dental Journal* 1990;169:164–7.
14. Dowling AH, Fleming GJP. Is encapsulation of posterior glass-ionomer restoratives the solution to clinically induced variability introduced on mixing? *Dental Materials* 2008;24:957–66.
15. International Organization for Standardization. ISO 9917-1. Dentistry – water-based cements. Part 1. Powder/liquid acid-base cements. 1st ed. 2003.
16. McCabe JF, Watts DC, Wilson HJ, Worthington HV. An investigation of test-house variability in the mechanical testing of dental materials. *Journal of Dentistry* 1990;18:90–7.

17. Darvell BW. Uniaxial compression tests and the validity of indirect tensile strength. *Journal of Material Science* 1990;25:757–80.
18. Fleming GJP, Dowling AH, Addison O. The crushing truth about glass ionomer restoratives: exposing the standard of the standard. *Journal of Dentistry* 2012;40:181–8.
19. Dowling AH, Fleming GJP, McGinley EL, Addison O. Improving the standard of the standard for glass ionomers: an alternative to the compressive fracture strength test for consideration? *Journal of Dentistry* 2012;40:189–201.
20. Kelly JR. Clinically relevant approach to failure testing of all-ceramic restorations. *Journal of Prosthetic Dentistry* 1999;81:652–61.
21. Kelly JR, Benetti P, Rungruananunt P, Bona AD. The slippery slope – critical perspectives on in vitro research methodologies. *Dental Materials* 2012;28:41–5.
22. Peterson IM, Pajares A, Lawn BR, Thompson VP, Rekow ED. Mechanical characterization of dental ceramics by Hertzian contacts. *Journal of Dental Research* 1998;77:589–602.
23. Lawn BR, Deng Y, Thompson VP. Use of contact testing in the characterization and design of all-ceramic crownlike layer structures: a review. *Journal of Prosthetic Dentistry* 2001;86:495–510.
24. Lawn BR, Deng Y, Miranda P, Pajares A, Chai H, Kim DK. Overview: damage in brittle layer structures from concentrated loads. *Journal of Materials Research* 2002;17:3019–36.
25. Jung YG, Wuttiphan S, Peterson IM, Lawn BR. Damage modes in dental layer structures. *Journal of Dental Research* 1999;78:887–97.
26. Deng Y, Lawn BR, Lloyd IK. Characterization of damage modes in dental ceramic bilayer structures. *Journal of Biomedical Materials Research* 2002;63:137–45.
27. Chai H, Lawn B. Fracture modes in brittle coatings with large interlayer modulus mismatch. *Journal of Materials Research* 1999;14:3805–17.
28. Harvey CK, Kelly JR. Contact damage as a failure mode during in vitro testing. *Journal of Prosthodontics* 1996;5:95–100.
29. Wang Y, Darvell BW. Failure mode of dental restorative materials under Hertzian indentation. *Dental Materials* 2007;23:1236–44.
30. Wang Y, Darvell BW. Failure behavior of glass ionomer cement under Hertzian indentation. *Dental Materials* 2008;24:1223–9.
31. Wang Y, Darvell BW. Interactive effect of indenter size and specimen thickness in Hertzian indentation test. *Dental Materials* 2010;26:539–44.
32. Darvell BW. Development of strength in dental silver amalgam. *Dental Materials* 2012;28:207–17.
33. Darvell BW. Effect of corrosion on the strength of dental silver amalgam. *Dental Materials* 2012;28:160–7.
34. Wang Y, Darvell BW. Hertzian load-bearing capacity of a ceramic-reinforced glass ionomer cement stored wet and dry. *Dental Materials* 2009;25:952–5.
35. Wang Y, Darvell BW. Effect of elastic modulus mismatch on failure behaviour of glass ionomer cement under Hertzian indentation. *Dental Materials* 2012;28:279–86.
36. Wasson EA, Nicholson JW. Effect of operator skill in determining the physical properties of glass-ionomer cements. *Clinical Materials* 1994;15:169–72.
37. Product specification for Chemfil Rock. Dentsply DeTrey: Konstanz, Germany.
38. Product specification for Fuji IX Fast Capsule. GC Europe: Leuven, Belgium.
39. Product specification for Ionofil Molar AC. Voco GmbH: Cuxhaven, Germany.
40. Product specification for Capmix. 3M ESPE: Seefeld, Germany.
41. Fleming GJP, Shortall ACC, Shelton RM, Marquis PM. Encapsulated versus hand-mixed zinc phosphate dental cements. *Biomaterials* 1999;20:2147–53.
42. McLean JW, Wilson AD. The clinical development of the glass-ionomer cement. III. The erosion lesion. *Australian Dental Journal* 1977;22:190–5.
43. White SN, Yub Z. Compressive and diametral tensile strengths of current adhesive luting agents. *Journal of Prosthetic Dentistry* 1993;69:568–72.
44. Berenbaum R, Brodie I. Measurement of tensile strength of brittle materials. *British Journal of Applied Physics* 1959;10:281–7.
45. Piddock V, Marquis PM, Wilson HJ. The mechanical strength and microstructure of all-ceramic crowns. *Journal of Dentistry* 1987;15:153–8.
46. Ban S, Hasegawa J, Anusavice KJ. Effect of loading conditions on bi-axial flexure strength of dental cements. *Dental Materials* 1992;8:100–4.
47. Product specification for polyamide – nylon 6,6 – 30% glass fiber reinforced rod. Goodfellow: Cambridge, Huntingdon, England.
48. Craig RG. Restorative dental materials. 13th ed. The oral environment. St. Louis: Mosby; 2012: 16.

### **3.3 FRACTURE TOUGHNESS TESTING: A DISCRIMINATORY MECHANICAL TESTING PERFORMANCE INDICATOR FOR GLASS-IONOMER RESTORATIVES.**

MS Baig, CH Lloyd, GJP Fleming (2015). Fracture toughness testing: A discriminatory mechanical testing performance indicator for glass-ionomer restoratives. *Dental Materials*, Article in press.

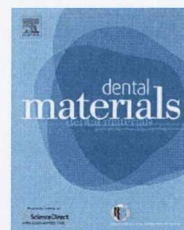
The HI test was identified as the most clinically relevant testing methodology and was able to discriminate between the encapsulated GI products investigated (Manuscript 3.2), although the Hertzian load bearing capacity was recorded as the maximum load-to-failure (Wang and Darvell, 2007) which was not an intrinsic material property. As  $K_{IC}$  is an intrinsic material property which represents the materials resistance to propagation of a pre-existing crack (Atkins and Mai, 1985), the current study examined the discriminatory potential of the SEN  $K_{IC}$  testing methodology for encapsulated GIs. To enable a valid comparison with the CFS, TFS, BFS (Dowling et al., 2012) and HI test results (Manuscript 3.2), the same encapsulated GIs were employed as previously. To further establish the discriminatory ability of the SEN  $K_{IC}$  testing methodology, the  $K_{IC}$  of hand-mixed GIs prepared with varying powder content for a constant weight of liquid was investigated. The hypothesis tested was that the SEN  $K_{IC}$  testing methodology would act as a discriminatory performance indicator for both encapsulated and hand-mixed GI products investigated. A linear deterioration in  $K_{IC}$  for the hand-mixed GI groups manipulated with progressively reduced powder content was expected. To ensure accurate determination of the crack-length for valid  $K_{IC}$  test results, the fracture surfaces of the fracture fragments from all specimens were scanned using a contact profilometer which enabled accurate quantification of the crack-length through the clear demarcation of two reproducible reference points.



ELSEVIER

Available online at [www.sciencedirect.com](http://www.sciencedirect.com)

ScienceDirect

journal homepage: [www.intl.elsevierhealth.com/journals/dema](http://www.intl.elsevierhealth.com/journals/dema)

## Fracture toughness testing: A discriminatory mechanical testing performance indicator for glass-ionomer restoratives?

Mirza Shahzad Baig<sup>a</sup>, Charles H. Lloyd<sup>b</sup>, Garry J.P. Fleming<sup>a,\*</sup>

<sup>a</sup> Materials Science Unit, Dublin Dental University Hospital, Trinity College Dublin, Dublin 2, Ireland

<sup>b</sup> Division of Oral and Maxillofacial Clinical Sciences, Dundee Dental Hospital and School, Park Place, Dundee DD1 4HR, Scotland, United Kingdom

### ARTICLE INFO

#### Article history:

Received 14 January 2015

Received in revised form

20 April 2015

Accepted 24 April 2015

#### Keywords:

Glass-ionomer restorative

Powder:liquid mixing ratio

Fracture toughness testing

Encapsulation

Hand-mixed

### ABSTRACT

**Objectives.** To investigate the single-edge notched (SEN) bend fracture toughness ( $K_{IC}$ ) testing methodology as a reproducible and discriminatory mechanical testing protocol for encapsulated and hand-mixed glass-ionomers (GI).

**Methods.** SEN bend test-pieces ( $35.0 \pm 0.1$  mm length,  $6.0 \pm 0.1$  mm width,  $3.0 \pm 0.1$  mm thickness with a sharp notch formed at mid-length by embedding a scalpel blade) were prepared for  $K_{IC}$  testing using three encapsulated GI products (Chemfil Rock, Fuji IXGP Fast Capsule and Ionofil Molar AC). In addition, test-pieces were prepared from a hand-mixed GI product (Ionofil Molar) which contained between 100% and 20% of the manufacturer's recommended powder content (in 10% decrements) for a constant weight of liquid. Groups of 20 test-pieces were prepared for each encapsulated GI product ( $n=3$ ) and hand-mixed GI powder:liquid mixing ratio ( $n=9$ ). Data were statistically analyzed and the coefficients of variation (CoV) determined for each encapsulated GI product and hand-mixed GI powder:liquid mixing ratio.

**Results.** The  $K_{IC}$  testing methodology failed to discriminate between the encapsulated GI products that were investigated ( $p=0.225$ ). For the hand-mixed GI, the  $K_{IC}$  testing methodology also failed to discriminate between the powder:liquid mixing ratios investigated ( $R^2=0.576$ ). The pooled CoV (10%) for the encapsulated GI products and for the powder:liquid mixing ratio groups (12%) identified the reproducibility of the test for this experiment. For the hand-mixed GI mixing ratio groups with between 100% to 50% of the recommended powder content, no trend could be discerned.

**Significance.** The  $K_{IC}$  testing methodology failed to discriminate between different encapsulated GI products and hand-mixed GI powder:liquid mixing ratio groups investigated, despite  $K_{IC}$  being an intrinsic material property and the coefficient of variation being acceptable.

© 2015 Academy of Dental Materials. Published by Elsevier Ltd. All rights reserved.

\* Corresponding author. Tel.: +353 1 612 7371; fax: +353 1 612 7297.

E-mail address: [garry.fleming@dental.tcd.ie](mailto:garry.fleming@dental.tcd.ie) (G.J.P. Fleming).

<http://dx.doi.org/10.1016/j.dental.2015.04.014>

0109-5641/© 2015 Academy of Dental Materials. Published by Elsevier Ltd. All rights reserved.

## 1. Introduction

The compressive fracture strength (CFS) test is the strength test specified by the International Organisation for Standardisation (ISO) [1] standard for water-based cements. Concerns have been raised regarding the reliability of the CFS testing protocol for glass-ionomers (GIs) in a ‘test-house variability’ study in 1990 [2] in which inter- and intra-operator variability was identified. Fleming et al. [3] revisited the CFS testing methodology given in ISO 9917-1:2007 [1] for GI products to identify the reproducibility of test results achieved in terms of inter- and intra-operator variabilities. These authors highlighted the batch censoring specified in the ISO 9917-1:2007 to be unsafe as it misidentified operator variability and therefore a statistical approach employing a minimum of 20 test-pieces [4] is required for a meaningful interpretation of the CFS data. They concluded that the CFS test could be performed reliably if test-piece preparation techniques and laboratory conditions are standardized, although such level of control is not routinely applied, as is evident from the large variation in CFS data reported in the dental literature [3].

To identify a potential replacement testing protocol for the CFS test, Dowling et al. [5] investigated the three-point flexure strength (TFS) and biaxial flexure strength (BFS) testing methodologies using three encapsulated GIs (Chemfil Rock, Fuji IX<sub>CP</sub> Fast Capsule and Ionofil Molar AC). With their results, these authors [5] could not differentiate between the reproducibility of the testing protocols investigated ( $p=0.632$ ), with the pooled coefficients of variation (CoV) of the CFS, TFS and BFS data reported being 10% (0.104), 12% (0.116) and 11% (0.109), respectively. Interestingly, both the TFS ( $p=0.271$ ) and BFS ( $p=0.134$ ) testing methodologies failed to discriminate between the three encapsulated GI products, despite being supplied by different manufacturers with different glass compositions, liquid compositions and powder:liquid mixing ratios. In contrast differences in CFS ( $p=0.001$ ) were evident. Baig et al. [6] used the same encapsulated GI products to examine the reliability of the Hertzian indentation (HI) testing protocol for disc-shaped test-pieces of 10 mm diameter and 3 mm thickness [7]. They [6] identified the HI test to be a reproducible testing methodology with a lower pooled CoV, 7% (0.071). In addition, the HI test was able to discriminate between these three encapsulated GI products ( $p<0.001$ ). However, the ‘Hertzian load-bearing capacity’ reported by Baig et al. [6] is the maximum load-to-failure, which was not a material property and therefore could be interpreted as the ‘quality of the cement’ rather than a ‘predictive value’ [8].

The validity of the CFS test has also been questioned because the stress at failure calculation does not take into account the failure mechanism operating during CFS testing, whereby cylindrical specimens fail by ‘some unresolved combination of tension and shear’ stresses [9,10]. The TFS [5], BFS [5] and HI [6] tests have been identified as valid testing methodologies for encapsulated GI products because failure occurs from the surface under tension. Bar-shaped test-pieces used for TFS testing are not geometrically representative of loading clinical GI restorations. Also, the force at failure will depend upon the perfection of the test-piece surface and well as any inherent material property. The loading geometry of

the disc shaped BFS test-piece eliminates the test-piece edge effect. This test-piece more closely resembles the surface area to volume ratio of a dental restoration, although loading such a test-piece through a 4 mm diameter ball when supported on an annulus [5] (i.e. in the absence of a supporting substructure) fails to replicate the situation met in vivo. In terms of simulating the clinical scenario, loading HI test-pieces using a 20 mm hard steel ball to simulate cusp contact [9,11] when resting freely on a dentin analogue seems most relevant, although the ‘Hertzian load-bearing capacity’ [6] recorded as the maximum load-to-failure is not a material property.

An ideal mechanical testing protocol for GIs should be reliable, valid and discriminatory between encapsulated GI products from different manufacturers and between hand-mixed GIs prepared at varying powder:liquid mixing ratios routinely employed in the clinic [12]. Fracture toughness ( $K_{IC}$ ) is an intrinsic material property, independent of specimen dimensions, that represents a material’s resistance to crack propagation [13] and has been employed to test resin-bonded composites (RBCs) [14–26], GIs [18–20,24,25,27–32], ceramics [33–35] and dental amalgams [20,24,25,36,37]. The aim of the current study was to investigate whether the single-edge notched (SEN) bend test-piece  $K_{IC}$  testing protocol is a reproducible and discriminatory testing methodology to act as a performance indicator for encapsulated and hand-mixed GI restorative materials. The hypotheses proposed were: (1) that the test would be a reliable and discriminatory mechanical testing protocol to act as a performance indicator by discriminating between different encapsulated GI products, and (2) that the presence of a linear deterioration in  $K_{IC}$  on reducing the powder content from the optimum that specified by the manufacturer for a hand-mixed GI restorative material is indicative of a reliable and discriminatory mechanical testing protocol.

## 2. Materials and methods

A polytetrafluoroethylene (PTFE) lined brass split-mould resting on top of a PTFE lined brass base plate [18] was used to prepare SEN bend test-pieces ( $35.0\pm 0.1$  mm length,  $6.0\pm 0.1$  mm width,  $3.0\pm 0.1$  mm thickness). Prior to test-piece manufacture, the PTFE lined surfaces (forming the two side walls) of the mould [18] (Fig. 1) were covered with two layers of transparent adhesive tape (Sellotape, Henkel Ltd., Winsford, Cheshire, UK) to facilitate test-piece removal. The mould was designed and constructed with PTFE on the surfaces in contact with the material to avoid adhesion. The PTFE was backed with brass to give the mould rigidity. However, applying adhesive tape to the walls and base produced an improvement. In addition the tape aided removal of the set cement. Peeling the tape from the top surface of the mould created a tab which could be lifted to apply a uniform force to the test-piece. This avoided direct and localized force on the test-piece which risked fracture during demoulding [12–16]. In addition, a single layer of the transparent adhesive tape was applied to the PTFE surface of the brass base plate (Fig. 1). Following application of the adhesive tape, the structural components of the split-mould were re-assembled and secured with multiple screws.



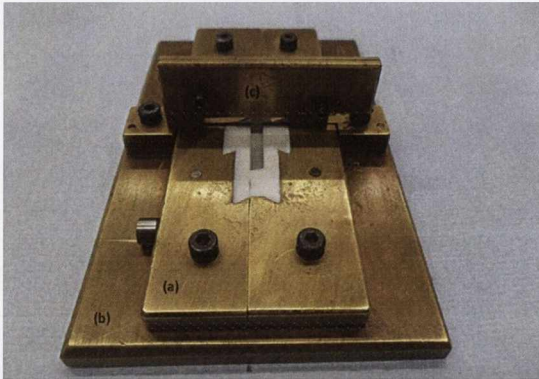


**Fig. 1** – A photograph of the structural components of a split-mould used for the preparation of single-edge notched (SEN) bend test-pieces highlighting (a) the PTFE lined brass split-mould (two parts), (b) the PTFE-lined brass base plate and (c) the straight edge surgical scalpel blade.

To eliminate the influence of sequence bias, randomization [5] of test-piece manufacture was performed by assigning a number to each test-piece to be made, such that a set of numbers were drawn daily to determine the sequence of test-piece manufacture. Only six SEN bend test-pieces were made daily to minimize the influence of operator fatigue [3]. A new scalpel blade was employed for each SEN bend specimen to ensure a consistent crack tip radius ( $0.3\ \mu\text{m}$ ) for all specimens manufactured.

### 2.1. Encapsulated glass-ionomer restoratives

To investigate and compare the discriminatory ability of the  $K_{IC}$  testing protocol between different encapsulated GIs with that of the mechanical testing methodologies investigated by Dowling et al. [5] (CFS, TFS and BFS) and Baig et al. [6] (HI), the same encapsulated GI products were used in the current study, namely: Chemfil Rock (Dentsply DeTrey, Konstanz, Germany; LOT 1208000039, shade A3), Fuji IX<sub>CP</sub> Fast Capsule (GC Europe, Leuven, Belgium; LOT 1305171, shade A2) and Ionofil Molar AC (Voco GmbH, Cuxhaven, Germany; LOT 1228502, shade A3). The powder within each GI capsule was loosened by tapping the side of the capsule against the laboratory bench. Following activation, the GI restorative capsules were vibratory mixed at 4300 oscillations per minute using a Capmix (3M ESPE, Seefeld, Germany) mechanical mixing machine [38]. In line with the manufacturer's instructions, Chemfil Rock capsules were mechanically mixed for 15 s [39], while Fuji IX<sub>CP</sub> Fast and Ionofil Molar AC were mixed for 10 s [40,41].

For Chemfil Rock and Fuji IX<sub>CP</sub> Fast, the mixed contents from five capsules were required for a single SEN bend test-piece. However, for Ionofil Molar AC four capsules provided sufficient amount of mixed GI for a single test-piece. To ensure consistent fabrication and to avoid delay between mixing capsules, assistance from a second operator was acquired. While the mixed content from a GI capsule was being transferred to the mould by the first operator, the second operator activated

and mixed the following GI capsule, thereby simulating 'four-handed dentistry' [42]. A sharp notch was formed in the test-piece by inserting a straight-edge surgical scalpel blade (Type 10A, Swann-Morton Ltd., Sheffield, UK) into a close-fitting slot located at mid-length of the split-mould (Fig. 1) which penetrated to half the width of the test-piece [14]. The contents of two GI capsules were transferred to the mould at mid-length, where the notch would be created and the blade pressed into the paste. The mixed contents from the remaining GI capsules were then transferred to the lateral aspects of the mould on each side of the blade. The filled mould was covered with strips of acetate, placed each side of the scalpel blade. To ensure adequate packing of the GI into the mould, pressure was applied to the top surface using a 1 kg weight. The filled mould assembly was transferred to an incubator (Climate Cabinet, Firlabo, Meyzieu, France) maintained at  $(37 \pm 1)^\circ\text{C}$  and 100% relative humidity for 1 h. After 1 h, the split-mould was disassembled, the test-piece removed, numbered and stored in 50 ml of distilled water at  $(37 \pm 1)^\circ\text{C}$  for 23 h prior to testing. This test-piece manufacturing procedure was repeated to prepare 20 SEN bend test-pieces for each encapsulated GI restorative under investigation.

### 2.2. Hand-mixed glass-ionomer restorative

To investigate the discriminatory ability of the  $K_{IC}$  testing protocol between GI test-pieces prepared at varying powder:liquid mixing ratios a hand-mixed GI restorative (Ionofil Molar: Voco GmbH, Cuxhaven, Germany; Powder: V50335, Liquid: V50375) was used to manufacture test-pieces with a progressively reduced (10% decrements) powder content to a minimum of 20% that recommended by the manufacturer (4:1, g:g) [43] for a constant weight of liquid. The powder:liquid mixing ratios investigated were chosen to replicate the mixing ratios reported to be routinely produced by operators in clinical practice and although the lowest powder content identified by the Billington et al. was 37% of that recommended by the manufacturers the authors included 30% and 20% powder contents for completeness [12]. The appropriate amount of the GI powder was weighed using a weighing boat on a balance accurate to 0.001 g (Sartorius Expert, Sartorius AG, Goettingen, Germany). The GI liquid was weighed and dispensed onto one end of a glass slab, the GI powder was transferred to the other end of the glass slab and divided into two equal halves. The first half of the powder was introduced into the liquid and mixed for 20 s using a stainless steel mixing spatula and followed by the second half, mixing for 20 s to ensure a total mixing time of 40 s.

Following mixing, the GI was transferred to the split-mould in three increments, one placed at the center of the mould cavity and the other two to each side of this. A sharp notch was formed in the test-piece as described previously. The filled split-mould was covered with acetate and the subsequent production procedure was the same as that for encapsulated GI products. The process was repeated such that 20 SEN bend test-pieces were produced for each of the powder:liquid mixing ratios ( $n = 9$ ) under investigation.

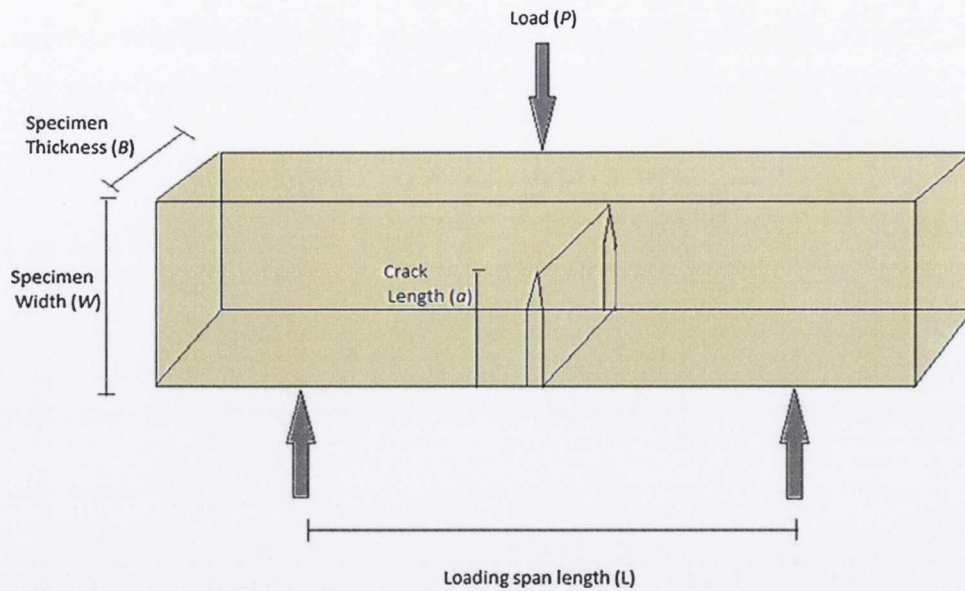


Fig. 2 – A schematic representation of the test-piece geometry of the single-edge notched (SEN) bend test-piece used in the current study illustrated, loaded in a three-point flexure.

### 2.3. Fracture toughness testing and profilometric analysis

The SEN bend test-pieces were loaded in a three-point flexure testing assembly (Fig. 2) at a crosshead speed of 0.1 mm/min using a universal testing machine (Instron Model 5565, High Wycombe, England). A micrometer screw gauge accurate to 1  $\mu\text{m}$  (Mitutoyo, Kawasaki, Japan) was used to measure the specimen width ( $W$ ) and thickness ( $B$ ) (To avoid accidental damage, these measurements were made after loading to failure). The crack length ( $a$ ) was determined by measuring the distance below the notch ( $W-a$ ) using a contact profilometer (Talsurf CLI 2000, Taylor-Hobson Precision, Leicester, UK). The two fracture fragments of each failed test-piece were secured on a stable platform with the fracture surfaces mounted adjacent to each other. The profilometric analysis was performed by scanning the fracture surfaces of the failed test-piece longitudinally across a rectangular area of 10 mm<sup>2</sup> (5 mm length and 1 mm width on each fracture fragment) using an induction gauge conisphere diamond stylus tip (2  $\mu\text{m}$  radius) at a speed of 2 mm/s. To determine the start and end points of the fracture surface, each scan included a section of the scalpel blade impression and the total length of the fracture surface. The scan resolution was 1001 points ( $x$ -direction) and 101 traces ( $y$ -direction) using a step size of 10  $\mu\text{m}$  ( $x$  and  $y$  direction). Following scanning, the TalyMap analysis software package (Taylor-Hobson Precision, Leicester, UK) was used to generate a detailed 3D profile representation of the fracture surfaces (Fig. 3). The length of the fracture surface ( $W-a$ ) was recorded as the distance (in mm) from the end of the scalpel blade impression to the lower edge of the fracture fragment (Fig. 4). The mean was determined by extracting and averaging three longitudinal traces from each fracture surface scan, one at mid-thickness and two at quarter-thickness points, such that the difference between any two of the three measurements

did not exceed 10% of the mean value [44]. The  $K_{IC}$  was then calculated using Eq. (1), obtained from ISO 12737:2010 [44].

$$K_{IC} = \frac{PL}{BW^{3/2}} f(a/W) \quad (1)$$

where  $P$  was the load-to-failure (N),  $L$  the loading span length (20 mm) and  $f(a/W)$  is a geometrical function dependant on  $a/W$  which was calculated using Eq. (2), provided in ISO 12737:2010 [44].

$$f(a/W) = \frac{3(a/W)^{1/2} [1.99 - (a/W)(1 - a/W)]}{2(1 + 2a/W)(1 - a/W)^{3/2}} \quad (2)$$

### 2.4. Statistical analyses

One-way analyses of variance (ANOVA) with Tukey's post hoc tests ( $p=0.05$ ) were performed for the  $K_{IC}$  data using IBM SPSS Statistics V22.0 (SPSS Inc., Chicago, IL, USA). The Shapiro-Wilk test ( $p<0.05$ ) and Levene's test of homogeneity ( $p<0.05$ ) were conducted to assess the normality and the homogeneity of variance of the data collected for test-pieces made using encapsulated and hand-mixed GI. Regression analyses ( $p<0.05$ ) were conducted to identify any trend within the encapsulated and hand-mixed  $K_{IC}$  data sets in terms of test-piece numbers. The coefficients of variation (CoV) of the encapsulated and hand-mixed  $K_{IC}$  data sets were determined. Additionally, for the hand-mixed GI powder:liquid mixing ratio groups, regression analyses ( $p<0.05$ ) were also employed to determine trends within the data sets as powder content was reduced.

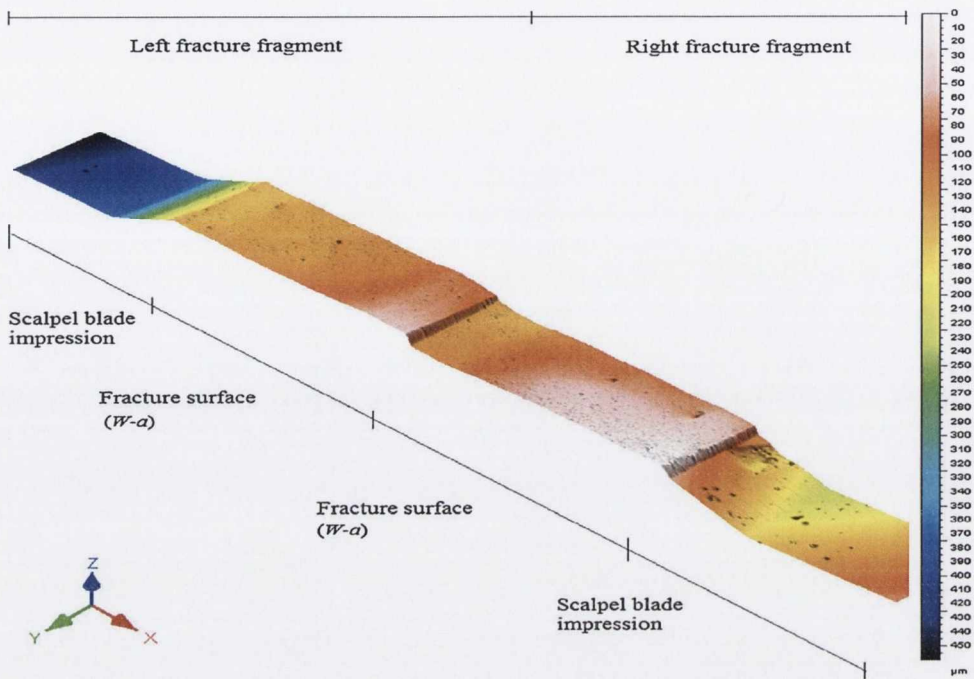


Fig. 3 – A three-dimensional representation of the fracture surfaces of a glass-ionomer single-edge notched (SEN) bend test-piece with alignment of the two fracture fragments (left and right).

### 3. Results

The SEN bend test-pieces from each encapsulated GI restorative ( $n=3$ ) and hand-mixed GI powder:liquid mixing ratio group ( $n=9$ ) fractured in a straight line with the crack extending from the apex of the preformed sharp notch to the opposite surface of the test-piece. No shear lips or edge effects were observed on any of the SEN bend test-piece fracture surfaces in

either the encapsulated ( $n=60$ ) or hand-mixed ( $n=180$ ) groups. All test-pieces had flat fracture surfaces.

The Shapiro-Wilk test confirmed that the  $K_{IC}$  data for the encapsulated GI products ( $p>0.253$ ) and those for hand-mixed GI powder:liquid ( $p>0.114$ ) were normally distributed. The Levene's test of homogeneity of variance showed that all data for the encapsulated GI products ( $p=0.212$ ) and the hand-mixed GI ( $p=0.400$ ) to be homogenous. The regression analyses identified no trend within the data sets in terms of

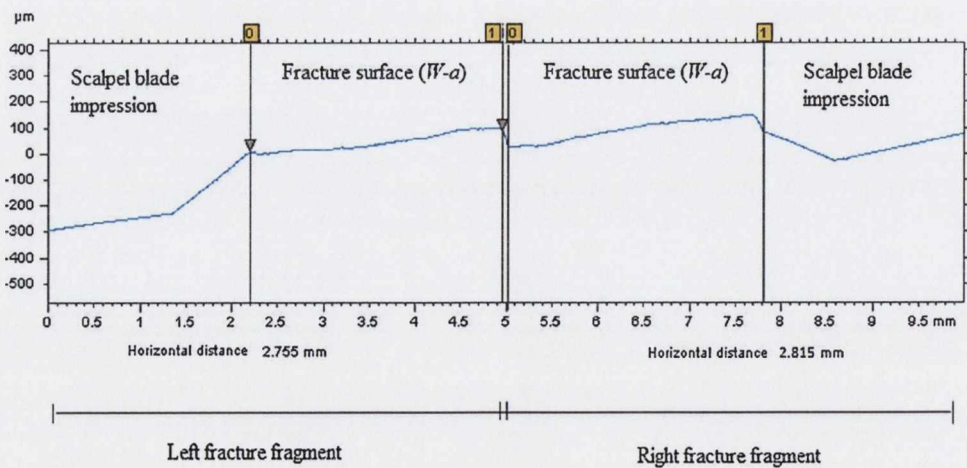


Fig. 4 – A profilometric trace extracted from the longitudinal scan (x-direction) of the fracture surfaces of two fracture fragments (left and right) of a glass-ionomer single-edge notched (SEN) bend test-piece. The length of the fracture surface ( $W-a$ ) on each fracture fragment measured in mm from the end of the scalpel blade impression (point 0) to the edge of the fracture fragment (point 1) for the left fracture fragment and from the edge of the fracture fragment (point 0) to the end of the scalpel blade impression (point 1) for the right fracture fragment.

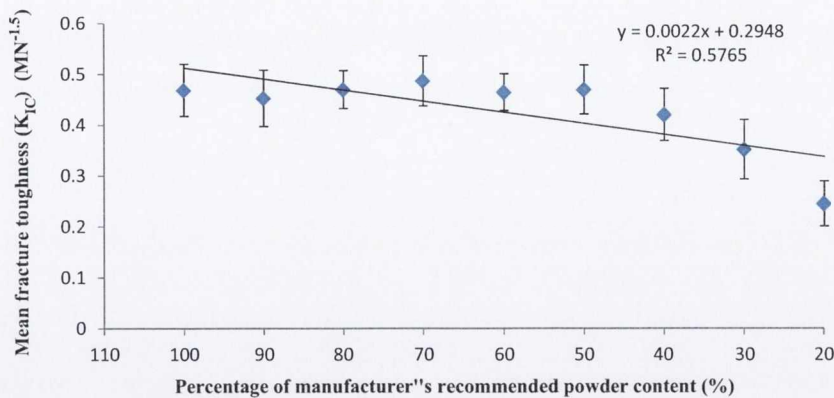


Fig. 5 – The mean fracture toughness ( $K_{IC}$ ) versus powder content when reduced from that recommended by the manufacturer (100%) in 10% increments to a minimum of 20% for a constant weight of liquid highlighting the non-linear deterioration in  $K_{IC}$  with reduced powder content indicated by  $R^2 = 0.576$  which is lower than the 0.95 required for a linear regression.

test-piece identification number for the encapsulated GI products ( $p > 0.069$ ) and also for the hand-mixed GI ( $p > 0.102$ ).

### 3.1. Encapsulated glass-ionomer restoratives

The one-way ANOVA of the  $K_{IC}$  data revealed no significant differences ( $p = 0.225$ ) between the three encapsulated GI products that were investigated. The Chemfil Rock test-pieces had a mean  $K_{IC}$  and associated standard deviation of  $0.488 \pm 0.045 MNm^{-1.5}$  with a CoV of 9% (0.091). The Fuji IXCP Fast test-pieces had a mean  $K_{IC}$  of  $0.490 \pm 0.046 MNm^{-1.5}$  and a CoV of 9% (0.095). The mean  $K_{IC}$  and associated standard deviation for Ionofil Molar AC was  $0.466 \pm 0.056 MNm^{-1.5}$  with a CoV of 12% (0.120). The pooled  $K_{IC}$  and CoV values for the three encapsulated GIs investigated were  $0.482 \pm 0.049 MNm^{-1.5}$  and 10% (0.102), respectively (Table 1).

### 3.2. Hand-mixed glass-ionomer restorative

The  $K_{IC}$  data for the hand-mixed GI powder:liquid mixing ratio groups prepared with a powder contents of between 100% and 20% that specified by the manufacturer (for a constant weight of liquid) did not produce a linear deterioration in the mean  $K_{IC}$  ( $R^2 = 0.576$ ; Fig. 5) and inspection gives an impression of two stages. There was no evident linear deterioration in the mean  $K_{IC}$  data from 100% to 50% ( $p = 0.586$ ). The mean  $K_{IC}$  and associated standard deviations for the control (100%) and 50% powder content groups were recorded at  $0.468 \pm 0.051 MNm^{-1.5}$  and  $0.469 \pm 0.048 MNm^{-1.5}$ , respectively. There is a clear decline in  $K_{IC}$  with each 10% reduction in powder content after 50% which was evident when a regression analysis was performed ( $p = 0.014$ ). The pooled  $K_{IC}$  for the hand-mixed powder:liquid mixing ratio groups investigated ( $n = 9$ ) showed a mean and standard deviation of  $0.425 \pm 0.087 MNm^{-1.5}$  with a pooled CoV value of 12% (0.117) for the hand-mixed powder:liquid mixing ratio groups investigated (Table 2).

## 4. Discussion

The stress intensity factor ( $K$ ) was proposed by Irwin [45] to describe the stress state at the crack tip of a material. Fracture occurs when the value of  $K$  exceeds a certain critical value ( $K_C$ ) for crack growth in the material [13]. For mode I tensile opening,  $K_C$  is denoted by  $K_{IC}$  and is referred to as the (plane strain) fracture toughness of the material, an intrinsic material property that determines the resistance of a material to the catastrophic propagation of a pre-existing crack [13]. The value of  $K_{IC}$  is affected by three properties, these being Young's modulus ( $E$ ), the Critical Strain Energy Release Rate ( $G_{IC}$ ) and Poisson's ratio ( $\nu$ ) through the relationship:  $K_{IC} = [G_{IC} E / (1 - \nu^2)]^{0.5}$ . For GIs the value of Poisson's ratio, measured by the ultrasound method (which is appropriate for the research reported in this paper) is in the region of 0.3 for products intended for use as restoratives but increases to 0.35 for luting cement products [46]. The greater water content to produce the necessary flow properties for a luting cement is the reason for the increase in Poisson's ratio [46]. Whereas this variation is relevant to all the materials in the present research, in practice the effect of the change is minimal [ $(1 - \nu^2)^{-0.5}$  is 1.05 for  $\nu = 0.3$  and 1.06 for  $\nu = 0.35$ ] and can be disregarded in this discussion. To a first approximation in this discussion  $K_{IC}$  can be taken as  $(G_{IC} E)^{0.5}$ .

In the absence of a specific standard for the measurement of  $K_{IC}$  in GI cements, researchers have employed the techniques described by the American Society for Testing and Materials International (ASTM International) [47] and ISO [44] for the  $K_{IC}$  testing of metallic materials. Owing to similarities of brittle fracture of GIs to dental ceramics, the ASTM International standard test method for determination of  $K_{IC}$  of advanced ceramics (ASTM C1421) appears to be more relevant when investigating the  $K_{IC}$  of GIs, although no publications employing ASTM C1421 [48] could be identified in the literature on  $K_{IC}$  testing of GIs. These prescribe strict geometry requirements for the metallic test-pieces which include a straight and horizontal crack front and very accurate measurement of the crack length. The test-piece must also have sufficient

**Table 1 – The mean fracture toughness ( $K_{IC}$ ), range of  $K_{IC}$  values and coefficient of variation (CoV) values for the three encapsulated glass-ionomers (GIs) investigated.**

Encapsulated GI	Mean $K_{IC}$ (MNm <sup>-1.5</sup> )	Range of $K_{IC}$ (MNm <sup>-1.5</sup> )	CoV
Chemfil Rock	0.488 ± 0.045	0.400–0.571	0.091
Fuji IX <sub>GP</sub> Fast	0.490 ± 0.046	0.365–0.546	0.095
Ionofil Molar AC	0.466 ± 0.056	0.375–0.561	0.102

thickness for constraint to maintain plane-strain conditions at the crack tip for most of the crack front. Theoretically, a Griffith pre-crack (a perfectly sharp crack) should be present, from which unstable crack growth can be initiated [49]. Therefore, the  $K_{IC}$  testing standards for metals and ceramics specify introducing a pre-crack with adequate sharpness from the apex of a notch in the SEN bend specimens prior to loading, although the method for pre-cracking varies for metallic and ceramic specimens which are required to be pre-cracked through fatigue cycling (ASTM 399:2009) [47] or loading the specimen using the bridge-flexure technique until a ‘pop-in’ pre-crack is heard or seen (ASTM C1421:2010) [48], respectively.

Pre-cracking is mandatory because the notch is machined (giving a rounded tip) in a material that has inherently high fracture toughness. In dentistry we enjoy a luxury that metallurgists do not have. We can mould the material in its pre-set plastic state around a sharp blade. When set, the impression left by the blade edge, the crack-tip, has the radius of that blade, typically 0.25 μm for a straight-edge surgical scalpel blade.

Ferracane et al. [21] investigated the effect of introducing a pre-crack from the moulded sharp notch in SEN bend test-pieces (30 mm length, 4.5 mm width, 2.1 mm thickness,  $n = 10$ ) on the resultant  $K_{IC}$  values of eight commercial RBCs. Results were inconclusive: for half the products tested pre-cracking had no significant effect. In the defence of the moulded sharp notch, Lloyd [50] cited the work of Hashemi and Williams [51] which showed that for brittle polymers the critical radius for adequate sharpness is more than two orders of magnitude greater than the radius of the crack-tip moulded around an embedded scalpel blade. Hashemi and Williams [51] demonstrated that a notch having a tip radius of 12.5 μm in polymers such as PMMA and PVC produce  $K_{IC}$  values that are comparable with those produced by pre-cracking. The critical radius for a valid result can be calculated and is greater than this. PMMA ( $K_{IC} = 1.95 \text{ MNm}^{-1.5}$ ) and PVC ( $K_{IC} = 2.84 \text{ MNm}^{-1.5}$ ) that have fracture toughness values similar to our dental materials.

For RBC products it is at best  $2.5 \text{ MNm}^{-1.5}$  and for GI products  $0.6 \text{ MNm}^{-1.5}$ . Sharp notches with crack tip radii of less than 10 μm have also been identified to produce comparable results to pre-cracked specimens for dental ceramics [52,53] and pyrolytic carbon/graphite composites [54] which further supports the use of sharp notched SEN bend specimens for  $K_{IC}$  testing of brittle materials.

There are fundamental issues that seem to be overlooked. The use of linear elastic fracture mechanics not only specifies a Griffith crack but also a perfectly elastic and homogeneous material, yet the concept has been applied successfully to real materials. In a particulate composite structure (whether RBC or GI) the initial crack front will confront more resistant particles as well as the matrix. Restrictions that apply to metallic structures in general may be less severe or even irrelevant when testing brittle organic materials.

The accurate determination of the position of the crack tip following pre-cracking [50] is difficult. Therefore, investigators [23,50,55] are in general agreement that although pre-cracking seems theoretically correct, invariably it will introduce errors when investigating brittle dental restorative materials, thereby negating any benefit produced. In the current study, SEN bend test-pieces were prepared with a sharp notch (0.3 μm crack tip radius [46]) moulded around a scalpel blade which has previously been shown to yield valid results that are indicative of the  $K_{IC}$  of the material [14–18,20,37]. This adequate sharpness was evident on profilometrically scanning the side surfaces of the SEN bend specimens, which highlighted crack tip radii of 0.3 μm.

Perhaps, of most relevance to the present research is the work of Hill and Labok [56] on zinc polycarboxylate cement, a material with a structure similar to GI. The values of fracture toughness obtained using compact tension test-pieces containing disc-cut ‘cracks’ were in excellent agreement with those obtained with double torsion test-pieces. The latter produces a perfectly sharp crack by growth during loading,

**Table 2 – The mean fracture toughness ( $K_{IC}$ ), range of  $K_{IC}$  values and coefficient of variation (CoV) values for the hand-mixed glass-ionomer (GI) powder:liquid mixing ratio groups investigated.**

% Powder content	Mean $K_{IC}$ (MNm <sup>-1.5</sup> )	Range of $K_{IC}$ (MNm <sup>-1.5</sup> )	CoV
100	0.468 ± 0.051	0.332–0.533	0.110
90	0.452 ± 0.055	0.315–0.536	0.122
80	0.469 ± 0.037	0.423–0.541	0.078
70	0.486 ± 0.049	0.392–0.584	0.101
60	0.464 ± 0.036	0.400–0.557	0.077
50	0.469 ± 0.048	0.386–0.563	0.102
40	0.420 ± 0.051	0.292–0.491	0.121
30	0.352 ± 0.058	0.260–0.461	0.163
20	0.246 ± 0.044	0.185–0.376	0.179

which Hill and Labok [56] say must happen with the CT test-piece as well.

In the dental literature on  $K_{IC}$  testing of GIs using SEN bend test-pieces, the majority of investigators [24,25,28,29,32] failed to report the methodology employed to accurately determine the crack length in the SEN test-piece, thereby assuming the crack length to be half of the test-piece width ( $a/W=0.5$ ). Some investigators have reported the use of a traveling microscope [18,20] or an optical microscope [31] for accurate quantification of the measurement of the crack length although images of the crack length were never supplied. In the current study, the crack length was determined after fracture by scanning the fracture surface of each fracture fragment using a contact profilometer, whereby three longitudinal traces were extracted from each scan, one at mid-thickness and two at quarter-thickness points [44]. The crack length was measured from two reproducible reference points namely, the end of the scalpel blade impression and the edge of the fracture fragment (Fig. 4). The profilometric analysis, therefore, ensured an accurate and reproducible measurement of the crack length, resulting from a clear demarcation of the two reference points. Such reproducibility, however, might not be guaranteed with optical microscopy measurements which could be subject to inter- and/or intra-operator variability.

The test-piece dimensions used in the present study have previously been validated by Lloyd and Mitchell [18] who investigated the  $K_{IC}$  of RBCs, GIs, and dental silicate restoratives. The test-piece thickness of 3 mm employed in the current study was in excess of the minimum requirement and the validity supported by the presence of flat fracture surfaces on all SEN bend test-pieces of the encapsulated GI restoratives ( $n=60$ ) and hand-mixed GI powder:liquid mixing ratio groups ( $n=180$ ), characteristic of plane strain conditions at the crack tip [22].

#### 4.1. Encapsulated glass-ionomer restoratives

The pooled CoV of 10% for the  $K_{IC}$  of the three encapsulated GIs investigated was in close agreement with those reported for the CFS (10%) [5], TFS (12%) [5], BFS (11%) [5] and HI (7%) [6] measurements for the same encapsulated GIs, highlighting good reproducibility of the  $K_{IC}$  data. The manufacturers of the three encapsulated GI products investigated disclosed that they contain different glass compositions, liquid compositions and different powder:liquid mixing ratios. (3.7:1 g:ml, 4.4:1 g:ml and 3.4:1, g:g for Chemfil Rock, Fuji IX<sub>CP</sub> Fast Capsule and Ionofil Molar AC, respectively). Nevertheless, the  $K_{IC}$  values for the three GIs  $0.488 \pm 0.045$ ,  $0.490 \pm 0.046$  and  $0.466 \pm 0.056 \text{ MNm}^{-1.5}$ , respectively were not significantly different ( $p=0.225$ ). Despite  $K_{IC}$  being an intrinsic material property, the apparent non-discriminatory nature of the  $K_{IC}$  testing protocol (for GI products) fails to offer any advantage over the CFS and HI tests investigated previously. Both had identified significant differences in CFS [5] and force-to-fracture [6] values between the same three encapsulated products. The interaction of many composition variables (such as the glass content; the acid present, its molecular weight and concentration; the water content) on both  $G_{IC}$  and  $E$  produce this result for  $K_{IC}$ . Manufacturers with different approaches to optimizing more empirical performance parameters would by

default also produce an optimized  $K_{IC}$ . The modes of failure in the three tests differ and they may have differing sensitivities to compositional changes.

#### 4.2. Hand-mixed glass-ionomer restorative

The microstructure of a set GI contains superficially reacted glass filler particles embedded in a polyacrylate salt matrix [57–60], such that the resistance to compressive, tensile and shear forces under loading during mastication is provided by the glass filler component rather than the weaker polyacrylate salt matrix [60]. In the current study, the  $K_{IC}$  testing methodology of using SEN bend test-pieces failed to discriminate between the hand-mixed GI restorative powder:liquid mixing ratio groups ( $n=9$ ) investigated, evident by the non-linear deterioration in  $K_{IC}$  ( $R^2=0.576$ ; Fig. 5). A further regression analyses of the  $K_{IC}$  data for the 100–50% powder content groups identified no trend within the data sets ( $p=0.586$ ). The relationship between  $K_{IC}$  and hand-mixed GI cements prepared with reduced powder content (from that recommended by the manufacturer) has not been demonstrated conclusively in the dental literature. A single publication by Mitsuhashi et al. [30] identified a progressive deterioration ( $R^2=0.9807$ ) in  $K_{IC}$  for a hand-mixed anterior GI restorative (Fuji II, GC Corporation, Tokyo, Japan) on reducing the powder content from 100% (i.e. the manufacturer's recommended ratio of 2.7:1, g:g,  $0.37 \text{ MNm}^{-1.5}$ ) to 74% ( $0.29 \text{ MNm}^{-1.5}$ ) and 37% ( $0.19 \text{ MNm}^{-1.5}$ ). However, care should be exercised when interpreting the reported  $K_{IC}$  data because these authors [30] employed notched ring-shaped test-pieces (4 mm inner radius, 8 mm outer radius, 3 mm thickness with a 1 mm radial notch) which were pre-cracked (0.96–2.32 mm) prior to testing. No scanning electron micrographs of the pre-cracked test-pieces were supplied to verify the extent of the pre-crack. It has been well established in the dental literature [23,50,55] that pre-cracking of  $K_{IC}$  test-pieces of brittle dental restorative materials can introduce errors in the determination of  $K_{IC}$ , through uncertainty in the pre-crack length. In addition, Mitsuhashi et al. [30] failed to report the standard deviations for their reported  $K_{IC}$  values and the number of test-pieces. A further complication is the low number of data points ( $n=3$ ).

Lucas et al. [29] and Miyazaki et al. [28] investigated a hand-mixed GI products produced by one manufacturer (GC Corporation, Tokyo, Japan), these being Fuji IX for posterior use and Fuji II for anterior use, respectively. These authors used the same test-piece geometry (SEN bend) and dimensions (25.0 mm length  $\times$  5.0 mm width  $\times$  2.5 mm thickness and a moulded sharp notch to 2.5 mm depth) loaded to failure at the same cross-head displacement rate (0.5 mm/min) following storage in the same storage media (distilled water at 37 °C) for the same time (24 h). Interestingly, the mean  $K_{IC}$  value reported for Fuji II ( $0.49 \pm 0.04 \text{ MNm}^{-1.5}$ ,  $n=6$ ) [28] was not significantly different from the mean  $K_{IC}$  value reported for Fuji IX ( $0.45 \pm 0.06 \text{ MNm}^{-1.5}$ ,  $n=12$ ) [29], despite the lower powder:liquid mixing ratio specified by the manufacturer for the anterior product Fuji II (2.7:1, g:g) compared with its posterior counterpart, Fuji IX (3.6:1, g:g). Although statistical confidence in the  $K_{IC}$  data reported by Lucas et al. [29] and Miyazaki et al. [28] could not be confirmed because of the small sample sizes, their  $K_{IC}$  data provide an indication of the non-discriminatory

nature of the  $K_{IC}$  testing methodology when it is employed for GIs products that have differing recommended mixing ratios.

The non-discriminatory nature of the  $K_{IC}$  testing methodology using SEN bend test-pieces for GI products has been shown in the dental literature [28,29]. Unfortunately, as explained already, it is not possible to confirm this using those results. In the current study,  $K_{IC}$  had mean values of  $0.468 \pm 0.051$  to  $0.469 \pm 0.048 \text{ MNm}^{-1.5}$  for the 50% and 100% powder content groups, respectively. The interaction of many composition variables (such as glass content; acid present, its molecular weight and concentration; water content) on both  $G_{IC}$  and  $E$  produce this result for  $K_{IC}$ . In exceptional circumstances, in a controlled research program (such as that reported by Wilson et al. [61]) for a series of simple experimental GI formulations in which one variable is progressively changed to study the effect,  $K_{IC}$  testing does produce discrimination in the way expected for the compositional change. Therefore, despite  $K_{IC}$  being an intrinsic material property, caution must be exercised when using it to differentiate commercial products with proven clinical performance. As a research tool it is, of course, well proven.

## 5. Conclusion

Based on the product range in this study, the  $K_{IC}$  testing methodology failed to discriminate between these products. For hand-mixed GIs prepared with a powder content reduced from that recommended by the manufacturer,  $K_{IC}$  was insensitive to a change which in practice would adversely affect clinical performance. This raises important issues. Despite  $K_{IC}$  being an intrinsic material property caution is required when using it to compare good quality GI products intended for the same application. GI is a material with low toughness and with the correct composition and production regime the range of values for products is within the scatter produced in well conducted tests.

## Acknowledgement

This work was funded by a Trinity College Dublin 1252 Studentship for MS Baig.

## REFERENCES

- [1] International Organisation for Standardisation ISO 9917-1:2007. Dentistry – water-based cements. Part 1. Powder/liquid acid–base cements.
- [2] McCabe JF, Watts DC, Wilson HJ, Worthington HV. An investigation of test-house variability in the mechanical testing of dental materials. *J Dent* 1990;18:90–7.
- [3] Fleming GJP, Dowling AH, Addison O. The crushing truth about glass ionomer restoratives: exposing the standard of the standard. *J Dent* 2012;40:181–8.
- [4] McCabe JF, Carrick TE. A statistical approach to the mechanical testing of dental materials. *Dent Mater* 1986;2:139–42.
- [5] Dowling AH, Fleming GJP, McGinley EL, Addison O. Improving the standard of the standard for glass ionomers: an alternative to the compressive fracture strength test for consideration? *J Dent* 2012;40:189–201.
- [6] Baig MS, Dowling AH, Fleming GJP. Hertzian indentation testing of glass-ionomer restoratives: a reliable and clinically relevant testing approach. *J Dent* 2013;41:968–73.
- [7] Wang Y, Darvell BW. Failure mode of dental restorative materials under Hertzian indentation. *Dent Mater* 2007;23:1236–44.
- [8] Wilson AD. Dental cements-general. Zinc oxide dental cements. Dental cement based on ion-leachable glasses. In: Von Fraunhofer JA, editor. Scientific aspects of dental materials. London: Butterworths; 1975. p. 131–221.
- [9] Darvell BW. Uniaxial compression tests and the validity of indirect tensile strength. *J Mater Sci* 1990;25:757–80.
- [10] Kendall K. Complexities of compression failure. *Proc R Soc Lond A* 1978;361:245–63.
- [11] Kelly JR. Clinically relevant approach to failure testing of all-ceramic restorations. *J Prosthet Dent* 1999;81:652–61.
- [12] Billington RW, Williams JA, Pearson GJ. Variation in powder/liquid ratio of restorative glass-ionomer cement used in dental practice. *Br Dent J* 1990;169:164–7.
- [13] Atkins AG, Mai YW. The mechanics of elastic fracture. In: Atkins AG, Mai YW, editors. Elastic and plastic fracture. Chichester, United Kingdom: Ellis Horwood Ltd.; 1985. p. 75–167.
- [14] Lloyd CH, Iannetta RV. The fracture toughness of dental composites. I. The development of strength and fracture toughness. *J Oral Rehabil* 1982;9:55–66.
- [15] Lloyd CH. The fracture toughness of dental composites. II. The environmental and temperature dependence of the stress intensification factor ( $K_{IC}$ ). *J Oral Rehabil* 1982;9:133–8.
- [16] Lloyd CH. Resistance to fracture in posterior composites. *Br Dent J* 1983;155:411–4.
- [17] Lloyd CH. The fracture toughness of dental composites. III. The effect of environment upon the stress intensification factor ( $K_{IC}$ ) after extended storage. *J Oral Rehabil* 1984;11:393–8.
- [18] Lloyd CH, Mitchell L. The fracture toughness of tooth coloured restorative materials. *J Oral Rehabil* 1984;11:257–72.
- [19] Goldman M. Fracture properties of composite and glass ionomer dental restorative materials. *J Biomed Mater Res* 1985;19:771–83.
- [20] Lloyd CH, Adamson M. The development of fracture toughness and fracture strength in posterior restorative materials. *Dent Mater* 1987;3:225–32.
- [21] Ferracane JL, Antonio RC, Matsumoto H. Variables affecting the fracture toughness of dental composites. *J Dent Res* 1987;66:1140–5.
- [22] Kovarik RE, Ergle JW, Fairhurst CW. Effects of specimen geometry on the measurement of fracture toughness. *Dent Mater* 1991;7:166–9.
- [23] Kovarik RE, Fairhurst CW. Effect of Griffith pre-cracks on measurement of composite fracture toughness. *Dent Mater* 1993;9:222–8.
- [24] Beatty MW, Pidaparti RMV. Elastic and fracture properties of dental direct filling materials. *Biomaterials* 1993;14:999–1002.
- [25] Pidaparti RMV, Beatty MW. Fracture toughness determination of dental materials by laboratory testing and finite element models. *J Biomed Mater Res* 1995;29:309–14.
- [26] Fujishima A, Ferracane JL. Comparison of four modes of fracture toughness testing for dental composites. *Dent Mater* 1996;12:38–43.
- [27] Hill RG, Wilson AD, Warrens CP. The influence of poly(acrylic acid) molecular weight on the fracture toughness of glass-ionomer cements. *J Mater Sci* 1989;24:363–71.
- [28] Miyazaki M, Moore BK, Onose H. Effect of surface coatings on flexural properties of glass ionomers. *Eur J Oral Sci* 1996;104:600–4.

- [29] Lucas ME, Arita K, Nishino M. Toughness, bonding and fluoride-release properties of hydroxyapatite-added glass ionomer cement. *Biomaterials* 2003;24:3787–94.
- [30] Mitsuhashi A, Hanaoka K, Teranaka T. Fracture toughness of resin-modified glass ionomer restorative materials: effect of powder/liquid ratio and powder particle size reduction on fracture toughness. *Dent Mater* 2003;19:747–57.
- [31] Ilie N, Hickel R, Valceanu AS, Huth KC. Fracture toughness of dental restorative materials. *Clin Oral Investig* 2012;16:489–98.
- [32] Elsaka SE, Hamouda IM, Swain MV. Titanium dioxide nanoparticles addition to a conventional glass-ionomer restorative: influence on physical and antibacterial properties. *J Dent* 2011;39:589–98.
- [33] Scherrer SS, Denry IL, Wiskott HWA. Comparison of three fracture toughness testing techniques using a dental glass and a dental ceramic. *Dent Mater* 1998;14:246–55.
- [34] Fischer H, Marx R. The fracture toughness of dental ceramics: comparison of bending and indentation method. *Dent Mater* 2002;18:12–9.
- [35] Quinn JB, Sundar V, Lloyd IK. Influence of microstructure and chemistry on the fracture toughness of dental ceramic. *Dent Mater* 2003;19:603–11.
- [36] Cruickshanks-Boyd DW, Lock WR. Fracture toughness of dental amalgams. *Biomaterials* 1983;4:234–42.
- [37] Lloyd CH, Adamson M. The fracture toughness ( $K_{IC}$ ) of amalgam. *J Oral Rehabil* 1985;12:59–68.
- [38] Product specification for Capmix. 3M ESPE: Seefeld, Germany.
- [39] Product specification for Chemfil Rock. Dentsply DeTrey: Konstanz, Germany.
- [40] Product specification for Fuji IX Fast Capsule. GC Europe: Leuven, Belgium.
- [41] Product specification for Ionofil Molar AC. Voco GmbH: Cuxhaven, Germany.
- [42] Paul JE. Four-handed dentistry. 1. Principles and techniques: a new look. *Dent Update* 1983;10:155–64.
- [43] Product specification for Ionofil Molar. Voco GmbH: Cuxhaven, Germany.
- [44] International Organisation for Standardisation ISO 12737:2010. Metallic materials – Plane-strain fracture toughness.
- [45] Irwin GR. Analysis of stresses and strains near the end of a crack traversing a plate. *J Appl Mech* 1957;24:361–4.
- [46] Akinomade AO, Nicholson JW. Poisson's ratio for glass polyalkenoate ("glass ionomer") cements determined by an ultrasonic method. *J Mater Sci Mater Med* 1995;6:483–5.
- [47] American Society for Testing and Materials ASTM E399:2009. Standard test method for linear-elastic plane strain fracture toughness  $K_{IC}$  of metallic materials.
- [48] American Society for Testing and Materials ASTM C1421:2010. Standard test method for determination of fracture toughness of advanced ceramics at ambient temperature.
- [49] Griffith AA. The phenomena of rupture and flow in solids. *Philos Trans R Soc Lond: Ser A* 1920;221:163–97.
- [50] Lloyd CH. Letter to the editor: The fracture toughness of composite filling materials and crack tip radius. *J Dent Res* 1988;67:883–4.
- [51] Hashemi S, Williams JG. Crack sharpness effects in fracture testing of polymers. *J Mater Sci* 1985;20:922–8.
- [52] Nishida T, Hanaki Y, Pezzotti G. Effect of notch-root radius on the fracture toughness of a fine-grained alumina. *J Am Ceram Soc* 1994;77:606–8.
- [53] Damani R, Gstrein R, Danzer R. Critical notch-root radius effect in SENB-S fracture toughness testing. *J Eur Ceram Soc* 1996;16:695–702.
- [54] Kruzic JJ, Kuskowski SJ, Ritchie RO. Simple and accurate fracture toughness testing methods for pyrolytic carbon/graphite composites used in heart-valve prostheses. *J Biomed Mater Res* 2005;74A:461–4.
- [55] Ferracane JL. Letter to the editor: The fracture toughness of composite filling materials and crack tip radius. *J Dent Res* 1988;67:884–5.
- [56] Hill RG, Labok SA. The influence of polyacrylic acid molecular weight on the fracture of zinc polycarboxylate cements. *J Mater Sci* 1991;26:67–74.
- [57] Brune D, Smith D. Microstructure and strength properties of silicate and glass ionomer cements. *Acta Odontol Scand* 1982;40:389–96.
- [58] Wilson AD, McLean JW. The setting reaction and its clinical consequences. In: Wilson AD, editor. *Glass-ionomer cement*. Chicago, IL: Quintessence Publishing Co., Inc.; 1988. p. 43–54.
- [59] Hatton PV, Brook IM. Characterisation of the ultrastructure of glass-ionomer (poly-alkenoate) cement. *Br Dent J* 1992;173:275–7.
- [60] Xie D, Brantley WA, Culbertson BM, Wang G. Mechanical properties and microstructures of glass-ionomer cements. *Dent Mater* 2000;16:129–38.
- [61] Wilson AD, Hill RG, Warrens CF, Lewis BG. The influence of polyacid molecular weight on some properties of glass-ionomer cements. *J Dent Res* 1989;68:89–94.



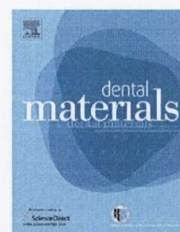
### **3.4 A DISCRIMINATORY MECHANICAL TESTING PERFORMANCE INDICATOR PROTOCOL FOR HAND-MIXED GLASS-IONOMER RESTORATIVES.**

MS Baig, AH Dowling, X Chen, GJP Fleming (2015). A discriminatory mechanical testing performance indicator protocol for hand-mixed glass-ionomer restoratives. *Dental Materials*, 31:273-283.

The non-discriminatory nature of the SEN  $K_{IC}$  testing methodology (Manuscript 3.3) for the encapsulated GI restoratives used for CFS, TFS, BFS (Dowling et al., 2012) and HI tests (Manuscript 3.2) was further highlighted for the hand-mixed GI groups. Therefore, the current study revisited the CFS, TFS, BFS and HI tests using the hand-mixed GI employed in Manuscript 3.3 to prepare GI groups with reduced powder content from that specified by the manufacturer for a constant weight of liquid. As resistance to compressive, tensile and shear forces under loading during mastication is provided by the reinforcing glass filler component rather than the weaker polyacrylate matrix, a deterioration in the mechanical properties was expected on reducing powder content (for a constant weight of liquid). The mechanical testing protocol of choice would, therefore, identify a linear deterioration in the property being investigated when the powder content is reduced from the optimum value specified by the manufacturer. The hypothesis investigated was that each mechanical testing methodology would act as a performance indicator by identifying a linear deterioration in the mechanical property being investigated as the powder content is reduced from the optimum value. The CM and TFM were determined from the stress-strain and load-deflection plots of the cylindrical CFS and bar-shaped TFS specimens, respectively. The fracture origin and failure mode of the HI specimens were determined by fractography.

Available online at [www.sciencedirect.com](http://www.sciencedirect.com)

ScienceDirect

journal homepage: [www.intl.elsevierhealth.com/journals/dema](http://www.intl.elsevierhealth.com/journals/dema)

# A discriminatory mechanical testing performance indicator protocol for hand-mixed glass-ionomer restoratives

Mirza Shahzad Baig<sup>a</sup>, Adam H. Dowling<sup>a</sup>, Xu Cao<sup>b</sup>, Garry J.P. Fleming<sup>a,\*</sup>

<sup>a</sup> Materials Science Unit, Dublin Dental University Hospital, Trinity College Dublin, Dublin 2, Ireland

<sup>b</sup> Barts and The London School of Medicine and Dentistry, Centre of Adult Oral Health, Turner Street, Whitechapel, London E1 2AD, UK

## ARTICLE INFO

### Article history:

Received 6 June 2014

Received in revised form

19 November 2014

Accepted 16 December 2014

### Keywords:

Glass-ionomer restorative

Powder:liquid mixing ratio

Compressive fracture testing

Three-point flexure testing

Biaxial flexure testing

Hertzian indentation testing

## ABSTRACT

**Objectives.** To identify a reproducible and discriminatory mechanical testing methodology to act as a performance indicator for hand-mixed glass-ionomer (GI) restoratives.

**Methods.** Groups of 20 (five batches of four) cylinders ( $6.0 \pm 0.1$  mm height,  $4.0 \pm 0.1$  mm diameter) for compressive fracture strength (CFS) and compressive modulus (CM) testing, bars ( $25.0 \pm 0.1$  mm length,  $2.0 \pm 0.1$  mm width,  $2.0 \pm 0.1$  mm thickness) for three-point flexure strength (TFS) and tensile flexural modulus (TFM) testing, discs ( $13.0 \pm 0.1$  mm diameter,  $1.0 \pm 0.1$  mm thickness and  $10.0 \pm 0.1$  mm diameter,  $3.10 \pm 0.03$  mm thickness) for biaxial flexure strength (BFS) and Hertzian indentation (HI) testing, respectively, were prepared using a hand-mixed GI restorative manipulated with 100–20% (in 10% increments) of the manufacturers recommended powder content for a constant weight of liquid. Data were statistically analyzed at  $p < 0.05$ , the coefficient of variation (CoV) was assessed for the four tests at each powder:liquid mixing ratio investigated ( $n = 9$ ) and a Weibull analysis performed on the CFS, TFS and BFS data to assess the reliability of the data sets. The failure mode and fracture origin of the HI specimens was assessed by fractography.

**Results.** For the hand-mixed GI restorative, a progressive reduction in the powder content (by 10% for a constant weight of liquid) resulted in a progressive linear deterioration ( $p < 0.001$ ) in the CFS ( $R^2 = 0.957$ ), CM ( $R^2 = 0.961$ ) and TFM ( $R^2 = 0.982$ ) data. However, no linear deterioration ( $p > 0.05$ ) was identified for the TFS ( $R^2 = 0.572$ ), BFS ( $R^2 = 0.81$ ) and HI ( $R^2 = 0.234$ ). The CoV and Weibull data identified distinct regions – three for the CFS and TFS data and two for the BFS data sets, within the range of powder:liquid mixing ratios investigated. Fractographic analysis of HI specimens revealed a transition in failure mode from bottom-initiated radial cracking to top-initiated cone cracking on reducing the powder content for a constant weight of liquid.

**Significance.** The CFS test is the only discriminatory performance indicator for hand-mixed GIs from amongst the four mechanical testing approaches (CFS, TFS, BFS and HI) investigated. The CM and TFM represent an intrinsic material property independent of specimen

\* Corresponding author. Tel.: +353 1 612 7371; fax: +353 1 612 7297.

E-mail address: [garry.fleming@dental.tcd.ie](mailto:garry.fleming@dental.tcd.ie) (G.J.P. Fleming).

<http://dx.doi.org/10.1016/j.dental.2014.12.012>

0109-5641/© 2014 Academy of Dental Materials. Published by Elsevier Ltd. All rights reserved.

dimensions and may be used as an adjunct to a mechanical testing approach when investigating hand-mixed GIs.

© 2014 Academy of Dental Materials. Published by Elsevier Ltd. All rights reserved.

## 1. Introduction

The discovery of glass-ionomers (GIs) by Wilson and Kent [1] in 1969 was accomplished on testing the 200th glass composition (G-200) and a clinically acceptable dental cement was realized [2]. G-200 remained the only glass composition capable of forming a GI suitable for clinical use prior to the discovery of the role of tartaric acid in the setting reaction [3]. Following the establishment of the role of tartaric acid as a chelating agent [3], further opportunities were identified for a number of glass compositions other than G-200 [2]. Since the original ground breaking research into the development of GIs, manufacturers and investigators have employed different glass formulations to improve the mechanical properties, enhance radiopacity and increase the reactivity of the glass powder by modifying the calcium fluoroaluminosilicate glass composition [4] with strontium [5], zirconia [6], lanthanum [7] and zinc [8]. Additionally, investigators have prepared aluminoborate [9] and zincsilicate [10,11] glass compositions for use in GIs with varied levels of success.

The compressive fracture strength (CFS) testing methodology is the only strength test specified in the International Organization for Standardization (ISO-9917-2003) [12] for GIs. However, the reliability [13] and validity [14] of the CFS testing protocol have been questioned [15]. A 'test-house variability' study in 1990 [13] identified inter-operator variability (between different test centers) was considerable and intra-operator variability (between individual operators) was also significant such that the poor reliability of the CFS testing protocol was 'inappropriate' for inclusion in the standard [12]. Additionally, the failure mode of dry gypsum cylinders was 'vertical split slabbing mode' but when wet with water or alcohol changed to failure on the 'diagonal planes running from top left to bottom right' [14]. However, the stress at failure calculation was independent of the failure mechanism [14] which raised concerns regarding the validity of the CFS test [14]. Alternative mechanical testing approaches including three-point flexure strength (TFS) [16], biaxial flexure strength (BFS) [16] and Hertzian indentation (HI) [17] tests have been suggested as potential replacement testing methodologies to be adopted in ISO-9917-2003 [12] – albeit for encapsulated GIs. Encapsulated GIs offer control over inaccurate dispensation of the powder and liquid components by the operator, where the optimum powder and liquid proportions are predetermined by the manufacturer [18,19]. The issue of identifying a reliable [13] and valid [14] testing methodology is complicated further for hand-mixed GIs as a result of the range of powder:liquid mixing ratios routinely employed clinically [20]. Interestingly, powder contents as low as 37% of that specified by the manufacturer were identified for Chemfil II, a hand-mixed GI, when prepared by 22 dental nurses – eleven employed in general dental practice and eleven from a

dental hospital setting [20]. Hand-mixed GIs tested in the laboratory are prone to large variations in the mechanical property data arising from inadequate control of the testing conditions [16] and the non-standardized nature of the product delivery systems namely powder scoops [20,21] and liquid dropper bottles [22,23]. The microstructure of a set GI is composed of unreacted glass core fillers sheathed by a siliceous hydrogel and dispersed in a polyacrylate matrix [24–27]. Therefore, the mechanical properties of GIs arise from the reinforcing glass phase where a linear deterioration on reducing the powder content from that specified by the manufacturer would be expected following testing with an appropriate testing methodology [28,29].

It is important to appreciate, however, that if one was charged with the task of delivering a novel reinforced GI restorative, the optimum powder:liquid mixing ratio [30] would need to be identified by hand-mixing the GI liquid with varying GI powder content and performing preliminary mechanical tests. The mechanical testing protocol of choice would therefore require to be discriminatory between the different powder:liquid mixing ratios employed, thereby identifying a linear deterioration when the powder content is reduced from the optimum value. As a result, the aim of the current study was to identify a reproducible and discriminatory testing methodology to act as a performance indicator for hand-mixed GI restorative materials. The hypotheses proposed was that each of the commonly used mechanical testing protocols employed to determine the performance of GIs (CFS, TFS, BFS and HI) would act as performance indicators by identifying the linear deterioration in the mechanical properties on reducing the powder content from that specified by the manufacturer.

## 2. Materials and methods

The GI restorative used (Ionofil Molar: Voco GmbH, Cuxhaven, Germany, Powder: V50335, Liquid: V50375) was hand-mixed for 40 s with the manufacturer's recommended powder:liquid mixing ratio (4:1 g:g) [31]. A glass slab was placed on a balance accurate to 0.001 g (Sartorius Expert, Sartorius AG, Goettingen, Germany), the appropriate weight of GI powder and liquid were dispensed and the powder divided into two equal portions. A stainless steel mixing spatula was used to mix half the powder with the liquid for 20 s, followed by the addition of the remaining powder for a further 20 s in a temperature ( $21 \pm 1^\circ\text{C}$ ) and humidity ( $50 \pm 5\%$ ) controlled laboratory [31]. To simulate the distribution of powder:liquid mixing ratios routinely produced by operators in clinical practice, GIs were prepared by reducing the manufacturers recommended powder content (in 10% increments for a constant weight of liquid) – to a minimum of 20%.

To identify a reproducible and discriminatory test methodology, 20 (five batches of four) specimens were prepared for each test methodology (CFS, TFS, BFS and HI) at the powder:liquid mixing ratios ( $n=9$ ) investigated. Specimen manufacture was randomized by assigning a number to each specimen batch and prior to specimen manufacture a number was drawn to determine the mixing ratio group to be manufactured. Only five batches of specimens were made daily to minimize the influence of operator fatigue [15].

### 2.1. Compressive fracture strength (CFS)

CFS specimens ( $6.0 \pm 0.1$  mm height,  $4.0 \pm 0.1$  mm diameter) were prepared using a polytetrafluoroethylene (PTFE) split-mold [23] resting on top of a PTFE base which was covered by an acetate strip. Alignment of the split-mold was achieved by inserting a locating pin and the split-mold was fixed using nylon wedges which ensured equal pressure was applied along its length. The GI restorative was consolidated to one side of the unfilled mold to avoid air trapping [23] and packed to excess before an acetate strip was used to cover the filled mold. Pressure was applied using a 1 kg weight, the assembly clamped and stored for 1 h in a water-bath ( $37 \pm 1^\circ\text{C}$ ). After 1 h, the mold assembly was disassembled, the specimens demoulded, numbered and stored in 50 ml of distilled water ( $37 \pm 1^\circ\text{C}$ ) for 23 h. Prior to CFS testing, the mean specimen diameter was calculated from three points along its length using a digital micrometer screw gauge reading to  $1 \mu\text{m}$  (Mitutoyo, Kawasaki, Japan). The flat ends of the specimen were covered with wet filter paper (Whatman No. 1, Whatman International Ltd., Maidstone, England) and a compressive load was applied to the long axis of the specimen at a crosshead speed of 1 mm/min (Instron Model 5565, High Wycombe, England). The load-to-failure was recorded and the CFS calculated using Eq. (1) [12].

$$\text{CFS} = \frac{4P}{\pi d^2} \quad (1)$$

where  $P$  was the load-to-failure (N) and  $d$  the mean specimen diameter (mm). Additionally, the individual stress/strain plots were used to determine the compressive modulus (CM) by calculating the slope of the initial linear segment.

### 2.2. Three-point flexure strength (TFS)

TFS specimens ( $25.0 \pm 0.1$  mm length,  $2.0 \pm 0.1$  mm width,  $2.0 \pm 0.1$  mm thickness) were prepared using an open-ended knife-edged PTFE mold [16] by condensing the GI along the length of the mold. The filled mold was covered with acetate, a 1 kg weight applied, clamped and transferred to the water-bath for 1 h. Following removal from the water-bath, the specimens were demoulded, numbered and transferred for 23 h to 50 ml of distilled water at  $37 \pm 1^\circ\text{C}$ . At 24 h, the specimens were loaded in a three-point flexure test rig at 1 mm/min and the load-to-failure recorded. The width and thickness of each fracture fragment was measured using the digital

micrometer screw gauge and the TFS was calculated using Eq. (2) [32].

$$\text{TFS} = \frac{3PL}{2bh^2} \quad (2)$$

where  $P$  was the load-to-failure (N),  $L$  the span between the two point supports (20 mm),  $b$  and  $h$  the mean specimen width (mm) and thickness (mm). In addition, the tensile flexural modulus (TFM) was calculated using Eq. (3) [32].

$$E = \left( \frac{\Delta P}{\Delta D} \right) \frac{L^3}{4bh^3} \quad (3)$$

where  $\left( \frac{\Delta P}{\Delta D} \right)$  was the gradient of the steepest linear portion of the load-deflection curve.

### 2.3. Biaxial flexure strength (BFS)

BFS specimens ( $13.0 \pm 0.1$  mm diameter,  $1.0 \pm 0.1$  mm thickness) were prepared using PTFE ring-molds resting on an acetate-covered glass slab [16] by condensing the GI into the center of the ring-mold to minimize air bubble incorporation. The filled mold was covered with an acetate strip, a 1 kg weight applied, clamped and transferred to the water bath for 1 h. The specimens were then demoulded, numbered and stored in 50 ml of distilled water ( $37 \pm 1^\circ\text{C}$ ) for 23 h prior to testing. The discs were centrally loaded using a 4 mm diameter ball-indenter on a 10 mm diameter knife-edge ring annulus covered with a thin sheet of rubber [33] at 1 mm/min. The load-to-failure was recorded and the BFS calculated using Eq. (4) [34].

$$\text{BFS} = \frac{P}{h^2} \left\{ (1 + \nu) \left[ 0.485 \ln \left( \frac{a}{h} \right) + 0.52 \right] + 0.48 \right\} \quad (4)$$

where  $a$  was the radius of the knife-edge ring annulus,  $\nu$  the Poisson's ratio and  $h$  the mean thickness of the fracture fragments measured using the digital micrometer screw gauge. In addition, the compressive extension at the maximum load was determined from the load-deflection plot for each specimen and the mean extension calculated.

### 2.4. Hertzian Indentation (HI)

Hertzian specimens ( $10.0 \pm 0.1$  mm diameter and  $3.1 \pm 0.03$  mm thickness) were prepared using polyetheretherketone (PEEK) and stainless steel ring-molds resting on an acetate-covered glass slab [17,35]. The GI was placed into the center of the ring-mold and the filled mold covered with acetate, a 1 kg weight applied, clamped and transferred to the water-bath for 1 h. After 1 h, the specimens were demoulded, numbered and stored for 23 h in 50 ml of distilled water at  $37 \pm 1^\circ\text{C}$  prior to testing. The specimens were tested resting freely on top of a 30% glass fiber reinforced polyamide substrate (Goodfellow Cambridge, Huntingdon, England), 10 mm diameter and 5 mm thickness, constrained in a brass holder [17,35]. The load was applied at 1 mm/min through a 20 mm diameter hard steel ball and a 20% drop in the peak compressive load value detected by the load cell was indicative of failure. In addition, the load-deflection plot

for each specimen was used to determine the compressive extension at the maximum load and the mean extension calculated. The number of fracture fragments was recorded and the thickness of each fracture fragment measured using the digital micrometer screw gauge. The fracture fragments were initially viewed under a stereomicroscope (Nikon Instruments Inc., USA) and selected specimens were viewed under a scanning electron microscope (SEM) to identify the fracture origin and failure mode.

### 2.5. Statistical analyses

The data were statistically analyzed using IBM SPSS Statistics V22.0 (Chicago, IL, USA). The Shapiro–Wilk test ( $p < 0.05$ ) was used to assess the normality of the data for each powder:liquid mixing ratio investigated. The homogeneity of variance of the data was determined using the Levene's test of homogeneity. Regression analyses ( $p < 0.05$ ) were performed to check for trends within the data sets regarding powder content, batch and specimen number. The coefficient of variation (CoV) namely the standard deviation divided by the mean was assessed for each test methodology (CFS, TFS, BFS and HI) at the powder:liquid mixing ratios ( $n=9$ ) investigated. The reliability of the CFS, TFS and BFS data sets were assessed by Weibull analyses (Eq. (5)) [36]. A Weibull analysis was not performed on the HI data as the HI test only generates a load-to-failure value.

$$P_f = 1 - \exp \left[ - \left( \frac{\sigma}{\sigma_0} \right)^m \right] \quad (5)$$

where  $m$  and  $\sigma_0$  are constants.  $m$  is known as the Weibull modulus characterizing the brittleness of a material [37] with a higher value of  $m$  indicative of a closer grouping of the data and  $\sigma_0$  is the normalizing constant or the characteristic stress (MPa). In addition, the  $R^2$ -value provided information regarding the defect population with an  $R^2 \geq 0.95$  representative of a uni-modal defect distribution and  $R^2 < 0.95$  indicative of a multi-modal defect distribution [38]. The 95% confidence intervals (CI) of the Weibull moduli were calculated for each data set investigated and differences were considered to be significant when the confidence intervals failed to overlap [39].

## 3. Results

The Shapiro–Wilk test identified that the mechanical testing protocol data for the various powder:liquid mixing ratio groups investigated were normally distributed ( $p > 0.05$ ). The Levene's test of homogeneity of variance identified the data for all powder:liquid mixing ratio groups investigated to be homogenous ( $p > 0.05$ ). The regression analyses highlighted no trends within the data sets in terms of batch ( $p > 0.05$ ) and specimen number ( $p > 0.05$ ) for the powder:liquid mixing ratios investigated.

### 3.1. CFS testing and analysis

Reducing the powder content (in 10% increments) from that recommended by the manufacturer for a constant weight of liquid resulted in a progressive ( $p < 0.001$ ) linear deterioration

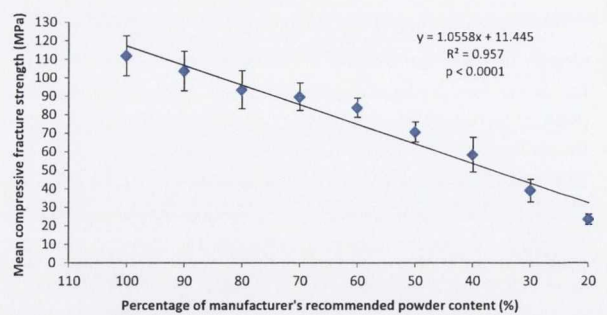


**Fig. 1 – Mean compressive fracture strength (CFS) versus powder content when reduced from that recommended by the manufacturer (100%) in 10% increments to a minimum of 20% for a constant weight of liquid highlighting the progressive linear deterioration in CFS with reduced powder content.**

in the mean CFS ( $R^2 = 0.957$ ; Fig. 1) and CM ( $R^2 = 0.961$ ; Fig. 2) data. When interpreting the CFS data sets, three distinct regions within the powder:liquid mixing ratios investigated ( $n=9$ ) were evident for the CoV analyses, namely, 100–80% (0.09–0.11), 70–50% (0.06–0.08) and 40–20% (0.12–0.16). The three distinct regions highlighted in the CoV analyses within the CFS data sets investigated were replicated using Weibull analyses (100–80% (9.5–10.7), 70–50% (12.7–16.8) and 40–20% (6.5–8.4)) (Table 1) since the Weibull modulus provides an indication of the grouping of the CFS data [37]. Most interesting, however, was the  $R^2$ -value which provided an indication of the defect population evident on testing. Reducing the powder content (for a constant weight of liquid) from that recommended by the manufacturer (100%) to 80% shows a progressive increase in  $R^2$ -value which at 70% is indicative of a single defect population ( $R^2 > 0.95$ ). A single defect population is also evident when the powder content was reduced to 40 and 30% of that recommended by the manufacturer (for a constant weight of liquid).

### 3.2. TFS testing and analysis

No progressive linear deterioration in mean TFS ( $R^2 = 0.572$ ; Fig. 3) but a progressive linear deterioration in mean TFM ( $R^2 = 0.982$ ; Fig. 4) was evident when the powder content was

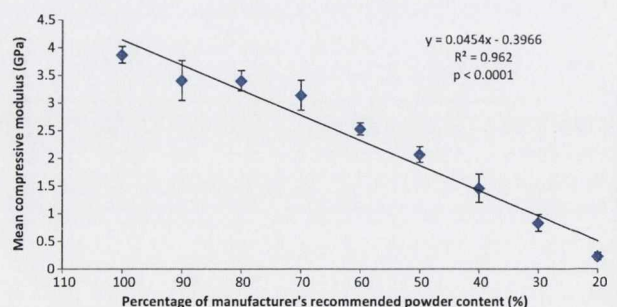


**Fig. 2 – Mean compressive modulus (CM) versus powder content for a constant weight of liquid highlighting the progressive linear deterioration in the CM data.**

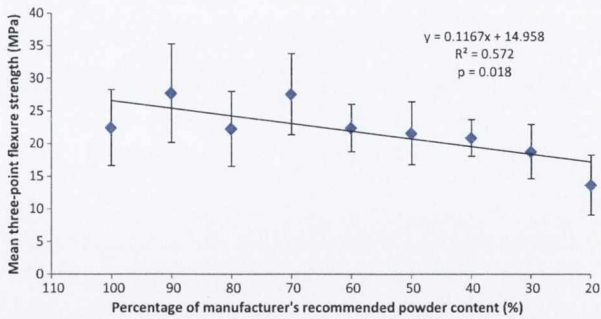


**Fig. 3 – Mean three-point flexure strength (TFS) versus powder content when reduced from that recommended by the manufacturer (100%) in 10% increments to a minimum of 20% for a constant weight of liquid highlighting the non-progressive linear deterioration in TFS data.**

progressively reduced (in 10% increments) from that recommended by the manufacturer for a constant weight of liquid. The TFS data was indicative of a multi-modal distribution ( $R^2=0.572$ ) and further statistical analysis of the progressively reduced powder contents from 100–60% identified no progressive deterioration in TFS ( $p=0.982$ ). The CoV analyses identified three distinct regions in the TFS data for specimen groups prepared at 100–70% (0.22–0.27), 60–40% (0.13–0.16) and 30–20% (0.21–0.33) of the manufacturer's recommended powder content (for a constant weight of liquid) (Table 2). The Weibull moduli were reflective of the CoV results and ranged from 3.8–4.7 (100–70%), 6.4–7.6 (60–40%) and 3.3–4.9 (30–20%) (Table 1).

**3.3. BFS testing and analysis**

When the powder content was reduced (in 10% increments) from that recommended by the manufacturer the mean BFS data was bi-modal ( $R^2=0.81$ ; Fig. 5) and did not show a linear deterioration for a constant weight of liquid from 100–60% ( $p=0.054$ ). The CoV and Weibull data was consistent for powder contents between 100 and 40% (0.12–0.15 and 6.4–8.5, respectively) but the CoV increased markedly for powder contents between 30 and 20% (0.19–0.30) while the Weibull moduli were reduced to 5.2 and 3.5, respectively. It was

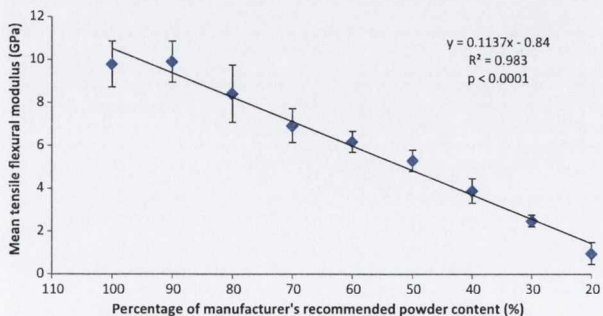


**Fig. 4 – Mean tensile flexural modulus (TFM) versus powder content highlighting a progressive linear deterioration in the TFM with reduced powder content.**

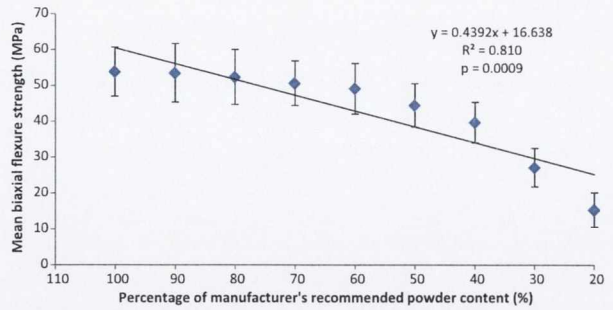


**Fig. 5 – Mean biaxial flexure strength (BFS) versus powder content reduced from that recommended by the manufacturer in 10% increments to a minimum of 20% highlighting a non-linear deterioration in the BFS data.**

interesting to note that the mean compressive extension during testing (Fig. 6) did not change regardless of reducing the powder content progressively (in 10% increments) from that recommended by the manufacturer.

**3.4. Hertzian indentation testing and analysis**

No linear deterioration ( $p=0.186$ ) in mean Hertzian load-bearing capacity ( $R^2=0.234$ ; Fig. 7) was evident when the powder content was progressively reduced (in 10% increments)

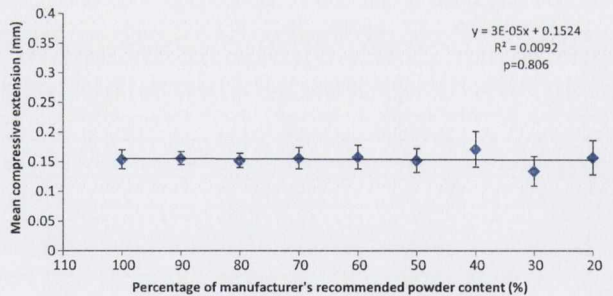


**Fig. 6 – Mean compressive extension for biaxial flexure strength (BFS) specimens versus powder content identifying a consistent compressive extension for the data.**

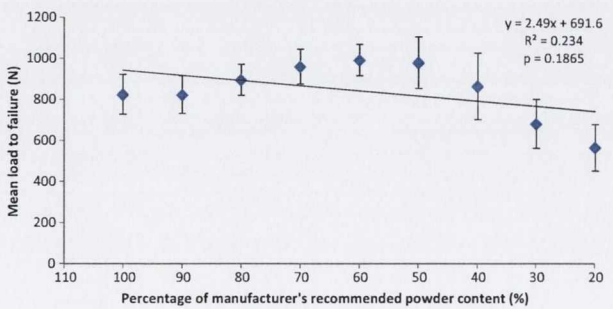


**Fig. 7 – Mean load-to-failure for Hertzian Indentation specimens versus powder content reduced from that recommended by the manufacturer in 10% increments to a minimum of 20%, identifying the non-linear deterioration in the load-to-failure data.**

**Table 1 – The Weibull moduli (*m*) and 95% confidence intervals (CI) for the compressive fracture strength (CFS), three-point flexure strength (TFS) and biaxial flexure strength (BFS) data sets for the powder:liquid mixing ratios investigated identifying distinct Weibull regions for CFS (100–80%, 70–50% and 40–20%), for TFS (100–70%, 60–40% and 30–20%) and for the BFS (100–40% and 30–20%) data sets.**

% Manufacturers powder content	CFS		TFS		BFS	
	<i>m</i>	CI	<i>m</i>	CI	<i>m</i>	CI
100	10.7	8.4–12.9	3.8	3.3–4.3	8.4	7.7–8.9
90	10.1	8.3–11.9	4.0	3.3–4.7	6.4	5.7–7.1
80	9.5	8.2–10.8	4.3	3.6–5.0	7.1	6.5–7.6
70	12.7	11.3–14.1	4.7	4.3–5.0	8.5	7.8–9.2
60	16.8	13.8–19.8	6.4	5.7–7.1	7.5	6.5–8.3
50	12.7	10.3–15.0	6.4	5.6–7.2	7.6	7.1–8.0
40	6.5	5.8–7.2	7.6	6.8–8.3	7.5	6.3–8.6
30	6.7	6.3–7.1	4.9	4.0–5.8	5.2	4.7–5.6
20	8.4	7.1–9.6	3.3	2.7–3.5	3.5	3.1–3.8

from that recommended by the manufacturer for a constant weight of liquid. Examination of the data highlighted the CoV decreased as the powder content was reduced (in 10% increments) to a minimum of 60% from that specified by the manufacturer for a constant weight of liquid (Table 2). A further reduction in the powder content (below 60%) resulted in an increase in the CoV for all groups (Table 2). Interestingly, there was a progressive increase ( $p < 0.001$ ) in mean compressive extension ( $R^2 = 0.967$ ; Fig. 8) on progressively reducing the powder content in 10% increments. On fractographic analysis, bottom-initiated radial cracking (Fig. 9a) was identified as the dominant failure mode for the control group specimens prepared at the manufacturer’s recommended powder content (for a constant weight of liquid). Reducing the powder content in 10% increments for a constant weight of liquid resulted in a transition in the dominant failure mode with mixed bottom-initiated radial cracking and top-initiated cone-cracking seen in the specimen group prepared with 50% of the manufacturer recommended powder content to solely cone cracking (Fig. 9b) in the 20% powder content group.

**4. Discussion**

The reinforcing glass particles embedded in the matrix of the hardened GI restorative enhance the resistance to compressive forces during masticatory function and crack propagation under loading [27]. As a result, the mechanical properties of

hand-mixed GIs vary depending on the powder content of the mix [20,28,29,40]. Incorporation of the optimum amount of reinforcing glass powder recommended by the manufacturer into the polymeric liquid is therefore crucial to maximizing the functional characteristics of hand-mixed GI restoratives when used in clinical practice [18,20]. GIs are tested in the laboratory using different mechanical testing protocols ranked in order of popularity as CFS, TFS, BFS and HI tests [16]. Owing to concerns regarding the reliability [13] and validity [14] of the CFS testing protocol [15], the TFS [16], BFS [16] and HI [17] tests have recently been advocated as potential replacement testing methodologies for adoption in ISO-9917-2003 [12] – albeit for encapsulated GI restoratives.

**4.1. Compressive fracture strength test**

The CFS test was identified as the only ‘truly’ discriminatory test amongst the four mechanical testing protocols investigated (CFS, TFS, BFS and HI) and highlighted a linear deterioration ( $p < 0.001$ ) in CFS (Fig. 1;  $R^2 = 0.957$ ) for the nine hand-mixed GI restorative groups prepared with reduced powder contents for a constant weight of liquid. This finding is in agreement with the reports in the dental literature where a linear deterioration was identified for the compressive fracture strength data ( $R^2 = 0.9987$  for  $n = 4$  [40],  $R^2 = 0.961–0.983$  for  $n = 6$  [28] and  $R^2 = 0.96–0.99$  for  $n = 6$  [29]) on reducing the GI powder content from that recommended by the manufacturer for a constant weight [28,29] or volume [40] of liquid.

**Table 2 – The mean coefficient of variation (CoV) values for the compressive fracture strength (CFS), three-point flexure strength (TFS), biaxial flexure strength (BFS) and Hertzian indentation (HI) data sets for the powder:liquid mixing ratios investigated.**

% Powder content	CFS	TFS	BFS	HI
100	0.097	0.257	0.127	0.117
90	0.103	0.270	0.151	0.111
80	0.110	0.256	0.145	0.084
70	0.083	0.224	0.122	0.088
60	0.062	0.161	0.143	0.077
50	0.076	0.165	0.136	0.128
40	0.160	0.133	0.141	0.187
30	0.156	0.219	0.195	0.173
20	0.118	0.331	0.308	0.198

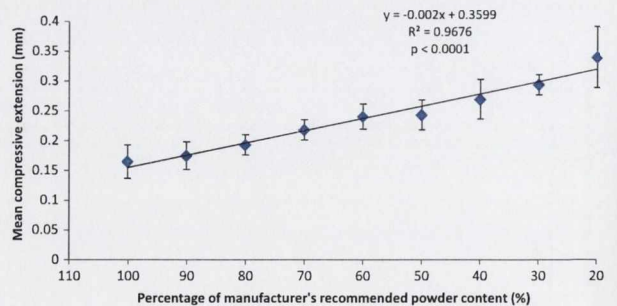


**Fig. 8 – Mean compressive extension for Hertzian Indentation specimens versus powder contents highlighting a progressive linear increase in the compressive extension with reduced powder content.**

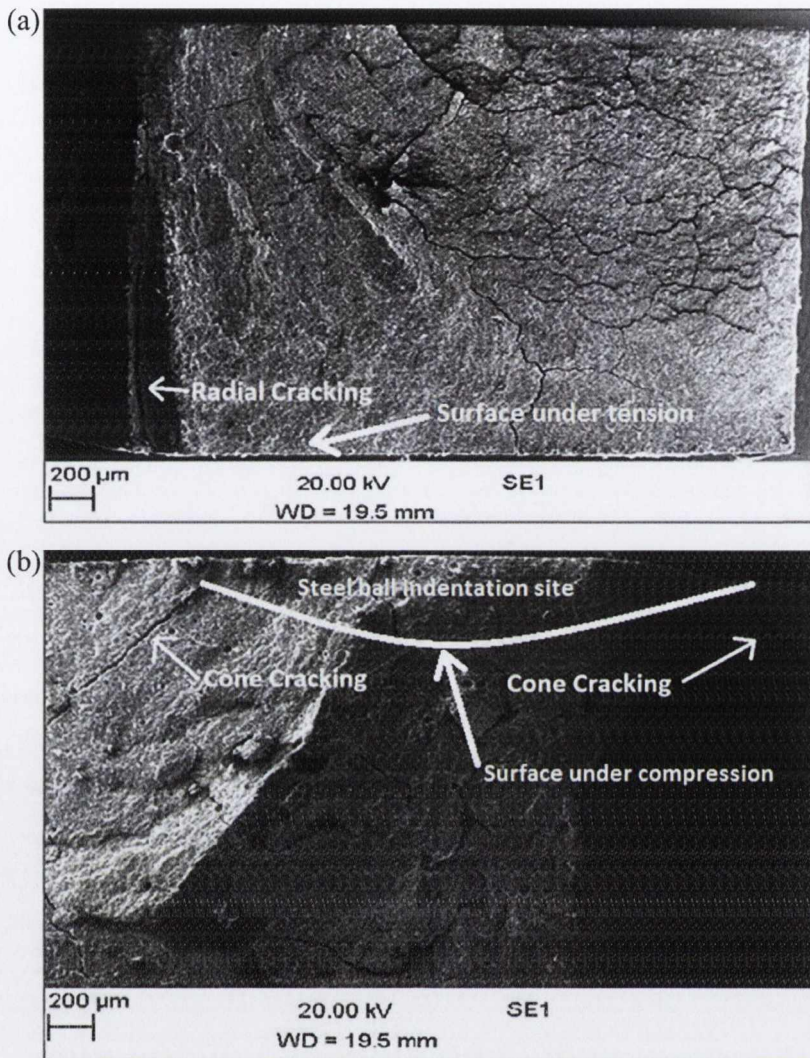


Fig. 9 – (a) Scanning electron micrograph of the fracture surface of a Hertzian Indentation specimen prepared at the manufacturers recommended powder content (100%) showing radial cracking initiating from the bottom surface which was in tension during testing. (b) Scanning electron micrograph of the fracture surface of a Hertzian Indentation specimen prepared with 20% of the manufacturers recommended powder content highlighting the modification in failure mode to cone cracking initiating from the top surface of the specimen which was in compression during testing.

Interestingly, while Fleming et al. [40] observed a linear deterioration in the CFS ( $R^2 = 0.999$ ) for an anterior hand-mixed GI restorative (Chemfil Superior) when the powder content was reduced from 100% (manufacturer's recommendation) to 90, 80 and 50% ( $n = 4$ ) for a constant volume of liquid, which contrasted with the finding of Dowling et al. [29] who reported a non-linear deterioration in CFS ( $R^2 = 0.94$ ) for Chemfil Superior. Although both Fleming et al. [40] and Dowling et al. [29] used adequate sample sizes ( $n = 20$  and  $n = 30$ , respectively) the Dowling study [29] assessed additional data points for powder contents of 70 and 60% to increase the number of groups investigated ( $n = 6$ ). This observation highlights the importance of the number of data points for the determination of a linear deterioration. In the current study, additional data points ( $n = 9$ ) identified the ability of the CFS testing methodology to

distinguish between GI restorative groups prepared at varying powder:liquid mixing ratios. The hypothesis that the CFS test would act as a performance indicator for a hand-mixed GI restorative by identifying a linear deterioration in the mean CFS when the powder content is progressively reduced (in 10% increments) for a constant weight of liquid was therefore accepted.

The current study also identified the CM to be discriminatory between the hand-mixed GI restorative groups ( $n = 9$ ) by showing a linear deterioration in the CM (Fig. 2;  $R^2 = 0.9619$ ) when the hand-mixed GI restorative was manipulated at reduced powder:liquid mixing ratios which are routinely encountered clinically. This finding is consistent with the linear deterioration identified for the compressive modulus ( $R^2 = 0.951$ – $0.974$  for  $n = 6$  [28] and  $R^2 = 0.95$ – $0.99$  for  $n = 6$  [29])



on reducing the GI powder content from that recommended by the manufacturer for a constant weight of liquid. Previously, Dowling et al. [28] identified the CM to be more sensitive to highlighting the impact of powder content variations than the CFS for hand-mixed GI restoratives and examination of the  $R^2$ -values in Figs. 1 and 2 confirms this observation. Therefore in line with the suggestions of Dowling et al. [28], the employment of an intrinsic material property, namely compressive modulus (CM), in combination with a non-intrinsic material property (CFS) is advantageous for hand-mixed GI restoratives. The CM information is contained within the CFS test data as the CM is determined by calculating the slope of the initial linear section of the stress/strain plot of each specimen tested in compression and as a result the authors encourage more researchers to quote both values in future studies.

Previously, porosity levels in CFS specimens have been shown to depend on air inclusion during mixing [41,42] or placement of the GI into the mold [41,42] during specimen manufacture. An increased powder content for a constant weight of liquid requires increased spatulation force to mix the powder and liquid components, which may result in air incorporation [41,42]. In the current study, an increase in the Weibull moduli and concomitant decrease in CoV as the powder content was reduced to 70, 60 and 50% of that specified by the manufacturer suggests easier mixing and better consolidation of the CFS specimens into the PTFE split-mold when compared with the CFS specimens prepared with 100, 90 and 80% of the manufacturer's powder content recommendation. However, the lower Weibull moduli for the groups prepared with powder contents which were further reduced to 40, 30 and 20% are indicative of pore inclusion on filling the mold as the GI mix becomes too fluidic such that it traps air while flowing into the mold. These findings are supported by the stereological findings based on a range of powder:liquid mixing ratios for different acid–base cements [21,41–43].

#### 4.2. Three-point flexure strength test

The TFS test failed to discriminate between the hand-mixed GI restorative groups ( $n=9$ ) prepared with reduced powder contents as evident by the non-linear deterioration in TFS ( $R^2=0.572$ ) shown in Fig. 3 where  $p=0.982$  for progressively reduced powder contents from 100–60%. Bonifacio et al. [44], Torabzadeh et al. [45] and Higgs et al. [46] failed to identify significant differences in the TFS for GIs mixed at the recommended powder:liquid mixing ratio and with 50% of the recommended powder content [44], 80% of the recommended powder content [45] or between a posterior and anterior hand-mixed GI restorative from the same manufacturer [46]. This observation occurred despite the reported powder:liquid mixing ratio of the posterior GI restorative (3.5:1 g:g) investigated being higher than the powder:liquid mixing ratio of its anterior counterpart (2.7:1 g:g) [46] which intuitively does not make sense. As a result, the findings of the current study indicate that the hypothesis that the TFS test would identify a linear deterioration for a hand-mixed GI restorative manipulated at reduced powder content (in 10% increments) for a constant weight of liquid and thereby act as a performance indicator was rejected.

The TFM is an intrinsic material property independent of specimen dimensions and is therefore capable of reproducing the internal structure of the material and any association with the neighboring atoms [47]. In the current study, the TFM was identified as a sensitive performance indicator which was able to discriminate between hand-mixed GI restorative mixing ratio groups ( $n=9$ ) prepared with reduced powder content (in 10% increments) from that advocated by the manufacturer for a constant weight of liquid, evident by the progressive ( $p<0.001$ ) linear deterioration in TFM (Fig. 4;  $R^2=0.982$ ). Previously, Bonifacio et al. [44] reported a statistically significant decrease in the TFM for a posterior hand-mixed GI restorative (Fuji IX;  $12.6 \pm 5.1$  GPa) when the powder content was reduced by 50% ( $7.2 \pm 4.6$  GPa) from that specified by the manufacturer for a constant volume of liquid. Owing to the additional data points ( $n=9$ ) investigated in the current study, a linear deterioration in the mean TFM data was identified for the hand-mixed GI restorative manipulated at reduced powder:liquid mixing ratios routinely produced by operators in clinical settings. Therefore, the TFM acted as a performance indicator for a hand-mixed GI restorative and the authors advocate determination of the TFM as an adjunct to a mechanical testing protocol when investigating the performance of hand-mixed GI restoratives.

The TFS of brittle materials like GIs is sensitive to surface imperfections [48] which may either be inherent to the GI or be introduced during manipulation of the GI and filling the mold [41,42]. However, on condensing the specimens against an acetate strip, to prevent the hand-mixed GI restorative from adhering to the glass slab, a consistent surface roughness is achieved regardless of the powder:liquid mixing ratio produced by the operator. Therefore the surface defect population would be expected to be similar for all groups. The lower Weibull modulus and concomitant increase in CoV of the hand-mixed GI control group is indicative of the difficulty in manipulation and consolidation of the hand-mixed GI restorative along the length of the open-ended knife-edged PTFE mold when mixed at the manufacturer's recommended powder:liquid mixing ratio. The Weibull moduli of the TFS data highlighted a narrowing in the data scatter as the powder content was reduced down to 30% of the optimum value identified by the manufacturer, which suggests that reducing the powder content results in easier mixing and better consolidation of the GI into the PTFE mold. The decrease in Weibull modulus as the powder content is further reduced to 20% of that specified by the manufacturer suggests that the mix had become so fluidic that air may have become incorporated during filling the mold [41,42].

#### 4.3. Biaxial flexure strength test

The non-linear deterioration in BFS (Fig. 5;  $R^2=0.81$ ) for the hand-mixed GI restorative groups ( $n=9$ ) prepared with reduced powder content (in 10% increments) from that proposed by the manufacturer for a constant weight of liquid demonstrates the non-discriminatory nature of the BFS test for hand-mixed GIs. This observation is in line with the findings of Higgs et al. [46] who reported the BFS of a posterior (Fuji IX;  $50.61 \pm 5.45$  MPa;  $n=8$ ) and an anterior (Fuji II;  $53.33 \pm 6.6$  MPa;  $n=10$ ) hand-mixed GI restorative, from the

same manufacturer (GC, International Corporation, Japan), to be statistically similar. The non-significant BFS data reported for the Fuji IX and Fuji II hand-mixed GI restoratives was unexpected as the powder:liquid mixing ratios reported by the manufacturer were 3.5:1 g:g and 2.7:1 g:g, respectively. However, confidence in the statistical analysis reported for the BFS of Fuji IX and Fuji II hand-mixed GI restoratives by Higgs et al. [46] could not be confirmed due to the small sample size ( $n < 20$ ) investigated. BFS specimens were prepared in the current study by condensing the hand-mixed GI restorative into a ring-mold resting on an acetate covered glass slab and covering with a second acetate strip to prevent the hand-mixed GI restorative from adhering to the glass slab. Therefore, all BFS specimen groups prepared with the hand-mixed GI restorative had a uniform surface finishing condition with an  $R_a$ -value of around  $0.10 \pm 0.01 \mu\text{m}$ . Previously, investigators [49,50] have shown that the BFS of brittle dental materials is dependent on roughness of the surface ( $R_a$ -value) under tension and is therefore a surface driven phenomenon. In the current study, owing to the uniform surface finishing condition of the BFS specimens prepared with the hand-mixed GI restorative at reduced powder content (in 10% increments) from that recommended by the manufacturer for a constant weight of liquid, the BFS test remained insensitive to powder content from 100–60% ( $p > 0.05$ ). The BFS test, therefore, failed to identify a linear deterioration when the powder content was reduced (in 10% increments) from that recommended by the manufacturer for a constant weight of liquid for a hand-mixed GI restorative and the hypothesis was rejected.

#### 4.4. Hertzian indentation test

The current investigation revealed the non-discriminatory nature of the Hertzian indentation test for hand-mixed GIs ( $p > 0.05$ ) by showing a non-linear deterioration in the Hertzian load-bearing capacity (Fig. 7;  $R^2 = 0.234$ ) for the hand-mixed GI restorative groups manipulated with reduced powder content (in 10% increments) from that specified by the manufacturer for a constant weight of liquid. In the current study, the hand-mixed GI specimens prepared at the powder:liquid mixing ratio identified by the manufacturer were tested while resting freely on top of a 30% glass fiber reinforced polyamide substrate [35,51,52]. The elastic modulus mismatch between the GI specimen and the substrate resulted in the generation of a tensile stress at the GI specimen/substrate interface on loading leading to radial crack formation at the bottom surface of the specimen [51]. The tensile initiated radial crack propagated upward through the thickness of the specimen, dissecting the specimen into two to four fracture fragments with smooth fracture surfaces [35,51,52], where the failure mode and origin were confirmed by fractography. This finding is consistent with the results reported by Wang and Darvell [35] who identified radial cracking as the dominant failure mode for a hand-mixed GI restorative (Amalgomer CR) of similar thickness (0.4–3.6 mm) to that investigated in the current study ( $3.10 \pm 0.03$  mm). However, this was not the case for the GI specimen groups manipulated at reduced powder contents. In the current study, a progressive reduction in the powder content resulted in an increase in the ductility of the hand-mixed GI restorative. This increased ductility

was attributed to the deterioration in the TFM as the powder content was reduced from that recommended by the manufacturer (Fig. 4), with a resultant progressive increase ( $p < 0.001$ ) in the indentation depth for the GI specimens tested under Hertzian indentation. The GI specimens prepared at reduced powder content, therefore, deformed prior to fracture where the initial point contact between the ball indenter and the specimen was transformed to a larger area of contact, evident by the progressive increase in the compressive extension (Fig. 8;  $R^2 = 0.967$ ). The failure mode therefore changed from brittle failure (Fig. 9a) to ductile (Fig. 9b) failure when the powder content was progressively reduced for a constant weight of liquid, as confirmed by fractography, such that top-initiated cone cracking began to appear (Fig. 9b) and bottom-initiated radial cracking (Fig. 9a) was no longer the dominant failure mode. The increase in the Hertzian load-bearing capacity as the powder content was reduced (Fig. 7) is therefore misleading when interpreting the load-to-failure data. The hypothesis that the Hertzian indentation test would act as a performance indicator for a hand-mixed GI restorative by identifying a linear deterioration in the mean load-bearing capacity when the powder content is progressively reduced was therefore rejected.

In summary, while the CFS test was identified as the only ‘truly’ discriminatory test amongst the four mechanical testing protocols investigated (CFS, TFS, BFS and HI), it is essential for any mechanical test used to evaluate the performance of dental restorative materials to demonstrate a clinically representative failure mode [17]. CFS testing has been advocated [53,54] for assessing powder/liquid acid–base cements and restoratives since loading during masticatory function results in stressing patterns analogous to those observed during CFS testing [53] and a high CFS was proposed as necessary to tolerate the functional forces routinely encountered in the posterior region of the mouth [54]. In TFS and BFS testing, the failure occurs in a state of pure tension under loading which is the mechanism by which brittle materials fail in vivo. However, BFS testing is advantageous over uniaxial TFS testing as the specimens are easier to prepare, clinically match the volume of a large posterior restoration with a reduced sensitivity to edge defects [16]. Unfortunately the preparation technique for TFS and BFS specimens prepared in the current study a uniform surface finishing condition which precluded the tests from being ‘truly’ discriminatory. The Hertzian indentation test is probably the most clinically relevant as the test simulates the loading conditions experienced by dental restorations under occlusal loading where opposing tooth contacts are simulated [51,52]. However, reducing the powder content was associated with a concomitant reduction in brittleness which nullified the discriminatory nature of the test owing to indenter penetration.

## 5. Conclusion

The CFS test is the only discriminatory performance indicator for hand-mixed GIs from amongst the four mechanical testing approaches (CFS, TFS, BFS and HI) investigated. The CM and TFM represent an intrinsic material property independent of specimen dimensions and may be used as an adjunct to a

mechanical testing approach when investigating hand-mixed GIs.

## Acknowledgement

This work was funded by a Trinity College Dublin 1252 Studentship for MS Baig.

## REFERENCES

- [1] Wilson AD, Kent BE. A new translucent cement for dentistry. The glass ionomer cement. *Br Dent J* 1972;132:133–5.
- [2] Wilson AD. A hard decade's work: steps in the invention of the glass-ionomer cement. *J Dent Res* 1996;75:1723–7.
- [3] Wilson AD, Crisp S, Ferner AJ. Reactions in glass-ionomer cements: IV. Effect of chelating comonomers on setting behaviour. *J Dent Res* 1976;55:489–95.
- [4] Kent BE, Lewis BG, Wilson AD. Glass-ionomer cement formulations: I. The preparation of novel fluoroaluminosilicate glasses high in fluorine. *J Dent Res* 1979;58:1607–19.
- [5] Product specification for Chemflex. De Trey, Konstanz, Germany, 2010.
- [6] Product specification for Amalomer CR. Advanced Healthcare, Tonbridge, UK, 2007.
- [7] Product specification for KetacMolar Easymix. 3M ESPE, Seefeld, Germany, 2013.
- [8] Product specification for Chemfil Rock. De Trey, Konstanz, Germany.
- [9] Neve AD, Piddock V, Combe EC. Development of novel dental cements I. Formation of aluminoborate glasses. *Clin Mater* 1992;9:7–12.
- [10] Darling M, Hill R. Novel polyalkenoate (glass ionomer) dental cements based on zinc silicate glasses. *Biomaterials* 1994;15:299–306.
- [11] Boyd D, Towler MR. The processing, mechanical properties and bioactivity of zinc based glass ionomer cements. *J Mater Sci Mater Med* 2005;16:843–50.
- [12] International Organization for Standardization. ISO 9917-1 – Dentistry – water-based cements. Part 1. Powder/liquid acid–base cements. 1st ed; 2003.
- [13] McCabe JF, Watts DC, Wilson HJ, Worthington HV. An investigation of test-house variability in the mechanical testing of dental materials. *J Dent* 1990;18:90–7.
- [14] Darvell BW. Uniaxial compression tests and the validity of indirect tensile strength. *J Mater Sci* 1990;25:757–80.
- [15] Fleming GJP, Dowling AH, Addison O. The crushing truth about glass ionomer restoratives: exposing the standard of the standard. *J Dent* 2012;40:181–8.
- [16] Dowling AH, Fleming GJP, McGinley EL, Addison O. Improving the standard of the standard for glass ionomers: an alternative to the compressive fracture strength test for consideration? *J Dent* 2012;40:189–201.
- [17] Baig MS, Dowling AH, Fleming GJP. Hertzian indentation testing of glass-ionomer restoratives: a reliable and clinically relevant testing approach. *J Dent* 2013;41:968–73.
- [18] Mount GJ. Clinical performance of glass-ionomers. *Biomaterials* 1998;19:573–9.
- [19] Nomoto R, McCabe JF. Effect of mixing methods on the compressive strength of glass-ionomer cements. *J Dent* 2001;29:205–10.
- [20] Billington RW, Williams JA, Pearson GJ. Variation in powder/liquid ratio of restorative glass-ionomer cement used in dental practice. *Br Dent J* 1990;169:164–7.
- [21] Fleming GJP, Zala DM. An assessment of encapsulated versus hand-mixed glass ionomer restoratives. *Oper Dent* 2003;28:168–77.
- [22] Eames WB, Monroe SD, Roan JD, O'Neal SJ. Proportioning and mixing of cements: a comparison of working times. *Oper Dent* 1977;2:97–104.
- [23] Fleming GJP, Shortall ACC, Shelton RM, Marquis PM. Encapsulated versus hand-mixed zinc phosphate dental cements. *Biomaterials* 1999;20:2147–53.
- [24] Brune D, Smith D. Microstructure and strength properties of silicate and glass ionomer cements. *Acta Odontol Scand* 1982;40:389–96.
- [25] Wilson AD, McLean JW. The setting reaction and its clinical consequences. In: Wilson AD, editor. *Glass-ionomer cement*. Chicago, IL: Quintessence Publishing Co., Inc.; 1988. p. 43–54.
- [26] Hatton PV, Brook IM. Characterisation of the ultrastructure of glass-ionomer (poly-alkenoate) cement. *Br Dent J* 1992;173:275–7.
- [27] Xie D, Brantley WA, Culbertson BM, Wang G. Mechanical properties and microstructures of glass-ionomer cements. *Dent Mater* 2000;16:129–38.
- [28] Dowling AH, Fleming GJP. Is encapsulation of posterior glass-ionomer restoratives the solution to clinically induced variability introduced on mixing? *Dent Mater* 2008;24:957–66.
- [29] Dowling AH, Fleming GJP. Are encapsulated anterior glass-ionomer restoratives better than their hand-mixed equivalents? *J Dent* 2009;37:133–40.
- [30] Crisp S, Lewis BG, Wilson AD. Characterization of glass-ionomer cements 2. Effect of the powder: liquid ratio on the physical properties. *J Dent* 1976;4:287–90.
- [31] Product specification for Ionofil Molar. Voco GmbH, Cuxhaven, Germany, 2013.
- [32] International Organization for Standardization. ISO 4049 – Dentistry – polymer-based filling, restorative and luting materials. 3rd ed; 2000. p. 15–8.
- [33] de With G, Wageman HHM. Ball-on-ring test revisited. *J Am Ceram Soc* 1989;72:1538–41.
- [34] Timoshenko S, Woinowsky-Krieger S. Symmetrical bending of circular plates. In: *Theory of plates and shells*. 2nd ed. New York: McGraw-Hill; 1959. p. 87–121.
- [35] Wang Y, Darvell BW. Failure mode of dental restorative materials under Hertzian indentation. *Dent Mater* 2007;23:1236–44.
- [36] Weibull W. A statistical distribution function of wide applicability. *J Appl Mech* 1951;18:293–7.
- [37] Trustrum K, Jayatilaka ADS. On estimating the Weibull modulus for a brittle material. *J Mater Sci* 1979;14:1080–4.
- [38] Lipson C, Sheth NJ. Statistical distributions. In: Lipson C, Sheth NJ, editors. *Statistical design and analysis of engineering experiments*. New York: McGraw-Hill; 1973. p. 372–415.
- [39] Thoman DR, Bain LJ, Antle CE. Inferences on the parameters of the Weibull distribution. *Technometrics* 1969;11:445–60.
- [40] Fleming GJP, Farooq AA, Barralet JE. Influence of powder/liquid mixing ratio on the performance of a restorative glass-ionomer dental cement. *Biomaterials* 2003;24:4173–9.
- [41] Fleming GJP, Shelton RM, Landini G, Marquis PM. The influence of mixing ratio on the toughening mechanisms of a hand-mixed zinc phosphate dental cement. *Dent Mater* 2001;17:14–20.
- [42] Fleming GJP, Landini G, Marquis PM. Properties of encapsulated and hand-mixed zinc phosphate dental cement. *Am J Dent* 2002;15:91–6.
- [43] Fleming GJP, Kenny SM, Barralet JE. The optimisation of the initial viscosity of an encapsulated glass-ionomer filling

- material following different mechanical mixing regimes. *J Dent* 2006;34:155–63.
- [44] Bonifacio CC, Kleverlaan CJ, Raggio DP, Werner A, de Carvalho RCR, van Amerongen WE. Physical-mechanical properties of glass ionomer cements indicated for atraumatic restorative treatment. *Aust Dent J* 2009;54:233–7.
- [45] Torabzadeh H, Ghasemi A, Shakeri S, Baghban AA, Razmavar S. Effect of powder/liquid ratio of glass ionomer cements on flexural and shear bond strengths to dentin. *Braz J Oral Sci* 2011;10:204–7.
- [46] Higgs WAJ, Lucksanasombool P, Higgs RJED, Swain MV. Evaluating acrylic and glass-ionomer cement strength using the biaxial flexure test. *Biomaterials* 2001;22:1583–90.
- [47] Braem MJA. Physical properties of glass-ionomer cements: Fatigue and elasticity. In: Davidson CL, Mjoer IA, editors. *Advances in glass-ionomer cements*. Berlin: Quintessence Publishing; 1999. p. 67–84.
- [48] Ban S, Anusavice KJ. Influence of test method on failure stress of brittle materials. *J Dent Res* 1990;69:1791–9.
- [49] Addison O, Marquis PM, Fleming GJP. Resin elasticity and the strengthening of all-ceramic restorations. *J Dent Res* 2007;86:519–23.
- [50] Hooi P, Addison O, Fleming GJP. Can a soda-lime glass be used to demonstrate how patterns of strength dependence are influenced by pre cementation and resin-cementation variables? *J Dent* 2013;41:24–30.
- [51] Wang Y, Darvell BW. Failure behavior of glass ionomer cement under Hertzian indentation. *Dent Mater* 2008;24:1223–9.
- [52] Wang Y, Darvell BW. Effect of elastic modulus mismatch on failure behaviour of glass ionomer cement under Hertzian indentation. *Dent Mater* 2012;28:279–86.
- [53] Yettram AL, Wright KW, Pickard HM. Finite element stress analysis of the crowns of normal and restored teeth. *J Dent Res* 1976;55:1004–11.
- [54] White SN, Yu Z. Compressive and diametral tensile strengths of current adhesive luting agents. *J Prosthet Dent* 1993;69:568–72.

## **4. GENERAL DISCUSSION**

### **4.1 THE NEED FOR A REINFORCED GI IN RESTORATIVE DENTISTRY**

Cost effective and predictable dental treatment is central to patient satisfaction regardless of whether the treatment is paid privately or by a third party. A systematic review of restoration longevity identified dental amalgam to be the material of choice due to the durability of the silver-tin alloy composition in the oral environment (Sheldon and Treasure, 1999). A study of 719,009 claims submitted to the Dental Practice Board (DPB) between 1991-2001 to investigate the dental factors associated with restoration type and size of the cavity confirmed that dental amalgam was the material of choice with single surface amalgam restorations producing a survival probability of 58% after 10 years (Lucarotti et al., 2005). Patient demand for the aesthetic restorative treatment of cavities in posterior teeth combined with the potential fear of mercury toxicity (Lutz, 1995) has led the dental profession to consider alternative materials to dental amalgam even though the clinical performance suggests a median survival time of over 11 years (Lucarotti et al., 2005). One limitation of the study conducted by Lucarotti et al. (2005) was that it was not possible to compare the performance of amalgam and tooth-coloured filling materials in load-bearing surfaces of posterior teeth. The General Dental Services (GDS) Regulations in England and Wales (under which auspices the data for the study was obtained) preclude the use of either RBCs or GIs in load-bearing surfaces of posterior teeth (Lucarotti et al., 2005). Accordingly, the RBCs were placed in class III, IV and V cavities and GIs in class III and V cavities with associated survival probabilities at 10 years of 43% and 38%, respectively (Lucarotti et al., 2005). The tooth-coloured restoratives were not randomly assigned to different cavities and as a result,

the relative performance of the tooth-coloured materials compared with dental amalgam could not be determined as they had not been applied to similar clinical scenarios.

Dental amalgam relies on mechanical interlocking for adhesion and necessitates the removal of sound tooth structure prior to placement such that the initial size of the cavity has to be extended (Lutz, 1995). The destruction of sound tooth structure is contraindicated since to date there is no replacement filling material available with the properties of natural dentition. Interestingly, Lucarotti et al. (2005) highlighted that whilst the performance of small class I dental amalgam restorations at 10 years produced a survival probability of 58%, this was reduced to only 43% when mesio-occlusal-distal (MOD) cavities were evaluated at 10 years.

Methacrylate RBC materials are currently considered to offer an aesthetic alternative to dental amalgam in load-bearing surfaces of posterior teeth. The free-radical polymerisation of dimethacrylate monomers during the light irradiation of RBCs involves bulk contraction (Davidson and Feilzer, 1997) and as a result polymerisation shrinkage of the RBC material may be manifested as shrinkage stress (Davidson et al., 1984). Cuspal movement on polymerisation may compromise the synergism at the restoration-tooth interface possibly leading to bacterial micro-leakage and ultimately to marginal staining, pulpal inflammation or necrosis, post-operative pain and secondary caries (Lutz et al., 1991; Christensen, 2000). Manufacturers have attempted to address the issues of excessive contraction on setting by removing triethyleneglycol dimethacrylate (TEGDMA) from monomeric formulations by employing urethane dimethacrylate (UDMA) and derivatives of bisphenol-A glycidyl methacrylate (BisGMA), such as bisphenol-A ethoxylated dimethacrylate (BisEMA). A reduction in the associated shrinkage due to the reduced concentration of carbon-to-carbon double bonds (Asmussen and Peutzfeldt, 1998) occurs, however, while cuspal movement on

polymerisation was reduced, no reduction in the associated gingival microleakage at the cervical dentine cavosurface margin was evident (Fleming et al., 2005). In addition, RBCs are time consuming and technique sensitive when placed clinically compared with dental amalgam and require a series of preconditioning treatments of the tooth structure to ensure adhesion (Peumans et al., 2005).

GIs are aesthetic and unique amongst dental restoratives in that they chemically bond to sound tooth structure without the need for preconditioning the tooth structure or the removal of sound tooth structure (Wilson and McLean, 1988d; Van Meerbeek et al., 2003). Clinically, GIs can be adequately placed and finished by the operator in a single patient visit and are reported to release fluoride ions which has been claimed to be therapeutic for secondary caries prevention (Forsten, 1998; Mayanagi et al., 2014). Unfortunately, conventional GI formulations are not advocated for load-bearing surfaces of posterior teeth according to the GDS Regulations in England and Wales. Despite the poor performance (38% at 10 years) in the investigation by Lucarotti et al. (2005), the authors suggested that the GIs would be placed in minimal intervention cavities with no associated loss of sound tooth structure such that in principle re-intervention of like with like (GI with GI) could allow a tooth to survive indefinitely even if the intervals were short. When placed in the posterior region of the mouth GIs have to resist masticatory forces during function and therefore optimisation of the CFS is important. As a result the minimum CFS stated in ISO 9917-1:2007 for GI restoratives is 100 MPa which is twice that stated for GI luting cements (50 MPa). Unfortunately, encapsulated GI restoratives often fail to meet the specification standards and suggestions have been made regarding reducing the 100 MPa value specified in the ISO standard. It is suggested that the failure to obtain the optimum hand-mixed powder:liquid mixing ratio (Mount and Makinson, 1978a; Billington et al., 1990) in combination with the utilisation of encapsulated GIs

(Fleming and Zala, 2003) may be contributing factors to the poor clinical performance highlighted by Lucarotti et al. (2005).

The published literature from January 1998 to May 2004 was reviewed to identify the clinical bonding effectiveness of resin-based adhesive systems (three or two-step etch and rinse, two or one-step self-etch) and GIs (conventional and resin modified) when restoring class V lesions (Peumans et al., 2005). The retention of non-carious class V restorations was identified as the 'most objective evaluation parameter' for investigating the clinical bonding effectiveness of adhesive restorations (Peumans et al., 2005). The reasons proposed included the lack of provision of macro-mechanical retention for class V lesions, the minimal requirement for tooth preparation, the ease of restoration due to adequate access for anterior and premolar teeth (Van Meerbeek et al., 1998), the increased incidence of class V lesions (Levitch et al., 1994) and the relatively insignificant influence of mechanical properties of the adhesive restorative materials (Browning et al., 2000). In accordance with the American Dental Association (ADA) guidelines for dentine and enamel adhesive materials, 6 and 18 month retention rates were required to be at least 95 and 90% for provisional and full acceptance, respectively (Peumans et al., 2005). The mean annual failure rate of GIs was highlighted to be  $1.9 \pm 1.8\%$  which was significantly lower when compared with the mean annual failure rates of the one-step self-etch ( $8.1 \pm 11.3\%$ ) and two-step etch and rinse adhesives ( $6.2 \pm 5.5\%$ ). The mean annual failure rates of the three-step etch and rinse and the two-step self-etch adhesive systems were not reported to be significantly lower than the mean annual failure rate of GIs, although the annual failure rates varied widely for the three-step etch and rinse (0-16%) and the two-step self-etch adhesives (0-19.3%) when compared with GIs (0-7.6%). In addition, GIs were the only adhesive category reviewed where 100 and 96% of the GIs investigated fulfilled the ADA guidelines for provisional and full acceptance,



respectively, when compared with the three-step etch and rinse (91 and 81%), two-step etch and rinse (79 and 51%), two-step self-etch (82 and 71%) and one-step self-etch (68 and 70%) resin-based adhesive systems. Although the brittle nature of GI restoratives precludes their use in thin sections (Xie et al., 2000), the clinical data for non-carious class V lesions restored with GIs confirm the superior clinical bonding effectiveness of GIs when compared with resin-based adhesives (Peumans et al., 2005).

Clinical studies on GIs used for the restoration of class I and class II cavities are routinely limited to deciduous dentition using the atraumatic restorative treatment (ART) approach (Taifour et al., 2002; Honkala et al., 2003; Yu et al., 2004), where GIs are placed under compromised conditions using only hand instrumentation (Frencken et al., 1996). Although some investigators have used ART for the permanent dentition in children (Yip et al., 2002; Gao et al., 2003; Frencken et al., 2006, 2007) or elderly patients (da Mata et al., 2015), the studies were limited to time periods of 12 (Yip et al., 2002), 24 (da Mata et al., 2015), 30 (Gao et al., 2003) or 76 months (Frencken et al., 2006, 2007). The evaluation of GIs placed using only hand instrumentation provides little comparative information on restoration survival when GIs are placed in general dental practice employing rotary instruments for caries removal, adequate moisture isolation and the application of a light cured protective varnish following placement of the GI into the cavity. Clinical data on the performance of GIs placed in class I and class II cavities in permanent dentition and not under ART conditions are rare. Short-term (24 months) survival data of 98% was reported for Fuji IX (GC Corporation) placed in class I (n=67) and class II (n=102) cavities of permanent molar (n=132) and premolar (n=37) teeth of 116 adult patients in three general dental practices in the UK (Burke et al., 2007). A single publication was identified in the dental literature reporting the long-term (72 months) survival data of class II GI restorations placed in

permanent dentition of adult patients in a routine dental setting (Scholtanus and Huysmans, 2007). A total of 116 class II GI restorations placed in permanent molar (n=78) and (n=38) premolar teeth were evaluated for 72 patients attending a Dutch private dental practice (Scholtanus and Huysmans, 2007). The cavities were filled with an encapsulated GI (Fuji IX) prior to conditioning the cavity walls with polyacrylic acid. Following finishing, the restorations were coated with Fuji LC varnish (GC Corporation) to protect the GI restorations from the deleterious effects of moisture contamination during clinical placement (Causton, 1981) and desiccation during the early stages of the setting reaction (Earl et al., 1989; Wilson, 1989). The GI restorations were inspected at 6 month intervals and restoration failure was defined as the need for re-intervention in the form of repair, partial or total replacement, fracture, secondary caries or excessive wear (Scholtanus and Huysmans, 2007). For the 116 class II GI restorations, no failure occurred within the first 18 months, although the failure rate increased to 5 and 40% at 36 and 72 months, respectively (Scholtanus and Huysmans, 2007). The failed restorations required intervention due to fracture of the marginal ridges of the restorations or loss of the GI in the proximal contact areas. Interestingly, no GI restorations observed in the short- (Burke et al., 2007) and long-term (Scholtanus and Huysmans, 2007) clinical studies failed due to secondary caries which may provide evidence to support the claimed therapeutic influence attributed to the fluoride release in GIs (Forsten, 1998; Mayanagi et al., 2014). The results of the only long-term study for GIs placed in class II cavities of permanent teeth of adult patients in dental practice (Scholtanus and Huysmans, 2007) suggests that further improvements in GI materials are required for GIs to be 'truly' advocated for the restoration of posterior dentition.

## 4.2 INTERNATIONAL ORGANISATION FOR STANDARDISATION

Guidance for the evaluation of dental materials is provided for by the ISO to ensure the reproducibility of test results, under standard conditions, between different test centres. The CFS testing protocol is the only strength test specified for inclusion in ISO 9917-1:2007 - the international standard for powder/liquid acid-base cements and restoratives (ISO 9917-1:2007). Investigators have suggested that loading during masticatory function results in stressing patterns analogous to compression during CFS testing (Yettram et al., 1976) such that a high CFS was advocated to tolerate the masticatory forces routinely encountered in the mouth (White and Yu, 1993). Disappointingly, despite specifications in the standard, a wide variation in testing conditions was identified in the dental literature for GIs such that a direct comparison between studies was impossible (Manuscript 3.1). The standard itself suffers from some inherent deficiencies which must be addressed to ensure consistent testing conditions for a valid comparison between studies. In addition, the reliability (McCabe et al., 1990) and validity (Darvell, 1990) of the CFS testing protocol have been questioned in the dental literature which cast doubts over its appropriateness for inclusion in ISO 9917-1:2007 (Fleming et al., 2012; Dowling et al., 2012).

Non-parallel specimen ends cause localised stress concentrations and premature failure during loading of CFS specimens (Lloyd and Mitchell, 1984; White and Yu, 1993). To accommodate for non-parallel specimen ends, a layer of a padding material is often placed between the cylindrical specimen ends and the loading platens of the testing apparatus. Interestingly, the use of a padding material has been reported to influence the CFS values determined (Darvell, 1990) but ISO 9917-1:2007 prescribe the use of filter paper as a

padding material to accommodate for non-parallel specimen ends which may be a deficiency in the standard (ISO 9917-1:2007).

Loading CFS specimens in a wet environment is more clinically relevant to accommodate for environmental assisted crack growth (Anusavice and Lee, 1989). Additionally, GI specimens are susceptible to desiccation (Earl et al., 1989; Wilson, 1989) such that testing in a dry environment would produce markedly reduced CFS values. To prevent desiccation and resultant cracking of the GI specimens, ISO 9917-1:2007 advocate the placement of a wet filter paper between the wet CFS specimen and the loading platens of the testing apparatus with the use of a freshly wet piece of filter paper recommended for each individual specimen tested. The lack of information detailed in studies investigating GIs in the dental literature, regarding the provision of a wet testing environment during testing, make it impossible to interpret the findings between different studies despite specification in the standard (Manuscript 3.1).

The time that GI specimens are stored in distilled water ( $37 \pm 1^\circ\text{C}$ ) influences the resultant CFS value due to maturation of the GI material (Crisp et al., 1976; Williams and Billington, 1991) following the initial stages of the setting reaction. GIs are reported to undergo a post-set hardening phase which continues for 24 h following the initial stages of the setting reaction and prior to the subsequent maturation stage which can continue over a time period of several months (Wilson and McLean, 1988b). Therefore, ISO 9917-1:2007 stipulate the CFS of GI specimens should be determined following conditioning in a mould for 1 h and water storage for  $23 \pm 0.5$  h, to ensure the completion of the post-set hardening phase. However, in the dental literature, CFS testing of GI specimens was routinely performed following 24 h (Miller et al., 1984; El Mallakh et al., 1987; Walls et al., 1987; Nakajima et

al., 1989; Kerby and Bleiholder, 1991; Williams et al., 1992; Nicholson et al., 1993; Culbertson and Kao, 1994; Yap et al., 2002; Gu et al., 2005; Yli-Urpo et al., 2005; Dowling et al., 2006, 2014; Moshaverinia et al., 2008a,b; Elsaka et al., 2011) or 1 week water storage (Kao et al., 1996; Culbertson et al., 1999; Yap et al., 2002; Yamazaki et al., 2005; Yli-Urpo et al., 2005; Moshaverinia et al., 2009) (Manuscript 3.1). It is evident that prolonged water storage (1 week) would increase the CFS values reported owing to the continuous maturation of GIs on setting (Crisp et al., 1976; Williams and Billington, 1991) such that a comparison between studies where CFS testing was performed following different water storage time intervals is of little value to the dental research community.

The CFS of brittle materials, namely GI restoratives, is influenced by the rate of compressive loading where an increase in the CFS value occurs with increasing loading rate owing to the reduced time available for environmental assisted crack growth (Li and White, 1999; Higgs et al., 2001a). The compressive loading rate advocated in ISO 9917-1:2007 for CFS testing of GI specimens is  $0.75 \pm 0.30$  mm/min. The CFS loading rates identified for studies reporting GI reinforcement strategies were 0.5 mm/min (Miller et al., 1984; Nakajima et al., 1989; Culbertson and Kao, 1994; Kao et al., 1996; Culbertson et al., 1999; Yamazaki et al., 2005; Moshaverinia et al., 2008a,b, 2009; Elsaka et al., 2011) and 1 mm/min (Walls et al., 1987; Kerby and Bleiholder, 1991; Williams et al., 1992; Nicholson et al., 1993; Yap et al., 2002; Gu et al., 2005; Yli-Urpo et al., 2005; Dowling et al., 2006, 2014), while El Mallakh et al. (1987) failed to report the loading rate employed (Manuscript 3.1). Although the compressive loading rates employed by the researchers (Miller et al., 1984; Walls et al., 1987; Nakajima et al., 1989; Kerby and Bleiholder, 1991; Williams et al., 1992; Nicholson et al., 1993; Culbertson and Kao, 1994; Kao et al., 1996; Culbertson et al., 1999; Yap et al., 2002; Gu et al., 2005; Yamazaki et al., 2005; Yli-Urpo et al., 2005; Dowling et al., 2006, 2014;

Moshaverinia et al., 2008a,b, 2009; Elsaka et al., 2011) were within the range recommended in ISO 9917-1:2007 (0.45-1.05 mm/min), a direct comparison between individual studies is not possible owing to the differences in the time available for environmental assisted crack growth to occur on loading to failure (Li and White, 1999; Higgs et al., 2001a) (Manuscript 3.1). Therefore, to avoid confusion and allow direct comparisons between studies, it is proposed that a standard loading rate for CFS testing of GIs must be specified in ISO 9917-1:2007 rather than the loading rate range provided for in the standard (ISO 9917-1:2007).

The CFS testing protocol in ISO 9917-1:2007 advocates testing cylindrical GI specimens of specific dimensions ( $6.0 \pm 0.1$  mm height and  $4.0 \pm 0.1$  mm diameter). Strength is not an intrinsic material property such that the height and diameter of the cylindrical specimen influence the maximum load-to-failure which in turn influences the CFS value recorded. In theory, a larger specimen has an increased likelihood of containing crack initiating defects which would reduce the CFS value recorded (Ritter, 1995). Despite the cylindrical specimen dimensions ( $6.0 \pm 0.1$  mm height and  $4.0 \pm 0.1$  mm diameter) being specified by inclusion in ISO 9917-1:2007, a wide variation in specimen dimensions was identified in studies pertaining to GI reinforcement strategies (Manuscript 3.1). These include studies employing specimen dimensions of 6 mm height and 3 mm diameter (El Mallakh et al., 1987), 6 mm height and 4 mm diameter (Yamazaki et al., 2005; Yli-Urpo et al., 2005; Dowling et al., 2006, 2014; Moshaverinia et al., 2008a,b, 2009; Elsaka et al., 2011), 6 mm height and 5 mm diameter (Walls et al., 1987), 8 mm height and 4 mm diameter (Yap et al., 2002; Gu et al., 2005) and 12 mm height and 6 mm diameter (Miller et al., 1984; Nakajima et al., 1989; Kerby and Bleiholder, 1991; Williams et al., 1992; Nicholson et al., 1993; Culbertson and Kao, 1994; Kao et al., 1996; Culbertson et al., 1999) (Manuscript 3.1). When testing the CFS of GI specimens, the wide variation in the specimen dimensions employed by dental

researchers prevents any direct comparison between studies which is a further embarrassment to the review process in the dental literature.

GIs are brittle dental materials, such that a distribution in the strength data is inevitable (Ritter, 1995). ISO 9917-1:2007 suggests CFS testing five cylindrical specimens and if four of the five CFS values are  $>100$  MPa then the GI restorative will pass the CFS criteria. If three or more of the five CFS values recorded are  $<100$  MPa, the GI restorative will fail the CFS criteria specified in ISO 9917-1:2007. If three specimens have a CFS value of  $>100$  MPa, an additional five specimens are tested and to pass the criteria specified in ISO 9917-1:2007, all additional five CFS values have to be  $>100$  MPa (ISO 9917-1:2007). The pass/fail criteria specified in ISO 9917-1:2007 for evaluation of GIs has been criticised in the dental literature (McCabe et al., 1990; Fleming et al., 2012). In a 'test-house variability' study involving three centres the CFS of a GI restorative (Ketac Fil) was investigated in accordance with ISO DP 9917:1987 (Harmonisation of test methods for dental cements). ISO DP 9917:1987 was a forerunner to ISO 9917-1:2003 which was superseded by ISO 9917-1:2007 - the current standard for powder/liquid acid-base cements and restoratives. The only significant change in the subsequent standards was the reduction in the minimum requirement of CFS from 130 MPa (ISO DP 9917:1987) to 100 MPa (ISO 9917-1:2003; ISO 9917-1:2007). In McCabe et al.'s (1990) study, cylindrical specimens (6 mm height, 4 mm diameter:  $n=30$ ) were prepared at each of the three test centres and six batches of five specimens were subjected to the pass/fail criteria specified in ISO DP 9917:1987. Interestingly, a clear fail was identified for all six batches in the first test centre, while two batches passed and four batches failed the pass/fail criteria in the second test centre. For the third test centre, a clear pass was identified for all six batches. The lack of reproducibility of the CFS test results was evident as inter- and intra-operator variability in different test centres

and the authors called for the identification of alternative testing methodologies for evaluating GIs (McCabe et al., 1990).

Recently, Fleming et al. (2012) revisited the CFS testing methodology for GIs and identified the reproducibility of test results achieved were susceptible to inter- and intra-operator variability by employing the batch censoring specified in ISO 9917-1:2003. To eliminate dispensing errors in powder:liquid mixing ratios (Billington et al., 1990; Fleming et al., 2003), Fleming et al. (2012) investigated the CFS of three encapsulated GI restoratives (Ketac Molar Aplicap; 3M ESPE, Fuji IX<sub>GP</sub> Fast; GC Corporation and Chemflex in Caps; Dentsply DeTrey) prepared by two operators using a vibratory (Capmix) and a centrifugal (Rotomix) mechanical mixing machine. Batch censoring specified in ISO 9917-1:2003 was highlighted to be unsafe as it misidentified operative variability and therefore a statistical approach employing a minimum of 20 specimens (McCabe and Carrick, 1986) was required for a meaningful interpretation of the CFS data sets. The authors concluded that the CFS test could be performed reliably if specimen preparation techniques and laboratory conditions were standardised, although such a level of control was not routinely applied in dental research as evident by the large variation in CFS data reported in the literature (Fleming et al., 2012).

Despite the demonstration that the CFS test could be performed reliably under controlled mixing and testing conditions (Fleming et al., 2012), the validity of the CFS testing methodology remained under scrutiny (Darvell, 1990). For cylindrical gypsum specimens loaded under axial compression, a pair of shear cones developed within the specimen adjacent to the contact points with the loading platens (Darvell, 1990). The shear stresses resulted in tensile forces acting outward from the central axis of the cylindrical specimen,



leading to lateral expansion of the specimen (Darvell, 1990) with a resultant formation of splitting 'wing' cracks (Renshaw and Schulson, 2001). The exact failure mechanism was, however, complex and involved the formation of crack linkages between wing cracks and secondary crack propagation, thereby splitting the cylinder into slender micro columns which separated from the specimen on axial compressive loading due to bending induced failure (Renshaw and Schulson, 2001). The cylindrical specimens were, therefore, identified to have fractured due to 'some unresolved combination of tension and shear stresses' and not solely by compressive stresses (Darvell, 1990). It should be noted, however, that the validity tests for the CFS testing protocol investigated by Darvell (1990) were performed on gypsum cylinders, where the failure mode of dry gypsum cylinders was identified to be 'vertical split slabbing mode' but when wet with water or alcohol changed to failure on the 'diagonal planes running from top left to bottom right'. It cannot be said with certainty whether the results for gypsum cylinders can be directly translated to cylindrical GI specimens which are a different class of material and despite their brittle nature, do not have any compositional resemblance to gypsum. Nevertheless, owing to concerns made in the dental literature regarding the reliability (McCabe et al., 1990) and validity (Darvell, 1990) of the CFS testing protocol, it was evident that there was a need for a definitive study to identify a valid and reliable alternative to the CFS testing protocol specified in ISO 9917-1:2007 for GIs.

### 4.3 A VALID, RELIABLE AND DISCRIMINATORY ALTERNATIVE MECHANICAL TESTING METHODOLOGY FOR ENCAPSULATED GIs

The results of a PubMed literature search (1990-2011) identified the four most commonly employed mechanical testing protocols for GIs (in order of popularity) were the CFS (n=154), DTS (n=76), TFS (n=62) and BFS (n=26) tests, while other less commonly used protocols included the HI and  $K_{IC}$  tests (Dowling et al., 2012). The use of testing methodologies other than that specified in ISO 9917-1:2007 for GIs is indicative of the lack of confidence in the dental research community regarding the reliability (McCabe et al., 1990) and validity (Darvell, 1990) of the CFS testing protocol. To identify a valid and reliable alternative testing methodology for GIs, Fleming et al.'s (2012) study was extended to an investigation using the most commonly employed testing methodologies for GIs, namely the CFS, TFS and BFS tests under standardised conditions, namely padding material (filter paper), loading rate (1 mm/min), environment (wet) and storage time (24 h) (Dowling et al., 2012). Although the DTS test was identified as the second most commonly used testing methodology for the assessment of GIs based on the PubMed literature search, the DTS test was not included in Dowling et al.'s (2012) investigation as the validity of the DTS test for brittle materials was thoroughly undermined by Darvell in 1990 (Darvell, 1990). The DTS test assumes a point contact between two knife edge supports and a disc-shaped or cylindrical specimen which is compressed diametrically. Theoretically, the tensile stresses generated on loading the disc or cylinder across the diameter pull the disc or cylinder in a vector half perpendicular to the diametral plane joining the two points of contact (Darvell, 1990). In practice, however, the knife edge supports are replaced by loading platens, thereby changing the point contacts to an area of contact which complicates the stress states within the specimen (Lloyd and Mitchell, 1984) such that failure does not occur solely by tensile

stresses but a combination of tensile, compressive and shear stresses (Darvell, 1990). The large shear stresses generated within the specimen in close approximation with the loading platens (Darvell, 1990) make it impossible to identify whether failure was initiated in tension or shear (Berenbaum and Brodie, 1959). Therefore, DTS testing of brittle materials has essentially been made redundant from the standards testing armamentarium, although some research groups employ DTS testing routinely notwithstanding the accepted reservations regarding the technique (Berenbaum and Brodie, 1959; Kendall, 1978; Lloyd and Mitchell, 1984; Darvell, 1990).

To eliminate dispensing errors with the powder and liquid constituents (Billington et al., 1990; Fleming et al., 2003) and to standardise the mixing regime, Dowling et al. (2012) used three encapsulated commercial GI restoratives, namely Chemfil Rock (Dentsply DeTrey), Fuji IX<sub>GP</sub> Fast (GC Corporation) and Ionofil Molar AC (Voco GmbH) (Dowling et al., 2012). Owing to the reproducible failure mode from the surface under tension observed for the bar-shaped TFS and disc-shaped BFS specimens, the TFS and BFS testing methodologies were identified as valid alternative mechanical testing protocols to the CFS test for the encapsulated GIs investigated. In terms of reproducibility, the authors could not statistically differentiate between the testing protocols investigated as the pooled CoV of the CFS, TFS and BFS data sets were reported at 10% (0.104), 12% (0.116) and 11% (0.109), respectively (Dowling et al., 2012). More interestingly, the TFS and BFS testing methodologies failed to discriminate between the encapsulated GI products, despite the GI products being supplied by different manufacturers with different glass compositions, liquid compositions and powder:liquid mixing ratios while differences in CFS values were evident (Dowling et al., 2012). Owing to the marked compositional and powder content variations in the three encapsulated GIs, the non-discriminatory results for the TFS and BFS tests were

confounding. This prompted the investigation of other mechanical testing methodologies identified for GIs in the dental literature (Dowling et al., 2012) to determine their discriminatory potential using the same encapsulated GI products to allow for comparison with the Dowling et al. (2012) study by eliminating product variability between the studies (Manuscripts 3.2 and 3.3). In the context of the overall investigation, the HI test (Manuscript 3.2) was investigated for reasons of increased clinical relevance while the  $K_{IC}$  test (Manuscript 3.3) was investigated as  $K_{IC}$  is an intrinsic material property.

#### **4.3.1 HERTZIAN INDENTATION TEST**

It is essential any mechanical test used to evaluate the performance of dental restorative materials demonstrates a failure mode which is representative of the clinical scenario *in vivo* (Kelly, 1999; Kelly et al., 2012). Bar-shaped specimens used for TFS testing are not geometrically representative of the clinical loading of GI restorations. Disc-shaped BFS specimens more closely resemble the surface area to volume ratio of a dental restoration, although loading discs through a 4 mm diameter ball when supported on a ring annulus in the absence of a supporting substructure fails to replicate the situation *in vivo*.

The HI test involves applying a load through a spherical indenter against a flat specimen surface until failure occurs and has been employed to test dental ceramics (Harvey and Kelly, 1996; Peterson et al., 1998; Chai and Lawn, 1999; Jung et al., 1999; Lawn et al., 2001, 2002; Deng et al., 2002), dental amalgams (Wang and Darvell, 2007, 2008, 2010; Darvell, 2012a,b), RBCs (Wang and Darvell, 2008) and GI restoratives (Wang and Darvell, 2007, 2008, 2009, 2012). In the initial part of the current investigation, the HI testing protocol was examined to identify a valid, reliable, discriminatory and clinically relevant testing protocol

for encapsulated GIs (Manuscript 3.2). The choice of the encapsulated GI restoratives used was based on those employed by Dowling et al. (2012) to enable a valid comparison between the reliability of the HI test results achieved with the CFS, TFS and BFS test results (Dowling et al., 2012).

The HI test simulates the loading conditions experienced by GI restorations under occlusal loading (Kelly, 1999; Wang and Darvell, 2007). Additionally, the specimens were tested while resting freely on top of a dentine analogue substrate material - which was reported by the manufacturer to be composed of a 30% glass fiber reinforced polyamide (nylon-6,6). The polyamide substrate was selected as a dentine analogue material as it was stated by the manufacturer to have an elastic modulus value of 10-11 GPa (Product specification) which was within the range of that reported for dentine at 11-18 GPa (Marshall et al., 1997). The elastic modulus mismatch between the GI restorative specimen and the dentine analogue substrate material results in the creation of a tensile stress at the specimen/dentine analogue interface on loading, leading to the initiation of radial cracks at the specimen bottom surface (Wang and Darvell, 2007, 2012). The tensile initiated radial crack propagates upward through the thickness of the specimen, dissecting the specimen into two to four fracture fragments with smooth fracture surfaces. Examination of the fracture surfaces highlighted fractographic features of the mirror, mist, hackle and macroscopic crack branching regions which facilitated the identification of the fracture origin and failure mode (Manuscript 3.2; Figure 1). The fractographic features were traced back to confirm the fracture origin which was identified to lie at the bottom surface of the specimen in contact with the substrate material for all of the specimens, thereby confirming that the specimens fractured by the clinically relevant failure mode of tensile initiated radial cracking at the GI restoration/dentine analogue interface.

The observations made for the encapsulated GI restorative disc-shaped specimens tested under HI (Manuscript 3.2) were in agreement with the findings of Wang and Darvell (2007, 2008, 2009, 2012) - the other researchers to have employed the HI testing methodology to GI restoratives over a range of specimen thicknesses. A regular fracture pattern with bottom initiated radial cracking from the surface under tension was observed as the principle failure mode for GI restorative disc-shaped specimens (Amalgomer CR) of thicknesses ranging from 0.4 to 3.6 mm (Wang and Darvell, 2007). Some evidence of cone cracking from the top surface under compression was identified only when the GI specimen thickness was increased from 4 to 7 mm (Wang and Darvell, 2007). In the present study, all specimens from the three encapsulated GI products had a regular fracture pattern with smooth fracture surfaces indicating that radial cracking was the dominant failure mode (Manuscript 3.2; Figure 1). The specimen thickness of  $3.14 \pm 0.07$  mm reported in Manuscript 3.2 was consistent with the bottom initiated radial cracking and regular fracture pattern observed for GI restoratives reported in the dental literature which is representative of the clinical failure mode for GI restoratives *in vivo* (Wang and Darvell, 2007, 2008, 2009, 2012), thereby confirming the validity of the HI testing protocol.

When the reliability of the HI testing protocol was assessed and compared with that of the CFS, TFS and BFS testing protocols (Dowling et al., 2012), the pooled CoV of 7% for the GI restorative data sets achieved using HI testing (Manuscript 3.2) was reduced compared with the pooled CoVs observed for the CFS (10%), TFS (12%) and BFS (11%) tests when data sets for the same encapsulated GI restoratives were investigated previously (Dowling et al., 2012). The reduced CoV in the load-to-failure data recorded for the encapsulated GI restoratives could be due to a number of factors relating to the mixing and testing conditions employed during HI testing. The specimen preparation technique employed to manufacture

the disc-shaped specimens is simple and does not require the operator to have a skill beyond that required of a dentist (Darvell, 2012a). The testing protocol is easy to perform with the specimen placed on top of the substrate constrained in a brass holder and aligned with the help of a centralising device, thereby minimising any critical alignment concerns. The use of encapsulated GI restoratives minimised operator induced variability on mixing and only five specimen batches were prepared each day which minimised the potential for operator fatigue (Fleming et al., 2012).

Contrary to the TFS and BFS tests (Dowling et al., 2012), The HI test was identified to be able to discriminate between the same three encapsulated GI products investigated (Manuscript 3.3). It must be noted, however, that the ‘Hertzian load-bearing capacity’ was recorded as the maximum load-to-failure (Wang and Darvell, 2007) which precluded it from being a material property, such that the Hertzian load-bearing capacity could possibly be interpreted (in line with the views of Alan Wilson) as the ‘quality of the cement’ rather than a ‘predictive value’ (Wilson, 1975). In the context of the overall investigation, it was considered useful to evaluate an intrinsic material property for GI restoratives which would be independent of variations in specimen dimensions, thereby providing a valid and reliable assessment of the GI products (Manuscript 3.4).  $K_{IC}$  is an intrinsic material property which represents the materials resistance to crack propagation (Atkins and Mai, 1985). As an intrinsic material property,  $K_{IC}$  would be expected to highlight differences between GI products with varying powder:liquid mixing ratios.

### 4.3.2 FRACTURE TOUGHNESS TEST

The stress intensity factor ( $K$ ) was proposed by Irwin (1957) to describe the stress state at the crack tip of a material. Fracture occurs when the value of  $K$  exceeds a certain critical value ( $K_C$ ) for crack growth in the material (Atkins and Mai, 1985). For mode I tensile opening,  $K_C$  is denoted by  $K_{IC}$  and is referred to as the plane-strain fracture toughness of the material, an intrinsic material property that determines the resistance of a material to the catastrophic propagation of a pre-existing crack (Atkins and Mai, 1985). As an intrinsic material property,  $K_{IC}$  is independent of specimen dimensions and has been employed to test dental ceramics (Scherrer et al., 1998; Fischer and Marx, 2002; Quinn et al., 2003), dental amalgams (Cruickshanks-Boyd and Lock, 1983; Lloyd and Adamson, 1985, 1987; Beatty and Pidaparti, 1993; Pidaparti and Beatty, 1995), RBCs (Lloyd and Iannetta, 1982; Lloyd, 1982, 1983, 1984; Lloyd and Mitchell, 1984; Goldman, 1985; Ferracane et al., 1987; Lloyd and Adamson, 1987; Kovarik et al., 1991; Beatty and Pidaparti, 1993; Kovarik and Fairhurst, 1993; Pidaparti and Beatty, 1995; Fujishima and Ferracane, 1996) and GIs (Lloyd and Mitchell, 1984; Goldman, 1985; Lloyd and Adamson, 1987; Hill et al., 1989; Beatty and Pidaparti, 1993; Pidaparti and Beatty, 1995; Miyazaki et al., 1996; Lucas et al., 2003; Mitsuhashi et al., 2003; Elsaka et al., 2011; Ilie et al., 2012).

In the absence of a specific standard for the measurement of  $K_{IC}$  in GIs, researchers have employed the techniques described by the ASTM International (ASTM 399:2009) and ISO (ISO 12737:2010) for the  $K_{IC}$  testing of metallic materials. Owing to similarities of brittle fracture of GIs to dental ceramics, the ASTM International standard test method for determination of  $K_{IC}$  of advanced ceramics (ASTM C1421:2010) appears to be more relevant when investigating the  $K_{IC}$  of GIs, although no publications employing ASTM C1421:2010



could be identified in the literature on  $K_{IC}$  testing of GIs. The  $K_{IC}$  testing standards prescribe strict geometry requirements for SEN bend specimens which include a straight and horizontal crack front. Theoretically, a Griffith pre-crack in the form of a perfectly sharp crack should be present, from which unstable crack growth can be initiated (Griffith, 1920). Therefore, the  $K_{IC}$  testing standards for metals and ceramics specify introducing a pre-crack with adequate sharpness from the apex of a notch in the SEN bend specimens prior to loading, although the method for pre-cracking varies for metallic and ceramic specimens which are required to be pre-cracked through fatigue cycling (ASTM 399:2009) or loading the specimen until a ‘pop-in’ pre-crack is heard or seen (ASTM C1421:2010), respectively.

The influence of introducing a pre-crack from the moulded sharp notch in SEN bend specimens (30 mm length, 4.5 mm width, 2.1 mm thickness:  $n=10$ ) on the resultant  $K_{IC}$  values was investigated for eight commercial RBCs (Ferracane et al., 1987). The pre-crack was introduced by tapping a razor blade into the moulded notch, although no images of the pre-crack were supplied to confirm the extent of the pre-crack (Ferracane et al., 1987). Results were inconclusive as for half the products tested, pre-cracking had no significant effect (Ferracane et al., 1987). On testing six additional commercial RBCs, only two showed a significant decrease in  $K_{IC}$  when pre-cracked (Ferracane, 1988). Interestingly, pre-cracking was identified to increase the  $K_{IC}$  values from  $1.38 \pm 0.08 \text{ MNm}^{-1.5}$  to  $1.66 \pm 0.25 \text{ MNm}^{-1.5}$  for one RBC product investigated, which erroneously implied that the notch was sharper than the actual pre-crack (Ferracane, 1988). In addition, all test groups for both studies (Ferracane et al., 1987; Ferracane, 1988) identified an increase in the standard deviation about the mean when pre-cracks were introduced into the specimen which suggests an inconsistency in the formation of the cracks. The inconsistency in forming pre-cracks was also evident for pyrolytic carbon/graphite composite SEN compact tension specimens which were pre-

cracked using the 'pop-in' technique, where an increase in the  $K_{IC}$  values and standard deviation was identified for the pre-cracked specimens ( $1.46 \pm 0.13 \text{ MNm}^{-1.5}$ ) when compared with the control ( $1.35 \pm 0.09 \text{ MNm}^{-1.5}$ ) which again confusingly implies a greater sharpness for the notch compared with the actual pre-crack (Kruzic et al., 2005).

Pre-cracking is mandatory because the notch is routinely machined into the metal or ceramic specimens which produces a rounded tip. However, in dentistry we enjoy a luxury that metallurgists do not have, where we can mould the material in its pre-set plastic state around a sharp scalpel blade. When set, the impression left by the blade edge, the crack tip, has the radius of that blade, typically  $0.25 \mu\text{m}$  for a straight-edge surgical scalpel blade. In the defence of the moulded sharp notch, Lloyd (1988) cited the work of Hashemi and Williams (1985) which showed that for brittle polymers the critical radius for adequate sharpness is more than two orders of magnitude greater than the radius of the crack-tip moulded around an embedded scalpel blade. A notch with a tip radius of  $12.5 \mu\text{m}$  in polymers such as polymethylmethacrylate (PMMA) and polyvinyl chloride (PVC) was identified to produce  $K_{IC}$  values comparable with those produced by pre-cracking. The critical radius for a valid result can be calculated and is greater than this. PMMA ( $1.95 \text{ MNm}^{-1.5}$ ) and PVC ( $2.84 \text{ MNm}^{-1.5}$ ) have  $K_{IC}$  values similar to our dental materials, where for RBC products it is at best  $2.5 \text{ MNm}^{-1.5}$  and for GI products  $0.6 \text{ MNm}^{-1.5}$ . Sharp notches with crack tip radii of less than  $10 \mu\text{m}$  have also been identified to produce comparable results to pre-cracked specimens for dental ceramics (Nishida et al., 1994; Damani et al., 1996) and pyrolytic carbon/graphite composites (Kruzic et al., 2005) which further supports the use of sharp notched SEN specimens for  $K_{IC}$  testing of brittle materials.

Perhaps, of most relevance to the present research is the work of Hill and Labok (1991) on zinc polycarboxylate cement, a material with a structure similar to GI. The values of  $K_{IC}$  obtained using compact tension specimens containing disc-cut 'cracks' were in agreement with those obtained with double torsion specimens. The latter produces a perfectly sharp crack by growth during loading, which Hill and Labok (1991) say must happen with the compact tension specimen as well. There are fundamental issues that seem to be overlooked, namely the use of linear elastic fracture mechanics not only specifies a Griffith crack but also a perfectly elastic and homogeneous material, yet the concept has been applied successfully to real materials. In a particulate composite structure (whether RBC or GI) the initial crack front will confront more resistant particles as well as the matrix. Restrictions that apply to metallic structures in general may be less severe or even irrelevant when testing brittle organic materials.

The accurate determination of the position of the crack tip following pre-cracking is an acknowledged problem (Lloyd, 1988; Kovarik and Fairhurst, 1993; Nishida et al., 1994). ASTM C1421:2010 recommends the use of an optical microscope to view the 'pop-in' crack as thin sharp cracks are not always discernible on the side surfaces of the specimen. This may involve repeated viewings under the optical microscope before a distinct through-thickness pre-crack is detectable. The standard further prescribes lapping of the side surfaces of the specimen or use of a dye penetrant, or both, to delineate the pre-crack which further highlights the difficulties in determination of the crack tip (ASTM C1421:2010). Therefore, investigators (Ferracane, 1988; Lloyd, 1988; Kovarik and Fairhurst, 1993) are in general agreement that although pre-cracking seems theoretically correct, invariably it will introduce errors when investigating brittle dental restorative materials, thereby negating any benefit produced. It must be noted that ASTM C1421:2010 was written for ceramic materials and the

potential prolonged exposure to the dry laboratory environment during the repeated viewings under the microscope for determination of the pre-crack length is less than ideal for GIs owing to their susceptibility to desiccation (Earl et al., 1989; Wilson, 1989) and resultant cracking (Wang and Darvell, 2009), which is a further limitation to pre-cracking of GIs. In the current investigation, SEN bend specimens were prepared with a sharp notch of 0.3  $\mu\text{m}$  crack tip radius moulded around a scalpel blade (Manuscript 3.3) which has previously been shown to yield valid results that are indicative of the  $K_{IC}$  of the material (Lloyd and Iannetta, 1982; Lloyd, 1982, 1983, 1984; Lloyd and Mitchell, 1984; Lloyd and Adamson, 1985, 1987). In addition, the employment of a new scalpel blade for each specimen manufactured ensured a consistent crack tip radius (0.3  $\mu\text{m}$ ) for all SEN bend specimens reported in Manuscript 3.3 which further validated the  $K_{IC}$  results.

The standards for  $K_{IC}$  testing of metallic (ASTM 399:2009; ISO 12737:2010) and ceramic materials (ASTM C1421:2010) prescribe an accurate measurement of the crack length to obtain a valid result for  $K_{IC}$ . A lack in reporting of the methodology employed to accurately determine the crack length in the SEN bend specimens was identified for the majority of GI SEN  $K_{IC}$  studies (Beatty and Pidaparti, 1993; Pidaparti and Beatty, 1995; Miyazaki et al., 1996; Lucas et al., 2003; Elsaka et al., 2011), where the crack length was assumed to be half of the specimen width (Manuscript 3.3). Although some investigations pertaining to SEN  $K_{IC}$  testing of GIs have reported the use of a travelling microscope (Lloyd and Mitchell, 1984; Lloyd and Adamson, 1987) or an optical microscope (Ilie et al., 2012) for quantification of the measurement of the crack length, images of the crack length were never supplied to confirm the extent of the crack. In the current study, the crack length was determined following fracture of the SEN bend specimen by scanning the fracture surface of each fracture fragment using a contact profilometer, whereby three longitudinal traces were

extracted from each scan, one at mid-thickness and two at quarter-thickness points (ASTM 399:2009; ISO 12737:2010; ASTM C1421:2010) (Figure 2.16). The crack length was measured from two reproducible reference points, namely the end of the scalpel blade impression and the edge of the fracture fragment (Figure 2.16). The profilometric analysis, therefore, ensured an accurate and reproducible measurement of the crack length, resulting from a clear demarcation of the two reference points (Figure 2.16). This level of accuracy, however, might not be guaranteed with the alternative techniques employed in the dental literature which would be subject to inter- and/or intra-operator variability.

To ensure a valid  $K_{IC}$  result, the SEN bend specimen must have sufficient thickness for constraint to maintain plane-strain conditions at the crack tip for most of the crack front (ASTM 399:2009; ISO 12737:2010; ASTM C1421:2010). The specimen dimensions employed in the current investigation have previously been validated for the SEN  $K_{IC}$  testing of RBCs, GIs and dental silicate restoratives (Lloyd and Mitchell 1984). The specimen thickness of 3 mm was in excess of the minimum requirement and the validity supported by the presence of flat fracture surfaces on all GI restorative SEN bend specimens which are characteristic of plane strain conditions at the crack tip (Kovarik et al., 1991).

The production of a notch with adequate sharpness of around 0.3  $\mu\text{m}$ , the accurate quantification of the crack length through profilometry of the fracture surfaces and the use of sufficiently thick specimens to ensure plane-strain conditions at the crack tip yielded valid  $K_{IC}$  values for the encapsulated GI restorative SEN bend specimens investigated (Manuscript 3.3). Good reproducibility of the  $K_{IC}$  data was highlighted by the pooled CoV of 10% (Manuscript 3.3; Table 1) which was in close agreement with the pooled CoVs for the CFS

(10%) (Dowling et al., 2012), TFS (12%) (Dowling et al., 2012), BFS (11%) (Dowling et al., 2012) and HI (7%) (Manuscript 3.2) tests reported for the same encapsulated GI products.

Despite  $K_{IC}$  being an intrinsic material property, the SEN  $K_{IC}$  testing protocol failed to discriminate between the three encapsulated GIs investigated, notwithstanding the compositional and powder content variations amongst the products reported by the manufacturers (Manuscript 3.3; Table 1). The non-discriminatory nature of the  $K_{IC}$  testing protocol failed to offer any obvious advantage over the CFS and HI tests which had identified significant differences in CFS (Dowling et al., 2012) and load-to-failure values (Manuscript 3.2) between the three encapsulated products. While the interaction of many compositional variables such as the glass content, acid (type, molecular weight and concentration) and water content on both critical strain energy release rate ( $G_{IC}$ ) and elastic modulus ( $E$ ) produced the non-discriminatory  $K_{IC}$  values, the loads to failure should not be overlooked. In the current investigation, the SEN  $K_{IC}$  specimens were loaded in a three-point flexure assembly using a 100 N load cell with a tolerance (standard error) of  $\pm 1\%$  (1 N) according to Instron (High Wycombe, England). On examination of the load-to-failure data, the values ranged from 7.8-11.9 N, 7.2-11.1 N and 7.4-11.2 N for Chemfil Rock, Fuji IX<sub>GP</sub> Fast and Ionofil Molar AC, respectively which suggests that the load-to-failure values were too low to be discriminatory. The low load bearing capacity of GI materials compared with alternative posterior filling materials (RBCs and dental amalgam) was considered to be responsible for the non-discriminatory  $K_{IC}$  data produced by the SEN  $K_{IC}$  testing methodology. Therefore, the non-discriminatory nature of the SEN  $K_{IC}$  testing methodology precluded the  $K_{IC}$  test from being advocated for testing GIs during GI development.

Despite differing sensitivities to compositional change, any mechanical testing protocol must distinguish between GIs manipulated with varying powder content. The discriminatory ability of a testing methodology for powder content variations becomes especially important in GI development, where the optimum powder content has to be identified by hand-mixing the GI liquid with varying GI powder contents by performing preliminary mechanical tests. As the resistance to compressive, tensile and shear forces under loading during mastication is provided by the reinforcing glass filler component rather than the weaker polyacrylate matrix (Xie et al., 2000), a deterioration in the mechanical properties would be expected on reducing the powder content from the optimum value specified by the manufacturer. The mechanical testing protocol of choice when investigating novel GI restoratives would therefore be required to be discriminatory between GIs manipulated with varying powder content by identifying a linear deterioration in the property being measured when the powder content is reduced from the optimum value. The linear deterioration in mechanical properties of GIs prepared with reduced powder content could not be illustrated by relying on using encapsulated GIs which was a significant oversight in the Fleming et al. (2012) and Dowling et al. (2012) studies.

#### **4.4 A DISCRIMINATORY MECHANICAL TESTING METHODOLOGY FOR GI DEVELOPMENT**

Since the initial GI developmental process would have to involve hand-mixing, the mixing and testing conditions reported by researchers investigating the reinforcement strategies for GIs were extensively reviewed which revealed a wide variation in the mixing and testing conditions employed (Manuscript 3.1). The large variation in mixing and testing conditions utilised when investigating GI reinforcement strategies makes any attempt at GI

reinforcement reported in the dental literature impossible to decipher (Manuscript 3.1). For novel GI development, the mechanical testing protocol of choice must be discriminatory to inform the researcher whether the reinforcement strategy has actually worked or not. Therefore, in the context of the overall investigation, the CFS, TFS, BFS, HI (Manuscript 3.4) and  $K_{IC}$  (Manuscript 3.3) testing methodologies for GI restoratives were revisited using a hand-mixed GI restorative prepared with varying powder contents. It was proposed that the discriminatory potential of each testing methodology would be highlighted on testing hand-mixed GI groups prepared by identifying a progressive reduction in reinforcing glass filler content. Consequently, the mechanical testing protocol of choice should identify a linear deterioration in the property being measured when the powder content is reduced from the optimum value.

#### **4.4.1 COMPRESSIVE FRACTURE STRENGTH TEST**

The CFS testing protocol has been criticised regarding the reliability (McCabe et al., 1990) and validity (Darvell, 1990), although reliable CFS test results can be obtained through a statistical approach employing a minimum of 20 specimens under controlled mixing and testing conditions (Fleming et al., 2012). In the current investigation, the CFS test was identified as the only 'truly' discriminatory test from amongst the five mechanical testing protocols investigated as a linear deterioration ( $p < 0.001$ ) in CFS ( $R^2 = 0.957$ ) was evident for the nine hand-mixed GI restorative groups prepared with reduced powder contents for a constant weight of liquid (Manuscript 3.4; Figure 1). This finding was in agreement with the reports in the dental literature where a linear deterioration in CFS with  $R^2 = 0.9987$  for  $n = 4$  (Fleming et al., 2003),  $R^2 = 0.961-0.983$  for  $n = 6$  (Dowling and Fleming, 2008) and  $R^2 = 0.96-0.99$  for  $n = 6$  (Dowling and Fleming, 2009) was identified on reducing the GI powder content



from that recommended by the manufacturer for a constant weight (Dowling and Fleming, 2008, 2009) or volume of liquid (Fleming et al., 2003).

While a linear deterioration in the CFS ( $R^2=0.9987$ ) was observed for an anterior hand-mixed GI restorative (Chemfil Superior) on reducing the powder content from that specified by the manufacturer (100%) to 90, 80 and 50% ( $n=4$ ) for a constant volume of liquid (Fleming et al., 2003), the finding contrasted with another study where a non-linear deterioration in CFS ( $R^2=0.94$ ) was reported for the same GI restorative (Dowling and Fleming, 2009). Although both studies used adequate sample sizes of  $n=20$  (Fleming et al., 2003) and  $n=30$  (Dowling and Fleming, 2009), the latter assessed additional data points for powder contents of 70 and 60% to increase the number of groups investigated to  $n=6$  (Dowling and Fleming, 2009). This observation highlighted the importance of the number of data points for the determination of a linear deterioration in the mechanical property being investigated. The ability of the CFS testing methodology to distinguish between the GI restorative groups prepared with progressively reduced powder content was further highlighted in the current investigation as a result of the additional data points assessed for powder contents of 40, 30 and 20% ( $n=9$ ) (Manuscript 3.4; Figure 1).

Incorporation of air bubbles during mixing (Fleming et al., 2001, 2002) or placement of the GI into the mould during specimen manufacture (Fleming et al., 2001, 2002) dictates the porosity levels in CFS specimens. An increased powder content for a constant weight of liquid requires increased spatulation force to form a homogenous mix which will result in air entrapment (Fleming et al., 2001, 2002). The increase in the Weibull moduli and concomitant decrease in CoV as the powder content was reduced to 70, 60 and 50% of that specified by the manufacturer suggests easier mixing and better consolidation of the CFS specimens into

the PTFE split-mould when compared with the CFS specimens prepared with 100, 90 and 80% of the manufacturer's recommended powder content (Manuscript 3.4; Tables 1 and 2). The reduced Weibull moduli for the groups prepared with powder contents which were further reduced to 40, 30 and 20% were indicative of pore inclusion on filling the mould as the GI mix became too fluidic and trapped air while flowing into the mould (Fleming et al., 2001, 2002) (Manuscript 3.4; Table 1). These findings in Manuscript 3.4 were supported by the stereological findings based on a range of powder:liquid mixing ratios for different acid-base cements (Fleming et al., 2001, 2002, 2003, 2006). Therefore, despite the criticism regarding the reliability (McCabe et al., 1990) and validity (Darvell, 1990) of the CFS testing protocol, the CFS test was identified as the only 'truly' discriminatory performance indicator for the hand-mixed GI restorative from amongst the five testing methodologies investigated (Manuscripts 3.3 and 3.4). The mechanical testing protocol of choice specified in the current ISO standard for powder/liquid acid-base cements and restoratives (ISO 9917-1:2007) was therefore highlighted as appropriate for GI development.

The CM would be expected to discriminate between the different powder content groups as the CM is an intrinsic material property independent of specimen dimensions. This was highlighted in the current investigation by a linear deterioration in the CM ( $R^2=0.9619$ ) when the hand-mixed GI restorative was manipulated with reduced powder content which suggested that the CM could act as a discriminatory performance indicator for hand-mixed GIs (Manuscript 3.4; Figure 2). The finding was also consistent with reports in the literature where a linear deterioration was identified in CM with  $R^2=0.951-0.974$  for  $n=6$  (Dowling and Fleming, 2008) and  $R^2=0.95-0.99$  for  $n=6$  (Dowling and Fleming, 2009) on reducing the GI powder content from that recommended by the manufacturer for a constant weight of liquid. In the dental literature, the CM was identified to be more sensitive to highlighting the impact

of powder content variations when compared with the CFS for hand-mixed GI restoratives (Dowling and Fleming, 2008). This observation was confirmed on examination of the  $R^2$ -values for the CFS ( $R^2=0.957$ ) and CM ( $R^2=0.9619$ ) data of the GI groups investigated in the current study (Manuscript 3.4; Figures 1 and 2) which suggested that the employment of an intrinsic material property (CM) in combination with a non-intrinsic material property (CFS) was advantageous when investigating hand-mixed GI restoratives (Manuscript 3.4). As the CM is determined by calculating the slope of the initial linear section of the stress-strain plot of each specimen tested in compression, the CM information is essentially contained within the CFS test data. Therefore, it was proposed that researchers should be encouraged to quote both values in future studies (Manuscript 3.4). In short, a further advantage of the CFS test was that the CM values could be obtained from the stress-strain plot of cylindrical CFS specimens loaded under compression as an intrinsic material property which may be employed as a reliable and discriminatory adjunct to the CFS test results when investigating the performance of novel GIs (Manuscript 3.4).

#### **4.4.2 THREE-POINT FLEXURE TEST**

Bar-shaped TFS specimens have a reproducible failure mode, namely from the surface under tension and have been identified as a valid and reliable alternative to the CFS test (Dowling et al., 2012). However, the TFS test results for different encapsulated GI products with varying powder content were non-discriminatory (Dowling et al., 2012). When employed for hand-mixed GIs prepared with varying powder content, the TFS test failed to discriminate between the hand-mixed GI restorative groups evident by the non-linear deterioration in TFS ( $R^2=0.572$ ) where  $p=0.982$  for progressively reduced powder contents from 100-60% (Manuscript 3.4; Figure 3). The fracture mode of TFS specimens is surface defect driven,

such that the TFS of brittle materials like GIs is sensitive to surface imperfections (Ban and Anusavice, 1990) which may either be inherent to the GI or be introduced during manipulation of the GI and filling the mould (Fleming et al., 2001, 2002). To prevent the hand-mixed GI restorative from adhering to the glass slab, the GI specimens were condensed against an acetate strip such that a consistent surface roughness was achieved regardless of the powder:liquid mixing ratio produced (Manuscript 3.4). Therefore, all GI powder:liquid mixing ratio groups would be expected to have a similar surface defect population irrespective of the powder content. Although the surface roughness ( $R_a$ -value) was not reported in Manuscript 3.4, it was identified to be  $0.10 \pm 0.01 \mu\text{m}$  using contact profilometry for specimens from all the powder:liquid mixing ratio groups investigated which was indicative of a uniform surface finishing condition. Therefore, the TFS test could not be advocated as a performance indicator when investigating novel GIs. The current observation of a uniform surface finish controlling the TFS is backed up by the dental literature. TFS testing of hand-mixed GIs failed to identify significant differences in the mean TFS values for GIs mixed at the recommended powder:liquid mixing ratio and when 50% (Bonifacio et al., 2013) or 80% (Torabzadeh et al., 2011) of the recommended powder content was employed. Additionally, no significant difference in TFS values was identified between a posterior (Fuji IX) and anterior (Fuji II) hand-mixed GI restorative from the same manufacturer (GC Corporation) despite the reported powder:liquid mixing ratio of the posterior GI restorative (3.5:1 g:g) investigated being higher than the powder:liquid mixing ratio of its anterior counterpart (2.7:1 g:g) (Higgs et al., 2001b).

The difficulty in manipulation and consolidation of the hand-mixed GI restorative along the length of the open-ended knife-edged PTFE mould when mixed at the manufacturer's recommended powder:liquid mixing ratio was evident by the lower Weibull modulus and

concomitant increase in CoV of the hand-mixed GI control group (Manuscript 3.4; Tables 1 and 2). A narrowing in the data scatter was identified for the Weibull moduli of the TFS data as the powder content was reduced down to 30% of the optimum value specified by the manufacturer which was indicative of easier mixing and better consolidation of the GI into the PTFE mould on reducing the powder content (Manuscript 3.4; Table 1). The decrease in Weibull modulus as the powder content was further reduced to 20% of that specified by the manufacturer suggested that the mix had become so fluidic that air may have become incorporated during filling the mould (Fleming et al., 2001, 2002) (Manuscript 3.4; Table 1).

The TFM is an intrinsic material property independent of specimen dimensions and is therefore capable of reproducing the internal structure of the material and any association with the neighbouring atoms (Braem, 1999). Therefore, like the CM, the TFM would be expected to act as a discriminatory performance indicator. This was confirmed in the current investigation, where the TFM was identified as a sensitive performance indicator which was able to discriminate between hand-mixed GI groups prepared with reduced powder content (in 10% increments) from that advocated by the manufacturer for a constant weight of liquid, evident by the progressive ( $p < 0.001$ ) linear deterioration in TFM ( $R^2 = 0.982$ ) (Manuscript 3.4; Figure 4). Previously, a statistically significant decrease in the TFM values for a posterior hand-mixed GI restorative (Fuji IX) was identified when the powder content was reduced to 50% of that specified by the manufacturer for a constant volume of liquid (Bonifacio et al., 2013). Owing to the additional data points ( $n=9$ ) investigated in the current study, a linear deterioration in the mean TFM data was identified for the hand-mixed GI restorative manipulated at reduced powder:liquid mixing ratios routinely produced by operators in clinical settings (Manuscript 3.4; Figure 4). Therefore, the TFM was identified as a reliable adjunct to a mechanical testing protocol when investigating the performance of hand-mixed

GI restoratives (Manuscript 3.4). It was proposed that the TFM should be determined and reported when testing bar-shaped specimens for TFS as the TFM information is contained within the load-to-failure and specimen deflection data for the bar-shaped specimens loaded in a three-point flexure test assembly (Manuscript 3.2).

#### **4.4.3 BIAXIAL FLEXURE STRENGTH TEST**

Disc-shaped BFS specimens are known to fracture from a reproducible failure mode from the surface under tension (Ban and Anusavice, 1990). However, the non-discriminatory behaviour of the BFS test results for three encapsulated GIs from different manufacturers (Dowling et al., 2012) was confounding which prompted the investigation of the discriminatory ability of the BFS test for powder content variations in hand-mixed GIs (Manuscript 3.4). The non-discriminatory nature of the BFS test for hand-mixed GIs was evident by the non-linear deterioration in BFS ( $R^2=0.81$ ) for the hand-mixed GI restorative groups ( $n=9$ ) prepared with reduced powder content (in 10% increments) from that proposed by the manufacturer for a constant weight of liquid (Manuscript 3.4; Figure 5). The BFS of brittle dental materials is dependent on  $R_a$ -value of the surface placed under tension and is therefore a surface defect driven phenomenon (Addison et al., 2007; Hooi et al., 2013). In the current investigation BFS specimens were prepared by condensing the hand-mixed GI restorative into a ring-mould resting on an acetate covered glass slab and covering with a second acetate strip to prevent the hand-mixed GI restorative from adhering to the glass slab (Manuscript 3.4). Therefore, all BFS specimen groups prepared with the hand-mixed GI restorative had a uniform surface finishing condition with an  $R_a$ -value of around  $0.10 \pm 0.01$   $\mu\text{m}$  irrespective of the powder content (Manuscript 3.4). Owing to the uniform surface finishing condition of the BFS specimens prepared with the hand-mixed GI restorative at

reduced powder content (in 10% increments) from that recommended by the manufacturer for a constant weight of liquid, the BFS test remained insensitive to powder content from 100-60% ( $p=0.054$ ) and therefore could not be advocated as a performance indicator for GI development (Manuscript 3.4; Figure 5). Previously, the BFS values of a posterior (Fuji IX;  $50.61 \pm 5.45$  MPa) and anterior (Fuji II;  $53.33 \pm 6.6$  MPa) hand-mixed GI restorative from the same manufacturer (GC Corporation) were reported to be statistically similar (Higgs et al., 2001b). The non-significant BFS data reported for the Fuji IX and Fuji II hand-mixed GI restoratives was unexpected as the powder:liquid mixing ratios reported by the manufacturer were 3.5:1 g:g and 2.7:1 g:g, respectively. Although confidence in the statistical analysis reported for the BFS values of Fuji IX ( $n=8$ ) and Fuji II ( $n=10$ ) hand-mixed GI restoratives could not be confirmed due to the small sample size ( $n<20$ ) investigated (Higgs et al., 2001b), the BFS test results highlighted the non-discriminatory nature of the BFS testing methodology.

Additionally, the Weibull modulus and CoV of the BFS data were consistent for the hand-mixed GI groups prepared with 100-40% of the manufacturer's recommended powder content which was indicative of the simple specimen preparation for BFS specimens (Manuscript 3.4; Tables 1 and 2). The decrease in Weibull modulus and concomitant increase in CoV as the powder content was further reduced to 30 and 20% of that specified by the manufacturer for a constant weight of liquid suggested that the mix had become too fluidic such that air inclusion may have occurred during filling the mould (Fleming et al., 2001, 2002) (Manuscript 3.4; Tables 1 and 2).

Examination of the compressive extension data identified a consistent compressive extension for the disc-shaped BFS specimens for all powder:liquid mixing ratio groups (Manuscript

3.4; Figure 6). Although the hand-mixed GI restorative became more ductile on reducing the powder content for a constant weight of liquid (Manuscript 3.4; Figure 4), this was not evident by the compressive extension data for the BFS specimens as all specimens fractured at similar loads to failure (30-40 N). The influence of the load-to-failure values on the compressive extension was evident for disc-shaped HI specimens (Manuscript 3.4; Figure 8) where the resultant increase in ductility of the hand-mixed GI restorative on reducing the powder content resulted in a transformation of the point contact between the indenter and the specimen into a larger area of contact such that the specimens were able to withstand increased loads to failure (Manuscript 3.4; Figure 7). For HI specimens the compressive extension was indicative of the displacement due to compressive strain at the contact zone owing to the increased load-to-failure values (800-1000N), however, for the BFS specimens the compressive extension was indicative of the deflection of the specimen. Therefore, the consistent compressive extension data for the BFS specimens prepared with reduced powder contents (Manuscript 3.4; Figure 6) was indicative of the non-discriminatory BFS test results (Manuscript 3.4; Figure 5).

In short, despite the apparent advantages of the BFS testing protocol, in terms of reduced sensitivity to specimen edge defects (Ban and Anusavice, 1990) and simple specimen preparation (Dowling et al., 2012), the BFS test failed to act as a discriminatory performance indicator for the hand-mixed GI groups investigated and therefore could not be advocated as a mechanical testing methodology of choice for GI development.



#### 4.4.4 HERTZIAN INDENTATION TEST

In terms of simulating the clinical scenario *in vivo*, loading disc-shaped specimens using a 20 mm hard steel ball to simulate cusp contact (Kelly, 1999) when resting freely on a dentine analogue intuitively is more clinically relevant (Wang and Darvell, 2007) when compared with the CFS, TFS and BFS tests. The current investigation revealed the non-discriminatory nature of the Hertzian indentation test for hand-mixed GIs by identifying a non-linear deterioration in the Hertzian load-bearing capacity ( $R^2=0.2345$ ) for the hand-mixed GI restorative groups manipulated with reduced powder content (in 10% increments) from that specified by the manufacturer for a constant weight of liquid (Manuscript 3.4; Figure 7). The hand-mixed GI specimens prepared at the powder:liquid mixing ratio identified by the manufacturer were tested while resting freely on top of a 30% glass fiber reinforced polyamide dentine analogue substrate material (Wang and Darvell, 2007). The elastic modulus mismatch between the GI specimen and the dentine analogue substrate material resulted in the generation of a tensile stress at the specimen/dentine analogue interface on loading, leading to radial crack formation at the bottom surface of the specimen (Wang and Darvell, 2007, 2012). The tensile initiated radial crack propagated upward through the thickness of the specimen, dissecting the specimen into two to four fracture fragments with smooth fracture surfaces (Manuscript 3.4; Figure 9a). This finding was consistent with the results reported by Wang and Darvell (2007) who identified radial cracking as the dominant failure mode for a hand-mixed GI restorative (Amalgomer CR) of similar thickness (0.4-3.6 mm) to that investigated in Manuscript 3.4 ( $3.10 \pm 0.03$  mm).

Although bottom initiated radial cracking from the surface under tension was observed for the GI control group (Manuscript 3.4; Figure 9a), this was not the case for the GI specimen

groups manipulated at reduced powder contents (Manuscript 3.4; Figure 9b). A progressive reduction in the powder content resulted in an increase in the ductility of the hand-mixed GI restorative which was attributed to the deterioration in the TFM as the powder content was reduced from that recommended by the manufacturer (Manuscript 3.4; Figure 4). The decrease in TFM was manifest as a resultant progressive increase in the indenter penetration for the GI specimens tested under HI such that the initial point contact between the ball indenter and the specimen was transformed to a larger area of contact evident by the progressive increase in the compressive extension (Manuscript 3.4; Figure 8). Fractographic analysis demonstrated a transition in failure mode from brittle failure (Manuscript 3.4; Figure 9a) to ductile failure (Manuscript 3.4; Figure 9b) when the powder content was progressively reduced for a constant weight of liquid where top-initiated cone cracking began to appear (Manuscript 3.4; Figure 9b) and bottom-initiated radial cracking was no longer the dominant failure mode (Manuscript 3.4; Figure 9a). Therefore, the GI specimens prepared at reduced powder content deformed prior to fracture such that the increase in the Hertzian load-bearing capacity on reducing the powder content was misleading when interpreting the load-to-failure data (Manuscript 3.4; Figure 7).

The ability of the HI testing methodology to distinguish between the encapsulated GI restoratives studied in Manuscript 3.2 was a result of the reproducible failure mode of bottom initiated radial cracking from the surface under tension for GIs mixed at the manufacturer's recommended powder:liquid ratio which was also highlighted for the hand-mixed GI control group in Manuscript 3.4 (Manuscript 3.4; Figure 9a). However, the HI test failed to offer any advantage when employed to investigate GIs prepared with powder contents reduced from that specified by the manufacturer owing to indenter penetration and transition in failure mode (Manuscript 3.4; Figure 9a,b). Therefore, despite the HI test being the most clinically

relevant testing methodology for GIs, the non-discriminatory nature of the HI test precluded the test from being a performance indicator and HI testing could not be advocated during GI development (Manuscript 3.4).

#### 4.4.5 FRACTURE TOUGHNESS TEST

The SEN  $K_{IC}$  test was expected to demonstrate a linear deterioration in  $K_{IC}$  on progressively reducing the powder content as  $K_{IC}$  is an intrinsic material property. As no difference in the  $K_{IC}$  was identified between the three encapsulated GIs investigated in Manuscript 3.3, despite the marked compositional and powder content variations, the SEN  $K_{IC}$  testing methodology was extended to hand-mixed GIs prepared with progressively reduced powder content to further highlight the discriminatory potential of the testing methodology (Manuscript 3.3). When employed to the hand-mixed GI powder:liquid mixing ratio groups, the SEN  $K_{IC}$  testing methodology failed to discriminate between the GI groups ( $n=9$ ) evident by the non-linear deterioration in  $K_{IC}$  ( $R^2=0.576$ ) which further highlighted the non-discriminatory behaviour of the SEN  $K_{IC}$  testing methodology (Manuscript 3.3; Figure 5). In the current investigation, the SEN  $K_{IC}$  specimens from all hand-mixed GI groups were loaded using a 100 N load cell with a tolerance (standard error) of  $\pm 1\%$  (1 N) in a three-point flexure assembly (Instron). The low load-to-failure values observed for the encapsulated GI products investigated in Manuscript 3.3 were also identified for the hand-mixed GI groups prepared with progressively reduced powder contents (Manuscript 3.3). Examination of the load-to-failure data of the SEN bend specimens from the 50 and 100% powder content groups highlighted mean load-to-failure values of  $8.9 \pm 1.2$  N and  $10.1 \pm 1.1$  N and associated mean  $K_{IC}$  values of  $0.469 \pm 0.048$   $MNm^{-1.5}$  and  $0.468 \pm 0.051$   $MNm^{-1.5}$ , respectively, thereby suggesting that the low loads to failure were responsible for the non-discriminatory  $K_{IC}$  test

results produced (Manuscript 3.3; Table 2). The SEN  $K_{IC}$  testing methodology therefore failed to act as a discriminatory performance indicator for the hand-mixed GI groups investigated, despite  $K_{IC}$  being an intrinsic material property and could not be advocated for testing novel GIs during GI development.

The relationship between  $K_{IC}$  and hand-mixed GIs prepared with powder contents reduced from that specified by the manufacturer has not been demonstrated conclusively in the dental literature. A progressive deterioration ( $R^2=0.9807$ ) in  $K_{IC}$  values was reported for a hand-mixed anterior GI restorative (Fuji II; GC Corporation) on reducing the powder content from that recommended by the manufacturer ( $0.37 \text{ MNm}^{-1.5}$ ) to 74% ( $0.29 \text{ MNm}^{-1.5}$ ) and 37% ( $0.19 \text{ MNm}^{-1.5}$ ) (Mitsuhashi et al., 2003). However, the  $K_{IC}$  data was reported for notched ring-shaped specimens (4 mm inner radius, 8 mm outer radius, 3 mm thickness with a 1 mm radial notch) which were pre-cracked prior to testing, although no scanning electron micrographs of the pre-cracked specimens were supplied to verify the extent of the pre-crack. Pre-cracking of  $K_{IC}$  specimens of brittle dental restorative materials can introduce errors in the determination of  $K_{IC}$  through uncertainty in the pre-crack length (Ferracane, 1988; Lloyd, 1988; Nishida et al., 1994). This uncertainty in the pre-crack length measurements was evident by the wide range in the pre-crack length reported which extended from 0.96 mm to 2.32 mm for the GI specimens prepared with reduced powder content (Mitsuhashi et al., 2003). The standard deviations for the  $K_{IC}$  values and the number of specimens tested were not supplied to confirm the power of the study. In addition, the low number of data points investigated ( $n=3$ ) further complicated interpretation of the results.

The SEN  $K_{IC}$  of a hand-mixed posterior (Fuji IX) and anterior GI restorative (Fuji II) from the same manufacturer (GC Corporation) was investigated by Lucas et al. (2003) and

Miyazaki et al. (1996), respectively. Both studies employed similar specimen geometries (SEN bend) and dimensions (25.0 mm length x 5.0 mm width x 2.5 mm thickness with a notch depth of 2.5 mm) loaded to failure at the same cross-head displacement rate (0.5 mm/min) following storage in the same storage media (distilled water at 37°C) for the same time (24 h). Interestingly, the mean  $K_{IC}$  value reported for Fuji II ( $0.49 \pm 0.04 \text{ MNm}^{-1.5}$ ) (Miyazaki et al., 1996) was not significantly different from the mean  $K_{IC}$  value reported for Fuji IX ( $0.45 \pm 0.06 \text{ MNm}^{-1.5}$ ) (Lucas et al., 2003), despite the lower powder:liquid mixing ratio reported by the manufacturer for the anterior product (Fuji II; 2.7:1 g:g) compared with its posterior counterpart (Fuji IX; 3.6:1 g:g). Statistical confidence in the  $K_{IC}$  data could not be confirmed owing to the small sample sizes of  $n=6$  (Miyazaki et al., 1996) and  $n=12$  (Lucas et al., 2003) employed in both studies, however, the  $K_{IC}$  data did provide an indication of the non-discriminatory nature of the  $K_{IC}$  testing methodology when employed for GIs products with varying recommended powder:liquid mixing ratios.

The mechanical testing methodologies investigated in the current study, namely the CFS, TFS, BFS, HI and  $K_{IC}$  tests revealed the CFS test to be the only 'truly' discriminatory performance indicator which remains the only test that can be advocated for use during development of a novel reinforced GI. In short, it is imperative that the mixing and testing conditions are standardised (Manuscript 3.1) and a discriminatory testing methodology is chosen (Manuscripts 3.2-3.4) for the assessment of the reinforcement strategy as the employment of a non-discriminatory testing methodology when investigating a reinforced GI would only misguide the direction of research into that reinforcement strategy (Manuscript 3.1).

## 5. CONCLUSIONS

The CFS test is the only strength test specified for GIs in ISO 9917-1:2007 and a high CFS has been proposed as necessary to tolerate the functional forces routinely encountered in the posterior region of the mouth since loading during masticatory function results in stressing patterns analogous to those observed during CFS testing. Any mechanical testing protocol employed to investigate novel reinforced GIs must be discriminatory for powder content variations since identification of the optimum powder:liquid ratio is one of the fundamental steps in GI development. In the current investigation:

- A wide variation in mixing and testing conditions was identified in the dental literature pertaining to GI reinforcement which prevented a valid assessment of the reported reinforcement strategies. When investigating a GI reinforcement strategy it is imperative that the mixing and testing conditions are standardised to allow for a valid comparison between studies. As a result, the identification of a discriminatory testing methodology was identified as essential when investigating novel reinforced GIs. It was highlighted that major improvements through a reinforcement strategy have yet to be made to enable clinical usage of GIs for the restoration of posterior dentition.
- Despite the criticism regarding the reliability and validity of the CFS testing methodology, the CFS test was identified as the only 'truly' discriminatory test from amongst the five mechanical testing protocols investigated namely the CFS, TFS, BFS, HI and  $K_{IC}$  tests as a linear deterioration in CFS was highlighted on progressively reducing the powder content from that recommended by the manufacturer for a constant weight of liquid.

- In TFS and BFS testing, failure occurs in a state of pure tension under loading which is the mechanism by which brittle materials fail *in vivo*. However, BFS testing is advantageous over uniaxial TFS testing as the specimens are easier to prepare, clinically match the volume of a large posterior restoration with a reduced sensitivity to edge defects. In the current study, the preparation technique employed for TFS and BFS specimens produced a uniform surface finishing condition for all specimens groups irrespective of the powder content which precluded the tests from being ‘truly’ discriminatory.
- The CM and TFM are intrinsic material properties and may be used as reliable adjuncts to a mechanical testing protocol when investigating novel hand-mixed GIs since both were identified as discriminatory performance indicators.
- The HI test was identified as the most clinically relevant as the test simulates the loading conditions experienced by dental restorations under occlusal loading where opposing tooth contacts are simulated. However, reducing the powder content associated increased ductility and a concomitant reduction in brittleness which nullified the discriminatory nature of the test owing to indenter penetration.
- For the SEN  $K_{IC}$  testing methodology, the non-discriminatory nature of the testing methodology was highlighted for both encapsulated GI products and the hand-mixed GI groups prepared with powder contents reduced from that recommended by the manufacturer, where the  $K_{IC}$  was insensitive to a change which in practice would adversely affect clinical performance. Despite  $K_{IC}$  being an intrinsic material property, the SEN  $K_{IC}$  testing methodology failed to act as a discriminatory

performance indicator owing to the low load-to-failure values recorded for the encapsulated and hand-mixed GIs investigated.

- In light of the results from the current investigation, a reassessment of the testing methodologies employed by investigators reporting different GI reinforcement strategies highlighted the employment of non-discriminatory testing methodologies, namely the TFS, BFS, HI and  $K_{IC}$  tests would be misguided. For studies reporting the use of a discriminatory testing methodology, namely the CFS test, poor control as well as lack in reporting of testing and mixing conditions employed were identified in the review (Manuscript 3.1).
- The ISO 9917-1:2007 needs to be more specific to eliminate problems with testing protocols between laboratories. As a result, the standard (ISO 9917-1:2007) should specify a set loading rate of 1 mm/min rather than the loading rate range ( $0.75 \pm 0.30$  mm/min) provided for in ISO 9917-1:2007 to enable comparison of nominally identical specimens tested in different faculties across the world. In addition, the standard (ISO 9917-1:2007) should advocate a statistical approach employing a minimum of 20 specimens for a meaningful interpretation of the CFS data sets that would avoid misidentification of operative variability by the pass/fail criteria currently specified in ISO 9917-1:2007.



## 6. RECOMMENDATIONS FOR FURTHER WORK

The current investigation has demonstrated that the CFS test is the only 'truly' discriminatory performance indicator for GIs (Manuscript 3.4), while the TFS (Manuscript 3.4), BFS (Manuscript 3.4), HI (Manuscripts 3.4) and  $K_{IC}$  (Manuscript 3.3) testing methodologies were identified to be non-discriminatory and therefore could not be advocated for investigating novel GIs. In addition, the CM and TFM were identified as discriminatory and reliable adjuncts to a mechanical testing protocol when investigating GI performance (Manuscript 3.4). In light of the findings from the current investigation, it is suggested that the GI reinforcement strategies highlighted in Manuscript 3.1 are revisited owing to the non-standardised mixing and testing conditions employed in every single study that was reviewed. The poor control in mixing and testing conditions employed limits any progress in GI development by preventing a valid comparison between studies such that all reinforcement strategies must be revisited under standardised mixing and testing conditions using the discriminatory CFS testing methodology. To supplement the CFS data, the discriminatory CM data should also be reported to highlight significant differences between groups.

From amongst the claimed improvements in mechanical properties of modified experimental GIs, the most noticeable findings were reported in a study by Elsaka et al. (2011) where the addition of 3 wt%  $TiO_2$  nano-powder to a conventional GI powder was identified to significantly increase the CFS, TFS and SEN  $K_{IC}$  of GIs prepared with the modified powder which suggests potential for GI reinforcement. Interestingly, the  $TiO_2$  reinforcement strategy was not pursued by the authors or other researchers despite the remarkable CFS, TFS and  $K_{IC}$  data reported for the modified GIs (Elsaka et al., 2011). When the same  $TiO_2$  nano-powder was added in 0.5 to 15 wt% to a conventional GI powder to prepare cylindrical CFS

specimens of the same dimensions (6 mm height, 4 mm diameter) that were tested under standardised ISO 9917-1:2007 conditions in the current Materials Science Unit, no improvement in CFS or CM could be identified which casts doubt on the data reported previously (Elsaka et al., 2011). The study reported by Elsaka et al. (2011) serves as an example for misquoted data which suggests that other studies highlighted in Manuscript 3.1 cannot be regarded as the ultimate source to the reported reinforcement. The reinforcement strategies in individual studies should therefore be revisited and a fresh start made under standardised mixing and testing conditions to enable verification of the claimed reinforcement and allow for a valid comparison between studies which is the only way forward to the development of a novel reinforced GI that could be 'truly' advocated for the restoration of posterior dentition.

Investigations in the dental literature reporting the influence of filler content variations in other posterior dental restorative materials like resin-based composites (RBCs) and dental ceramics should also be performed under standardised mixing and testing conditions to enable a valid comparison between studies. The majority of studies in the dental literature reporting the influence of filler content on the mechanical properties of RBCs have employed commercial products, notwithstanding the marked variation in filler particle size, filler composition, filler density and resin composition between different products which fails to enable a valid assessment for filler content variations. Therefore, future studies investigating the influence of filler content variations on the mechanical properties of RBCs should employ RBCs with the same filler particle size, filler composition, filler density and resin composition to enable a valid assessment of the reinforcing filler content.

## 7. REFERENCES

Addison O, Marquis PM, Fleming GJP. Resin elasticity and the strengthening of all-ceramic restorations. *Journal of Dental Research* 2007; **86**: 519 - 23.

Akinmade AO, Braybrook HJ. Dental Cement. *US Patent* 1995; 5,411,584.

Akinmade AO, Nicholson JW. Poisson's ratio for glass polyalkenoate ('glass-ionomer') cements determined by an ultrasonic method. *Journal of Materials Science: Materials in Medicine* 1995; **6**: 483 - 5.

American Society for Testing and Materials (ASTM) International E399:2009. Standard test method for linear-elastic plane-strain fracture toughness  $K_{IC}$  of metallic materials.

American Society for Testing and Materials (ASTM) International C1421:2010. Standard test method for determination of fracture toughness of advanced ceramics at ambient temperature.

Anstice HM, Nicholson JW. Investigation of the post-hardening reaction in glass-ionomer cements based on polyvinylphosphonic acid. *Journal of Materials Science: Materials in Medicine* 1995; **6**: 420 - 5.

Anusavice KJ, Lee RB. Effect of firing temperature and water exposure on crack propagation in unglazed porcelain. *Journal of Dental Research* 1989; **68**: 1075 - 81.

Asmussen E, Peutzfeldt A. Influence of UEDMA, BisGMA and TEGDMA on selected mechanical properties of experimental resin composites. *Dental Materials* 1998; **14**: 51 - 6.

Atkins AG, Mai YW. The mechanics of elastic fracture. In: Atkins AG and Mai YW, editors. *Elastic and plastic fracture*. Ellis Horwood Ltd., Chichester; 1985, p. 75 - 167.

Ban S, Anusavice KJ. Influence of test method on failure stress of brittle materials. *Journal of Dental Research* 1990; **69**: 1791 - 9.

Beatty MW, Pidaparti RMV. Elastic and fracture properties of dental direct filling materials. *Biomaterials* 1993; **14**: 999 - 1002.

Berenbaum R, Brodie I. Measurement of tensile strength of brittle materials. *British Journal of Applied Physics* 1959; **10**: 281 - 7.

Bhamra G, Palin WM, Fleming GJP. The effect of surface roughness on the flexure strength of an alumina reinforced all-ceramic crown material. *Journal of Dentistry* 2002; **30**: 153 - 60.

Billington RW, Williams JA, Pearson GJ. Variation in powder/liquid ratio of a restorative glass-ionomer cement used in dental practice. *British Dental Journal* 1990; **169**: 164 - 7.

Bonifacio CC, de Jager N, Kleverlaan CJ. Mechanical behaviour of a bi-layer glass-ionomer. *Dental Materials* 2013; **29**: 1020 - 5.

Braem MJA. Physical properties of glass-ionomer cements: Fatigue and elasticity. In: Davidson CL and Mjoer IA, editors. *Advances in glass-ionomer cements*. Quintessence Publishing, Berlin, Germany; 1999, p. 67 - 84.

British Standards BS 5199:1975. Specification for resin-based dental filling materials.

Browning WD, Brackett WW, Gilpatrick RO. Two-year clinical comparison of a microfilled and a hybrid resin-based composite in non-carious class V lesions. *Operative Dentistry* 2000; **25**: 46 - 50.

Brune D, Smith D. Microstructure and strength properties of silicate and glass-ionomer cements. *Acta Odontologica Scandinavica* 1982; **40**: 389 - 96.

Bucknall CB. In: Haward RN, editor. *The physics of glassy polymers*. Applied Science Publishers, London; 1973, p. 363 - 412.

Burke FJT, Siddons C, Phipps S, Bardha J, Crisp RJ and Dopheide B. Clinical performance of reinforced glass-ionomer restorations placed in UK dental practices. *British Dental Journal* 2007; **203**: E2.

Causton BE. The physico-mechanical consequences of exposing glass-ionomer cements to water during setting. *Biomaterials* 1981; **2**: 112 - 5.

Chai H, Lawn B. Fracture modes in brittle coatings with large interlayer modulus mismatch. *Journal of Materials Research* 1999; **14**: 3805 - 17.

Christensen GJ. Curing restorative resin - a significant controversy. *Journal of the American Dental Association* 2000; **131**: 1067 - 9.

Crisp S, Lewis BG, Wilson AD. Gelation of polyacrylic acid aqueous solutions and the measurement of viscosity. *Journal of Dental Research* 1975a; **54**: 1173 - 5.

Crisp S, Ferner AJ, Lewis BG, Wilson AD. Properties of improved glass-ionomer cement formulations. *Journal of Dentistry* 1975b; **3**: 125 - 30.

Crisp S, Lewis BG, Wilson AD. Characterisation of glass-ionomer cements. 1. Long term hardness and compressive strength. *Journal of Dentistry* 1976; **4**: 162 - 6.

Crisp S, Wilson AD. Reactions in glass-ionomer cements. V. Effect of incorporating tartaric acid in the cement liquid. *Journal of Dental Research* 1976; **55**: 1023 - 31.

Crisp S, Lewis BG, Wilson AD. Characterisation of glass-ionomer cements. 3. Effect of polyacid concentration on the physical properties. *Journal of Dentistry* 1977; **5**: 51 - 6.

Crisp S, Wilson AD. Cements comprising acrylic and itaconic acid copolymers and fluoroaluminosilicate glass powder. *US Patent* 1977; 1,532,954.

Crisp S, Lewis BG, Wilson AD. Characterisation of glass-ionomer cements. 5. The effect of the tartaric acid concentration in the liquid component. *Journal of Dentistry* 1979; **7**: 304 - 12.

Crisp S, Kent BE, Lewis BG, Ferner AJ, Wilson AD. Glass-ionomer cement formulations. II. The synthesis of novel polycarboxylic acids. *Journal of Dental Research* 1980; **59**: 1055 - 63.

Croll TP, Phillips RW. Glass-ionomer silver cermet restorations for primary teeth. *Quintessence International* 1986; **17**: 607 - 15.

Cruickshanks-Boyd DW, Lock WR. Fracture toughness of dental amalgams. *Biomaterials* 1983; **4**: 234 - 42.

Culbertson BM, Kao EC. Water soluble polymers containing amino acid residues for dental restoratives. *US Patent* 1994; 5,369,142.

Culbertson BM, Xie D, Thakur A. New matrix resins for glass polyalkenoates or glass-ionomers with pendant amino acid residues. *Journal of Macromolecular Science - Pure and Applied Chemistry* 1999; **A36**: 681 - 96.

Culbertson BM. Glass-ionomer dental restoratives. *Progress in Polymer Science* 2001; **26**: 577 - 604.

Culbertson BM. New polymeric materials for use in glass-ionomer cements. *Journal of Dentistry* 2006; **34**: 556 - 65.

da Mata C, Allen PF, McKenna G, Cronin M, O'Mahony D, Woods N. Two-year survival of ART restorations placed in elderly patients: a randomised controlled clinical trial. *Journal of Dentistry* 2015; **43**: 405 - 11.

Damani R, Gstrein R, Danzer R. Critical notch-root radius effect in SENB-S fracture toughness testing. *Journal of the European Ceramic Society* 1996; **16**: 695 - 702.

Darling M, Hill R. Novel polyalkenoate (glass-ionomer) dental cements based on zinc silicate glasses. *Biomaterials* 1994; **15**: 299 - 306.

Darvell BW. Cements and liners. In: Darvell BW, editor. *Materials Science for Dentistry*. Darvell BW, Hong Kong; 2002, p. 190 - 221.

Darvell BW. Effect of corrosion on the strength of dental silver amalgam. *Dental Materials* 2012a; **28**: 160 - 7.

Darvell BW. Development of strength in dental silver amalgam. *Dental Materials* 2012b; **28**: 207 - 17.

Darvell BW. Uniaxial compression tests and the validity of indirect tensile strength. *Journal of Materials Science* 1990; **25**: 757 - 80.

Davidson CL, de Gee AJ, Feilzer AJ. The competition between the composite - dentin bond strength and the polymerisation contraction stress. *Journal of Dental Research* 1984; **63**: 1396 - 9.

Davidson CL, Feilzer AJ. Polymerisation shrinkage and polymerisation shrinkage stress in polymer-based restoratives. *Journal of Dentistry* 1997; **25**: 435 - 40.



de Barra E, Hill RG. Influence of polyacrylic acid content on the fracture behaviour of glass polyalkenoate cements. *Journal of Materials Science* 1998; **33**: 5487 - 97.

de Barra E, Hill RG. Influence of glass composition on the properties of glass polyalkenoate cements. Part III: influence of fluorite content. *Biomaterials* 2000; **21**: 563 - 9.

de Gennes PG. In: de Gennes PG, editor. *Scaling concepts in polymer physics*. Cornell University Press, Ithaca, New York, USA; 1979, p. 219 - 44.

de With G, Wageman HHM. Ball-on-ring test revisited. *Journal of the American Ceramic Society* 1989; **72**: 1538 - 41.

Debb S, Nicholson JW. The effect of strontium oxide in glass-ionomer cements. *Journal of Materials Science: Materials in Medicine* 1999; **10**: 471 - 4.

Deng Y, Lawn BR, Lloyd IK. Characterization of damage modes in dental ceramic bilayer structures. *Journal of Biomedical Materials Research* 2002; **63**: 137 - 45.

Dowling AH, Stamboulis A, Fleming GJP. The influence of montmorillonite clay reinforcement on the performance of a glass-ionomer restorative. *Journal of Dentistry* 2006; **34**: 802 - 10.

Dowling AH, Fleming GJP. The impact of montmorillonite clay addition on the in vitro wear resistance of a glass-ionomer restorative. *Journal of Dentistry* 2007; **35**: 309 - 17.

Dowling AH, Fleming GJP. Is encapsulation of posterior glass-ionomer restoratives the solution to clinically induced variability introduced on mixing? *Dental Materials* 2008; **24**: 957 - 66.

Dowling AH, Fleming GJP. Are encapsulated anterior glass-ionomer restoratives better than their hand-mixed equivalents? *Journal of Dentistry* 2009; **37**: 133 - 40.

Dowling AH, Fleming GJP. The influence of polyacrylic acid number average molecular weight and concentration in solution on the compressive fracture strength and modulus of a glass-ionomer restorative. *Dental Materials* 2011a; **27**: 535 - 43.

Dowling AH, Fleming GJP. Can polyacrylic acid molecular weight mixtures improve the compressive fracture strength and elastic modulus of a glass-ionomer restorative? *Dental Materials* 2011b; **27**: 1170 - 9.

Dowling AH, Fleming GJP, McGinley EL, Addison O. Improving the standard of the standard for glass-ionomers: an alternative to the compressive fracture strength test for consideration? *Journal of Dentistry* 2012; **40**: 189 - 201.

Dowling AH, Schmitt WS, Fleming GJP. Modification of titanium dioxide particles to reinforce glass-ionomer restoratives. *Dental Materials* 2014; **30S**: e159 - 60.

Dupree R, Holland D, Mortuza MG, Collins JA, Lockyer MWG. Magic angle spinning NMR of alkali phosphoaluminosilicate glasses. *Journal of Non-Crystalline Solids* 1989; **112**: 111 - 9.

Eames WB, Monroe SD, Roan JD, O'Neal SJ. Proportioning and mixing of cements: a comparison of working times. *Operative Dentistry* 1977; **2**: 97 - 104.

Earl MSA, Mount GJ, Hume WR. The effect of varnishes and other surface treatments on water movement across the glass-ionomer cement surface. *Australian Dental Journal* 1989; **34**: 326 - 9.

Edwards SF. Statistical mechanics of polymerized material. *Proceedings of the Physical Society of London* 1967; **92**: 9 - 16.

El Mallakh B, Sarkar NK, Kamar A. Does metal incorporation improve glass-ionomer properties? *Journal of Dental Research* 1987; **66**: Special Issue B113 (Abstract 50).

Ellis J, Anstice M, Wilson AD. The glass polyphosphonate cement: a novel glass-ionomer cement based on polyvinylphosphonic acid. *Clinical Materials* 1991; **7**: 341 - 6.

Elsaka SE, Hamouda IM, Swain MV. Titanium dioxide nanoparticles addition to a conventional glass-ionomer restorative: influence on physical and antibacterial properties. *Journal of Dentistry* 2011; **39**: 589 - 98.

Fennell B, Hill RG. The influence of polyacrylic acid molar mass and concentration on the properties of polyalkenoate cements. Part I: compressive strength. *Journal of Materials Science* 2001a; **36**: 5193 - 202.

Fennell B, Hill RG. The influence of polyacrylic acid molar mass and concentration on the properties of polyalkenoate cements. Part II: Young's modulus and flexural strength. *Journal of Materials Science* 2001b; **36**: 5177 - 83.

Fennel B, Hill RG. The influence of polyacrylic acid molar mass and concentration on the properties of polyalkenoate cements. Part III: fracture toughness and toughness. *Journal of Materials Science* 2001c; **36**: 5185 - 92.

Ferracane JL, Antonio RC, Matsumoto H. Variables affecting the fracture toughness of dental composites. *Journal of Dental Research* 1987; **66**: 1140 - 5.

Ferracane JL. Letter to the editor: the fracture toughness of composite filling materials and crack tip radius. *Journal of Dental Research* 1988; **67**: 884 - 5.

Fischer H, Marx R. The fracture toughness of dental ceramics: comparison of bending and indentation method. *Dental Materials* 2002; **18**: 12 - 9.

Fleming GJP, Shortall ACC, Shelton RM, Marquis PM. Encapsulated versus hand-mixed zinc phosphate dental cements. *Biomaterials* 1999; **20**: 2147 - 53.

Fleming GJP, Shelton RM, Landini G, Marquis PM. The influence of mixing ratio on the toughening mechanisms of a hand-mixed zinc phosphate dental cement. *Dental Materials* 2001; **17**: 14 - 20.

Fleming GJP, Landini G, Marquis PM. Properties of encapsulated and hand-mixed zinc phosphate dental cement. *American Journal of Dentistry* 2002; **15**: 91 - 6.

Fleming GJP, Farooq AA, Barralet JE. Influence of powder/liquid mixing ratio on the performance of a restorative glass-ionomer dental cement. *Biomaterials* 2003; **24**: 4173 - 9.

Fleming GJP, Zala DM. An assessment of encapsulated versus hand-mixed glass-ionomer restoratives. *Operative Dentistry* 2003; **28**: 168 - 77.

Fleming GJP, Hall D, Shortall ACC, Burke FJT. Cuspal movement and microleakage in premolar teeth restored with posterior filling materials of varying reported volumetric shrinkage values. *Journal of Dentistry* 2005; **33**: 139 - 46.

Fleming GJP, Kenny SM, Barralet JE. The optimisation of the initial viscosity of an encapsulated glass-ionomer filling material following different mechanical mixing regimes. *Journal of Dentistry* 2006; **34**: 155 - 63.

Fleming GJP, Dowling AH, Addison O. The crushing truth about glass-ionomer restoratives: exposing the standard of the standard. *Journal of Dentistry* 2012; **40**: 181 - 8.

Forsten L. Fluoride release and uptake by glass-ionomers and related materials and its clinical effect. *Biomaterials* 1998; **19**: 503 - 8.

Frencken JE, Pilot T, Songpaisan Y, Phantumvanit P. Atraumatic restorative treatment (ART): rationale, technique and development. *Journal of Public Health Dentistry* 1996; **56** (Special Issue 3): 135 - 40.

Frencken JE, Taifour D, van't Hof MA. Survival of ART and amalgam restorations in permanent teeth of children after 6.3 years. *Journal of Dental Research* 2006; **85**: 622 - 6.

Frencken JE, van't Hof MA, Taifour D, Al-Zaher I. Effectiveness of ART and traditional amalgam approach in restoring single-surface cavities in posterior teeth of permanent dentitions in school children after 6.3 years. *Community Dental Oral Epidemiology* 2007; **35**: 207 - 14.

Fujishima A, Ferracane JL. Comparison of four modes of fracture toughness testing for dental composites. *Dental Materials* 1996; **12**: 38 - 43.

Gao W, Peng D, Smales RJ, Yip KH. Comparison of atraumatic restorative treatment and conventional restorative procedures in a hospital clinic: evaluation after 30 months. *Quintessence International* 2003; **34**: 31 - 7.

Goldman M. Fracture properties of composite and glass-ionomer dental restorative materials. *Journal of Biomedical Materials Research* 1985; **19**: 771 - 83.

Gonzalez AE. Viscoelasticity of ionomer gels. 2. The elastic moduli. *Polymer* 1984; **25**: 1469 - 74.

Griffin SG, Hill RG. Influence of poly(acrylic acid) molar mass on the fracture properties of glass polyalkenoate cements. *Journal of Materials Science* 1998; **33**: 5383 - 96.

Griffin SG, Hill RG. Influence of glass composition on the properties of glass polyalkenoate cements. Part I: influence of aluminium to silicon ratio. *Biomaterials* 1999; **20**: 1579 - 86.

Griffin SG, Hill RG. Influence of glass composition on the properties of glass polyalkenoate cements. Part II: influence of phosphate content. *Biomaterials* 2000; **21**: 399 - 403.

Griffith AA. The phenomena of rupture and flow in solids. *Philosophical Transactions of the Royal Society of London Series A* 1920; **221**: 163 - 97.

Gu Y, Yap AUJ, Cheang C, Khor KA. Effects of incorporation of HA/ZrO<sub>2</sub> into glass-ionomer cement (GIC). *Biomaterials* 2005; **26**: 713 - 20.

Hannigan A, Lynch CD. Statistical methodology in oral and dental research: pitfalls and recommendations. *Journal of Dentistry* 2013; **41**: 385 - 92.

Harvey CK, Kelly JR. Contact damage as a failure mode during *in vitro* testing. *Journal of Prosthodontics* 1996; **5**: 95 - 100.

Hashemi S, Williams JG. Crack sharpness effects in fracture testing of polymers. *Journal of Materials Science* 1985; **20**: 922 - 8.

Hatton PV, Brook IM. Characterisation of the ultrastructure of glass-ionomer (polyalkenoate) cement. *British Dental Journal* 1992; **173**: 275 - 7.

Heurich E, Beyer M, Jandt KD, Reichert J, Herold V, Schnabelrauch M, Sigusch BW. Quantification of dental erosion - A comparison of stylus profilometry and confocal laser scanning microscopy (CLSM). *Dental Materials* 2010; **26**: 326 - 36.

Higgs WAJ, Lucksanasombool P, Higgs RJED, Swain MV. Comparison of the material properties of PMMA and glass-ionomer based cements for use in orthopaedic surgery. *Journal of Materials Science: Materials in Medicine* 2001a; **12**: 453 - 60.

Higgs WAJ, Lucksanasombool P, Higgs RJED, Swain MV. Evaluating acrylic and glass-ionomer cement strength using the biaxial flexure test. *Biomaterials* 2001b; **22**: 1583 - 90.

Hill RG, Wilson AD. A rheological study of the role of additives on the setting of glass-ionomer cements. *Journal of Dental Research* 1988; **67**: 1446 - 50.

Hill RG, Wilson AD, Warrens CP. The influence of polyacrylic acid molecular weight on the fracture toughness of glass-ionomer cements. *Journal of Materials Science* 1989; **24**: 363 - 71.

Hill RG, Labok SA. The influence of polyacrylic acid molecular weight on the fracture of zinc polycarboxylate cements. *Journal of Materials Science* 1991; **26**: 67 - 74.



Honkala E, Behbehani J, Ibricevic H, Kerosuo E, Al-Jame G. The atraumatic restorative treatment (ART) approach to restoring primary teeth in a standard dental clinic. *International Journal of Paediatric Dentistry* 2003; **13**: 172 - 9.

Hooi P, Addison O, Fleming GJP. Can a soda-lime glass be used to demonstrate how patterns of strength dependence are influenced by pre cementation and resin-cementation variables? *Journal of Dentistry* 2013; **41**: 24 - 30.

Hooi P, Addison O, Fleming GJP. Strength determination of brittle materials as curved monolithic structures. *Journal of Dental Research* 2014; **93**: 412 - 6.

Ilie N, Hickel R, Valceanu AS, Huth KC. Fracture toughness of dental restorative materials. *Clinical Oral Investigations* 2012; **16**: 489 - 98.

International Organisation for Standardisation ISO DP 9917:1987. Harmonisation of test methods for dental cements.

International Organisation for Standardisation ISO 4049:2000. Dentistry - polymer-based filling, restorative and luting materials.

International Organisation for Standardisation ISO 9917-1:2003. Dentistry - water-based cements. Part 1. Powder/liquid acid-base cements.

International Organisation for Standardisation ISO 9917-1:2007. Dentistry - water-based cements. Part 1. Powder/liquid acid-base cements.

International Organisation for Standardisation ISO 12737:2010. Metallic materials - determination of plane-strain fracture toughness.

Irwin GR. Analysis of stresses and strains near the end of a crack traversing a plate. *Journal of Applied Mechanics* 1957; **24**: 361 - 4.

Isgro G, Addison O, Fleming GJP. Deformation of dental ceramic following adhesive cementation. *Journal of Dental Research* 2010; **89**: 87 - 90.

Isgro G, Addison O, Fleming GJP. The deformation and strength of a dental ceramic following resin-cement coating. *Journal of Dentistry* 2011; **39**: 122 - 7.

Jung YG, Wuttiphan S, Peterson IM, Lawn BR. Damage modes in dental layer structures. *Journal of Dental Research* 1999; **78**: 887 - 97.

Kakaboura A, Fragouli C, Silikas N. Evaluation of surface characteristics of dental composites using profilometry, scanning electron, atomic force microscopy and gloss-meter. *Journal of Materials Science: Materials in Medicine* 2007; **18**: 155 - 63.

Kao EC, Culbertson BM, Xie D. Preparation of glass-ionomer cement using N-acryloyl-substituted amino acid monomers: evaluation of physical properties. *Dental Materials* 1996; **12**: 44 - 51.

Kaplan AE, Williams J, Billington RW, Braden M. Effects of variation in particle size on biaxial flexural strength of two conventional glass-ionomer cements. *Journal of Oral Rehabilitation* 2004; **31**: 373 - 8.

Kelly JR, Benetti P, Rungruangant P, Bona AD. The slippery slope - critical perspectives on *in vitro* research methodologies. *Dental Materials* 2012; **28**: 41 - 5.

Kelly JR, Giordano R, Pober R, Cima MJ. Fracture surface analysis of dental ceramics: clinically failed restorations. *International Journal of Prosthodontics* 1990; **3**: 430 - 40.

Kelly JR. Clinically relevant approach to failure testing of all-ceramic restorations. *Journal of Prosthetic Dentistry* 1999; **81**: 652 - 61.

Kendall K. Complexities of compression failure. *Proceedings of the Royal Society of London Series A* 1978; **361**: 245 - 63.

Kent BE, Lewis BG, Wilson AD. Glass-ionomer cement formulations: I. The preparation of novel fluoroaluminosilicate glasses high in fluorine. *Journal of Dental Research* 1979; **58**: 1607 - 19.

Kerby RE, Bleiholder RF. Physical properties of stainless-steel and silver-reinforced glass-ionomer cements. *Journal of Dental Research* 1991; **70**: 1358 - 61.

Khouw-Liu VHW, Anstice HM, Pearson GJ. An *in vitro* investigation of polyvinylphosphonic acid based cement with four conventional glass-ionomer cements. Part 2: maturation in relation to surface hardness. *Journal of Dentistry* 1999a; **27**: 359 - 65.

Khouw-Liu VHW, Anstice HM, Pearson GJ. An *in vitro* investigation of polyvinylphosphonic acid based cement with four conventional glass-ionomer cements. Part 1: flexural strength and fluoride release. *Journal of Dentistry* 1999b; **27**: 351 - 7.

Kilpatrick NM, Murray JJ, McCabe JF. The use of a reinforced glass-ionomer cermet for the restoration of primary molars: a clinical trial. *British Dental Journal* 1995; **179**: 175 - 9.

Kirkpatrick RJ, Brow RK. Nuclear magnetic resonance investigation of the structure of phosphate and phosphate containing glasses: a review. *Solid State Nuclear Magnetic Resonance* 1995; **5**: 9 - 21.

Kobayashi M, Kon M, Miyai K, Asaoka K. Strengthening of glass-ionomer cement by compounding short fibres. *Biomaterials* 2000; **21**: 2051 - 8.

Kovarik RE, Ergle JW, Fairhurst CW. Effects of specimen geometry on the measurement of fracture toughness. *Dental Materials* 1991; **7**: 166 - 9.

Kovarik RE, Fairhurst CW. Effect of Griffith pre-cracks on measurement of composite fracture toughness. *Dental Materials* 1993; **9**: 222 - 8.

Kruzic JJ, Kuskowski SJ, Ritchie RO. Simple and accurate fracture toughness testing methods for pyrolytic carbon/graphite composites used in heart-valve prostheses. *Journal of Biomedical Materials Research* 2005; **74A**: 461 - 4.

Lawn BR, Deng Y, Thompson VP. Use of contact testing in the characterization and design of all-ceramic crown like layer structures: a review. *Journal of Prosthetic Dentistry* 2001; **86**: 495 - 510.

Lawn BR, Deng Y, Miranda P, Pajares A, Chai H, Kim DK. Overview: damage in brittle layer structures from concentrated loads. *Journal of Materials Research* 2002; **17**: 3019 - 36.

Levitch LC, Bader JD, Shugars DA, Heymann HO. Non-carious cervical lesions. *Journal of Dentistry* 1994; **22**: 195 - 207.

Li ZC, White SN. Mechanical properties of dental luting cements. *Journal of Prosthetic Dentistry* 1999; **81**: 597 - 609.

Lipson C, Sheth NJ. Statistical distributions. In: Lipson C, Sheth NJ, editors. *Statistical design and analysis of engineering experiments*. McGraw-Hill, New York, USA; 1973, p. 372 - 415.

Lloyd CH. The fracture toughness of dental composites. II. The environmental and temperature dependence of the stress intensification factor ( $K_{IC}$ ). *Journal of Oral Rehabilitation* 1982; **9**: 133 - 8.

Lloyd CH, Iannetta RV. The fracture toughness of dental composites. I. The development of strength and fracture toughness. *Journal of Oral Rehabilitation* 1982; **9**: 55 - 66.

Lloyd CH. Resistance to fracture in posterior composites. *British Dental Journal* 1983; **155**: 411 - 4.

Lloyd CH. The fracture toughness of dental composites. III. The effect of environment upon the stress intensification factor ( $K_{IC}$ ) after extended storage. *Journal of Oral Rehabilitation* 1984; **11**: 393 - 8.

Lloyd CH, Mitchell L. The fracture toughness of tooth coloured restorative materials. *Journal of Oral Rehabilitation* 1984; **11**: 257 - 72.

Lloyd CH, Adamson M. The fracture toughness ( $K_{IC}$ ) of amalgam. *Journal of Oral Rehabilitation* 1985; **12**: 59 - 68.

Lloyd CH, Adamson M. The development of fracture toughness and fracture strength in posterior restorative materials. *Dental Materials* 1987; **3**: 225 - 32.

Lloyd CH. Letter to the editor: the fracture toughness of composite filling materials and crack tip radius. *Journal of Dental Research* 1988; **67**: 883 - 4.

Lohbauer U, Walker J, Nikolaenko S, Werner J, Clare A, Petschelt A, Greil P. Reactive fibre reinforced glass-ionomer cements. *Biomaterials* 2003; **24**: 2901 - 7.

Lucarotti PJ, Holder RL, Burke FJT. Outcome of direct restorations placed within the general dental services in England and Wales (Part 1): variation by type of restoration and re-intervention. *Journal of Dentistry* 2005; **33**: 805 - 15.

Lucas ME, Arita K, Nishino M. Toughness, bonding and fluoride-release properties of hydroxyapatite-added glass-ionomer cement. *Biomaterials* 2003; **24**: 3787 - 94.

Lucksanasombool P, Higgs WAJ, Higgs RJED, Swain MV. Toughness of glass fibres reinforced glass-ionomer cements. *Journal of Materials Science* 2002; **37**: 101 - 8.

Lutz F, Kreici I, Barbakow F. Quality and durability of marginal adaptation in bonded composite restorations. *Dental Materials* 1991; **7**: 107 - 13.

Lutz F. The postamalgam age. *Operative Dentistry* 1995; **20**: 218 - 22.

Marshall GW, Marshall SJ, Kinney JH, Balooch M. The dentin substrate: structure and properties related to bonding. *Journal of Dentistry* 1997; **25**: 441 - 58.

Mathis RS, Ferracane JL. Properties of a glass-ionomer/resin-composite hybrid material. *Dental Materials* 1989; **5**: 355 - 8.

Mayanagi G, Igarashi K, Washio J, Domon-Tawaraya H, Takahashi N. Effect of fluoride-releasing restorative materials on bacteria-induced pH fall at the bacteria-material interface: an *in vitro* model study. *Journal of Dentistry* 2014; **42**: 15 - 20.

McCabe JF, Carrick TE. A statistical approach to the mechanical testing of dental materials. *Dental Materials* 1986; **2**: 139 - 42.

McCabe JF, Watts DC, Wilson HJ, Worthington HV. An investigation of test-house variability in the mechanical testing of dental materials. *Journal of Dentistry* 1990; **18**: 90 - 7.

McLean JW, Wilson AD. Fissure sealing and filling with an adhesive glass-ionomer cement. *British Dental Journal* 1974; **136**: 269 - 76.

McLean JW, Wilson AD, Prosser HJ. Development and use of water-hardening glass-ionomer luting cements. *Journal of Prosthetic Dentistry* 1984; **52**: 175 - 81.

McLean JW, Gasser O. Glass-cermet cements. *Quintessence International* 1985; **16**: 333 - 43.

McLean JW. Cermet cements. *Journal of the American Dental Association* 1990; **120**: 43 - 47.

McMillan PW. Crystallisation and devitrification. In: Roberts JP, Popper P, editors. *Glass-Ceramics*. Academic Press Inc., London, UK; 1964, p. 7 - 60.

Mecholsky JJ, Rice RW, Freiman SW. Prediction of fracture energy and flaw size in glasses from measurements of mirror size. *Journal of the American Ceramic Society* 1974; **57**: 440 - 3.



Mecholsky JJ. Fractography: determining the sites of fracture initiation. *Dental Materials* 1995; **11**: 113 - 6.

Miller D, Marker VA, Okabe T, Simmons JJ. Formulation and evaluation of dental amalgam alloy added to glass-ionomer. *Journal of Dental Research* 1984; **63**: Special Issue B231 (Abstract 545).

Mitchell CA, Douglas WH, Cheng YS. Fracture toughness of conventional, resin-modified glass-ionomer and composite luting cements. *Dental Materials* 1999; **15**: 7 - 13.

Mitsuhashi A, Hanaoka K, Teranaka T. Fracture toughness of resin-modified glass-ionomer restorative materials: effect of powder/liquid ratio and powder particle size reduction on fracture toughness. *Dental Materials* 2003; **19**: 747 - 57.

Miyazaki M, Moore BK, Onose H. Effect of surface coatings on flexural properties of glass-ionomers. *European Journal of Oral Science* 1996; **104**: 600 - 4.

Morrell R. Measurement good practice guide no. 12: biaxial flexure strength testing of ceramic materials. *National Physics Laboratory* 2007.

Moshaverinia A, Ansari S, Moshaverinia M, Roohpour N, Darr J, Rehman I. Effects of incorporation of hydroxyapatite and fluoroapatite nanobioceramics into conventional glass-ionomer cements (GIC). *Acta Biomaterialia* 2008a; **4**: 432 - 40.

Moshaverinia A, Ansari S, Movasaghi Z, Billington RW, Darr JA, Rehman IU. Modification of conventional glass-ionomer cements with N-vinylpyrrolidone containing polyacids, nano-hydroxy and fluoroapatite to improve mechanical properties. *Dental Materials* 2008b; **24**: 1381 - 90.

Moshaverinia A, Roohpour N, Darr JA, Rehman IU. Synthesis and characterisation of a novel N-vinylcaprolactam-containing acrylic acid terpolymer for applications in glass-ionomer dental cements. *Acta Biomaterialia* 2009; **5**: 2101 - 8.

Moshaverinia A, Brantley WA, Chee WWL, Roohpour N, Ansari S, Zheng F, Heshmati RH, Darr JA, Schricker SR, Rehman IU. Measure of microhardness, fracture toughness and flexural strength of N-vinylcaprolactam (NVC)-containing glass-ionomer dental cements. *Dental Materials* 2010; **26**: 1137 - 43.

Mount GJ, Makinson OF. Clinical characteristics of a glass-ionomer cement. *British Dental Journal* 1978a; **145**: 67 - 71.

Mount GJ, Makinson OF. Letter to the editor. *British Dental Journal* 1978b; **145**: 125.

Mount GJ. Description of glass-ionomer cements. In: Mount GJ, editor. *An atlas of glass-ionomer cements: a clinician's guide*. Martin Dunitz, London, UK; 1994, p. 1 - 24.

Musanje L, Shu M, Darvell BW. Water sorption and mechanical behaviour of cosmetic direct restorative materials in artificial saliva. *Dental Materials* 2001; **17**: 394 - 401.

Nakajima H, Hashimoto H, Marker VA, Hanaoka K, Miyakuni S, Teranaka T, Iwamoto T, Okabe T. Static and dynamic mechanical properties of glass-ionomers. *Journal of Dental Research* 1989; **68**: Special Issue B273 (Abstract 735).

Neve AD, Piddock V, Combe EC. Development of novel dental cements. I. Formulation of aluminoborate glasses. *Clinical Materials* 1992a; **9**: 7 - 12.

Neve AD, Piddock V, Combe EC. Development of novel dental cements. II. Cement properties. *Clinical Materials* 1992b; **9**: 13 - 20.

Neve AD, Piddock V, Combe EC. The effect of glass heat treatment on the properties of a novel polyalkenoate cement. *Clinical Materials* 1993; **12**: 113 - 6.

Nicholson JW, Brookman PJ, Lacy OM, Wilson AD. Fourier transform infrared spectroscopic study of the role of tartaric acid in glass-ionomer dental cements. *Journal of Dental Research* 1988; **67**: 1451 - 4.

Nicholson JW, Hawkins SJ, Smith JE. The incorporation of hydroxyapatite into glass-polyalkenoate ('glass-ionomer') cements: a preliminary study. *Journal of Materials Science: Materials in Medicine* 1993; **4**: 418 - 21.

Nicholson JW, Abiden F. Changes in compressive strength on ageing in glass polyalkenoate (glass-ionomer) cements prepared from acrylic/maleic acid copolymers. *Biomaterials* 1997; **18**: 59 - 62.

Nicholson JW. Chemistry of glass-ionomer cements: a review. *Biomaterials* 1998; **19**: 485 - 94.

Nishida T, Hanaki Y, Pezzotti G. Effect of notch-root radius on the fracture toughness of a fine-grained alumina. *Journal of the American Ceramic Society* 1994; **77**: 606 - 8.

Oilo M, Gjerdet NR. Fractographic analyses of all-ceramic crowns: a study of 27 clinically fractured crowns. *Dental Materials* 2013; **29**: e78 - 84.

Oldfield CWB, Ellis B. Fibrous reinforcement of glass-ionomer cements. *Clinical Materials* 1991; **7**: 313 - 23.

Paul JE. Four-handed dentistry. 1. Principles and techniques: a new look. *Dental Update* 1983; **10**: 155 - 64.

Pearson GJ, Atkinson AS. Long-term flexural strength of glass-ionomer cements. *Biomaterials* 1991; **12**: 658 - 60.

Peters MCRB, DeLong R, Pintado MR, Pallesen U, Qvist V, Douglas WH. Comparison of two measurement techniques for clinical wear. *Journal of Dentistry* 1999; **27**: 479 - 85.

Peterson IM, Pajares A, Lawn BR, Thompson VP, Rekow ED. Mechanical characterization of dental ceramics by Hertzian contacts. *Journal of Dental Research* 1998; **77**: 589 - 602.

Peumans M, Kanumilli P, De Munck J, Van Landuyt K, Lambrechts P, Van Meerbeek B. Clinical effectiveness of contemporary adhesives: a systematic review of current clinical trials. *Dental Materials* 2005; **21**: 864 - 81.

Pidaparti RMV, Beatty MW. Fracture toughness determination of dental materials by laboratory testing and finite element models. *Journal of Biomedical Materials Research* 1995; **29**: 309 - 14.

Prentice P. The influence of molecular weight on the fracture of thermoplastic glassy polymers. *Journal of Materials Science* 1985; **20**: 1445 - 54.

Product specification for Chemfil Rock. Dentsply DeTrey: Konstanz, Germany.

Product specification for Diamond Carve. Associated Dental Products Ltd.: Wiltshire, UK.

Product specification for Fuji IX<sub>GP</sub> Fast. GC Europe: Leuven, Belgium.

Product specification for Ionofil Molar AC. Voco GmbH: Cuxhaven, Germany.

Product specification for Ionofil Molar. Voco GmbH: Cuxhaven, Germany.

Product specification for Ketac Molar. 3M ESPE: St. Paul, Minnesota, USA.

Product specification for Ketac Fil. 3M ESPE: St. Paul, Minnesota, USA.

Product specification for polyamide nylon 6,6 - 30% glass fiber reinforced rod. Goodfellow: Cambridge, Huntingdon, England.

Prosser HJ, Powis DR, Brant P, Wilson AD. Characterisation of glass-ionomer cements. 7. The physical properties of current materials. *Journal of Dentistry* 1984; **12**: 231 - 40.

Prosser HJ, Powis DR, Wilson AD. Glass-ionomer cements of improved flexural strength. *Journal of Dental Research* 1986; **65**: 146 - 8.

Quinn JB, Sundar V, Lloyd IK. Influence of microstructure and chemistry on the fracture toughness of dental ceramic. *Dental Materials* 2003; **19**: 603 - 11.

Quinn JB, Quinn GD, Kelly JR, Scherrer SS. Fractographic analyses of three ceramic whole crown restoration failures. *Dental Materials* 2005; **21**: 920 - 9.

Quinn GD. Fractography of ceramics and glasses. *NIST Recommended Practice Guide* 2007.

Renshaw CE, Schulson EM. Universal behaviour in compressive failure of brittle materials. *Nature* 2001; **412**: 897 - 900.

Ritter JE. Predicting lifetimes of materials and materials structures. *Dental materials* 1995; **11**: 142 - 6.

Sarkar NK, El Mallakh B, Graves R. Silver release from metal-reinforced glass-ionomers. *Dental Materials* 1988; **4**: 103 - 4.

Sced I, Wilson AD. Polycarboxylic acid hardenable compositions. *British Patent* 1980; 2,028,855A.

Scherrer SS, Denry IL, Wiskott HWA. Comparison of three fracture toughness testing techniques using a dental glass and a dental ceramic. *Dental Materials* 1998; **14**: 246 - 55.

Scherrer SS, Quinn JB, Quinn GD, Kelly JR. Failure analysis of ceramic clinical cases using qualitative fractography. *International Journal of Prosthodontics* 2006; **19**: 185 - 92.

Schmitt W, Purrmann R, Jochum P, Gasser O. Mixing component for dental glass-ionomer cements. *US Patent* 1982; 4,360,605.

Schmitt W, Purrmann R, Jochum P, Gasser O. Calcium depleted aluminium fluorosilicate glass powder for use in dental or bone cements. *US Patent* 1983; 4,376,835.

Scholtanus JD, Huysmans MCDNJM. Clinical failure of class II restorations of a highly viscous glass-ionomer material over a 6-year period: a retrospective study. *Journal of Dentistry* 2007; **35**: 156 - 62.

Seiler H. Secondary electron emission in the scanning electron microscope. *Journal of Applied Physics* 1983; **54**: 1 - 18.

Sheldon T, Treasure E. Dental restoration: what type of filling? *Effective Health Care* 1999; **5**: 1 - 11.

Simmons JJ. The miracle mixture: glass-ionomer and alloy powder. *Texas Dental Journal* 1983; **100**: 6 - 12.

Simmons JJ. Silver-alloy powder and glass-ionomer cement. *Journal of the American Dental Association* 1990; **120**: 49 - 52.

Skinner JC, Prosser HJ, Scott RP, Wilson AD. Adhesion of carboxylate cements to hydroxyapatite. *Biomaterials* 1986; **7**: 438 - 40.

Smith DC. Development of glass-ionomer cement systems. *Biomaterials* 1998; **19**: 467 - 78.

Swinscow TDV. In: Swinscow TDV, editor. *Statistics at square one*. BMJ Publishing group, London, UK; 1996.

Taifour D, Frencken JE, Beiruti N, van't Hof MA, Truin GJ. Effectiveness of glass-ionomer (ART) and amalgam restorations in the deciduous dentition: results after 3 years. *Caries Research* 2002; **36**: 437 - 44.

Theocharopoulos A, Zou R, Hill R, Cattell M. Wear quantification of human enamel and dental glass-ceramics using white light profilometry. *Wear* 2010; **269**: 930 - 6.

Thoman DR, Bain LJ, Antle CE. Inferences on the parameters of the Weibull distribution. *Technometrics* 1969; **11**: 445 - 60.



Thompson JY, Anusavice KJ, Naman A, Morris HF. Fracture surface characterisation of clinically failed all-ceramic crowns. *Journal of Dental Research* 1994; **73**: 1824 - 32.

Timoshenko S, Woinowsky-Krieger S. Symmetrical bending of circular plates. In: Timoshenko S, Woinowsky-Krieger S, editors. *Theory of plates and shells*. McGraw-Hill, New York, USA; 1959, p. 87 - 121.

Torabzadeh H, Ghasemi A, Shakeri S, Baghban AA, Razmavar S. Effect of powder/liquid ratio of glass-ionomer cements on flexural and shear bond strengths to dentin. *Brazilian Journal of Oral Science* 2011; **10**: 204 - 7.

Truong VT, Cock DJ, Padmanathan N. Fatigue crack propagation in posterior dental composites and prediction of clinical wear. *Journal of Applied Biomaterials* 1990; **1**: 21 - 30.

Trustrum K, Jayatilaka ADS. On estimating the Weibull modulus for a brittle material. *Journal of Materials Science* 1979; **14**: 1080 - 4.

Van Meerbeek B, Perdigao J, Lambrechts P, Vanherle G. The clinical performance of adhesives. *Journal of Dentistry* 1998; **26**: 1 - 20.

Van Meerbeek B, De Munck J, Yoshida Y, Inoue S, Vargas M, Vijay P. Buonocore memorial lecture. Adhesion to enamel and dentin: current status and future challenges. *Operative Dentistry* 2003; **28**: 215 - 35.

Vihola H, Laukkanen A, Hirvonen J, Tenhu H. Binding and release of drugs into and from thermosensitive poly(N-vinylcaprolactam) nanoparticles. *European Journal of Pharmaceutical Sciences* 2002; **16**: 69 - 74.

Walls AWG, Adamson J, McCabe JF, Murray JJ. The properties of glass polyalkenoate (ionomer) cement incorporating sintered metallic particles. *Dental Materials* 1987; **3**: 113 - 6.

Wang Y, Darvell BW. Failure mode of dental restorative materials under Hertzian indentation. *Dental Materials* 2007; **23**: 1236 - 44.

Wang Y, Darvell BW. Failure behavior of glass-ionomer cement under Hertzian indentation. *Dental Materials* 2008; **24**: 1223 - 9.

Wang Y, Darvell BW. Hertzian load-bearing capacity of a ceramic-reinforced glass-ionomer cement stored wet and dry. *Dental Materials* 2009; **25**: 952 - 5.

Wang Y, Darvell BW. Interactive effect of indenter size and specimen thickness in Hertzian indentation test. *Dental Materials* 2010; **26**: 539 - 44.

Wang Y, Darvell BW. Effect of elastic modulus mismatch on failure behaviour of glass-ionomer cement under Hertzian indentation. *Dental Materials* 2012; **28**: 279 - 86.

Watt IM. In: Watt IM, editor. *The principles and practice of electron microscopy*. University Press, Cambridge, UK; 1997.

Weibull W. A statistical distribution function of wide applicability. *Journal of Applied Mechanics* 1951; **18**: 293 - 7.

White SN, Yu Z. Compressive and diametral tensile strengths of current adhesive luting agents. *Journal of Prosthetic Dentistry* 1993; **69**: 568 - 72.

Whitehead SA, Shearer AC, Watts DC, Wilson NHF. Surface texture changes of a composite brushed with 'tooth whitening' dentifrices. *Dental Materials* 1996; **12**: 315 - 8.

Whitehead SA, Shearer AC, Watts DC, Wilson NHF. Comparison of two stylus methods for measuring surface texture. *Dental Materials* 1999; **15**: 79 - 86.

Williams JA, Billington RW. Changes in compressive strength of glass-ionomer restorative materials with respect to time periods of 24 h to 4 months. *Journal of Oral Rehabilitation* 1991; **18**: 163 - 8.

Williams JA, Billington RW, Pearson GJ. The comparative strengths of commercial glass-ionomer cements with and without metal additions. *British Dental Journal* 1992; **172**: 279 - 82.

Wilson AD, Batchelor RF. Dental Silicate Cements. I. The chemistry of erosion. *Journal of Dental Research* 1967a; **46**: 1078 - 85.

Wilson AD, Batchelor RF. Dental silicate cements. II. Preparation and durability. *Journal of Dental Research* 1967b; **46**: 1425 - 32.

Wilson AD, Batchelor RF. Dental silicate cements. III. Environment and durability. *Journal of Dental Research* 1968; **47**: 115 - 20.

Wilson AD. Dental silicate cements. IV. Alternative liquid cement formers. *Journal of Dental Research* 1968; **47**: 1133 - 6.

Wilson AD, Kent BE. Surgical cement. *British Patent* 1969; 1,316,129.

Wilson AD, Kent BE. A new translucent cement for dentistry. The glass-ionomer cement. *British Dental Journal* 1972; **132**: 133 - 5.

Wilson AD. Dental cements - general. Zinc oxide dental cements. Dental cement based on ion-leachable glasses. In: Von Fraunhofer JA, editor. *Scientific aspects of dental materials*. Butterworths, London, UK; 1975, p. 131 - 221.

Wilson AD, Crisp S, Ferner AJ. Reactions in glass-ionomer cements. IV. Effect of chelating comonomers on setting behaviour. *Journal of Dental Research* 1976; **55**: 489 - 95.

Wilson AD, Crisp S, Abel G. Characterisation of glass-ionomer cements. 4. Effect of molecular weight on physical properties. *Journal of Dentistry* 1977; **5**: 117 - 20.

Wilson AD, Crisp S, Prosser HJ, Lewis BG, Merson SA. Aluminosilicate glasses for polyelectrolyte cements. *Industrial and Engineering Chemistry Product Research and Development* 1980; **19**: 263 - 70.

Wilson AD, Prosser HJ. A survey of inorganic and polyelectrolyte cements. *British Dental Journal* 1984; **157**: 449 - 54.

Wilson AD, McLean JW. Scientific and clinical development. In: Wilson AD and McLean JW, editors. *Glass-ionomer cement*. Quintessence Publishing Co., Inc., Chicago, Illinois, USA; 1988a, p. 13 - 20.

Wilson AD, McLean JW. The setting reaction and its clinical consequences. In: Wilson AD, McLean JW, editors. *Glass-ionomer cement*. Quintessence Publishing Co., Inc., Chicago, Illinois, USA; 1988b, p. 43 - 56.

Wilson AD, McLean JW. Composition. In: Wilson AD, McLean JW, editors. *Glass-ionomer cement*. Quintessence Publishing Co., Inc., Chicago, Illinois, USA; 1988c, p. 21 - 42.

Wilson AD, McLean JW. Adhesion. In: Wilson AD and McLean JW, editors. *Glass-ionomer cement*. Quintessence Publishing Co., Inc., Chicago, Illinois, USA; 1988d, p. 83 - 99.

Wilson AD. Developments in glass-ionomer cements. *International Journal of Prosthodontics* 1989; **2**: 438 - 46.

Wilson AD, Ellis J. Polyvinylphosphonic acid and metal oxide or cermet or glass-ionomer cement. *British Patent* 1989; 2,219,289A.

Wilson AD, Hill RG, Warrens CP, Lewis BG. The influence of polyacid molecular weight on some properties of glass-ionomer cements. *Journal of Dental Research* 1989; **68**: 89 - 94.

Wilson AD. Glass-ionomer cements - origins, development and future. *Clinical Materials* 1991; **7**: 275 - 82.

Wilson AD, Nicholson JW. Polyalkenoate cements. In: Wilson AD, Nicholson JW, editors. *Acid-base cements: Their biomedical and industrial applications*. University Press, Cambridge, UK; 1993, p. 90 - 196.

Wilson AD. A hard decade's work: steps in the invention of the glass-ionomer cement. *Journal of Dental Research* 1996; **75**: 1723 - 7.

Wood D, Hill R. Structure-property relationship in ionomer glasses. *Clinical Materials* 1991; **7**: 301 - 12.

Xie D, Culbertson BM, Johnston W. Improved flexural strength of N-vinylpyrrolidone modified acrylic acid copolymers for glass-ionomers. *Journal of Macromolecular Science - Pure and Applied Chemistry* 1998; **A35**: 1615 - 29.

Xie D, Brantley WA, Culbertson BM, Wang G. Mechanical properties and microstructures of glass-ionomer cements. *Dental Materials* 2000; **16**: 129 - 38.

Yamazaki T, Brantley W, Culbertson B, Seghi R, Schricker S. The measure of wear in N-vinylpyrrolidone (NVP) modified glass-ionomer cements. *Polymers for Advanced Technology* 2005; **16**: 113 - 6.

Yap AUJ, Pek YS, Kumar RA, Cheang P, Khor KA. Experimental studies on a new bioactive material: HA Ionomer cements. *Biomaterials* 2002; **23**: 955 - 62.

Yettram AL, Wright KW, Pickard HM. Finite element stress analysis of the crowns of normal and restored teeth. *Journal of Dental Research* 1976; **55**: 1004 - 11.

Yip KH, Smales RJ, Gao W, Peng D. The effects of two cavity preparation methods on the longevity of glass-ionomer cement restorations: an evaluation after 12 months. *Journal of the American Dental Association* 2002; **133**: 744 - 51.

Yli-Urpo H, Lassila LVJ, Narhi T, Vallittu PK. Compressive strength and surface characterisation of glass-ionomer cements modified by particles of bioactive glass. *Dental Materials* 2005; **21**: 201 - 9.

Yoshida Y, Van Meerbeek B, Nakayama Y, Yoshioka M, Snauwaert J, Abe Y, Lambrechts P, Vanherle G, Okazaki O. Adhesion to and decalcification of hydroxyapatite by carboxylic acids. *Journal of Dental Research* 2001; **80**: 1565 - 9.

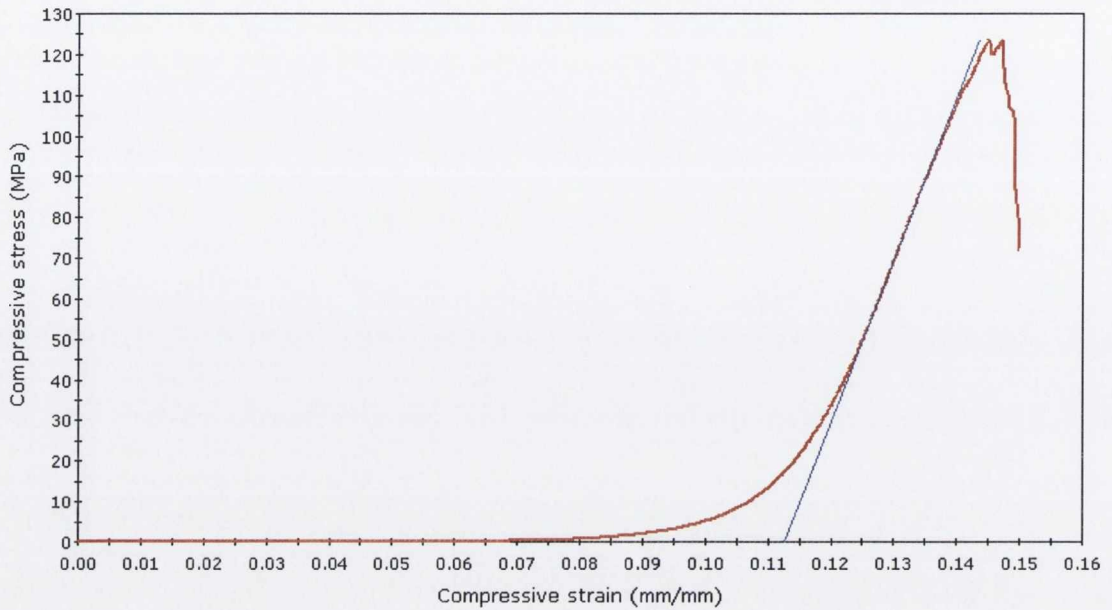
Yu C, Gao XJ, Deng DM, Yip HK, Smales RJ. Survival of glass-ionomer restorations placed in primary molars using atraumatic restorative treatment (ART) and conventional cavity preparations: 2-year results. *International Dental Journal* 2004; **54**: 42 - 66.

Zachariasen WH. Atomic arrangement in glass. *Journal of the American Chemistry Society* 1932; **54**: 3841 - 51.

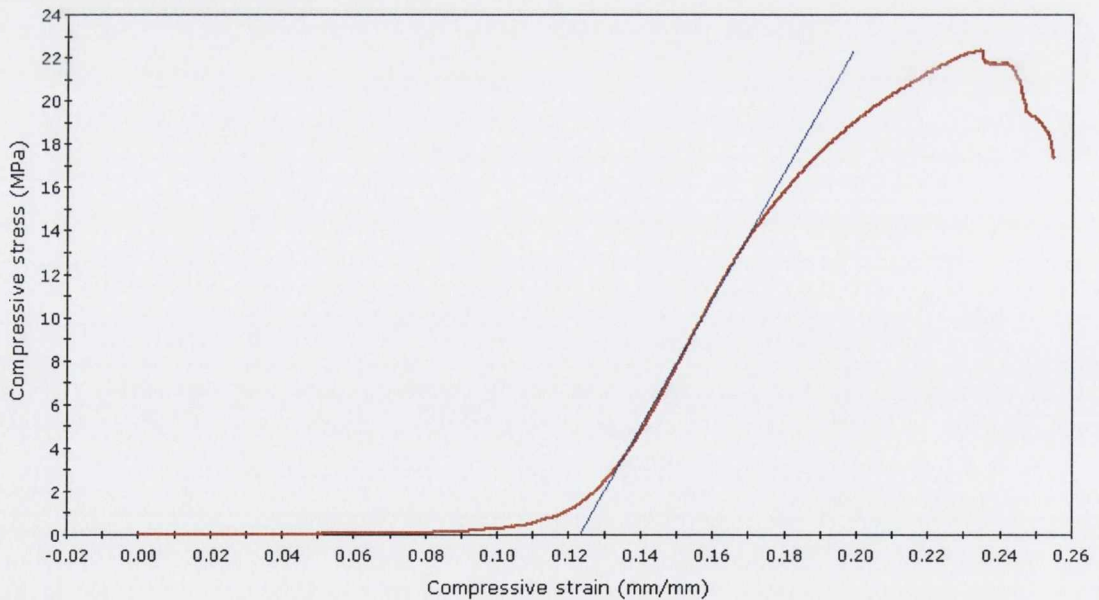
Zeng K, Oden A, Rowcliffe D. Flexure tests on dental ceramics. *International Journal of Prosthodontics* 1996; **9**: 434 - 9.



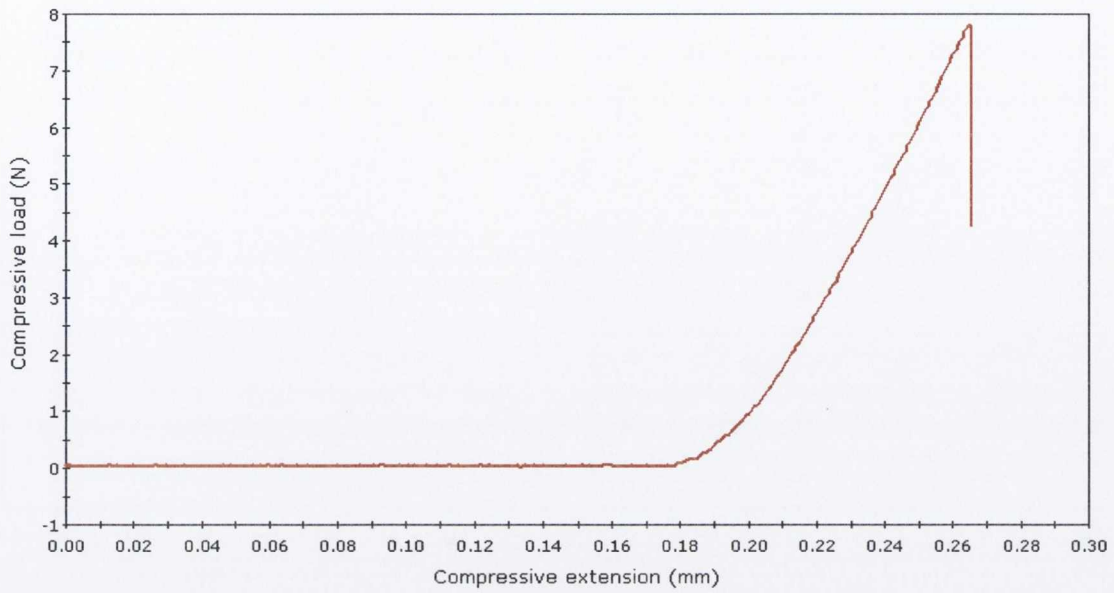
## APPENDIX



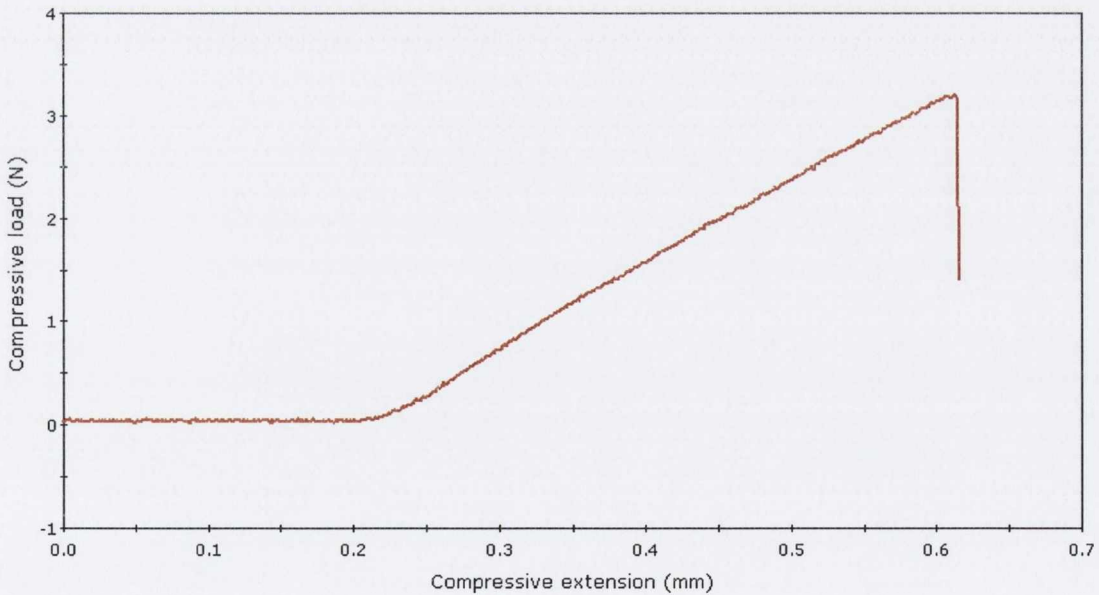
**Appendix Figure 1.** A stress-strain plot of a cylindrical compressive fracture strength (CFS) specimen prepared with the manufacturer's recommended powder content (100%) highlighting a maximum stress of 120 MPa and a compressive strain of 0.07 mm/mm. The compressive modulus (CM) was calculated from the initial linear segment of the stress-strain graph.



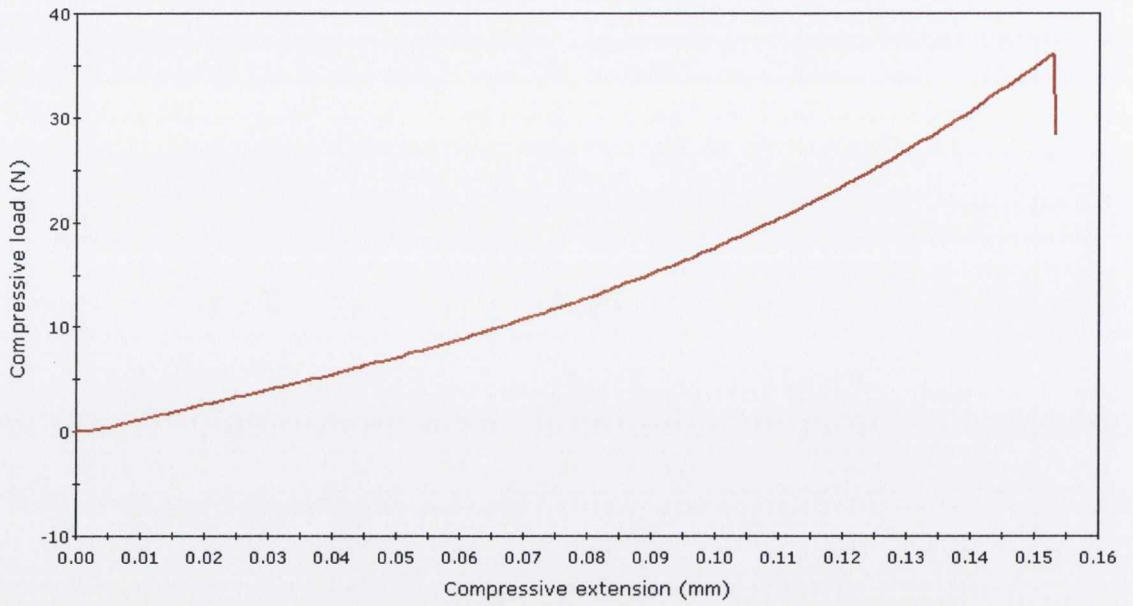
**Appendix Figure 2.** A stress-strain plot of a cylindrical compressive fracture strength (CFS) specimen prepared with 20% of the manufacturer's recommended powder content highlighting a maximum stress of 22 MPa and a compressive strain of 0.16 mm/mm. The compressive modulus (CM) was calculated from the initial linear segment of the stress-strain graph.



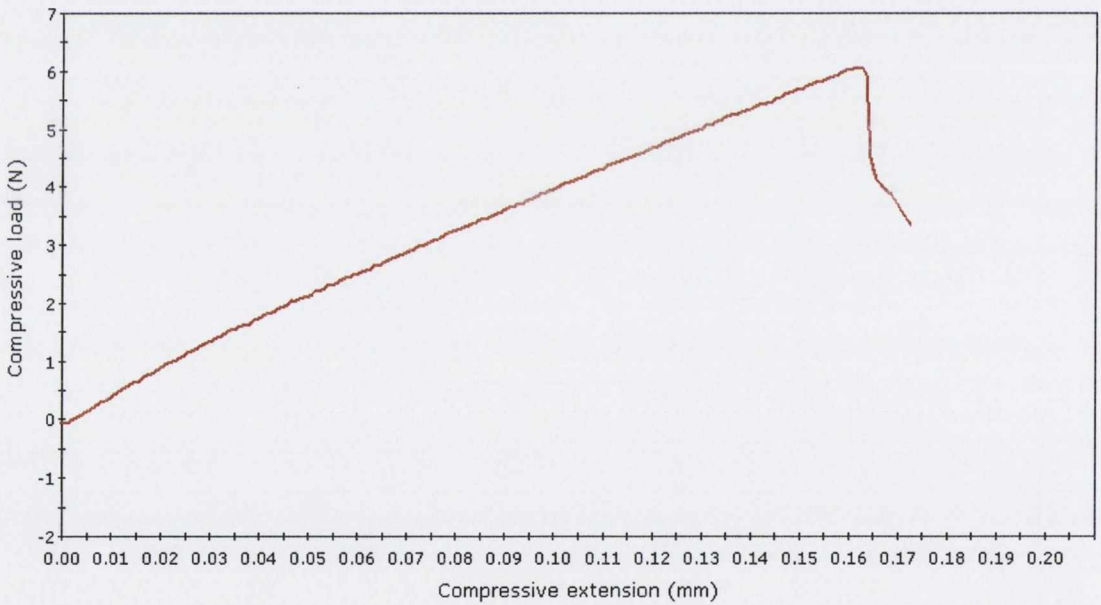
**Appendix Figure 3.** A load-deflection plot of a bar-shaped three-point flexure strength (TFS) specimen prepared with the manufacturer’s recommended powder content (100%) highlighting a maximum load of 8 N and a compressive extension of 0.09 mm. The three-point flexure modulus (TFM) was calculated from the initial linear segment of the load-deflection plot.



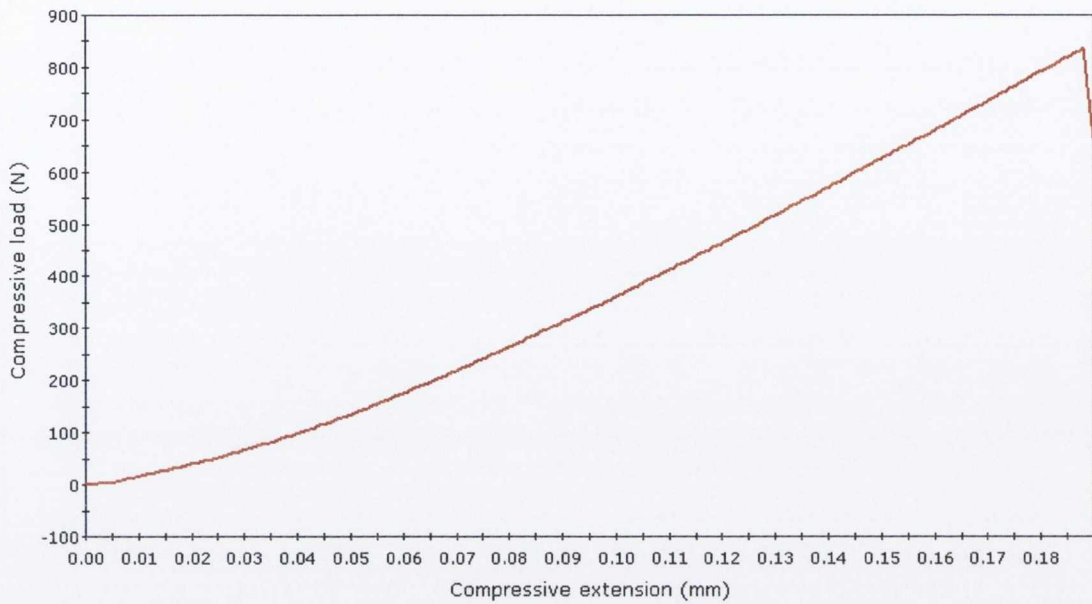
**Appendix Figure 4.** A load-deflection plot of a bar-shaped three-point flexure strength (TFS) specimen prepared with 20% of the manufacturer’s recommended powder content highlighting a maximum load of 3 N and a compressive extension of 0.4 mm. The three-point flexure modulus (TFM) was calculated from the initial linear segment of the load-deflection plot.



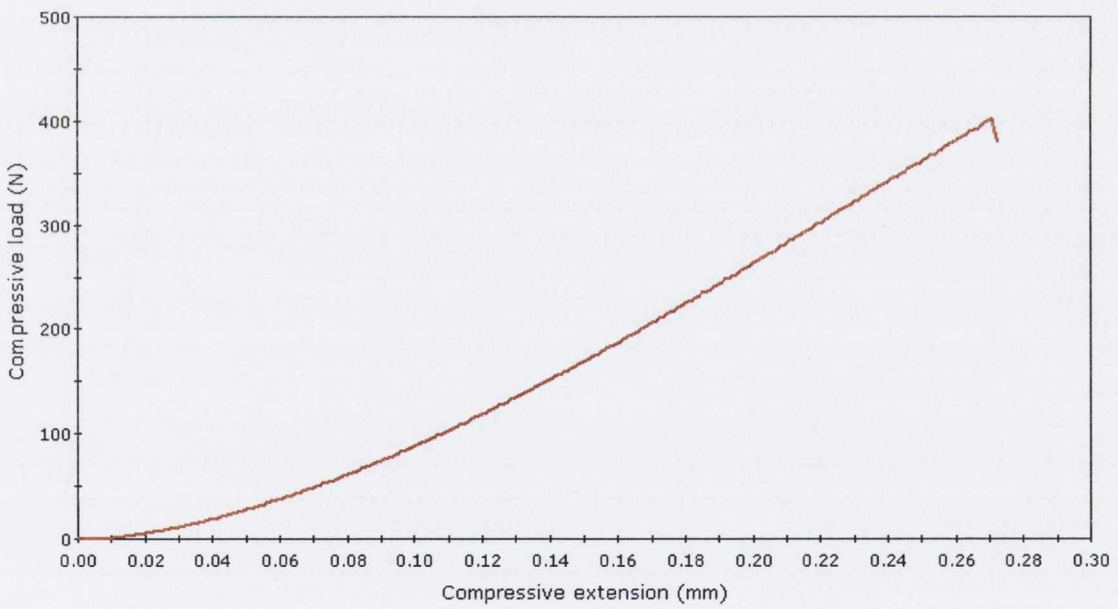
**Appendix Figure 5. A load-deflection plot of a disc-shaped biaxial flexure strength (BFS) specimen prepared with the manufacturer's recommended powder content (100%) highlighting a maximum load of 35 N and a compressive extension of 0.15 mm.**



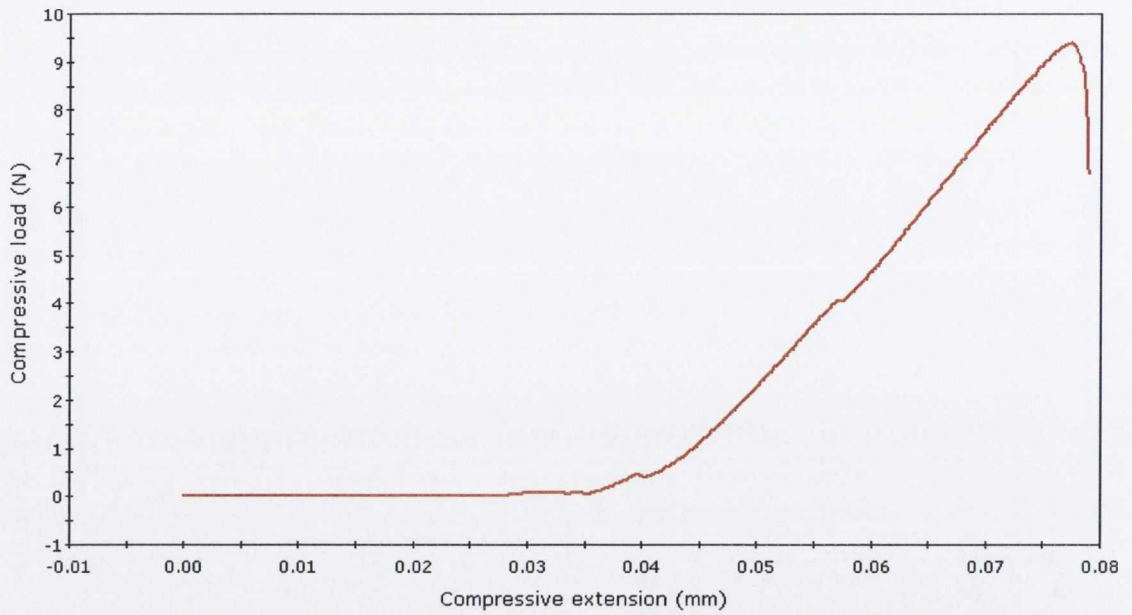
**Appendix Figure 6. A load-deflection plot of a disc-shaped biaxial flexure strength (BFS) specimen prepared with 20% of the manufacturer's recommended powder content highlighting a maximum load of 6 N and a compressive extension of 0.16 mm.**



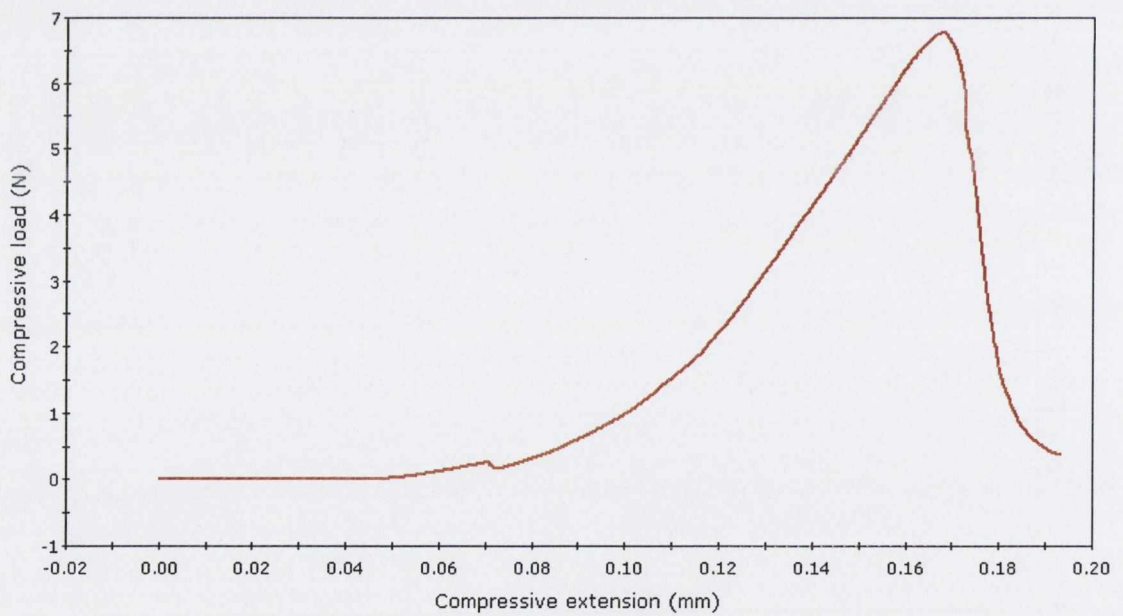
**Appendix Figure 7. A load-deflection plot of a disc-shaped Hertzian Indentation (HI) specimen prepared with the manufacturer's recommended powder content (100%) highlighting a maximum load of 800 N and a compressive extension of 0.19 mm.**



**Appendix Figure 8. A load-deflection plot of a disc-shaped Hertzian Indentation (HI) specimen prepared with 20% of the manufacturer's recommended powder content highlighting a maximum load of 400 N and a compressive extension of 0.27 mm.**



**Appendix Figure 9.** A load-deflection plot of a single-edge notched (SEN) fracture toughness ( $K_{IC}$ ) specimen prepared with the manufacturer's recommended powder content (100%) highlighting a maximum load of 9 N and a compressive extension of 0.04 mm.



**Appendix Figure 10.** A load-deflection plot of a single-edge notched (SEN) fracture toughness ( $K_{IC}$ ) specimen prepared with 20% of the manufacturer's recommended powder content highlighting a maximum load of 6.5 N and a compressive extension of 0.13 mm.

CFS data: hand-mixed GIs

100%

Sp No	1	2	3	Thickness	Load	Compr Str	Mean CS	Modulus	Mean Modulus
1				3.95	1,363.30	111.25	111.25	4.077	4.077
2				3.98	1,278.20	102.74	102.74	3.777	3.777
3				3.97	1,433.21	115.78	115.78	3.898	3.898
4				3.98	1,719.40	138.20	138.20	4.081	4.081
5				3.97	1,377.26	111.26	111.26	3.655	3.655
6				3.98	1,489.04	119.69	119.69	3.923	3.923
7				3.99	1,336.92	106.92	106.92	3.809	3.809
8				4.02	1,643.03	129.45	129.45	4.04	4.04
						<b>116.91</b>		<b>3.91</b>	
						<b>11.86</b>		<b>0.15</b>	
						<b>0.101418</b>		<b>0.039553</b>	
9			4	3.97	1330.73	105.90	105.90	3.692	3.692
10				3.97	1216.34	98.26	98.26	3.669	3.669
11				3.99	1359.82	108.75	108.75	3.638	3.638
12				3.96	1314.45	106.72	106.72	3.914	3.914
13				3.97	1310.95	105.90	105.90	3.922	3.922
14				3.96	1481.43	120.28	120.28	4.013	4.013
15				3.96	1288.73	104.64	104.64	4.08	4.08
16				3.95	1514.74	123.61	123.61	4.002	4.002
						<b>109.26</b>		<b>3.86625</b>	
						<b>8.44</b>		<b>0.174196</b>	
						<b>0.08</b>		<b>0.045056</b>	
17				3.97	1250.15	100.99	100.99	3.776	3.776
18				4.01	1254.83	99.36	99.36	3.799	3.799
19				3.99	1262.13	100.94	100.94	3.788	3.788
20				3.95	1480.4	120.81	120.81	3.907	3.907
						<b>105.53</b>	<b>111.57</b>	<b>3.82</b>	<b>3.87</b>
						<b>10.22</b>	<b>10.79</b>	<b>0.06</b>	<b>0.15</b>
						<b>0.096817</b>	<b>0.096739</b>	<b>0.015822</b>	<b>0.038057</b>

CFS data: hand-mixed GIs									
90%	1	2	3	Thickness	Load	Compr Str	Mean CS	Modulus	Mean Modulus
Sp No	1	2	3	3					
1				4	1194.56	95.06	95.06	3.217	3.217
2				3.98	1196.38	96.16	96.16	2.792	2.792
3				3.98	1278.75	102.78	102.78	3.542	3.542
4				3.98	1613.36	129.68	129.68	3.173	3.173
5				3.95	1261.48	102.94	102.94	3.199	3.199
6				3.95	1217.37	99.34	99.34	3.174	3.174
7				3.93	1261.22	103.97	103.97	3.218	3.218
8				3.89	1438.38	121.03	121.03	2.328	2.328
						<b>106.37</b>		<b>3.080375</b>	
						<b>12.36372</b>		<b>0.36476</b>	
						<b>0.116231</b>		<b>0.118414</b>	
9				3.97	1306.93	105.58	105.58	3.541	3.541
10				3.96	1173.58	95.29	95.29	3.722	3.722
11				3.99	1249.62	99.94	99.94	3.665	3.665
12				3.95	1338.85	109.26	109.26	3.671	3.671
13				3.94	1364.59	111.92	111.92	3.523	3.523
14				3.93	1403.03	115.66	115.66	3.859	3.859
15				3.92	993.39	82.31	82.31	3.569	3.569
16				3.96	1284.97	104.33	104.33	3.549	3.549
						<b>103.04</b>		<b>3.637375</b>	
						<b>10.58576</b>		<b>0.115281</b>	
						<b>0.102738</b>		<b>0.031693</b>	
17				3.98	1184.66	95.22	95.22	3.776	3.454
18				3.93	1152.07	94.97	94.97	3.799	3.68
19				3.91	1134.26	94.46	94.46	3.788	3.645
20				3.91	1289.82	107.42	107.42	3.907	3.638
						<b>98.02</b>	<b>103.37</b>	<b>3.8175</b>	<b>3.40795</b>
						<b>6.27</b>	<b>10.66</b>	<b>0.06</b>	<b>0.36195</b>
						<b>0.064013</b>	<b>0.10315</b>	<b>0.015822</b>	<b>0.106208</b>

CFS data: hand-mixed GIs									
Sp No	1	2	3	Thickness Load	Compr Str	Mean CS	Modulus	Mean Modulus	
1	4	1194.28	95.04	95.04	3.259	3.259	3.259		
2	3.98	1082.9	87.04	87.04	3.186	3.186	3.186		
3	3.97	1093.64	88.35	88.35	3.366	3.366	3.366		
4	3.94	1339.99	109.91	109.91	3.686	3.686	3.686		
5	3.95	1174.91	95.88	95.88	3.46	3.46	3.46		
6	3.97	1101.15	88.96	88.96	3.081	3.081	3.081		
7	4	1087.76	86.56	86.56	3.133	3.133	3.133		
8	3.98	1090.75	87.67	87.67	3.199	3.199	3.199		
			<b>92.43</b>		<b>3.29625</b>				
			<b>7.918253</b>		<b>0.199845</b>				
			<b>0.085672</b>		<b>0.060628</b>				
9	3.97	1286.64	103.94	103.94	3.359	3.359	3.359		
10	3.97	1164.84	94.10	94.10	3.388	3.388	3.388		
11	3.99	1412.68	112.98	112.98	3.601	3.601	3.601		
12	4.01	1327.41	105.11	105.11	3.437	3.437	3.437		
13	3.94	1136.35	93.20	93.20	3.39	3.39	3.39		
14	3.97	1101.38	88.97	88.97	3.22	3.22	3.22		
15	3.94	1252.43	102.72	102.72	3.457	3.457	3.457		
16	3.95	1250.54	102.05	102.05	3.411	3.411	3.411		
			<b>100.39</b>		<b>3.407875</b>				
			<b>7.774611</b>		<b>0.106213</b>				
			<b>0.077448</b>		<b>0.031167</b>				
17	3.93	922.45	76.04	76.04	2.539	2.539	2.539	3.454	
18	3.99	932.79	74.60	74.60	2.705	2.705	2.705	3.68	
19	3.97	1058.3	85.49	85.49	2.759	2.759	2.759	3.645	
20	3.96	1085.68	88.15	88.15	2.865	2.865	2.865	3.638	
			<b>81.07</b>	<b>93.34</b>	<b>2.717</b>	<b>3.4025</b>			
			<b>6.75</b>	<b>10.27</b>	<b>0.14</b>	<b>0.183963</b>			
			<b>0.083292</b>	<b>0.110044</b>	<b>0.050059</b>	<b>0.054067</b>			



CFS data: hand-mixed GIs

Sp No	1	2	3	Thickness	Load	Compr Str	Mean CS	Modulus	Mean Modulus
1			3.99	1024.81	81.96	81.96	2.855	2.855	2.855
2			3.96	1098.41	89.18	89.18	2.903	2.903	2.903
3			3.99	1198.16	95.83	95.83	3.104	3.104	3.104
4			4.01	1247.55	98.78	98.78	3.169	3.169	3.169
5			3.97	1248.85	100.89	100.89	3.176	3.176	3.176
6			3.99	1174.95	93.97	93.97	3.103	3.103	3.103
7			3.94	1124.81	92.26	92.26	3.091	3.091	3.091
8			3.89	1078.85	90.78	90.78	3.294	3.294	3.294
					<b>92.96</b>		<b>3.086875</b>		
					<b>5.933935</b>		<b>0.144289</b>		
					<b>0.063837</b>		<b>0.046743</b>		
9			3.93	1153.18	95.07	95.07	2.971	2.971	2.971
10			3.98	1100.78	88.48	88.48	3.008	3.008	3.008
11			3.99	1015.08	81.18	81.18	2.819	2.819	2.819
12			3.98	1247.09	100.24	100.24	3.148	3.148	3.148
13			3.99	1242.84	99.40	99.40	3.074	3.074	3.074
14			3.99	1088.72	87.07	87.07	2.818	2.818	2.818
15			3.96	965.6	78.40	78.40	2.879	2.879	2.879
16			3.98	1085.36	87.24	87.24	3	3	3
					<b>89.63</b>		<b>2.964625</b>		
					<b>8.005151</b>		<b>0.118803</b>		
					<b>0.089308</b>		<b>0.040074</b>		
17			3.91	1026.49	85.49	85.49	2.605	2.605	3.454
18			3.94	963.52	79.03	79.03	2.588	2.588	3.68
19			3.95	954.46	77.89	77.89	2.463	2.463	3.645
20			3.91	1050.04	87.45	87.45	2.829	2.829	3.638
					<b>82.46</b>	<b>89.53</b>	<b>2.62125</b>	<b>3.14145</b>	
					<b>4.72</b>	<b>7.45</b>	<b>0.15</b>	<b>0.272063</b>	
					<b>0.057206</b>	<b>0.08325</b>	<b>0.058097</b>	<b>0.086604</b>	

CFS data: hand-mixed GIs									
60%									
Sp No	1	2	3	Thickness	Load	Compr Str	Mean CS	Modulus	Mean Modulus
1				3.99	1032.91	82.61	82.61	2.549	2.549
2				3.96	1020.4	82.85	82.85	2.494	2.494
3				3.98	999.48	80.34	80.34	2.411	2.411
4				3.96	1178.95	95.72	95.72	2.804	2.804
5				3.96	1074.59	87.25	87.25	2.614	2.614
6				3.97	1027.15	82.98	82.98	2.5	2.5
7				3.98	1010.96	81.26	81.26	2.54	2.54
8				3.94	1080.76	88.64	88.64	2.648	2.648
						<b>85.21</b>		<b>2.57</b>	
						<b>5.11</b>		<b>0.119567</b>	
						<b>0.060028</b>		<b>0.046524</b>	
9				3.96	1034.28	83.98	83.98	2.483	2.483
10				3.98	985.6	79.22	79.22	2.441	2.441
11				4.02	1046.1	82.42	82.42	2.45	2.45
12				3.91	942.99	78.54	78.54	2.468	2.468
13				3.93	1083.3	89.30	89.30	2.542	2.542
14				3.92	910.55	75.45	75.45	2.429	2.429
15				3.96	965.93	78.43	78.43	2.431	2.431
16				4	1135.84	90.39	90.39	2.536	2.536
						<b>82.21</b>		<b>2.4725</b>	
						<b>5.383172</b>		<b>0.04489</b>	
						<b>0.065477</b>		<b>0.018156</b>	
17				3.97	964.26	77.90	77.90	2.355	2.355
18				3.99	1024.02	81.90	81.90	2.693	2.693
19				3.92	1096.86	90.88	90.88	2.665	2.665
20				3.97	1034.48	83.57	83.57	2.574	2.574
						<b>83.56</b>	<b>83.68</b>	<b>2.57175</b>	<b>2.53135</b>
						<b>5.43</b>	<b>5.18</b>	<b>0.15</b>	<b>0.11</b>
						<b>0.064988</b>	<b>0.061932</b>	<b>0.059558</b>	<b>0.043535</b>

CFS data: hand-mixed GIs

Sp No	1	2	3	Thickness	Load	Compr Str	Mean CS	Modulus	Mean Modulus
1				3.95	831.35	67.84	67.84	1.918	1.918
2				4.01	688.66	54.53	54.53	1.922	1.922
3				3.93	843.03	69.50	69.50	2.045	2.045
4				3.95	858.03	70.02	70.02	2.059	2.059
5				3.95	929.87	75.88	75.88	2.1	2.1
6				3.96	879.16	71.38	71.38	2.003	2.003
7				3.93	752.28	62.02	62.02	1.949	1.949
8				3.9	841.61	70.45	70.45	2.149	2.149
						<b>67.70</b>		<b>2.018125</b>	
						<b>6.57</b>		<b>0.084934</b>	
						<b>0.097096</b>		<b>0.042086</b>	
9				3.98	894.87	71.93	71.93	1.989	1.989
10				4.02	875.07	68.94	68.94	2.011	2.011
11				3.97	878.95	71.01	71.01	2.116	2.116
12				3.99	981.23	78.48	78.48	2.279	2.279
13				3.95	868.46	70.87	70.87	2.038	2.038
14				3.98	879.2	70.67	70.67	2.098	2.098
15				3.91	887.1	73.88	73.88	2.236	2.236
16				3.93	958.8	79.04	79.04	2.466	2.466
						<b>73.10</b>		<b>2.154125</b>	
						<b>3.76</b>		<b>0.162746</b>	
						<b>0.051368</b>		<b>0.075551</b>	
17				3.98	872.06	70.10	70.10	1.914	1.914
18				3.96	831.96	67.55	67.55	2.009	2.009
19				3.95	906.42	73.97	73.97	2.114	2.114
20				3.94	897.85	73.64	73.64	2.001	2.001
						<b>71.31</b>	<b>70.58</b>	<b>2.0095</b>	<b>2.0708</b>
						<b>3.06</b>	<b>5.37</b>	<b>0.08</b>	<b>0.14</b>
						<b>0.042929</b>	<b>0.076127</b>	<b>0.040746</b>	<b>0.065428</b>

CFS data: hand-mixed GIs									
40%									
SpNo	1	2	3	Thickness	Load	Compr Str	Mean CS	Modulus	Mean Modulus
1				4.05	869.67	67.51	67.51	1.815	1.815
2				4.01	724.54	57.37	57.37	1.582	1.582
3				3.95	815.17	66.52	66.52	1.777	1.777
4				3.99	798.85	63.89	63.89	1.695	1.695
5				3.96	763.49	61.99	61.99	1.705	1.705
6				3.99	831.45	66.50	66.50	1.615	1.615
7				4.06	780.85	60.32	60.32	1.61	1.61
8				4.01	821	65.01	65.01	1.589	1.589
						<b>63.64</b>		<b>1.67</b>	
						<b>3.51</b>		<b>0.09</b>	
						<b>0.055224</b>		<b>0.053042</b>	
9				3.98	835.05	67.12	67.12	1.735	1.735
10				3.94	788.68	64.69	64.69	1.724	1.724
11				3.96	654.54	53.14	53.14	1.236	1.236
12				3.97	603.68	48.77	48.77	1.195	1.195
13				3.94	567.39	46.54	46.54	1.27	1.27
14				3.93	625.32	51.55	51.55	1.237	1.237
15				3.92	636.09	52.71	52.71	1.166	1.166
16				3.94	615.48	50.48	50.48	1.27	1.27
						<b>54.37</b>		<b>1.35</b>	
						<b>7.46</b>		<b>0.23</b>	
						<b>0.137117</b>		<b>0.173057</b>	
17				3.93	957.93	78.97	78.97	1.293	1.293
18				3.93	638.8	52.66	52.66	1.312	1.312
19				3.94	623.57	51.14	51.14	1.473	1.473
20				3.93	490.35	40.42	40.42	0.907	0.907
						<b>55.79968</b>	<b>58.36</b>	<b>1.24625</b>	<b>1.46</b>
						<b>16.38</b>	<b>9.34</b>	<b>0.24</b>	<b>0.26</b>
						<b>0.293527</b>	<b>0.159979</b>	<b>0.192697</b>	<b>0.175622</b>

CFS data: hand-mixed GIs

Sp No	1	2	3	Thickness	Load	Compr Str	Mean CS	Modulus	Mean Modulus
1				3.94	595.35	48.83	48.83	1.129	1.129
2				3.96	533.86	43.35	43.35	0.945	0.945
3				3.98	529.9	42.59	42.59	0.845	0.845
4				3.98	601.25	48.33	48.33	0.881	0.881
5				4	583.57	46.44	46.44	0.962	0.962
6				4	566.54	45.08	45.08	0.974	0.974
7				4.02	580.42	45.73	45.73	1.088	1.088
8				4.01	496.95	39.35	39.35	0.987	0.987
						<b>44.96</b>		<b>0.98</b>	
						<b>3.14</b>		<b>0.10</b>	
						<b>0.069731</b>		<b>0.097487</b>	
9				4.03	522.11	40.93	40.93	0.926	0.926
10				4.04	504.48	39.35	39.35	0.922	0.922
11				3.94	459.72	37.71	37.71	0.713	0.713
12				3.92	403.84	33.46	33.46	0.632	0.632
13				3.98	402.36	32.34	32.34	0.62	0.62
14				3.97	390.64	31.56	31.56	0.64	0.64
15				3.99	466.78	37.33	37.33	0.727	0.727
16				3.94	463.17	37.99	37.99	0.78	0.78
						<b>36.33</b>		<b>0.75</b>	
						<b>3.44</b>		<b>0.12</b>	
						<b>0.094704</b>		<b>0.16524</b>	
17				3.96	446.82	36.28	36.28	0.729	0.729
18				3.94	339.65	27.86	27.86	0.697	0.697
19				3.97	454.76	36.74	36.74	0.727	0.727
20				4	379.43	30.19	30.19	0.752	0.752
						<b>32.76711</b>	<b>39.07</b>	<b>0.72625</b>	<b>0.83</b>
						<b>4.43</b>	<b>6.10</b>	<b>0.02</b>	<b>0.15</b>
						<b>0.13513</b>	<b>0.156129</b>	<b>0.031063</b>	<b>0.183132</b>

CFS data: hand-mixed GIs									
20%	1	2	3	Thickness Load	Compr Str	Mean CS	Modulus	Mean Modulus	
Sp No									
1				4.13	264.1	19.71	19.71	0.163	0.163
2				4.18	343.17	25.01	25.01	0.154	0.154
3				4.19	353.6	25.64	25.64	0.164	0.164
4				4.14	317.04	23.55	23.55	0.166	0.166
5				4.21	344.62	24.76	24.76	0.188	0.188
6				4.18	319.78	23.30	23.30	0.168	0.168
7				4.13	318.2	23.75	23.75	0.183	0.183
8				4.13	286.63	21.40	21.40	0.162	0.162
						<b>23.39</b>		<b>0.17</b>	
						<b>1.97</b>		<b>0.01</b>	
						<b>0.084302</b>		<b>0.067293</b>	
9				4.15	336.28	24.86	24.86	0.21	0.206
10				4.16	269.05	19.80	19.80	0.18	0.179
11				4.11	318.92	24.04	24.04	0.282	0.282
12				3.97	351.68	28.41	28.41	0.391	0.391
13				4.07	252.81	19.43	19.43	0.26	0.26
14				4.06	252.13	19.48	19.48	0.273	0.273
15				4.06	376.31	29.07	29.07	0.322	0.322
16				4.06	289.14	22.33	22.33	0.293	0.293
						<b>23.43</b>		<b>0.28</b>	
						<b>3.87</b>		<b>0.07</b>	
						<b>0.165355</b>		<b>0.238354</b>	
17				4.12	322.71	24.21	24.21	0.286	0.286
18				4.03	310.4	24.33	24.33	0.279	0.279
19				4.09	345.46	26.29	26.29	0.305	0.305
20				4.15	325	24.03	24.03	0.305	0.305
						<b>24.71547</b>	<b>23.67</b>	<b>0.29375</b>	<b>0.24</b>
						<b>1.06</b>	<b>2.73</b>	<b>0.01</b>	<b>0.07</b>
						<b>0.042891</b>	<b>0.115129</b>	<b>0.04528</b>	<b>0.297627</b>

TFS data: hand-mixed GIs

Batch No.	Spec No.	Width (mm)		Thickness (mm)		Span (mm)	Width (mm)	Thickness (mm)		Force (N)	Strength (MPa)	Deflection (GPa)	Modulus (GPa)		Mean Stre	Modulus	
		1	2	1	2			1	2				1	2			
1	1	2.221	2.164	2.282	2.12	20	2.2515	2.142	7.81	22.68096	0.082	8.608685	22.68096	8.608685			
	2	2.141	2.138	2.135	2.156	20	2.138	2.147	5.46	16.62042	0.06479	7.965459	16.62042	7.965459			
	3	2.104	2.1	2.195	2.104	20	2.1495	2.102	9.96	31.46138	0.0994	10.03847	31.46138	10.03847			
	4	2.101	2.14	2.123	2.116	20	2.112	2.128	9.08	28.48196	0.08259	10.80388	28.48196	10.80388			
	5	2.049	2.136	2.055	2.073	20	2.052	2.1045	8.42	27.79445	0.08117	10.84732	27.79445	10.84732			
2	1	2.114	2.129	2.121	2.103	20	2.1175	2.116	4.97	15.72617	0.0594	8.341219	15.72617	8.341219			
	2	2.254	2.095	2.179	2.139	20	2.2165	2.117	6.16	18.60341	0.06148	9.528983	18.60341	9.528983			
	3	2.078	2.097	2.103	2.095	20	2.0905	2.096	3.63	11.85756	0.03782	9.972203	11.85756	9.972203			
	4	2.093	2.069	2.052	2.087	20	2.0725	2.078	4.84	16.22486	0.05191	10.02751	16.22486	10.02751			
	5	2.048	2.126	2.058	2.088	20	2.053	2.107	4.89	16.09578	0.0508	10.02519	16.09578	10.02519			
3	1	2.122	2.15	2.118	2.13	20	2.12	2.14	5.24	16.19158	0.05425	9.297889	16.19158	9.297889			
	2	2.214	2.24	2.223	2.123	20	2.2185	2.1815	10.15	28.84147	0.08997	9.796552	28.84147	9.796552			
	3	2.101	2.086	2.071	2.123	20	2.086	2.1045	5.77	18.73635	0.0603	9.842998	18.73635	9.842998			
	4	2.156	2.059	2.045	2.065	20	2.1005	2.062	8.48	28.48506	0.08975	10.26131	28.48506	10.26131			
	5	2.019	2.096	2.032	2.097	20	2.0255	2.0965	6.81	22.94808	0.08403	8.684122	22.94808	8.684122			
4	1	2.103	2.133	2.122	2.182	20	2.1125	2.1575	9.15	27.91541	0.0791	10.905	27.91541	10.905			
	2	2.187	2.172	2.245	2.12	20	2.216	2.146	8.89	26.13327	0.09202	8.822479	26.13327	8.822479			
	3	2.092	2.104	2.064	2.092	20	2.078	2.098	8.21	26.92824	0.09131	9.371148	26.92824	9.371148			
	4	2.035	2.109	2.035	2.055	20	2.035	2.082	7.41	25.20076	0.07196	11.21374	25.20076	11.21374			
	5	2.032	2.109	2.042	2.136	20	2.037	2.1225	6.94	22.6879	0.05894	12.09053	22.6879	12.09053			
												<b>9.576574</b>					
												<b>0.604642</b>					
												<b>0.063138</b>					
												<b>23.04051</b>					
												<b>5.673106</b>					
												<b>0.246223</b>					
												<b>7.1135</b>	<b>25.77312</b>	<b>0.07215</b>	<b>10.48058</b>	<b>22.48075</b>	<b>9.822233</b>
												<b>1.916211</b>	<b>1.993715</b>	<b>0.017196</b>	<b>1.349974</b>	<b>5.772442</b>	<b>1.040941</b>
												<b>0.269377</b>	<b>0.077356</b>	<b>0.238344</b>	<b>0.128807</b>	<b>0.256773</b>	<b>0.105978</b>

TFS data: hand-mixed GIs

90%

Batch No.	Spec No.	Width (mm)	Thickness (mm)	Width (mm)	Thickness (mm)	Span (mm)	Width (mm)	Thickness (mm)	Force (N)	Strength (MPa)	Deflection Modulus (GPa)	Mean Stre Modulus	
1	1	2.218	2.153	2.229	2.202	20	2.2235	2.1775	6.04	17.18718	0.05242	10.03826	
	2	2.102	2.077	2.103	2.098	20	2.1025	2.0875	6.72	22.004	0.07084	9.919854	
	3	2.104	2.1	2.081	2.121	20	2.0925	2.1105	7.7	24.78425	0.07475	10.47341	
	4	2.062	2.051	2.032	2.026	20	2.047	2.0385	6.18	21.79568	0.07021	10.15242	
	5	2.044	2.1	2.041	2.099	20	2.0425	2.0995	8.71	29.02322	0.08615	10.69752	
2	1	2.141	2.145	2.138	2.122	20	2.1395	2.1335	9.39	28.92606	0.08379	10.78731	
	2	2.253	2.189	2.223	2.127	20	2.238	2.158	8.31	23.9199	0.08503	8.690493	
	3	2.09	2.117	2.113	2.126	20	2.1015	2.1215	7.15	22.67837	0.07027	10.14163	
	4	2.062	2.089	2.135	2.069	20	2.0985	2.079	6.18	20.44051	0.06398	10.24476	
	5	2.05	2.118	2.043	2.079	20	2.0465	2.0985	8.68	28.89424	0.08661	10.59847	
3	1	2.06	2.097	2.141	2.082	20	2.1005	2.0895	8.05	26.33357	0.09104	9.22877	
	2	2.054	2.082	2.049	2.115	20	2.0515	2.0985	7.14	23.70992	0.08327	9.04568	
	3	2.114	2.125	2.129	2.13	20	2.1215	2.1275	8.09	25.27479	0.09542	8.300177	
	4	2.288	2.209	2.256	2.12	20	2.272	2.1645	10.43	29.39558	0.10265	8.820115	
	5	2.089	2.107	2.114	2.125	20	2.1015	2.116	8.44	26.90934	0.09733	8.710625	
4	1	2.1	2.114	2.111	2.123	20	2.1055	2.1185	12.66	40.19229	0.10707	11.81287	
	2	2.177	2.12	2.247	2.213	20	2.212	2.1665	15.68	45.30695	0.14114	9.877903	
	3	2.068	2.08	2.099	2.114	20	2.0835	2.097	6.35	20.7924	0.07638	8.654366	
	4	2.077	2.11	2.037	2.069	20	2.057	2.0895	12.41	41.45472	0.12091	10.93901	
	5	2.021	2.096	2.033	2.058	20	2.027	2.077	10.23	35.09701	0.1034	10.89486	
								<b>8.727</b>	<b>36.56867</b>	<b>0.088133</b>	<b>10.4358</b>	<b>27.706</b>	<b>9.901425</b>
								<b>2.513455</b>	<b>9.544869</b>	<b>0.020528</b>	<b>1.208825</b>	<b>7.497602</b>	<b>0.961479</b>
								<b>0.288009</b>	<b>0.261012</b>	<b>0.232919</b>	<b>0.115834</b>	<b>0.270613</b>	<b>0.097105</b>



TFS data: hand-mixed GIs

Batch No.	Spec No.	Width (mm)	Thickness (mm)	Width (mm)	Thickness (mm)	Span (mm)	Width (mm)	Thickness (mm)	Force (N)	Strength (MPa)	Deflection (GPa)	Modulus (GPa)	Mean Stre	Mean Modulus
1	1	2.205	2.135	2.269	2.085	20	2.237	2.11	5.32	16.02515	0.06892	7.346543	16.02515	7.346543
	2	2.125	2.114	2.115	2.115	20	2.12	2.1145	6.63	20.98377	0.09311	7.105396	20.98377	7.105396
	3	2.098	2.127	2.126	2.116	20	2.112	2.1215	6.52	20.57732	0.08791	7.355569	20.57732	7.355569
	4	2.064	2.064	2.177	2.068	20	2.1205	2.066	7.67	25.42247	0.08909	9.208039	25.42247	9.208039
	5	2.051	2.068	2.045	2.098	20	2.048	2.083	7.34	24.78043	0.10308	7.69403	24.78043	7.69403
2	1	2.1	2.101	2.101	2.087	20	2.1005	2.094	5.96	19.41295	0.06264	9.866697	19.41295	9.866697
	2	2.209	2.143	2.207	2.214	20	2.208	2.1785	5.44	15.57421	0.0502	9.494092	15.57421	9.494092
	3	2.021	2.054	2.035	2.058	20	2.028	2.056	7.63	26.70125	0.08586	10.08385	26.70125	10.08385
	4	2.054	2.065	2.089	2.079	20	2.0715	2.072	4.99	16.83284	0.05879	9.212402	16.83284	9.212402
	5	2.035	2.04	2.153	2.034	20	2.094	2.037	8.09	27.93258	0.07755	11.78819	27.93258	11.78819
3	1	2.124	2.124	2.123	2.133	20	2.1235	2.1285	12.59	39.25974	0.14292	8.603784	39.25974	8.603784
	2	2.237	2.167	2.211	2.124	20	2.224	2.1455	5.08	14.88652	0.06814	6.78846	14.88652	6.78846
	3	2.108	2.1	2.089	2.089	20	2.0985	2.0945	7.2	23.46303	0.07969	9.371489	23.46303	9.371489
	4	2.032	2.094	2.062	2.094	20	2.047	2.094	6.26	20.92302	0.08184	8.139371	20.92302	8.139371
	5	2.076	2.077	2.063	2.095	20	2.0695	2.086	5.56	18.5226	0.06531	9.063935	18.5226	9.063935
4	1	2.1	2.08	2.1	2.08	20	2.1	2.08	7.99	26.38287	0.1091	7.750732	26.38287	7.750732
	2	2.19	2.13	2.19	2.11	20	2.19	2.12	7.96	24.26155	0.10473	7.284844	24.26155	7.284844
	3	2.05	2.08	2.04	2.04	20	2.045	2.06	4.94	17.07735	0.08586	6.436816	17.07735	6.436816
	4	2.02	2.09	2	2.08	20	2.01	2.085	7.58	26.02449	0.09876	8.425659	26.02449	8.425659
	5	2.02	2.04	1.99	2.03	20	2.005	2.035	5.77	20.84749	0.09361	7.295851	20.84749	7.295851
									<b>6.826</b>	<b>22.91875</b>	<b>0.085356</b>	<b>7.43878</b>	<b>22.29458</b>	<b>8.415787</b>
									1.745359	3.932587	0.02106	0.727891	5.705117	1.341179
									0.255693	0.171588	0.246737	0.097851	0.255897	0.159365

TFS data: hand-mixed GlS

70%

Batch No.	Spec No.	Width (mm)	Thickness (mm)	Width (mm)	Thickness (mm)	Span (mm)	Width (mm)	Thickness (mm)	Force (N)	Strength (MPa)	Deflection Modulus (GPa)	Mean Stre	Modulus	Mean Modulus
1	1	2.189	2.096	2.192	2.105	20	2.1905	2.1005	5.79	17.97261	0.08016	7.116059	17.97261	7.116059
	2	2.048	2.088	2.037	2.106	20	2.0425	2.097	12.45	41.58452	0.20715	6.382004	41.58452	6.382004
	3	2.121	2.106	2.096	2.107	20	2.1085	2.1065	6.77	21.70768	0.10646	6.453186	21.70768	6.453186
	4	2.064	2.064	2.121	2.051	20	2.0925	2.0575	8.04	27.22903	0.11191	7.883737	27.22903	7.883737
	5	2.01	2.03	2.01	2.03	20	2.01	2.03	4.82	17.45742	0.09616	5.962088	17.45742	5.962088
2	1	2.084	2.064	2.082	2.09	20	2.083	2.077	7.12	23.77054	0.08935	8.53919	23.77054	8.53919
	2	2.187	2.093	2.183	2.151	20	2.185	2.122	6.5	19.81949	0.09818	6.342095	19.81949	6.342095
	3	2.052	2.065	2.08	2.067	20	2.066	2.066	8.57	29.15487	0.12514	7.517846	29.15487	7.517846
	4	2.03	2.027	2.081	2.006	20	2.0555	2.0165	6.77	24.29942	0.10065	7.981651	24.29942	7.981651
	5	2.006	2.038	2.004	2.057	20	2.005	2.0475	7.91	28.2316	0.12229	7.516738	28.2316	7.516738
3	1	2.109	2.096	2.106	2.105	20	2.1075	2.1005	8.36	26.97209	0.13084	6.542747	26.97209	6.542747
	2	2.215	2.147	2.223	2.138	20	2.219	2.1425	9.6	28.27441	0.1488	5.9126	28.27441	5.9126
	3	2.074	2.084	2.083	2.096	20	2.0785	2.09	10.41	34.3977	0.14779	7.424151	34.3977	7.424151
	4	2.05	2.106	2.04	2.08	20	2.045	2.093	9.81	32.85175	0.18077	5.788575	32.85175	5.788575
	5	2.099	2.096	2.14	2.074	20	2.1195	2.085	10.75	35.0013	0.17264	6.482543	35.0013	6.482543
4	1	2.048	2.067	2.083	2.074	20	2.0655	2.0705	8.36	28.32382	0.14568	6.26016	28.32382	6.26016
	2	2.131	2.106	2.2	2.04	20	2.1655	2.073	8.05	25.95137	0.13498	6.183016	25.95137	6.183016
	3	2.032	2.053	2.058	2.067	20	2.045	2.06	9.54	32.97933	0.154204	6.921301	32.97933	6.921301
	4	2.041	2.013	1.992	2.033	20	2.0165	2.023	6.26	22.75651	0.09908	7.568895	22.75651	7.568895
	5	1.991	2.002	1.985	2.021	20	1.988	2.0115	8.72	32.5223	0.14083	7.653759	32.5223	7.653759
								<b>8.23</b>	<b>28.50667</b>	<b>0.129653</b>	<b>6.917426</b>	<b>27.56289</b>	<b>6.921617</b>	
								<b>1.856876</b>	<b>4.351936</b>	<b>0.033298</b>	<b>0.696055</b>	<b>6.173593</b>	<b>0.795028</b>	
								<b>0.225623</b>	<b>0.152664</b>	<b>0.256821</b>	<b>0.100623</b>	<b>0.223982</b>	<b>0.114862</b>	

TFS data: hand-mixed GIs

Batch No.	Spec No.	Width (mm)	Thickness (mm)	Width (mm)	Thickness (mm)	Span (mm)	Width (mm)	Thickness (mm)	Force (N)	Strength (MPa)	Deflection (GPa)	Modulus (GPa)	Mean Stre	Mean Modulus
1	1	2.251	2.094	2.21	2.174	20	2.2305	2.134	7.75	22.88927	0.12171	5.875164	22.88927	5.875164
	2	2.112	2.115	2.122	2.099	20	2.117	2.107	8.97	28.6328	0.15411	5.878644	28.6328	5.878644
	3	2.077	2.092	2.105	2.092	20	2.091	2.092	5.72	18.75167	0.10114	5.90832	18.75167	5.90832
	4	2.054	2.07	2.172	2.055	20	2.113	2.0625	7.24	24.1642	0.12517	6.240034	24.1642	6.240034
	5	2.035	2.076	2.045	2.046	20	2.04	2.061	4.83	16.72177	0.08543	6.331441	16.72177	6.331441
2	1	1.987	2.033	2.022	2.031	20	2.0045	2.032	4.99	18.08707	0.08927	6.647339	18.08707	6.647339
	2	2.061	2.045	2.061	2.07	20	2.061	2.0575	5.23	17.98313	0.08674	6.717609	17.98313	6.717609
	3	2.184	2.133	2.174	2.052	20	2.179	2.0925	7.19	22.60799	0.10785	6.678595	22.60799	6.678595
	4	2.025	2.04	2.059	2.057	20	2.042	2.0485	6.14	21.49621	0.10391	6.732516	21.49621	6.732516
	5	2.128	2.035	2.024	2.038	20	2.076	2.0365	7.29	25.4011	0.11422	7.280057	25.4011	7.280057
3	1	2.019	2.093	2.05	2.087	20	2.0345	2.09	6.22	20.9972	0.11162	6.000422	20.9972	6.000422
	2	2.103	2.107	2.106	2.103	20	2.1045	2.105	7.95	25.57615	0.14791	5.47639	25.57615	5.47639
	3	2.139	2.086	2.035	2.055	20	2.087	2.0705	6.35	21.29227	0.12077	5.676707	21.29227	5.676707
	4	2.235	2.069	2.205	2.166	20	2.22	2.1175	6.23	18.77628	0.11043	5.353129	18.77628	5.353129
	5	2.062	2.06	2.095	2.07	20	2.0785	2.065	7.65	25.89361	0.14569	5.73788	25.89361	5.73788
4	1	2.046	2.046	2.053	2.045	20	2.0495	2.0455	7.78	27.21786	0.15169	5.847985	27.21786	5.847985
	2	2.143	2.102	2.206	2.034	20	2.1745	2.068	5.4	17.42026	0.09318	6.026845	17.42026	6.026845
	3	2.035	2.03	2.012	2.04	20	2.0235	2.035	7.44	26.63558	0.14388	6.064654	26.63558	6.064654
	4	2.001	2.023	2.103	2.004	20	2.052	2.0135	7.04	25.38711	0.12986	6.472842	25.38711	6.472842
	5	1.999	1.991	1.999	2.013	20	1.999	2.002	6.02	22.54119	0.11382	6.594819	22.54119	6.594819
									6.6715	23.8404	0.11792	6.201429	22.42364	6.17707
									1.123801	4.016179	0.021979	0.317226	3.62179	0.493109
									0.168448	0.168461	0.186389	0.051154	0.161517	0.079829

TFS data: hand-mixed GIs

50%

Batch No.	Spec No.	Width (mm)	Thickness (mm)	Width (mm)	Thickness (mm)	Span (mm)	Width (mm)	Thickness (mm)	Force (N)	Strength (MPa)	Deflection Modulus (GPa)	Mean Stre Modulus	
1	1	2.12	2.098	2.111	2.098	20	2.1155	2.098	5.16	16.62444	0.09244	5.714658	
	2	2.103	2.085	2.082	2.089	20	2.0925	2.087	5.44	17.90646	0.1085	5.27189	
	3	2.165	2.068	2.044	2.053	20	2.1045	2.0605	5.53	18.56745	0.09575	6.274073	
	4	2.039	2.106	2.049	2.061	20	2.044	2.0835	5.88	19.88065	0.12502	5.088226	
	5	1.99	2.01	2.01	2.05	20	2	2.03	5.86	21.33029	0.15638	4.479487	
2	1	2.113	2.023	2.156	2.04	20	2.1345	2.0315	5.54	18.86693	0.12757	4.853383	
	2	2.024	2.023	2.024	2	20	2.024	2.0115	4.53	16.59468	0.10643	5.167655	
	3	1.991	1.999	2.023	2.002	20	2.007	2.0005	5.51	20.58014	0.12138	5.650299	
	4	2.048	1.977	1.964	1.985	20	2.006	1.981	4.86	18.52071	0.10617	5.870568	
	5	1.962	1.98	1.956	2.008	20	1.959	1.994	6.5	25.03513	0.15273	5.48036	
3	1	1.973	1.951	1.961	1.989	20	1.967	1.97	6.42	25.23013	0.13845	6.16693	
	2	2.004	1.994	1.977	1.999	20	1.9905	1.9965	5.91	22.34642	0.13884	5.374434	
	3	1.942	1.977	1.947	1.979	20	1.9445	1.978	6.35	25.04001	0.14106	5.982918	
	4	2.106	2.033	2.119	2.021	20	2.1125	2.027	6.5	22.46624	0.13701	5.393034	
	5	2.02	2	2.038	2.032	20	2.029	2.016	6.68	24.30159	0.14332	24.30159	
4	1	2.01	2.013	2.019	2.027	20	2.0145	2.02	4.71	17.18985	0.11351	4.99799	
	2	2.095	2.053	2.157	1.994	20	2.126	2.0235	7.76	26.7432	0.22608	3.897236	
	3	1.977	2.005	2.003	2.003	20	1.99	2.004	7.63	28.6416	0.1756	5.42605	
	4	2.025	1.968	1.95	1.965	20	1.9875	1.9665	6.27	24.47337	0.13587	6.106396	
	5	1.938	2.005	1.956	1.969	20	1.947	1.987	5.7	22.2451	0.16781	4.447618	
								<b>5.937</b>	<b>23.85862</b>	<b>0.135496</b>	<b>4.975058</b>	<b>21.62922</b>	<b>5.36252</b>
								<b>0.857101</b>	<b>4.434284</b>	<b>0.031143</b>	<b>0.854947</b>	<b>3.577913</b>	<b>0.617185</b>
								<b>0.144366</b>	<b>0.185857</b>	<b>0.229846</b>	<b>0.171847</b>	<b>0.16542</b>	<b>0.115092</b>

TFS data: hand-mixed GIs

Batch No.	Spec No.	Width (mm)	Thickness (mm)	Width (mm)	Thickness (mm)	Span (mm)	Width (mm)	Thickness (mm)	Force (N)	Strength (MPa)	Deflection (GPa)	Modulus (GPa)	Mean Stre	Mean Modulus
1	1	2.196	2.137	2.221	2.089	20	2.2085	2.113	7.02	21.35807	0.18543	3.634053	21.35807	3.634053
	2	2.104	2.092	2.099	2.094	20	2.1015	2.093	6.11	19.91107	0.18111	3.501803	19.91107	3.501803
	3	2.032	2.063	2.04	2.028	20	2.036	2.0455	6.28	22.11588	0.21001	3.432207	22.11588	3.432207
	4	2.064	2.077	2.099	2.068	20	2.0815	2.0725	4.53	15.20036	0.13229	3.696078	15.20036	3.696078
	5	2.045	2.051	2.189	2.04	20	2.117	2.0455	6.38	21.60837	0.19371	3.635627	21.60837	3.635627
2	1	2.019	2.001	2.021	2.009	20	2.02	2.005	6.44	23.79178	0.19794	3.996573	23.79178	3.996573
	2	2.131	2.08	2.128	2.019	20	2.1295	2.0495	5.29	17.74204	0.15221	3.791587	17.74204	3.791587
	3	1.996	2.004	2.053	2.138	20	2.0245	2.071	5.15	17.79305	0.14361	3.988361	17.79305	3.988361
	4	2.048	1.977	1.971	1.988	20	2.0095	1.9825	5.48	20.81553	0.1546	4.527656	20.81553	4.527656
	5	1.942	1.975	1.965	1.973	20	1.9535	1.974	5.37	21.16352	0.17222	4.15017	21.16352	4.15017
3	1	2.216	2.137	2.179	2.09	20	2.1975	2.1135	6.59	20.14064	0.19499	3.258123	20.14064	3.258123
	2	2.102	2.076	2.086	2.057	20	2.094	2.0665	6.53	21.9072	0.20885	3.383964	21.9072	3.383964
	3	2.135	2.052	2.029	2.038	20	2.082	2.045	6.63	22.84375	0.23014	3.235868	22.84375	3.235868
	4	2.072	2.058	2.056	2.07	20	2.064	2.064	6.64	22.6548	0.23523	3.110761	22.6548	3.110761
	5	2.002	2.044	2.026	2.04	20	2.014	2.042	6.35	22.68423	0.23782	3.114072	22.68423	3.114072
4	1	1.999	1.988	2.046	2	20	2.0225	1.994	5.26	19.62312	0.14979	4.379948	19.62312	4.379948
	2	2.099	2.078	2.089	2.015	20	2.094	2.0465	4.5	15.39337	0.11393	4.401417	15.39337	4.401417
	3	1.972	1.989	2.003	1.985	20	1.9875	1.987	6.67	25.50024	0.17354	4.930097	25.50024	4.930097
	4	1.933	1.955	2.041	1.951	20	1.987	1.953	6.38	25.25455	0.17613	4.89455	25.25455	4.89455
	5	1.911	1.944	1.936	1.93	20	1.9235	1.937	5.15	21.40805	0.16126	4.569088	21.40805	4.569088
									<b>20.03875</b>		<b>3.579953</b>			
									<b>2.825998</b>		<b>0.108913</b>			
									<b>0.141027</b>		<b>0.030423</b>			
									<b>20.26118</b>		<b>4.09087</b>			
									<b>2.550706</b>		<b>0.275349</b>			
									<b>0.125891</b>		<b>0.067308</b>			
									<b>5.9375</b>	<b>21.43586</b>	<b>0.180241</b>	<b>4.63502</b>	<b>20.94548</b>	<b>3.8816</b>
									<b>0.764921</b>	<b>4.210108</b>	<b>0.034158</b>	<b>0.263821</b>	<b>2.787615</b>	<b>0.579377</b>
									<b>0.128829</b>	<b>0.196405</b>	<b>0.189514</b>	<b>0.056919</b>	<b>0.133089</b>	<b>0.149262</b>

TFS data: hand-mixed GIs												
30%												
Batch No.	Spec No.	Width (mm)	Thickness (mm)	Width (mm)	Thickness (mm)	Span (mm)	Width (mm)	Thickness (mm)	Force (N)	Strength (MPa)	Deflection (GPa)	Mean Stre Modulus
1	1	2.032	1.995	2.104	1.95	20	2.068	1.9725	6.3	23.48969	0.29386	2.701646
	2	1.954	1.922	1.953	1.953	20	1.9535	1.9375	7.22	29.53668	0.40385	2.516567
	3	1.936	1.952	1.96	1.907	20	1.948	1.9295	6.44	26.63966	0.34352	2.679418
	4	1.898	1.9	1.892	1.916	20	1.895	1.908	3.52	15.30728	0.19119	2.797455
	5	1.876	1.891	1.895	1.897	20	1.8855	1.894	4.12	18.27393	0.24382	2.638101
										<b>22.64945</b>		
										<b>5.85479</b>		
										<b>0.258496</b>		
2	1	1.976	1.988	1.983	1.966	20	1.9795	1.977	4.42	17.13857	0.21736	2.65887
	2	2.085	1.991	2.1	2.007	20	2.0925	1.999	5.5	19.73299	0.27935	2.355809
	3	1.969	1.977	1.964	1.99	20	1.9665	1.9835	5.27	20.43495	0.26726	2.569899
	4	2.043	1.921	1.942	1.934	20	1.9925	1.9275	5.09	20.62775	0.29875	2.388132
	5	1.964	1.951	1.905	1.941	20	1.9345	1.946	4.97	20.35276	0.28176	2.474627
										<b>19.6574</b>		
										<b>1.447402</b>		
										<b>0.073631</b>		
3	1	2.179	2.041	2.139	2.103	20	2.159	2.072	5.64	18.25443	0.29261	2.007234
	2	1.978	2.021	2.002	2.012	20	1.99	2.0165	4.63	17.16535	0.2673	2.12307
	3	2.018	2.032	2.016	2.012	20	2.017	2.022	4.38	15.93409	0.23747	2.21231
	4	2.041	2.045	2.05	2.046	20	2.0455	2.0455	4.39	15.38818	0.2355	2.129637
	5	1.997	2.008	2.099	1.999	20	2.048	2.0035	4.2	15.32717	0.21316	2.39263
										<b>16.41384</b>		
										<b>1.266445</b>		
										<b>0.077157</b>		
										<b>0.142859</b>		
										<b>0.065743</b>		
4	1	1.917	1.915	1.93	1.919	20	1.9235	1.917	3.7	15.70314	0.20884	2.614927
	2	2.016	1.898	2.031	1.997	20	2.0235	1.9475	3.46	13.52506	0.21372	2.166334
	3	1.895	1.905	1.926	1.902	20	1.9105	1.9035	4.49	19.45874	0.24985	2.727667
	4	1.86	1.898	1.879	1.893	20	1.8695	1.8955	4.71	21.03629	0.24914	2.969687
	5	1.882	1.877	1.868	1.887	20	1.875	1.882	3.07	13.86817	0.17149	2.864636
										<b>4.776</b>	<b>16.71828</b>	<b>2.66865</b>
										<b>1.061163</b>	<b>3.372893</b>	<b>0.311338</b>
										<b>0.222187</b>	<b>0.201749</b>	<b>0.208894</b>
										<b>0.25799</b>	<b>2.66865</b>	<b>18.85974</b>
										<b>0.053893</b>	<b>0.311338</b>	<b>4.137424</b>
										<b>0.116665</b>	<b>0.219379</b>	<b>0.108256</b>

TFS data: hand-mixed Glis

Batch No.	Spec No.	Width (mm)	Thickness (mm)	Width (mm)	Thickness (mm)	Span (mm)	Width (mm)	Thickness (mm)	Force (N)	Strength (MPa)	Deflection (GPa)	Modulus (GPa)	Mean Stire	Mean Modulus
1	1	2.123	2.099	2.157	2.13	20	2.14	2.1145	3.2	10.03326	0.39635	0.798113	10.03326	0.798113
	2	2.033	2.055	2.088	2.087	20	2.0605	2.071	3.09	10.48931	0.4734	0.713259	10.48931	0.713259
	3	2.222	2.1	2.224	2.095	20	2.223	2.0975	4.25	13.03667	0.5564	0.744709	13.03667	0.744709
	4	2.08	2.088	2.162	2.075	20	2.121	2.0815	4.01	13.09098	0.46972	0.892618	13.09098	0.892618
	5	2.122	2.089	2.117	2.104	20	2.1195	2.0965	3.44	11.07788	0.42665	0.825655	11.07788	0.825655
2	1	2.016	1.932	2.006	1.98	20	2.011	1.956	3.99	15.55766	0.5504	0.963398	15.55766	0.963398
	2	1.909	1.902	1.887	1.926	20	1.898	1.914	3.18	13.72045	0.46948	1.01793	13.72045	1.01793
	3	1.932	1.908	1.938	1.922	20	1.935	1.915	3.42	14.45869	0.58515	0.860204	14.45869	0.860204
	4	1.936	1.896	1.882	1.891	20	1.909	1.8935	3.93	17.22572	0.54446	1.113922	17.22572	1.113922
	5	2.25	2.15	2.22	2.18	20	2.235	2.165	2.9	8.304738	0.65221	0.392093	8.304738	0.392093
3	1	1.947	1.87	1.995	1.914	20	1.971	1.892	2.25	9.56698	0.77736	0.433651	9.56698	0.433651
	2	1.846	1.839	1.836	1.873	20	1.841	1.856	1.89	8.940737	0.62407	0.514601	8.940737	0.514601
	3	1.863	1.841	1.855	1.857	20	1.859	1.849	2.72	12.83917	0.91618	0.505275	12.83917	0.505275
	4	2.16	2.14	2.16	2.12	20	2.16	2.13	2.77	8.479848	0.64051	0.414373	8.479848	0.414373
	5	2.14	2.13	2.14	2.16	20	2.14	2.145	2.6	7.921843	0.60664	0.40586	7.921843	0.40586
4	1	1.876	1.864	1.878	1.876	20	1.877	1.87	4.59	20.97908	0.42173	1.773451	20.97908	1.773451
	2	1.947	1.892	1.997	1.914	20	1.972	1.903	4.47	18.77778	0.38445	1.711096	18.77778	1.711096
	3	1.838	1.855	1.821	1.845	20	1.8295	1.85	3.81	18.25452	0.40835	1.610923	18.25452	1.610923
	4	1.806	1.829	1.898	1.827	20	1.852	1.828	4.43	21.47492	0.42955	1.823268	21.47492	1.823268
	5	1.815	1.826	1.811	1.847	20	1.813	1.8365	4.35	21.34179	0.40153	1.929437	21.34179	1.929437
									<b>3.4645</b>	<b>20.16562</b>	<b>0.53673</b>	<b>1.769635</b>	<b>13.7786</b>	<b>0.972192</b>
									<b>0.790446</b>	<b>1.527889</b>	<b>0.139358</b>	<b>0.119419</b>	<b>4.567346</b>	<b>0.519826</b>
									<b>0.228156</b>	<b>0.075767</b>	<b>0.259644</b>	<b>0.067483</b>	<b>0.331481</b>	<b>0.534695</b>

BFS data: hand-mixed GIs									
100%									
Batch 1	1	2	3	4	Thickness	Load	Biax Str	Biax Str	Compressive extension
1	1.113	1.128		4	1.1205	25.83	43.18335	43.18335	0.125
2	1.18	1.176			1.178	34.16	50.89382	50.89382	0.140
3	1.192	1.236			1.214	39.21	54.49943	54.49943	0.154
4	1.151	1.144			1.1475	42.12	66.66245	66.66245	0.165
5	1.077	1.083			1.08	27.24	49.56229	49.56229	0.134
							<b>52.96027</b>		0.174
							<b>8.682215</b>		0.171
							<b>0.163938</b>		0.180
Batch 2	1	2	3	4	Thickness	Load	Biax Str	Biax Str	Compressive extension
1	1.2	1.246		4	1.223	40.24	54.98562	54.98562	0.157
2	1.188	1.202			1.195	39.34	56.70672	56.70672	0.161
3	1.168	1.184			1.176	37.85	56.61272	56.61272	0.140
4	1.205	1.196			1.2005	37.69	53.75595	53.75595	0.151
5	1.17	1.185			1.1775	31.66	47.21534	47.21534	0.141
							<b>53.85527</b>		0.139
							<b>3.908662</b>		0.143
							<b>0.072577</b>		0.168
Batch 3	1	2	3	4	Thickness	Load	Biax Str	Biax Str	Compressive extension
1	1.177	1.149		4	1.163	38.15	58.54191	58.54191	0.146
2	1.147	1.136			1.1415	25.49	40.83237	40.83237	0.148
3	1.166	1.17			1.168	31.1	47.25417	47.25417	<b>0.154</b>
4	1.119	1.13			1.1245	29.11	48.26961	48.26961	<b>0.016</b>
5	1.152	1.162			1.157	34.74	53.94817	53.94817	<b>0.107</b>
							<b>49.76925</b>		
							<b>6.761386</b>		
							<b>0.135855</b>		
Batch 4	1	2	3	4	Thickness	Load	Biax Str	Biax Str	Compressive extension
1	1.18	1.173		4	1.1765	33.17	49.5642	49.5642	
2	1.172	1.207			1.1895	44.46	64.77237	64.77237	
3	1.215	1.169			1.192	40.98	59.41412	59.41412	
4	1.085	1.072			1.0785	32.86	59.97888	59.97888	
5	1.179	1.147			1.163	39.76	61.01249	61.01249	
							<b>58.94841</b>	<b>53.8833</b>	
							<b>5.646259</b>	<b>6.844852</b>	
							<b>0.095783</b>	<b>0.127031</b>	



BFS data: hand-mixed GIs									
90%									
Batch 1	1	2	3	4	Thickness	Load	Biax Str	Biax Str	Compressive extension
1	1.213	1.152	1.212	4	1.192333	30.53	44.23484	44.23484	0.143
2	1.158	1.172			1.165	33.45	51.12688	51.12688	0.157
3	1.141	1.164			1.1525	31.79	49.81215	49.81215	0.154
4	1.1	1.193			1.1465	20.49	32.49426	32.49426	0.131
5	1.154	1.156	1.101		1.137	29.4	47.52595	47.52595	0.157
							<b>45.03882</b>		0.167
							<b>7.484106</b>		0.158
							<b>0.16617</b>		0.156
Batch 2	1	2	3	4	Thickness	Load	Biax Str	Biax Str	Compressive extension
1	1.173	1.139		4	1.156	37	57.5723	57.5723	0.160
2	1.165	1.167			1.166	35.59	54.29035	54.29035	0.136
3	1.114	1.117			1.1155	38.35	64.7776	64.7776	0.153
4	1.251	1.124			1.1875	38.28	55.98574	55.98574	0.171
5	1.199	1.218			1.2085	35.97	50.52266	50.52266	0.164
							<b>56.62973</b>		0.166
							<b>5.254999</b>		0.145
							<b>0.092796</b>		0.162
Batch 3	1	2	3	4	Thickness	Load	Biax Str	Biax Str	Compressive extension
1	1.207	1.202		4	1.2045	29.92	42.34765	42.34765	0.170
2	1.203	1.208			1.2055	38.53	54.42962	54.42962	0.150
3	1.187	1.195			1.191	44.33	64.39557	64.39557	<b>0.156</b>
4	1.161	1.147			1.154	38.11	59.53644	59.53644	<b>0.011</b>
5	1.16	1.134			1.147	38.63	61.20028	61.20028	<b>0.071</b>
							<b>56.38191</b>		
							<b>8.633631</b>		
							<b>0.153128</b>		
Batch 4	1	2	3	4	Thickness	Load	Biax Str	Biax Str	Compressive extension
1	1.191	1.243		4	1.217	34.63	47.86012	47.86012	
2	1.169	1.184			1.1765	37.03	55.332	55.332	
3	1.127	1.144			1.1355	35.24	57.13984	57.13984	
4	1.19	1.203			1.1965	44.57	64.05991	64.05991	
5	1.149	1.131			1.14	35.24	56.62201	56.62201	
							<b>56.20277</b>	<b>53.56331</b>	
							<b>5.769456</b>	<b>8.1134</b>	
							<b>0.102654</b>	<b>0.151473</b>	

BFS data: hand-mixed GIs									
80%									
Batch 1	1	2	3	4	Thickness	Load	Biax Str	Biax Str	Compressive extension
1	1.188	1.146		4	1.167	24.52	37.32994	37.32994	0.141
2	1.132	1.12		4	1.126	36.29	59.99107	59.99107	0.175
3	0.988	0.989		4	0.9885	18.51	41.25909	41.25909	0.150
4	1.099	1.093		4	1.096	27.71	48.74225	48.74225	0.159
5	1.114	1.093		4	1.1035	31.84	55.13582	55.13582	0.171
							<b>48.49163</b>		0.149
							<b>9.398644</b>		0.156
							<b>0.19382</b>		0.140
Batch 2	1	2	3	4	Thickness	Load	Biax Str	Biax Str	Compressive extension
1	1.118	1.14		4	1.129	36.11	59.32917	59.32917	0.134
2	1.088	1.087		4	1.0875	37.42	67.01055	67.01055	0.148
3	1.109	1.099		4	1.104	29.57	51.15167	51.15167	0.159
4	1.112	1.098		4	1.105	33.98	58.65808	58.65808	0.159
5	1.105	1.14		4	1.1225	28.74	47.85166	47.85166	0.159
							<b>56.80022</b>		0.132
							<b>7.517994</b>		0.151
							<b>0.132359</b>		0.133
Batch 3	1	2	3	4	Thickness	Load	Biax Str	Biax Str	Compressive extension
1	1.157	1.164		4	1.1605	33.06	50.98333	50.98333	0.155
2	1.128	1.155		4	1.1415	35.08	56.19457	56.19457	0.162
3	1.153	1.186		4	1.1695	36.32	55.02262	55.02262	<b>0.152</b>
4	1.135	1.111		4	1.123	32.91	54.73854	54.73854	<b>0.012</b>
5	1.118	1.115		4	1.1165	23.85	40.20248	40.20248	<b>0.079</b>
							<b>51.42831</b>		
							<b>6.572883</b>		
							<b>0.127807</b>		
Batch 4	1	2	3	4	Thickness	Load	Biax Str	Biax Str	Compressive extension
1	1.205	1.175		4	1.19	30.72	44.71165	44.71165	
2	1	1.009		4	1.0045	21.88	47.01004	47.01004	
3	1.11	1.096		4	1.103	33.35	57.81082	57.81082	
4	1.096	1.112		4	1.104	34.14	59.05708	59.05708	
5	1.112	1.103		4	1.1075	32.6	55.9842	55.9842	
							<b>52.91476</b>	<b>52.40873</b>	
							<b>6.581749</b>	<b>7.625231</b>	
							<b>0.124384</b>	<b>0.145495</b>	

BFS data: hand-mixed GIs									
70%									
Batch 1	1	2	3	4	Thickness	Load	Biax Str	Biax Str	Compressive extension
1	1.083	1.072		1.0775	21.59	39.49197	39.49197	0.141	
2	1.167	1.167		1.167	30.86	46.98214	46.98214	0.158	
3	1.06	1.059		1.0595	29.22	55.5566	55.5566	0.154	
4	1.054	1.042		1.048	25.15	49.031	49.031	0.145	
5	1.056	1.08		1.068	29.49	55.05076	55.05076	0.155	
						<b>49.22249</b>		0.141	
						<b>6.592204</b>		0.160	
						<b>0.133927</b>		0.146	
Batch 2	1	2	3	4	Thickness	Load	Biax Str	Biax Str	Compressive extension
1	1.221	1.193		1.207	31.45	44.30073	44.30073	0.160	
2	1.207	1.216		1.2115	41.07	57.35692	57.35692	0.187	
3	1.139	1.173		1.156	30.76	47.86281	47.86281	0.186	
4	1.051	1.054		1.0525	20.46	39.49739	39.49739	0.180	
5	1.107	1.094		1.1005	29.01	50.55062	50.55062	0.187	
						<b>47.91369</b>		0.143	
						<b>6.708541</b>		0.161	
						<b>0.140013</b>		0.147	
Batch 3	1	2	3	4	Thickness	Load	Biax Str	Biax Str	Compressive extension
1	1.077	1.075		1.076	32.72	60.04253	60.04253	0.152	
2	1.152	1.193		1.1725	38.39	57.81621	57.81621	0.140	
3	1.154	1.139		1.1465	34.65	54.95003	54.95003	<b>0.156</b>	
4	1.163	1.128		1.1455	36.84	58.54056	58.54056	<b>0.018</b>	
5	1.048	1.058		1.053	23.48	45.27803	45.27803	<b>0.113</b>	
						<b>55.32547</b>			
						<b>5.913612</b>			
						<b>0.106888</b>			
Batch 4	1	2	3	4	Thickness	Load	Biax Str	Biax Str	Compressive extension
1	1.098	1.108		1.103	32.66	56.61473	56.61473		
2	1.087	1.057		1.072	25.3	46.82534	46.82534		
3	1.045	1.017		1.031	22.4	45.33905	45.33905		
4	1.076	1.076		1.076	27.84	51.08754	51.08754		
5	1.049	1.064		1.0565	27.04	51.74742	51.74742		
						<b>50.32282</b>	<b>50.69612</b>		
						<b>4.451761</b>	<b>6.20026</b>		
						<b>0.088464</b>	<b>0.122302</b>		

BFS data: hand-mixed GIs									
60%									
Batch	1	2	3	4	Thickness	Load	Biax Str	Biax Str	Compressive extension
Batch 1	1	1.104	1.077	1.0905	27.11	48.24139	48.24139	0.165	
	2	1.026	1.041	1.0335	29.07	58.51369	58.51369	0.185	
	3	1.05	1.081	1.0655	30.38	57.01816	57.01816	0.192	
	4	1.108	1.126	1.117	37.71	63.5	63.5	0.206	
	5	1.065	1.054	1.0595	23.78	45.21342	45.21342	0.170	
						<b>54.49733</b>		<b>0.133</b>	
						<b>7.564088</b>		<b>0.135</b>	
						<b>0.138797</b>		<b>0.158</b>	
Batch 2	1	0.99	1.032	1.011	20.75	43.92821	43.92821	0.164	
	2	0.996	1.009	1.0025	22.8	49.21086	49.21086	0.162	
	3	0.987	0.991	0.989	27.01	60.13606	60.13606	0.154	
	4	0.974	0.969	0.9715	21.84	50.65345	50.65345	0.157	
	5	1.022	1.018	1.02	26.91	55.82364	55.82364	0.158	
						<b>51.95044</b>		<b>0.135</b>	
						<b>6.235976</b>		<b>0.156</b>	
						<b>0.120037</b>		<b>0.149</b>	
Batch 3	1	1.207	1.172	1.1895	31.88	46.44496	46.44496	0.158	
	2	1.173	1.172	1.1725	31.86	47.98188	47.98188	0.152	
	3	1.087	1.108	1.0975	30.38	53.27109	53.27109	0.125	
	4	1.146	1.126	1.136	29.81	48.28642	48.28642	<b>0.158</b>	
	5	1.07	1.06	1.065	20.94	39.34324	39.34324	<b>0.020</b>	
						<b>47.06552</b>		<b>0.125</b>	
						<b>5.021408</b>			
						<b>0.10669</b>			
Batch 4	1	1.13	1.115	1.1225	26.06	43.3895	43.3895		
	2	1.098	1.103	1.1005	23.01	40.09547	40.09547		
	3	1.025	1.024	1.0245	23.04	47.31561	47.31561		
	4	0.975	0.976	0.9755	20.74	47.65208	47.65208		
	5	1.038	1.066	1.052	19.52	37.72387	37.72387		
						<b>43.23531</b>	<b>49.18715</b>		
						<b>4.370787</b>	<b>7.035558</b>		
						<b>0.101093</b>	<b>0.143036</b>		

BFS data: hand-mixed GIs									
50%									
Batch 1	1	2	3	4	Thickness	Load	Biax Str	Biax Str	Compressive extension
	0.99	0.979		0.9845	22.17	49.87814	49.87814	0.177	
	0.94	0.967		0.9535	20.01	48.4374	48.4374	0.173	
	1.025	1.013		1.019	25.76	53.55829	53.55829	0.184	
	0.987	1.005		0.996	22.78	49.90571	49.90571	0.180	
	0.878	0.895		0.8865	13.47	38.50854	38.50854	0.131	
						<b>48.05762</b>		0.123	
						<b>5.663838</b>		0.144	
						<b>0.117855</b>		0.133	
Batch 2	1	2	3	4	Thickness	Load	Biax Str		
	0.975	0.967		0.971	16.15	37.50079	37.50079	0.136	
	1.016	1.033		1.0245	20.83	42.77709	42.77709	0.145	
	1.115	1.052		1.0835	20.49	37.00481	37.00481	0.155	
	1.01	1.002		1.006	24.65	52.78076	52.78076	0.154	
	0.994	1.001		0.9975	21.14	46.15351	46.15351	0.181	
						<b>43.24339</b>		0.167	
						<b>6.548758</b>		0.128	
						<b>0.15144</b>		0.146	
Batch 3	1	2	3	4	Thickness	Load	Biax Str		
	1.062	1.083		1.0725	21.9	40.48923	40.48923	0.119	
	1.025	1.022		1.0235	23.24	47.83331	47.83331	0.155	
	0.997	0.995		0.996	20.54	44.99839	44.99839	<b>0.152</b>	
	1.073	1.045		1.059	27.5	52.34301	52.34301	<b>0.020</b>	
	1.042	1.028		1.035	23.24	46.62341	46.62341	<b>0.131</b>	
						<b>46.45747</b>			
						<b>4.310131</b>			
						<b>0.092776</b>			
Batch 4	1	2	3	4	Thickness	Load	Biax Str		
	1.024	1.039		1.0315	17.62	35.62439	35.62439		
	1.004	1.015		1.0095	20.88	44.35407	44.35407		
	1.074	1.063		1.0685	23.97	44.69818	44.69818		
	1.039	1.055		1.047	16.41	32.06215	32.06215		
	1.099	1.128		1.1135	26.61	45.13327	45.13327		
						<b>40.37441</b>	<b>44.53322</b>		
						<b>6.099914</b>	<b>6.06293</b>		
						<b>0.151084</b>	<b>0.136144</b>		

BFS data: hand-mixed GIs									
40%									
Batch 1	1	2	3	4	Thickness	Load	Biax Str	Biax Str	Compressive extens
1	1.176	1.156		4	1.166	33.58	51.22422	51.22422	0.264
2	1.104	1.076		4	1.09	29.29	52.17558	52.17558	0.223
3	0.924	0.93		4	0.927	16.12	41.61726	41.61726	0.178
4	1.101	1.097	1.089	4	1.095667	22.45	39.51746	39.51746	0.196
5	0.954	0.955		4	0.9545	13.65	32.9629	32.9629	0.153
							<b>43.49949</b>		0.159
							<b>8.145015</b>		0.167
							<b>0.187244</b>		0.146
Batch 2	1	2	3	4	Thickness		Biax Str		0.154
1	0.912	0.943	0.932	4	0.929	15.04	38.63832	38.63832	0.151
2	0.973	0.966		4	0.9695	19.62	45.71967	45.71967	0.151
3	0.934	0.933		4	0.9335	14.4	36.58799	36.58799	0.147
4	0.881	0.871	0.864	4	0.872	15.58	46.24734	46.24734	0.153
5	0.957	0.946		4	0.9515	16.31	39.67096	39.67096	0.153
							<b>41.37286</b>		0.147
							<b>4.356731</b>		0.194
							<b>0.105304</b>		0.171
Batch 3	1	2	3	4	Thickness		Biax Str		0.174
1	1.179	1.219		4	1.199	20.86	29.83783	29.83783	0.178
2	0.992	0.989		4	0.9905	18.49	41.02422	41.02422	0.158
3	0.973	0.98		4	0.9765	18.25	41.83288	41.83288	<b>0.171</b>
4	0.991	1		4	0.9955	17.81	39.06249	39.06249	<b>0.030</b>
5	0.974	0.958		4	0.966	16.49	38.74521	38.74521	<b>0.174</b>
							<b>38.10052</b>		
							<b>4.798218</b>		
							<b>0.125936</b>		
Batch 4	1	2	3	4	Thickness		Biax Str		
1	1.065	1.08		4	1.0725	20.21	37.36472	37.36472	
2	1.059	1.059		4	1.059	19.01	36.1833	36.1833	
3	1.107	1.134		4	1.1205	21.47	35.89417	35.89417	
4	1.062	1.06		4	1.061	20.18	38.24426	38.24426	
5	1.04	1.031		4	1.0355	16.78	33.62628	33.62628	
							<b>36.26255</b>	<b>39.80885</b>	
							<b>1.748845</b>	<b>5.635521</b>	
							<b>0.048227</b>	<b>0.141565</b>	

**BFS data: hand-mixed GIs**

30%		1	2	3	4	Thickness	Load	Biax Str	Biax Str	Compressive extension
<b>Batch 1</b>										
1	0.957	0.949	0.953	13.61	32.98471	32.98471	0.182			
2	0.889	0.894	0.8915	11.91	33.61476	33.61476	0.162			
3	0.886	0.877	0.8815	9.29	26.90338	26.90338	0.148			
4	0.971	0.977	0.974	14.8	34.12433	34.12433	0.187			
5	0.933	0.953	0.943	6.5	16.13766	16.13766	0.130			
					<b>28.75297</b>		0.137			
					<b>7.631565</b>		0.135			
					<b>0.265418</b>		0.131			
<b>Batch 2</b>										
1	1.018	0.987	0.982	12.7	27.8441	27.8441	0.155			
2	0.851	0.884	0.871	8.91	26.51752	26.51752	0.110			
3	0.946	0.94	0.943	10.7	26.56508	26.56508	0.148			
4	0.916	0.923	0.9195	9.27	24.38067	24.38067	0.136			
5	0.96	0.968	0.964	15.12	35.69506	35.69506	0.121			
					<b>28.20048</b>		0.120			
					<b>4.370169</b>		0.093			
					<b>0.154968</b>		0.144			
<b>Batch 3</b>										
1	0.883	0.873	0.878	8.04	23.4956	23.4956	0.129			
2	0.961	0.939	0.95	11.3	27.58441	27.58441	0.113			
3	0.963	0.876	0.9195	12.01	31.58704	31.58704	<b>0.134</b>			
4	0.94	0.912	0.926	9.78	25.31151	25.31151	<b>0.025</b>			
5	0.943	0.849	0.896	10	27.90165	27.90165	<b>0.185</b>			
					<b>27.17604</b>					
					<b>3.048455</b>					
					<b>0.112174</b>					
<b>Batch 4</b>										
1	0.937	0.947	0.942	8.25	20.53215	20.53215				
2	0.975	0.992	0.9835	15.72	35.44928	35.44928				
3	0.938	0.945	0.9415	8.4	20.93084	20.93084				
4	0.948	0.951	0.9495	10.68	26.10232	26.10232				
5	0.954	0.938	0.946	9.05	22.30606	22.30606				
					<b>25.06413</b>	<b>27.29841</b>				
					<b>6.208039</b>	<b>5.332967</b>				
					<b>0.247686</b>	<b>0.195358</b>				

**BFS data: hand-mixed GIs**

**20%**

Batch	1	2	3	4	Thickness	Load	Biax Str	Biax Str	Compressive extension
Batch 1	1	0.882	0.877	4	0.8795	6.69	19.47451	19.47451	0.187
	2	0.91	0.923	4	0.9165	4.68	12.40088	12.40088	0.177
	3	1.011	1.022	4	1.0165	10.94	22.87406	22.87406	0.221
	4	0.876	0.869	4	0.8725	8.54	25.31685	25.31685	0.166
	5	0.886	0.879	4	0.8825	8.35	24.11875	24.11875	0.180
						<b>20.83701</b>		0.144	
						<b>5.196466</b>		0.160	
						<b>0.249386</b>		0.130	
Batch 2	1	0.918	0.926	4	0.922	7.22	18.87167	18.87167	0.095
	2	0.883	0.906	4	0.8945	6.07	17.00116	17.00116	0.165
	3	0.89	0.882	0.867	0.879667	3.76	10.94059	10.94059	0.159
	4	0.917	0.912	4	0.9145	5.11	13.60799	13.60799	0.129
	5	0.917	0.93	4	0.9235	3.33	8.671716	8.671716	0.161
						<b>13.81862</b>		0.121	
						<b>4.197617</b>		0.195	
						<b>0.303765</b>		0.177	
Batch 3	1	0.964	0.987	4	0.9755	7.92	18.19694	18.19694	0.147
	2	0.923	0.924	4	0.9235	5.75	14.97368	14.97368	0.164
	3	0.881	0.885	4	0.883	4.69	13.52945	13.52945	0.121
	4	0.917	0.907	4	0.912	5.97	15.99784	15.99784	<b>0.157</b>
	5	0.927	0.928	4	0.9275	5.43	14.00146	14.00146	<b>0.029</b>
						<b>15.33988</b>		<b>0.186</b>	
						<b>1.857337</b>			
						<b>0.121079</b>			
Batch 4	1	1.104	1.057	4	1.086	9.21	16.54536	16.54536	
	2	1.111	1.057	1.097	1.092667	6.46	11.44305	11.44305	
	3	1.048	1.079	1.11	1.0635	6.2	11.68666	11.68666	
	4	1.068	1.064	4	1.066	6.98	13.08618	13.08618	
	5	1.038	1.044	4	1.041	4.27	8.453527	8.453527	
						<b>12.24296</b>	<b>15.55962</b>		
						<b>2.938147</b>	<b>4.792949</b>		
						<b>0.239987</b>	<b>0.308038</b>		





HI data: encapsulated GIs

Chemfil Rock

Batch 1	Thickness				Mean	Load	Load
1	3.164	3.154	3.157	3.163	3.1595	1382.43	1382.43
2	3.128	3.143	3.129	3.145	3.13625	1035.66	1035.66
3	3.134	3.095	3.137	3.104	3.1175	1171.4	1171.4
4	3.13	3.144	3.124	3.112	3.1275	1299.8	1299.8
						1222.323	
Batch 2	Thickness				Mean	Load	
1	3.071	3.072	3.041	3.049	3.05825	1174.95	1174.95
2	3.115	3.08	3.06	3.11	3.09125	1244.56	1244.56
3	3.084	3.111			3.0975	1035.88	1035.88
4	3.09	3.062	3.042	3.042	3.059	1171.79	1171.79
						1156.795	
Batch 3	Thickness				Mean	Load	
1	3.008	3.04	3.017	3.035	3.025	1177.19	1177.19
2	3.117	3.101	3.112	3.09	3.105	1233.74	1233.74
3	3.169	3.155	3.2	3.207	3.18275	1263.12	1263.12
4	3.005	3.009	3.009		3.007667	1159.28	1159.28
						1208.333	
Batch 4	Thickness				Mean	Load	
1	3.082	3.043	3.065	3.057	3.06175	1206.42	1206.42
2	3.116	3.133	3.121	3.126	3.124	1264.7	1264.7
3	3.023	3.021	3.012	3.021	3.01925	1255.08	1255.08
4	3.047	3.077	3.091	3.126	3.08525	1097.36	1097.36
						1205.89	
Batch 5	Thickness				Mean	Load	
1	3.134	3.147	3.183	3.188	3.163	1304.11	1304.11
2	3.072	3.066	3.028	3.054	3.035	1173.61	1173.61
3	3.119	3.108	3.116	3.121	3.116	1386.71	1386.71
4	3.073	3.039	3.082	3.044	3.0595	980.34	980.34
						1211.193	
						<b>1200.907</b>	<b>1200.907</b>
						<b>107.8834</b>	<b>107.8834</b>
						<b>0.089835</b>	<b>0.089835</b>

HI data: encapsulated GIs

Fuji IX		Mean		Load	
Batch 1	Thickness				
1	3.131	3.138	3.119	3.132	
2	3.158	3.111	3.157	3.135	1035.52
3	3.166	3.166	3.155	3.158	1049.94
4	3.092	3.099	3.095	3.092	1055.13
					948.56
					1022.288
Batch 2	Thickness				
1	3.126	3.133	3.144	3.141	
2	3.139	3.128	3.134		1092.51
3	3.138	3.137	3.133		1051.57
4	3.095	3.087	3.082	3.084	1071.17
					984.12
					1049.843
Batch 3	Thickness				
1	3.14	3.108	3.144	3.158	
2	3.207	3.22	3.201	3.229	1067.24
3	3.235	3.182	3.184	3.224	1040.41
4	3.17	3.163	3.164	3.174	1050.28
					959.21
					1029.285
Batch 4	Thickness				
1	3.133	3.129	3.119		
2	3.191	3.165	3.146	3.179	1042.49
3	3.136	3.123	3.143		1073
4	3.184	3.171	3.182		928.37
					1081.08
					1031.235
Batch 5	Thickness				
1	3.141	3.144	3.108	3.129	
2	3.217	3.219	3.208	3.208	944.93
3	3.164	3.164	3.176	3.177	1115.72
4	3.098	3.081	3.097		1081.08
					1086.2
					1056.983
					1037.927
					54.68625
					0.052688

HI data: hand-mixed GIs

100%

Batch	Thickness	Mean	Load
Batch 1			
1	3.162 3.167 3.177 3.167	3.16825	851.45
2	3.141 3.145 3.088 3.117	3.12275	835.95
3	3.085 3.095 3.092 3.097	3.09225	864.91
4	3.143 3.135 3.146 3.155	3.14475	857.79
Batch 2			
1	3.145 3.156 3.155 3.149	3.15125	710.27
2	3.093 3.085 3.114 3.097	3.09725	843.02
3	3.079 3.08 3.086 3.079	3.081	941.45
4	3.129 3.126 3.12 3.12	3.125	501.59
Batch 3			
1	3.116 3.12 3.103 3.093	3.108	857.01
2	3.115 3.127 3.109 3.125	3.119	813.14
3	3.08 3.071 3.087 3.092	3.0825	879.4
4	3.147 3.138 3.141 3.148	3.1435	851.87
Batch 4			
1	3.169 3.161 3.121 3.112	3.14075	691.73
2	3.125 3.144 3.158 3.149	3.144	830.37
3	3.102 3.122 3.088 3.07	3.112	766.78
4	3.08 3.071 3.088 3.088	3.07725	845.45
Batch 5			
1	3.091 3.04 3.095 3.07	3.074	842.61
2	3.088 3.101 3.085 3.091	3.09125	888.51
3	3.138 3.123 3.143 3.136	3.135	875.93
4	3.061 3.061 3.084 3.071	3.06925	905.03
			<b>822.713</b>
			<b>95.91983</b>
			<b>0.11659</b>

HI data: hand-mixed Glis

90%		Thickness		Mean	Load	
Batch 1						
1	3.164	3.154	3.157	3.163	698.35	698.35
2	3.128	3.143	3.129	3.145	706.1	706.1
3	3.134	3.095	3.137	3.104	885.45	885.45
4	3.13	3.144	3.124	3.112	984.95	984.95
Batch 2						
			Thickness	Mean	Load	
1	3.071	3.072	3.041	3.049	779.5	779.5
2	3.115	3.08	3.06	3.11	886.92	886.92
3	3.084	3.111	3.071	3.088667	892.59	892.59
4	3.09	3.062	3.042	3.059	861.87	861.87
Batch 3						
			Thickness	Mean	Load	
1	3.134	3.147	3.183	3.188	919.98	919.98
2	3.072	3.066	3.028	3.054	839.62	839.62
3	3.119	3.108	3.116	3.121	780.08	780.08
4	3.073	3.039	3.082	3.0595	613.67	613.67
Batch 4						
			Thickness	Mean	Load	
1	3.008	3.04	3.017	3.035	912.22	912.22
2	3.117	3.101	3.112	3.09	853.27	853.27
3	3.169	3.155	3.2	3.207	791.09	791.09
4	3.005	3.009	3.009	3.007667	685	685
Batch 5						
			Thickness	Mean	Load	
1	3.082	3.043	3.065	3.057	799.83	799.83
2	3.116	3.133	3.121	3.126	859.15	859.15
3	3.023	3.021	3.012	3.021	851.12	851.12
4	3.047	3.077	3.091	3.126	844.34	844.34
					822.255	822.255
					91.48559	91.48559
					0.111262	0.111262

HI data: hand-mixed GIs

80%

Batch	Thickness	Mean	Load
Batch 1	1 3.18 3.088 3.118 3.168	3.1385	964.47
	2 3.372 3.311 3.374	3.352333	922.87
	3 3.147 3.14 3.141 3.156	3.146	911.68
	4 3.155 3.175 3.149	3.159667	788.11
Batch 2	1 3.169 3.186 3.192 3.169	3.179	848.74
	2 3.282 3.307 3.291 3.276	3.289	961.6
	3 3.325 3.297 3.332 3.3	3.3135	922.65
	4 3.391 3.391 3.373 3.373	3.382	913.14
Batch 3	1 3.134 3.104 3.106 3.106	3.114667	850.57
	2 3.085 3.105 3.103 3.088	3.09525	831.16
	3 3.215 3.208	3.2115	756.39
	4 3.218 3.208 3.209 3.217	3.213	964.37
Batch 4	1 3.298 3.259 3.235 3.273	3.26625	986.14
	2 3.142 3.142 3.153	3.145667	936.31
	3 3.146 3.12 3.136 3.136	3.1345	969.57
	4 3.265 3.243 3.218 3.283	3.25225	770.62
Batch 5	1 3.199 3.204 3.186 3.182	3.19275	792.64
	2 3.339 3.356 3.357 3.339	3.34775	898.22
	3 3.115 3.119 3.114 3.105	3.11325	996.9
	4 3.199 3.173 3.203 3.15	3.18125	883.56
		<b>893.4855</b>	
		<b>75.06165</b>	
		<b>0.08401</b>	

HI data: hand-mixed GIs

70%		Thickness		Mean		Load	
<b>Batch 1</b>							
1	3.131	3.138	3.119	3.132	3.13	940.52	940.52
2	3.158	3.111	3.157	3.135	3.14025	881.93	881.93
3	3.166	3.166	3.155	3.158	3.16125	1039.47	1039.47
4	3.092	3.099	3.095	3.092	3.0945	1016.47	1016.47
<b>Batch 2</b>							
Thickness							
1	3.126	3.133	3.144	3.141	3.136	946.45	946.45
2	3.139	3.128	3.134		3.133667	828.3	828.3
3	3.138	3.137	3.133		3.136	909.5	909.5
4	3.095	3.087	3.082	3.084	3.087	879.22	879.22
<b>Batch 3</b>							
Thickness							
1	3.14	3.108	3.144	3.158	3.1375	1061.65	1061.65
2	3.207	3.22	3.201	3.229	3.21425	1041.68	1041.68
3	3.235	3.182	3.184	3.224	3.20625	1111.97	1111.97
4	3.17	3.163	3.164	3.174	3.16775	1118.89	1118.89
<b>Batch 4</b>							
Thickness							
1	3.141	3.144	3.108	3.129	3.1305	963.51	963.51
2	3.217	3.219	3.208	3.208	3.213	1001.26	1001.26
3	3.164	3.164	3.176	3.177	3.17025	912.58	912.58
4	3.098	3.081	3.097		3.092	931.14	931.14
<b>Batch 5</b>							
Thickness							
1	3.133	3.129	3.119		3.127	859.54	859.54
2	3.191	3.165	3.146	3.179	3.17025	881.09	881.09
3	3.136	3.123	3.143		3.134	920.96	920.96
4	3.184	3.171	3.182		3.179	895.34	895.34
							<b>957.0735</b>
							<b>84.16061</b>
							<b>0.087935</b>

HI data: hand-mixed GIs									
60%									
Batch 1									
				Thickness			Mean	Load	Load
1	3.101	3.125	3.087	3.008			3.08025	835.28	835.28
2	3.119	3.046	3.148	3.178			3.12275	1042.98	1042.98
3	3.2	3.111	3.156				3.155667	1069.03	1069.03
4	3.217	3.219	3.208	3.208			3.213	1080.69	1080.69
Batch 2									
				Thickness			Mean	Load	Load
1	3.214	3.167	3.177	3.167			3.18125	978.65	978.65
2	3.141	3.145	3.101	3.117			3.126	1080.63	1080.63
3	3.138	3.137	3.133				3.136	1062.67	1062.67
4	3.095	3.087	3.082	3.084			3.087	1034.76	1034.76
Batch 3									
				Thickness			Mean	Load	Load
1	3.162	3.167	3.177	3.167			3.16825	994.34	994.34
2	3.141	3.145	3.088	3.117			3.12275	972.06	972.06
3	3.085	3.095	3.092	3.097			3.09225	997.4	997.4
4	3.143	3.135	3.146	3.155			3.14475	923.68	923.68
Batch 4									
				Thickness			Mean	Load	Load
1	3.145	3.156	3.155	3.006			3.1155	942.47	942.47
2	3.121	3.085	3.114	3.097			3.10425	923.25	923.25
3	3.079	3.077	3.086	3.079			3.08025	801.97	801.97
4	3.129	3.126	3.12				3.125	1004.07	1004.07
Batch 5									
				Thickness			Mean	Load	Load
1	3.082	3.043	3.065	3.057			3.06175	1063.09	1063.09
2	3.162	3.101	3.121	3.126			3.1275	1007.27	1007.27
3	3.023	3.021	3.012	3.002			3.0145	1010.74	1010.74
4	3.047	3.077	3.091	3.126			3.08525	963	963
								<b>989.4015</b>	<b>989.4015</b>
								<b>76.32915</b>	<b>76.32915</b>
								<b>0.077147</b>	<b>0.077147</b>





HI data: hand-mixed GIs

40%

Batch	Thickness	Mean	Load
Batch 1	3.113	3.141	1021.59
	3.2	3.141	1021.59
	3.119	3.141	1021.59
	3.132	3.141	1021.59
Batch 2	3.158	3.14025	808.13
	3.111	3.14025	808.13
	3.157	3.14025	808.13
	3.135	3.14025	808.13
Batch 3	3.115	3.14225	738.17
	3.166	3.14225	738.17
	3.13	3.14225	738.17
	3.158	3.14225	738.17
Batch 4	3.092	3.0975	762
	3.111	3.0975	762
	3.095	3.0975	762
	3.111	3.0975	762
Batch 5	3.126	3.1305	989.2
	3.111	3.1305	989.2
	3.144	3.1305	989.2
	3.141	3.1305	989.2
Batch 6	3.139	3.133667	875.6
	3.128	3.133667	875.6
	3.134	3.133667	875.6
	3.133	3.133667	875.6
Batch 7	3.137	3.15675	650.27
	3.137	3.15675	650.27
	3.133	3.15675	650.27
	3.133	3.15675	650.27
Batch 8	3.095	3.087	707.97
	3.087	3.087	707.97
	3.082	3.087	707.97
	3.084	3.087	707.97
Batch 9	3.101	3.12775	918.18
	3.108	3.12775	918.18
	3.144	3.12775	918.18
	3.158	3.12775	918.18
Batch 10	3.207	3.1925	1282.68
	3.22	3.1925	1282.68
	3.114	3.1925	1282.68
	3.229	3.1925	1282.68
Batch 11	3.235	3.19475	1144.5
	3.136	3.19475	1144.5
	3.184	3.19475	1144.5
	3.224	3.19475	1144.5
Batch 12	3.17	3.16775	761.09
	3.163	3.16775	761.09
	3.164	3.16775	761.09
	3.174	3.16775	761.09
Batch 13	3.114	3.12375	709.75
	3.144	3.12375	709.75
	3.108	3.12375	709.75
	3.129	3.12375	709.75
Batch 14	3.217	3.18275	833.02
	3.098	3.18275	833.02
	3.208	3.18275	833.02
	3.208	3.18275	833.02
Batch 15	3.164	3.16625	781.64
	3.164	3.16625	781.64
	3.176	3.16625	781.64
	3.161	3.16625	781.64
Batch 16	3.098	3.092	959.45
	3.081	3.092	959.45
	3.097	3.092	959.45
	3.097	3.092	959.45
Batch 17	3.133	3.127	695.5
	3.129	3.127	695.5
	3.119	3.127	695.5
	3.119	3.127	695.5
Batch 18	3.191	3.17025	954.31
	3.165	3.17025	954.31
	3.146	3.17025	954.31
	3.179	3.17025	954.31
Batch 19	3.136	3.143	769.59
	3.123	3.143	769.59
	3.143	3.143	769.59
	3.17	3.143	769.59
Batch 20	3.184	3.14175	868.15
	3.171	3.14175	868.15
	3.182	3.14175	868.15
	3.03	3.14175	868.15
Total			861.5395
Total			161.1688
Total			0.187071

HI data: hand-mixed GIs

30%

Batch	Thickness	Mean	Load
Batch 1	1 3.2 3.155 3.143 3.212	3.1775	673.3
	2 3.161 3.123 3.143 3.171	3.1495	686
	3 3.198 3.171 3.21 3.144	3.18075	624
	4 3.366 3.16 3.182 3.199	3.22675	673.25
Batch 2	1 3.126 3.134 3.212 3.141	3.15325	763.21
	2 3.139 3.133 3.22 3.189	3.17025	811.23
	3 3.137 3.082 3.084 3.187	3.1225	836.41
	4 3.161 3.17 3.155 3.14	3.1565	628
Batch 3	1 3.134 3.104 3.106	3.114667	481
	2 3.085 3.105 3.103 3.088	3.09525	574
	3 3.215 3.109	3.162	612
	4 3.218 3.208 3.209	3.211667	540
Batch 4	1 3.213 3.12 3.136 3.136	3.15125	903
	2 3.28 3.243 3.218 3.283	3.256	618.99
	3 3.231 3.298 3.146 3.151	3.2065	591
	4 3.16 3.142 3.265	3.189	542
Batch 5	1 3.142 3.153 3.189 3.17	3.1635	769
	2 3.12 3.136 3.142 3.156	3.1385	850
	3 3.296 3.298 3.259 3.201	3.2635	633.91
	4 3.231 3.199 3.202 3.178	3.2025	804.57
			680.7435
			117.9886
			0.173323



KIC data: encapsulated GIs																									
SpecNo	W1	W2	W	B1	B2	B	C1.1	C1.2	C1.3	C1	C2.1	C2.2	C2.3	C2	a1	(W1-C1a2)	(W2-C1a	a/W	P	L	KIC	KIC			
	[mm]	[mm]	[m]	[mm]	[mm]	[m]									[mm]	[mm]	[m]		[N]	[m]	[Nm <sup>-1.5</sup> ]	[Nm <sup>-1.5</sup> ]			
Ionofill Molar AC																									
1	5.828	5.875	0.0059	2.732	2.669	0.0027	2.697	2.675	2.631	2.668	2.741	2.748	2.741	2.743	3.160	3.132	0.00315	0.538	8.682	0.02	432678	0.433			
2	6.213	6.021	0.0061	2.656	2.736	0.0027	2.617	2.617	2.624	2.619	2.690	2.704	2.697	2.697	3.594	3.324	0.00346	0.565	10.662	0.02	548549	0.549			
3	5.682	5.898	0.0058	2.709	2.676	0.0027	2.617	2.631	2.646	2.631	2.675	2.661	2.661	2.666	3.051	3.232	0.00314	0.543	9.965	0.02	514619	0.515			
4	5.941	5.825	0.0059	2.731	2.690	0.0027	2.675	2.631	2.641	2.668	2.668	2.661	2.690	2.673	3.300	3.152	0.00323	0.548	10.989	0.02	561476	0.561			
5	5.972	6.032	0.0060	2.628	2.737	0.0027	2.602	2.602	2.617	2.607	2.661	2.617	2.661	2.646	3.365	3.386	0.00338	0.562	9.813	0.02	516367	0.516			
6	5.971	6.039	0.0060	2.708	2.739	0.0027	2.704	2.704	2.719	2.709	2.755	2.755	2.763	2.758	3.262	3.281	0.00327	0.545	9.770	0.02	475914	0.476			
7	6.010	6.020	0.0060	2.718	2.813	0.0028	2.573	2.573	2.734	2.627	2.653	2.653	2.449	2.585	3.383	3.435	0.00341	0.567	8.023	0.02	414653	0.415			
8	6.099	6.116	0.0061	2.787	2.775	0.0028	2.719	2.719	2.792	2.743	2.690	2.704	2.653	2.682	3.356	3.434	0.00339	0.556	7.898	0.02	381612	0.382			
9	5.904	5.740	0.0058	2.739	2.736	0.0027	2.792	2.807	2.821	2.807	2.828	2.828	2.887	2.848	3.097	2.892	0.00299	0.514	11.228	0.02	514923	0.515			
10	6.081	6.134	0.0061	2.729	2.711	0.0027	2.748	2.748	2.719	2.738	2.763	2.777	2.807	2.782	3.343	3.352	0.00335	0.548	8.990	0.02	432255	0.432			
11	6.059	5.961	0.0060	2.754	2.726	0.0027	2.734	2.734	2.734	2.734	2.726	2.668	2.675	2.690	3.325	3.271	0.00330	0.549	9.666	0.02	473845	0.474			
12	6.008	6.105	0.0061	2.783	2.792	0.0028	2.690	2.970	2.690	2.783	2.697	2.734	2.697	2.709	3.225	3.396	0.00331	0.547	8.859	0.02	418739	0.419			
13	5.844	5.912	0.0059	2.623	2.725	0.0027	2.734	2.748	2.734	2.739	2.734	2.661	2.573	2.656	3.105	3.256	0.00318	0.541	10.246	0.02	518282	0.518			
14	6.000	5.919	0.0060	2.746	2.719	0.0027	2.763	2.734	2.777	2.758	2.675	2.675	2.763	2.704	3.242	3.215	0.00323	0.542	9.582	0.02	465570	0.466			
15	5.799	5.979	0.0059	2.767	2.753	0.0028	2.763	2.734	2.763	2.753	2.807	2.821	2.792	2.807	3.046	3.172	0.00311	0.528	11.061	0.02	517080	0.517			
16	5.877	5.987	0.0059	2.745	2.716	0.0027	2.748	2.748	2.734	2.743	2.704	2.704	2.719	2.709	3.134	3.278	0.00321	0.540	10.366	0.02	505328	0.505			
17	6.022	5.927	0.0060	2.659	2.741	0.0027	2.719	2.704	2.690	2.704	2.690	2.675	2.675	2.680	3.318	3.247	0.00328	0.549	7.946	0.02	399671	0.400			
18	5.916	5.926	0.0059	2.765	2.706	0.0027	2.690	2.646	2.631	2.656	2.661	2.675	2.631	2.656	3.260	3.270	0.00327	0.551	7.395	0.02	374829	0.375			
19	5.997	5.886	0.0059	2.730	2.766	0.0027	2.682	2.661	2.675	2.673	2.741	2.763	2.719	2.741	3.324	3.145	0.00323	0.544	8.824	0.02	432247	0.432			
20	6.071	5.872	0.0060	2.771	2.711	0.0027	2.763	2.719	2.748	2.743	2.697	2.682	2.712	2.697	3.328	3.175	0.00325	0.544	8.798	0.02	428905	0.429			
			<b>0.0060</b>			<b>0.0027</b>			<b>2.704</b>					<b>2.706</b>			<b>0.00326</b>	<b>0.546</b>	<b>9.438</b>			<b>0.466</b>			
			<b>0.0001</b>			<b>0.0000</b>			<b>0.059</b>					<b>0.060</b>			<b>0.00011</b>	<b>0.012</b>	<b>1.136</b>			<b>0.056</b>			
			<b>0.0157</b>			<b>0.0116</b>			<b>0.022</b>					<b>0.022</b>			<b>0.03433</b>	<b>0.022</b>	<b>0.120</b>			<b>0.120</b>			

KIC data: encapsulated GIs																							
SpecNo	W1	W2	W	B1 [m]	B2	B	C1.1	C1.2	C1.3	C1	C2.1	C2.2	C2.3	C2	a1 [mm]	a1 [W1-C1a2]	a2 [W2-C2a]	a/W	P	L	K1C	K1C	
	[mm]	[mm]	[m]	[mm]	[mm]	[m]									[mm]	[mm]	[mm]		[N]	[m]	[Nm <sup>-1.5</sup> ]	[MNm <sup>-1.5</sup> ]	
Chemfil Rock																							
1	6.170	6.121	0.0061	2.845	2.831	0.0028	2.748	2.704	2.704	2.704	2.7187	2.588	2.602	2.668	2.6193	3.451	3.502	0.00348	0.566	9.094	0.02	441777	0.442
2	6.049	6.272	0.0062	2.799	2.808	0.0028	2.719	2.743	2.748	2.748	2.7367	2.69	2.682	2.682	2.6847	3.312	3.587	0.00345	0.560	10.405	0.02	499575	0.500
3	6.041	5.989	0.0060	2.811	2.759	0.0028	2.734	2.719	2.719	2.7240	2.712	2.712	2.712	2.617	2.6803	3.317	3.308	0.00331	0.551	9.921	0.02	481185	0.481
4	6.160	5.997	0.0061	2.696	2.722	0.0027	2.704	2.69	2.734	2.7093	2.741	2.741	2.726	2.7360	3.451	3.261	0.00336	0.552	8.853	0.02	436533	0.437	
5	6.000	5.957	0.0060	2.738	2.726	0.0027	2.807	2.807	2.792	2.8020	2.792	2.821	2.865	2.8260	3.198	3.131	0.00316	0.529	10.685	0.02	495607	0.496	
6	6.098	6.177	0.0061	2.753	2.752	0.0028	2.807	2.748	2.777	2.7773	2.712	2.741	2.77	2.7410	3.321	3.436	0.00338	0.550	9.964	0.02	473883	0.474	
7	6.018	5.972	0.0060	2.728	2.734	0.0027	2.661	2.69	2.975	2.7753	2.755	2.697	2.719	2.7237	3.243	3.248	0.00325	0.541	11.304	0.02	544027	0.544	
8	6.291	6.157	0.0062	2.696	2.720	0.0027	2.661	2.675	2.646	2.6607	2.675	2.704	2.704	2.6943	3.630	3.463	0.00355	0.570	10.225	0.02	518348	0.518	
9	6.050	6.094	0.0061	2.782	2.771	0.0028	2.807	2.792	2.807	2.8020	2.69	2.807	2.777	2.7580	3.248	3.336	0.00329	0.542	10.891	0.02	507156	0.507	
10	6.353	6.213	0.0063	2.783	2.770	0.0028	2.734	2.734	2.69	2.7193	2.69	2.763	2.734	2.7290	3.634	3.484	0.00356	0.566	11.854	0.02	570873	0.571	
11	6.247	6.016	0.0061	2.756	2.767	0.0028	2.661	2.661	2.675	2.6657	2.661	2.719	2.675	2.6850	3.581	3.331	0.00346	0.564	9.749	0.02	484867	0.485	
12	6.101	6.262	0.0062	2.760	2.753	0.0028	2.763	2.763	2.734	2.7533	2.763	2.675	2.675	2.7043	3.348	3.558	0.00345	0.559	10.531	0.02	509026	0.509	
13	6.114	6.268	0.0062	2.735	2.756	0.0027	2.631	2.646	2.69	2.6557	2.734	2.734	2.748	2.7387	3.458	3.529	0.00349	0.564	10.516	0.02	519731	0.520	
14	6.145	6.247	0.0062	2.768	2.774	0.0028	2.763	2.734	2.719	2.7387	2.631	2.631	2.617	2.6263	3.406	3.621	0.00351	0.567	9.154	0.02	452086	0.452	
15	6.120	6.442	0.0063	2.759	2.777	0.0028	2.734	2.748	2.763	2.7483	2.748	2.734	2.777	2.7530	3.372	3.689	0.00353	0.562	9.086	0.02	432352	0.432	
16	6.104	6.265	0.0062	2.738	2.749	0.0027	2.646	2.682	2.631	2.6530	2.58	2.704	2.704	2.6627	3.451	3.602	0.00353	0.570	10.479	0.02	530209	0.530	
17	6.145	6.178	0.0062	2.728	2.721	0.0027	2.653	2.653	2.653	2.6530	2.617	2.704	2.624	2.6483	3.492	3.530	0.00351	0.570	7.818	0.02	399923	0.400	
18	6.241	6.291	0.0063	2.755	2.758	0.0028	2.507	2.580	2.624	2.5703	2.602	2.617	2.631	2.6167	3.671	3.674	0.00367	0.586	9.834	0.02	514702	0.515	
19	6.199	6.199	0.0062	2.750	2.831	0.0028	2.595	2.624	2.624	2.6143	2.646	2.588	2.661	2.6317	3.585	3.567	0.00358	0.577	10.387	0.02	527440	0.527	
20	6.197	6.310	0.0063	2.742	2.741	0.0027	2.682	2.653	2.653	2.6627	2.690	2.719	2.675	2.6947	3.534	3.615	0.00357	0.572	8.930	0.02	446974	0.447	
			<b>0.0062</b>			<b>0.0028</b>			<b>2.707</b>						<b>2.698</b>		<b>0.00345</b>	<b>0.561</b>	<b>9.984</b>			<b>0.488</b>	
			<b>0.0001</b>			<b>0.0000</b>			<b>0.063</b>						<b>0.054</b>		<b>0.00013</b>	<b>0.013</b>	<b>0.952</b>			<b>0.045</b>	
			<b>0.0147</b>			<b>0.0116</b>			<b>0.023</b>						<b>0.020</b>		<b>0.03672</b>	<b>0.024</b>	<b>0.095</b>			<b>0.091</b>	



K1C data: hand-mixed G1s

SpecNo	W1 [mm]	W2 [mm]	W [mm]	B1 [mm]	B2 [mm]	B [mm]	C1.1	C1.2	C1.3	C1	C2.1	C2.2	C2.3	C2	a1 [mm]	a2 [mm]	a3 [mm]	a/W	P [N]	L [m]	K1C [Nm <sup>-1.5</sup> ]	K1C [MNm <sup>-1.5</sup> ]
<b>100%</b>																						
1	6.016	6.188	0.0061	2.787	2.773	0.0028	2.763	2.755	2.814	2.777	2.77	2.78	2.75	2.765	3.239	3.423	0.00333	0.546	9.370	0.02	438089	0.438
2	6.287	6.044	0.0062	2.790	2.800	0.0028	2.726	2.785	2.77	2.760	2.79	2.78	2.73	2.768	3.527	3.276	0.00340	0.552	9.643	0.02	450535	0.451
3	6.155	6.312	0.0062	2.796	2.770	0.0028	2.799	2.785	2.785	2.790	2.81	2.87	2.87	2.846	3.365	3.466	0.00342	0.548	10.383	0.02	473111	0.473
4	6.096	6.068	0.0061	2.732	2.731	0.0027	2.785	2.712	2.726	2.741	2.69	2.68	2.68	2.682	3.355	3.386	0.00337	0.554	9.339	0.02	459611	0.460
5	6.101	6.497	0.0063	2.767	2.732	0.0027	2.704	2.682	2.712	2.699	2.74	2.75	2.70	2.731	3.402	3.766	0.00358	0.569	9.132	0.02	446451	0.446
6	6.327	6.28	0.0063	2.780	2.763	0.0028	2.741	2.755	2.712	2.736	2.75	2.78	2.71	2.746	3.591	3.534	0.00356	0.565	9.513	0.02	454711	0.455
7	6.085	6.071	0.0061	2.736	2.726	0.0027	2.872	2.858	2.931	2.887	2.89	2.94	2.85	2.894	3.198	3.177	0.00319	0.524	10.338	0.02	460430	0.460
8	6.172	6.316	0.0062	2.765	2.753	0.0028	2.858	2.916	2.799	2.858	2.85	2.82	2.87	2.845	3.314	3.471	0.00339	0.543	11.005	0.02	496521	0.497
9	6.341	6.268	0.0063	2.737	2.715	0.0027	2.799	2.843	2.858	2.833	2.76	2.85	2.87	2.826	3.508	3.442	0.00347	0.551	9.692	0.02	448187	0.448
10	6.206	6.351	0.0063	2.729	2.704	0.0027	2.894	2.858	2.792	2.848	2.86	2.79	2.83	2.826	3.358	3.525	0.00344	0.548	10.664	0.02	492741	0.493
11	6.342	6.433	0.0064	2.735	2.754	0.0027	2.828	2.887	2.872	2.862	2.91	2.87	2.88	2.885	3.480	3.548	0.00351	0.550	7.961	0.02	357274	0.357
12	6.348	6.477	0.0064	2.751	2.749	0.0028	2.88	2.843	2.843	2.855	2.80	2.84	2.85	2.828	3.493	3.649	0.00357	0.557	7.275	0.02	331589	0.332
13	6.232	6.258	0.0062	2.728	2.725	0.0027	2.916	2.872	2.785	2.858	2.73	2.82	2.85	2.802	3.374	3.456	0.00342	0.547	11.278	0.02	521131	0.521
14	6.178	6.342	0.0063	2.768	2.777	0.0028	2.872	2.77	2.828	2.823	2.88	2.79	2.82	2.831	3.355	3.511	0.00343	0.548	10.040	0.02	456926	0.457
15	6.199	6.023	0.0061	2.732	2.676	0.0027	2.639	2.843	2.814	2.765	2.79	2.79	2.82	2.800	3.434	3.223	0.00333	0.545	10.866	0.02	519040	0.519
16	5.956	6.295	0.0061	2.731	2.727	0.0027	2.741	2.814	2.712	2.756	2.75	2.65	2.73	2.709	3.200	3.586	0.00339	0.554	10.669	0.02	519532	0.520
17	6.371	6.145	0.0063	2.709	2.722	0.0027	2.828	2.799	2.828	2.818	2.81	2.78	2.82	2.802	3.553	3.343	0.00345	0.551	10.590	0.02	496764	0.497
18	6.284	6.244	0.0063	2.717	2.642	0.0027	2.901	2.799	2.858	2.853	2.94	2.81	2.82	2.855	3.431	3.389	0.00341	0.544	11.479	0.02	532651	0.533
19	6.205	6.07	0.0061	2.712	2.723	0.0027	2.901	2.901	2.931	2.911	2.73	2.88	2.95	2.856	3.294	3.214	0.00325	0.530	10.945	0.02	492144	0.492
20	6.231	6.123	0.0062	2.740	2.727	0.0027	2.799	2.726	2.785	2.770	2.79	2.87	2.76	2.807	3.461	3.316	0.00339	0.549	10.813	0.02	509605	0.510
			<b>0.00622</b>			<b>0.00274</b>				<b>2.810</b>				<b>2.805</b>			<b>0.00342</b>	<b>0.549</b>	<b>10.050</b>			<b>0.468</b>
			<b>0.00010</b>			<b>0.00003</b>				<b>0.057</b>				<b>0.057</b>			<b>0.00010</b>	<b>0.010</b>	<b>1.081</b>			<b>0.051</b>
			<b>0.01567</b>			<b>0.01072</b>				<b>0.020</b>				<b>0.020</b>			<b>0.02897</b>	<b>0.018</b>	<b>0.108</b>			<b>0.110</b>



KIC data: hand-mixed G1s

SpecNo	W1 [mm]	W2 [mm]	W [mm]	B1 [mm]	B2 [mm]	B [mm]	C1.1	C1.2	C1.3	C1	C2.1	C2.2	C2.3	C2	a1 [mm]	W1-C1a2 [mm]	W2-C1a2 [mm]	a/W	P [N]	L [m]	KIC [Nm <sup>1.5</sup> ]	KIC [MNm <sup>1.5</sup> ]
<b>90%</b>																						
1	6.1	6.059	0.0060795	2.753	2.768	0.0028	2.799	2.828	2.741	2.789	2.748	2.836	2.836	2.807	3.311	3.252	0.00328	0.540	9.636	0.02	446817	0.447
2	6.216	6.203	0.0062095	2.757	2.731	0.0027	2.755	2.726	2.682	2.721	2.777	2.792	2.719	2.763	3.495	3.440	0.00347	0.558	10.201	0.02	491796	0.492
3	6.03	5.987	0.0060085	2.732	2.72	0.0027	2.682	2.668	2.741	2.697	2.646	2.661	2.617	2.641	3.333	3.346	0.00334	0.556	8.891	0.02	449054	0.449
4	6.07	6.043	0.0060565	2.745	2.78	0.0028	2.909	2.858	2.785	2.851	2.843	2.909	2.777	2.843	3.219	3.200	0.00321	0.530	9.698	0.02	437228	0.437
5	6.174	6.136	0.006155	2.745	2.727	0.0027	2.77	2.785	2.719	2.758	2.734	2.763	2.755	2.751	3.416	3.385	0.00340	0.553	8.899	0.02	427024	0.427
6	6.153	6.095	0.006124	2.728	2.669	0.0027	2.653	2.668	2.712	2.678	2.646	2.704	2.675	2.675	3.475	3.420	0.00345	0.563	10.543	0.02	536252	0.536
7	6.177	6.283	0.00623	2.723	2.735	0.0027	2.697	2.755	2.77	2.741	2.631	2.719	2.777	2.709	3.436	3.574	0.00351	0.563	10.484	0.02	513253	0.513
8	6.048	6.33	0.006189	2.697	2.69	0.0027	2.624	2.697	2.682	2.668	2.675	2.719	2.69	2.695	3.380	3.635	0.00351	0.567	7.407	0.02	376601	0.377
9	6.077	6.259	0.006168	2.71	2.749	0.0027	2.682	2.741	2.719	2.714	2.777	2.734	2.755	2.755	3.363	3.504	0.00343	0.557	8.115	0.02	394762	0.395
10	6.216	6.092	0.006154	2.803	2.804	0.0028	2.624	2.755	2.697	2.692	2.734	2.602	2.748	2.695	3.524	3.397	0.00346	0.562	7.945	0.02	385266	0.385
11	6.175	6.356	0.0062655	2.718	2.69	0.0027	2.697	2.741	2.741	2.726	2.704	2.763	2.748	2.738	3.449	3.618	0.00353	0.564	8.911	0.02	438538	0.439
12	6.213	6.241	0.006227	2.735	2.722	0.0027	2.755	2.755	2.77	2.760	2.734	2.734	2.807	2.758	3.453	3.483	0.00347	0.557	9.795	0.02	470943	0.470
13	6.479	6.207	0.006343	2.713	2.737	0.0027	2.785	2.858	2.887	2.843	2.719	2.894	2.821	2.811	3.636	3.396	0.00352	0.554	9.274	0.02	429721	0.430
14	6.114	6.358	0.006236	2.738	2.722	0.0027	2.843	2.814	2.755	2.804	2.88	2.88	2.821	2.860	3.310	3.498	0.00340	0.546	9.812	0.02	452144	0.452
15	5.981	6.38	0.0061805	2.728	2.734	0.0027	2.828	2.901	2.872	2.867	2.777	2.807	2.807	2.797	3.114	3.583	0.00335	0.542	10.541	0.02	485329	0.485
16	6.16	6.095	0.0061275	2.685	2.67	0.0027	2.799	2.814	2.814	2.809	2.85	2.865	2.792	2.836	3.351	3.259	0.00331	0.539	10.659	0.02	502972	0.503
17	6.044	6.26	0.006152	2.736	2.741	0.0027	2.799	2.814	2.77	2.794	2.821	2.807	2.777	2.802	3.250	3.458	0.00335	0.545	11.136	0.02	520915	0.521
18	6.231	6.53	0.0063805	2.733	2.742	0.0027	2.901	2.799	2.916	2.872	2.967	2.976	2.909	2.951	3.359	3.579	0.00347	0.544	10.553	0.02	465176	0.465
19	6.387	6.351	0.006369	2.741	2.745	0.0027	2.872	2.858	2.858	2.863	2.88	2.85	2.807	2.846	3.524	3.505	0.00351	0.552	6.932	0.02	314506	0.315
20	5.995	6.083	0.006039	2.714	2.704	0.0027	2.828	2.828	2.755	2.804	2.79200	2.836	2.865	2.831	3.191	3.252	0.00322	0.533	10.77	0.02	503208	0.503
										<b>2.773</b>				<b>2.778</b>				<b>0.00341</b>	<b>9.5101</b>			<b>0.452</b>
										<b>0.066</b>				<b>0.075</b>				<b>9.89E-05</b>	<b>1.193277</b>			<b>0.055</b>
										<b>0.024</b>				<b>0.027</b>				<b>0.029004</b>	<b>0.019</b>	<b>0.125475</b>		<b>0.122</b>

K1C data: hand-mixed G1s																						
SpecNo	W1 [mm]	W2 [mm]	W [m]	B1 [m] [mm]	B2 [mm]	B [m]	C1.1	C1.2	C1.3	C1	C2.1	C2.2	C2.3	C2	a1 [W1-C1a2] [mm]	a2 [W2-C2a] [mm]	a/W [m]	P [N]	L [m]	K1C [Nm <sup>-1.5</sup> ]	K1C [MNm <sup>-1.5</sup> ]	
80%																						
1	6.157	6.056	0.0061065	2.751	2.749	0.0028	2.85	2.865	2.814	2.843	2.785	2.843	2.785	2.804	3.314	3.252	0.00328	0.538	9.386	0.02	430810	0.431
2	6.116	6.191	0.0061535	2.718	2.723	0.0027	2.828	2.785	2.828	2.814	2.777	2.777	2.704	2.753	3.302	3.438	0.00337	0.548	8.899	0.02	422528	0.423
3	6.094	6.107	0.0061005	2.702	2.676	0.0027	2.726	2.734	2.726	2.729	2.69	2.712	2.748	2.717	3.365	3.390	0.00338	0.554	9.289	0.02	461537	0.462
4	6.113	6.167	0.00614	2.724	2.716	0.0027	2.69	2.777	2.697	2.721	2.748	2.755	2.697	2.733	3.392	3.434	0.00341	0.556	9.509	0.02	466014	0.466
5	6.116	6.18	0.006148	2.783	2.836	0.0028	2.814	2.828	2.814	2.819	2.865	2.836	2.845	2.849	3.297	3.331	0.00331	0.539	9.698	0.02	433492	0.433
6	6.069	6.133	0.006101	2.756	2.804	0.0028	2.712	2.712	2.639	2.688	2.792	2.836	2.719	2.782	3.381	3.351	0.00337	0.552	10.093	0.02	481665	0.482
7	6.133	6.076	0.0061045	2.739	2.737	0.0027	2.668	2.682	2.653	2.668	2.602	2.675	2.617	2.631	3.465	3.445	0.00346	0.566	8.949	0.02	455611	0.456
8	6.135	6.223	0.006179	2.716	2.687	0.0027	2.989	2.974	2.901	2.955	2.85	2.85	2.953	2.884	3.180	3.339	0.00326	0.528	9.87	0.02	437987	0.438
9	6.024	6.086	0.006055	2.648	2.68	0.0027	2.697	2.653	2.639	2.663	2.646	2.675	2.646	2.656	3.361	3.430	0.00340	0.561	9.849	0.02	512174	0.512
10	6.294	6.206	0.00625	2.674	2.717	0.0027	2.609	2.58	2.639	2.609	2.675	2.675	2.646	2.665	3.685	3.541	0.00361	0.578	9.807	0.02	511410	0.511
11	6.32	6.174	0.006247	2.751	2.721	0.0027	2.668	2.726	2.741	2.712	2.748	2.704	2.704	2.719	3.608	3.455	0.00353	0.565	10.781	0.02	529437	0.529
12	6.235	6.264	0.0062495	2.775	2.765	0.0028	2.704	2.726	2.755	2.728	2.777	2.748	2.719	2.748	3.507	3.516	0.00351	0.562	9.319	0.02	446145	0.446
13	6.087	6.199	0.006143	2.66	2.709	0.0027	2.755	2.741	2.741	2.746	2.777	2.763	2.734	2.758	3.341	3.441	0.00339	0.552	8.748	0.02	428387	0.428
14	6.18	6.079	0.0061295	2.636	2.641	0.0026	2.565	2.58	2.609	2.585	2.792	2.865	2.792	2.816	3.595	3.263	0.00343	0.559	8.891	0.02	456110	0.456
15	6.203	6.357	0.00628	2.738	2.725	0.0027	2.872	2.843	2.799	2.838	2.874	2.865	2.777	2.839	3.365	3.518	0.00344	0.548	9.316	0.02	427784	0.428
16	6.647	6.388	0.0065175	2.724	2.715	0.0027	2.872	2.931	2.916	2.906	2.923	2.821	2.88	2.875	3.741	3.513	0.00363	0.557	12.045	0.02	541174	0.541
17	6.087	6.249	0.006168	2.695	2.711	0.0027	2.828	2.872	2.843	2.848	2.836	2.894	2.88	2.870	3.239	3.379	0.00331	0.537	10.958	0.02	502217	0.502
18	6.253	6.046	0.0061495	2.732	2.709	0.0027	2.859	2.843	2.77	2.824	2.805	2.865	2.821	2.830	3.429	3.216	0.00332	0.540	10.429	0.02	483158	0.483
19	6.123	6.208	0.0061655	2.756	2.769	0.0028	2.843	2.799	2.828	2.823	2.88	2.792	2.909	2.860	3.300	3.348	0.00332	0.539	9.938	0.02	449830	0.450
20	6.129	6.26	0.0061945	2.721	2.673	0.0027	2.843	2.77	2.741	2.785	2.85	2.821	2.865	2.845	3.344	3.415	0.00338	0.546	10.714	0.02	504310	0.504
			<b>0.00618</b>			<b>0.00272</b>				<b>2.765</b>				<b>2.782</b>			<b>0.00341</b>	<b>0.551</b>	<b>9.8244</b>			<b>0.469</b>
			<b>0.00010</b>			<b>0.00004</b>				<b>0.097</b>				<b>0.078</b>			<b>0.000101</b>	<b>0.012</b>	<b>0.831515</b>			<b>0.037</b>
			<b>0.01602</b>			<b>0.01490</b>				<b>0.035</b>				<b>0.028</b>			<b>0.029793</b>	<b>0.022</b>	<b>0.084638</b>			<b>0.078</b>

KIC data: hand-mixed G1s																							
SpecNo	W1 [mm]	W2 [mm]	W [mm]	B1 [mm]	B2 [mm]	B [mm]	C1.1	C1.2	C1.3	C1	C2.1	C2.2	C2.3	C2	a1 [mm]	a1 (W1-C1)a2 (W2-C1)a [mm]	a/W	P [N]	L [m]	K1C [Nm <sup>-1.5</sup> ]	K1C [MNm <sup>-1.5</sup> ]		
<b>70%</b>																							
1	6.182	6.135	0.0061585	2.766	2.752	0.0028	2.682	2.697	2.697	2.697	2.692	2.704	2.748	2.777	2.743	3.490	3.392	0.00344	0.559	8.721	0.02	423803	0.424
2	6.044	5.868	0.005956	2.664	2.691	0.0027	2.609	2.624	2.682	2.682	2.638	2.69	2.675	2.661	2.675	3.406	3.193	0.00330	0.554	8.867	0.02	459022	0.459
3	6.208	5.912	0.00606	2.655	2.687	0.0027	2.7	2.726	2.777	2.758	2.748	2.792	2.741	2.760	2.760	3.450	3.152	0.00330	0.545	9.645	0.02	472383	0.472
4	5.898	6.126	0.006012	2.749	2.719	0.0027	2.69	2.668	2.624	2.661	2.529	2.529	2.507	2.522	2.522	3.237	3.604	0.00342	0.569	8.012	0.02	422531	0.423
5	6.159	6.004	0.0060815	2.671	2.672	0.0027	2.595	2.631	2.58	2.602	2.661	2.631	2.653	2.648	2.648	3.557	3.356	0.00346	0.568	9.802	0.02	518738	0.519
6	6.021	6.208	0.0061145	2.659	2.632	0.0026	2.682	2.653	2.661	2.665	2.675	2.675	2.697	2.682	2.682	3.356	3.526	0.00344	0.563	9.528	0.02	495011	0.495
7	6.023	6.105	0.006064	2.687	2.652	0.0027	2.639	2.682	2.712	2.678	2.69	2.69	2.734	2.705	2.705	3.345	3.400	0.00337	0.556	10.334	0.02	526490	0.526
8	5.986	6.1	0.006043	2.662	2.661	0.0027	2.595	2.609	2.639	2.614	2.661	2.675	2.602	2.646	2.646	3.372	3.454	0.00341	0.565	11.024	0.02	583675	0.584
9	6.418	6.359	0.0063885	2.709	2.744	0.0027	2.77	2.726	2.741	2.746	2.792	2.734	2.734	2.753	2.753	3.672	3.606	0.00364	0.570	10.201	0.02	493569	0.494
10	6.221	6.266	0.0062435	2.758	2.74	0.0027	2.712	2.712	2.755	2.726	2.748	2.748	2.763	2.753	2.753	3.495	3.513	0.00350	0.561	11.239	0.02	541684	0.542
11	5.957	6.204	0.0060805	2.659	2.658	0.0027	2.697	2.697	2.682	2.692	2.692	2.719	2.719	2.719	2.717	3.265	3.487	0.00338	0.555	9.709	0.02	492915	0.493
12	6.021	6.039	0.00603	2.685	2.707	0.0027	2.712	2.726	2.748	2.729	2.748	2.748	2.77	2.755	2.755	3.292	3.284	0.00329	0.545	9.31	0.02	455990	0.456
13	6.061	6.093	0.006077	2.683	2.706	0.0027	2.682	2.697	2.697	2.692	2.692	2.69	2.646	2.69	2.675	3.369	3.418	0.00339	0.558	9.342	0.02	473646	0.474
14	6.071	6.143	0.006107	2.633	2.662	0.0026	2.726	2.712	2.697	2.697	2.712	2.734	2.704	2.69	2.709	3.359	3.434	0.00340	0.556	10.024	0.02	509438	0.509
15	6.027	6.161	0.006094	2.669	2.69	0.0027	2.726	2.726	2.77	2.741	2.836	2.777	2.792	2.802	2.802	3.286	3.359	0.00332	0.545	10.488	0.02	508711	0.509
16	6.155	6.289	0.006222	2.763	2.735	0.0027	2.799	2.785	2.799	2.799	2.794	2.821	2.734	2.821	2.792	3.361	3.497	0.00343	0.551	8.919	0.02	417028	0.417
17	6.313	6.333	0.006323	2.712	2.655	0.0027	2.887	2.88	2.916	2.894	2.894	2.776	2.938	2.869	2.869	3.419	3.464	0.00344	0.544	10.099	0.02	461145	0.461
18	6.039	5.872	0.0059555	2.621	2.669	0.0026	2.755	2.741	2.755	2.750	2.865	2.821	2.734	2.807	2.807	3.289	3.065	0.00318	0.533	8.023	0.02	392006	0.392
19	5.903	6.274	0.0060885	2.683	2.693	0.0027	2.828	2.828	2.828	2.828	2.85	2.865	2.786	2.834	2.834	3.075	3.440	0.00326	0.535	11.275	0.02	527247	0.527
20	6.148	6.004	0.006076	2.641	2.668	0.0027	2.785	2.726	2.843	2.785	2.748	2.807	2.807	2.787	2.787	3.363	3.217	0.00329	0.541	11.295	0.02	548314	0.548
						<b>0.00269</b>				<b>2.720</b>					<b>2.732</b>			<b>0.00338</b>	<b>0.554</b>	<b>9.79285</b>			<b>0.486</b>
						<b>0.00004</b>				<b>0.072</b>					<b>0.079</b>			<b>0.000101</b>	<b>0.011</b>	<b>0.993641</b>			<b>0.049</b>
						<b>0.01357</b>				<b>0.026</b>					<b>0.029</b>			<b>0.029842</b>	<b>0.020</b>	<b>0.101466</b>			<b>0.101</b>

KIC data: hand-mixed GIs																						
SpectNo	W1	W2	W	B1 [m]	B2	B	C1.1	C1.2	C1.3	C1	C2.1	C2.2	C2.3	C2	a1 [mm]	a1 (W1-C1)a2 (W2-C2)a	a/W	P	L	K1C	K1C	
[mm]	[mm]	[mm]	[m]	[mm]	[mm]	[mm]	[mm]	[mm]	[mm]	[mm]	[mm]	[mm]	[mm]	[mm]	[mm]	[mm]	[N]	[m]	[Nm <sup>^-1.5</sup> ]	[MNm <sup>^-1.5</sup> ]	[MNm <sup>^-1.5</sup> ]	
60%																						
1	5.873	5.952	0.0059125	2.646	2.639	0.0026	2.624	2.624	2.675	2.641	2.588	2.646	2.653	2.629	3.232	3.323	0.00328	0.554	9.321	0.02	495031	0.495
2	6.173	6.12	0.0061465	2.751	2.75	0.0028	2.726	2.682	2.704	2.704	2.704	2.704	2.653	2.687	3.469	3.433	0.00345	0.561	8.887	0.02	438671	0.439
3	6.198	6.22	0.006209	2.709	2.714	0.0027	2.741	2.734	2.763	2.746	2.704	2.697	2.682	2.694	3.452	3.526	0.00349	0.562	8.407	0.02	415257	0.415
4	5.981	6.045	0.006013	2.644	2.636	0.0026	2.639	2.639	2.624	2.634	2.69	2.704	2.69	2.695	3.347	3.350	0.00335	0.557	8.291	0.02	433632	0.434
5	6.014	5.985	0.005995	2.631	2.621	0.0026	2.741	2.639	2.726	2.702	2.704	2.777	2.748	2.743	3.312	3.242	0.00328	0.546	9.375	0.02	476549	0.477
6	6.072	6.213	0.0061425	2.681	2.651	0.0027	2.697	2.668	2.653	2.673	2.719	2.704	2.631	2.685	3.399	3.528	0.00346	0.564	10.839	0.02	557364	0.557
7	5.973	5.779	0.005876	2.632	2.612	0.0026	2.704	2.69	2.682	2.692	2.755	2.734	2.58	2.690	3.281	3.089	0.00319	0.542	9.407	0.02	487104	0.487
8	5.921	5.969	0.005945	2.663	2.608	0.0026	2.682	2.624	2.646	2.651	2.748	2.734	2.609	2.697	3.270	3.272	0.00327	0.550	8.741	0.02	455110	0.455
9	6.027	5.838	0.0059325	2.644	2.618	0.0026	2.675	2.69	2.631	2.665	2.697	2.639	2.609	2.648	3.362	3.190	0.00328	0.552	9.292	0.02	489410	0.489
10	6.036	5.799	0.0059175	2.601	2.635	0.0026	2.58	2.639	2.712	2.644	2.777	2.675	2.617	2.690	3.392	3.109	0.00325	0.549	7.6	0.02	399908	0.400
11	5.989	6.089	0.006039	2.651	2.683	0.0027	2.697	2.704	2.668	2.690	2.704	2.704	2.668	2.692	3.299	3.397	0.00335	0.554	8.354	0.02	425993	0.426
12	6.365	6.103	0.006234	2.685	2.711	0.0027	2.566	2.682	2.631	2.626	2.661	2.573	2.609	2.614	3.739	3.489	0.00361	0.580	8.619	0.02	453505	0.454
13	5.984	5.833	0.0059085	2.612	2.593	0.0026	2.748	2.712	2.682	2.714	2.653	2.763	2.69	2.702	3.270	3.131	0.00320	0.542	9.071	0.02	468707	0.469
14	5.953	6.118	0.0060355	2.684	2.656	0.0027	2.697	2.77	2.748	2.738	2.704	2.704	2.697	2.702	3.215	3.416	0.00332	0.549	9.947	0.02	498190	0.498
15	6.069	5.919	0.005994	2.628	2.642	0.0026	2.712	2.639	2.763	2.705	2.719	2.668	2.682	2.690	3.364	3.229	0.00330	0.550	8.889	0.02	456897	0.457
16	5.965	6.08	0.0060225	2.616	2.637	0.0026	2.668	2.668	2.668	2.668	2.661	2.646	2.697	2.668	3.297	3.412	0.00335	0.557	8.702	0.02	456530	0.457
17	6.033	5.899	0.005966	2.68	2.668	0.0027	2.741	2.682	2.631	2.685	2.748	2.704	2.639	2.697	3.348	3.202	0.00328	0.549	8.931	0.02	453894	0.454
18	5.679	6.071	0.005875	2.659	2.616	0.0026	2.58	2.609	2.697	2.629	2.631	2.631	2.675	2.646	3.050	3.425	0.00324	0.551	9.593	0.02	509597	0.510
19	5.959	6.013	0.005986	2.631	2.607	0.0026	2.741	2.755	2.697	2.731	2.748	2.821	2.748	2.772	3.228	3.241	0.00323	0.540	8.884	0.02	445252	0.445
20	6.045	5.989	0.006017	2.631	2.634	0.0026	2.712	2.726	2.726	2.721	2.734	2.748	2.719	2.734	3.324	3.255	0.00329	0.547	9.326	0.02	471620	0.472
			<b>0.00601</b>			<b>0.00265</b>				<b>2.683</b>				<b>2.689</b>			<b>0.00332</b>	<b>0.553</b>	<b>9.0238</b>			<b>0.464</b>
			<b>0.00010</b>			<b>0.00004</b>				<b>0.038</b>				<b>0.037</b>			<b>0.000107</b>	<b>0.009</b>	<b>0.680594</b>			<b>0.036</b>
			<b>0.01730</b>			<b>0.01376</b>				<b>0.014</b>				<b>0.014</b>			<b>0.032243</b>	<b>0.016</b>	<b>0.075422</b>			<b>0.077</b>

KIC data: hand-mixed GIs																						
SpectNo	W1 [mm]	W2 [mm]	W [mm]	B1 [mm]	B2 [mm]	B [mm]	C1.1	C1.2	C1.3	C1	C2.1	C2.2	C2.3	C2	a1 [mm]	a1-C1a2 [mm]	W2-C2a [mm]	a/W	P [N]	L [m]	KIC [Nm <sup>-1.5</sup> ]	KIC [MNm <sup>-1.5</sup> ]
50%																						
1	5.993	6.226	0.0061095	2.669	2.699	0.0027	2.58	2.558	2.588	2.575	2.544	2.566	2.609	2.573	3.418	3.653	0.00354	0.579	7.284	0.02	395625	0.396
2	6.016	5.878	0.005947	2.552	2.587	0.0026	2.478	2.609	2.69	2.592	2.792	2.631	2.639	2.687	3.424	3.191	0.00331	0.556	8.634	0.02	470387	0.470
3	6.13	6.193	0.0061615	2.722	2.736	0.0027	2.712	2.726	2.726	2.721	2.675	2.69	2.675	2.680	3.409	3.513	0.00346	0.562	9.404	0.02	466519	0.467
4	5.808	5.641	0.0057245	2.593	2.611	0.0026	2.668	2.653	2.675	2.665	2.675	2.661	2.661	2.666	3.143	2.975	0.00306	0.534	7.296	0.02	385713	0.386
5	5.915	5.991	0.005953	2.609	2.616	0.0026	2.858	2.858	2.734	2.817	2.938	2.821	2.785	2.848	3.098	3.143	0.00312	0.524	11.007	0.02	528311	0.528
6	6.129	6.237	0.006183	2.667	2.661	0.0027	2.507	2.464	2.639	2.537	2.573	2.456	2.515	2.515	3.592	3.722	0.00366	0.592	8.438	0.02	475781	0.476
7	5.757	5.89	0.0058235	2.609	2.587	0.0026	2.507	2.522	2.522	2.517	2.529	2.544	2.544	2.539	3.240	3.351	0.00330	0.566	7.971	0.02	458883	0.459
8	6.033	5.839	0.005936	2.574	2.609	0.0026	2.522	2.58	2.646	2.583	2.631	2.661	2.624	2.639	3.450	3.200	0.00333	0.560	9.062	0.02	498002	0.498
9	5.973	6.2	0.0060865	2.689	2.773	0.0027	2.624	2.639	2.668	2.644	2.646	2.661	2.558	2.622	3.329	3.578	0.00345	0.567	9.803	0.02	505267	0.505
10	5.917	5.895	0.005906	2.603	2.581	0.0026	2.507	2.609	2.595	2.570	2.529	2.602	2.558	2.563	3.347	3.332	0.00334	0.565	8.21	0.02	463044	0.463
11	5.943	5.821	0.005882	2.611	2.577	0.0026	2.639	2.682	2.697	2.673	2.69	2.69	2.704	2.695	3.270	3.126	0.00320	0.544	9.283	0.02	487934	0.488
12	5.616	5.821	0.0057185	2.645	2.587	0.0026	2.653	2.646	2.675	2.658	2.646	2.653	2.682	2.660	2.958	3.161	0.00306	0.535	7.557	0.02	398830	0.399
13	5.906	6.01	0.005958	2.589	2.592	0.0026	2.69	2.682	2.697	2.690	2.682	2.646	2.719	2.682	3.216	3.328	0.00327	0.549	8.525	0.02	448446	0.448
14	5.905	5.935	0.00592	2.54	2.541	0.0025	2.639	2.609	2.675	2.641	2.661	2.734	2.741	2.712	3.264	3.223	0.00324	0.548	9.115	0.02	491438	0.491
15	5.692	6.224	0.005958	2.613	2.576	0.0026	2.755	2.682	2.785	2.741	2.646	2.675	2.646	2.656	2.951	3.568	0.00326	0.547	7.93	0.02	413575	0.414
16	5.693	5.444	0.0055685	2.455	2.48	0.0025	2.755	2.712	2.741	2.736	2.653	2.675	2.704	2.677	2.957	2.767	0.00286	0.514	9.803	0.02	532400	0.532
17	5.832	5.732	0.005782	2.578	2.58	0.0026	2.551	2.704	2.682	2.646	2.719	2.726	2.69	2.712	3.186	3.020	0.00310	0.537	7.996	0.02	423493	0.423
18	6.194	6.284	0.006239	2.689	2.708	0.0027	2.755	2.726	2.741	2.741	2.704	2.763	2.792	2.753	3.453	3.531	0.00349	0.560	10.303	0.02	503793	0.504
19	6.096	6.092	0.006094	2.689	2.632	0.0027	2.668	2.77	2.77	2.736	2.763	2.777	2.763	2.768	3.360	3.324	0.00334	0.548	11.395	0.02	562772	0.563
20	5.959	6.058	0.0060085	2.632	2.636	0.0026	2.77	2.712	2.712	2.731	2.807	2.807	2.704	2.773	3.228	3.285	0.00326	0.542	9.599	0.02	478372	0.478
			0.00595			0.00262				2.661				2.671				0.00328	0.551	8.93075		0.469
			0.00017			0.00006				0.080				0.082				0.000187	0.018	1.163402		0.048
			0.02867			0.02426				0.030				0.031				0.056951	0.033	0.130269		0.102

K1C data: hand-mixed G1s

SpecNo	W1 [mm]	W2 [mm]	W [mm]	B1 [m] [mm]	B2 [mm]	B [m]	C1.1	C1.2	C1.3	C1	C2.1	C2.2	C2.3	C2	a1 [W1-C1] a2 [W2-C2] a [mm] [mm] [m]	a/W	P [N]	L [m]	K1C [Nm <sup>Λ</sup> -1.5]	K1C [MNm <sup>Λ</sup> -1]	
40%																					
1	6.14	5.99	0.006065	2.665	2.633	0.0026	2.464	2.5	2.544	2.503	2.573	2.566	2.529	2.556	3.637	3.434	0.00354	6.576	0.02	371735	0.372
2	5.954	5.826	0.005889	2.622	2.563	0.0026	2.624	2.646	2.631	2.634	2.602	2.58	2.58	2.587	3.320	3.239	0.00328	7.302	0.02	400989	0.401
3	5.83	5.645	0.0057375	2.541	2.52	0.0025	2.668	2.624	2.675	2.656	2.661	2.641	2.653	2.652	3.174	2.993	0.00308	8.702	0.02	476425	0.476
4	5.909	5.644	0.0057765	2.601	2.5	0.0026	2.566	2.544	2.544	2.551	2.558	2.551	2.551	2.553	3.358	3.091	0.00322	7.664	0.02	442584	0.443
5	5.887	5.586	0.0057365	2.56	2.596	0.0026	2.58	2.566	2.551	2.566	2.646	2.617	2.597	2.620	3.321	2.966	0.00314	7.515	0.02	418768	0.419
6	5.638	5.675	0.0056565	2.529	2.578	0.0026	2.697	2.624	2.646	2.656	2.777	2.704	2.624	2.702	2.982	2.973	0.00298	7.674	0.02	409873	0.410
7	5.695	5.623	0.005659	2.49	2.507	0.0025	2.595	2.595	2.507	2.566	2.602	2.558	2.602	2.587	3.129	3.036	0.00308	7.258	0.02	421100	0.421
8	5.886	5.711	0.0057985	2.531	2.576	0.0026	2.726	2.755	2.712	2.731	2.777	2.748	2.734	2.753	3.155	2.958	0.00306	8.938	0.02	460988	0.461
9	5.952	6.066	0.006009	2.669	2.658	0.0027	2.507	2.522	2.544	2.524	2.529	2.529	2.536	2.531	3.428	3.535	0.00348	6.804	0.02	382713	0.383
10	5.808	5.843	0.0058255	2.53	2.544	0.0025	2.595	2.595	2.624	2.605	2.69	2.704	2.646	2.680	3.203	3.163	0.00318	8.06	0.02	443536	0.444
11	5.734	5.916	0.005825	2.571	2.533	0.0026	2.536	2.566	2.558	2.553	2.573	2.529	2.536	2.546	3.181	3.370	0.00328	6.507	0.02	376335	0.376
12	5.613	5.844	0.0057285	2.576	2.543	0.0026	2.609	2.566	2.551	2.575	2.573	2.675	2.602	2.617	3.038	3.227	0.00313	6.544	0.02	366565	0.367
13	5.809	5.688	0.0057485	2.567	2.573	0.0026	2.609	2.609	2.522	2.580	2.631	2.573	2.661	2.622	3.229	3.066	0.00315	7.785	0.02	433132	0.433
14	6.178	6.236	0.006207	2.702	2.663	0.0027	2.639	2.624	2.624	2.629	2.675	2.631	2.617	2.641	3.549	3.595	0.00357	6.785	0.02	355903	0.356
15	5.797	5.812	0.0058045	2.532	2.582	0.0026	2.536	2.595	2.595	2.575	2.617	2.573	2.602	2.597	3.222	3.215	0.00322	8.702	0.02	491160	0.491
16	5.811	5.646	0.0057285	2.498	2.591	0.0025	2.595	2.595	2.668	2.619	2.602	2.602	2.646	2.617	3.192	3.029	0.00311	8.184	0.02	455091	0.455
17	5.969	5.854	0.0059115	2.528	2.463	0.0025	2.639	2.668	2.675	2.661	2.763	2.807	2.77	2.780	3.308	3.074	0.00319	8.836	0.02	472782	0.473
18	5.648	5.813	0.0057305	2.539	2.574	0.0026	2.624	2.609	2.668	2.634	2.529	2.675	2.631	2.612	3.014	3.201	0.00311	8.406	0.02	463958	0.464
19	6.394	6.596	0.006495	2.695	2.68	0.0027	2.609	2.639	2.551	2.600	2.69	2.646	2.661	2.666	3.794	3.930	0.00386	5.563	0.02	292264	0.292
20	5.802	5.888	0.005845	2.578	2.62	0.0026	2.566	2.609	2.697	2.624	2.675	2.719	2.661	2.685	3.178	3.203	0.00319	8.839	0.02	471503	0.472
			<b>0.00586</b>			<b>0.00258</b>				<b>2.602</b>				<b>2.630</b>		<b>0.00324</b>	<b>0.553</b>	<b>7.6322</b>		<b>0.420</b>	
			<b>0.00020</b>			<b>0.00006</b>				<b>0.054</b>				<b>0.066</b>		<b>0.000214</b>	<b>0.018</b>	<b>0.960422</b>		<b>0.051</b>	
			<b>0.03466</b>			<b>0.02144</b>				<b>0.021</b>				<b>0.025</b>		<b>0.065978</b>	<b>0.033</b>	<b>0.125838</b>		<b>0.121</b>	

K1C data: hand-mixed G1s

SpecNo	W1	W2	W	B1 [mm]	B2	B	C1.1	C1.2	C1.3	C1	C2.1	C2.2	C2.3	C2	a1 [mm]	a2 [mm]	a/W	P [N]	L [m]	K1C [Nm^-1.5]	K1C [Nm^-1.5]			
	[mm]	[mm]	[m]	[mm]	[mm]	[mm]	[mm]	[mm]	[mm]	[mm]	[mm]	[mm]	[mm]	[mm]	[mm]	[mm]	[m]	[N]	[m]					
30%																								
1	5.808	5.949	0.0058785	2.632	2.709	0.0027	2.522	2.522	2.544	2.544	2.529	2.515	2.558	2.558	2.544	3.279	3.405	0.00334	0.569	4.731	0.02	263719	0.264	
2	5.611	5.5	0.0055555	2.497	2.497	0.0025	2.595	2.639	2.595	2.595	2.610	2.588	2.602	2.602	2.597	3.001	2.903	0.00295	0.531	6.774	0.02	386414	0.386	
3	5.51	5.461	0.0054855	2.493	2.507	0.0025	2.478	2.522	2.522	2.522	2.507	2.529	2.544	2.515	2.529	3.003	2.932	0.00297	0.541	5.191	0.02	311318	0.311	
4	6.039	6.066	0.0060525	2.711	2.682	0.0027	2.726	2.595	2.675	2.665	2.631	2.646	2.653	2.643	2.643	3.374	3.423	0.00340	0.561	5.973	0.02	307760	0.308	
5	5.529	5.603	0.005566	2.494	2.484	0.0025	2.668	2.544	2.434	2.549	2.442	2.434	2.5	2.459	2.459	2.980	3.144	0.00306	0.550	7.198	0.02	437965	0.438	
6	5.349	5.601	0.005475	2.423	2.431	0.0024	2.712	2.77	2.734	2.739	2.704	2.734	2.712	2.717	2.717	2.610	2.884	0.00275	0.502	6.803	0.02	370555	0.371	
7	5.698	5.737	0.0057175	2.445	2.419	0.0024	2.536	2.493	2.434	2.488	2.5	2.5	2.456	2.485	2.485	3.210	3.252	0.00323	0.565	6.325	0.02	398718	0.399	
8	5.746	5.496	0.005621	2.441	2.443	0.0024	2.575	2.573	2.551	2.566	2.52	2.507	2.456	2.494	2.494	3.180	3.002	0.00309	0.550	7.557	0.02	461248	0.461	
9	5.817	5.615	0.005716	2.463	2.456	0.0025	2.42	2.536	2.434	2.463	2.427	2.529	2.42	2.459	2.459	3.354	3.156	0.00326	0.569	5.58	0.02	353429	0.353	
10	5.359	6.08	0.0057195	2.415	2.466	0.0024	2.609	2.609	2.609	2.609	2.609	2.617	2.631	2.602	2.617	2.750	3.463	0.00311	0.543	5.029	0.02	292439	0.292	
11	5.432	5.696	0.005564	2.485	2.376	0.0024	2.58	2.493	2.595	2.556	2.719	2.894	2.821	2.811	2.811	2.876	2.885	0.00288	0.518	6.876	0.02	384235	0.384	
12	5.476	5.748	0.005612	2.433	2.466	0.0024	2.536	2.522	2.551	2.536	2.558	2.588	2.544	2.563	2.563	2.940	3.185	0.00306	0.546	6.622	0.02	398101	0.398	
13	5.704	5.835	0.0057695	2.4	2.51	0.0025	2.712	2.624	2.668	2.668	2.602	2.675	2.675	2.651	2.651	3.036	3.184	0.00311	0.539	6.84	0.02	384853	0.385	
14	5.898	5.807	0.0058525	2.538	2.532	0.0025	2.624	2.609	2.653	2.629	2.617	2.646	2.748	2.670	2.670	3.269	3.137	0.00320	0.547	5.871	0.02	322059	0.322	
15	5.936	6.19	0.006063	2.66	2.588	0.0026	2.551	2.653	2.595	2.600	2.631	2.631	2.661	2.661	2.661	3.336	3.549	0.00344	0.568	5.013	0.02	270829	0.271	
16	5.642	5.389	0.0055155	2.445	2.464	0.0025	2.653	2.653	2.595	2.634	2.602	2.719	2.631	2.651	2.651	3.008	2.738	0.00287	0.521	5.583	0.02	316401	0.316	
17	5.615	5.739	0.005677	2.451	2.458	0.0025	2.653	2.682	2.653	2.663	2.631	2.646	2.631	2.636	2.636	2.952	3.103	0.00303	0.533	6.94	0.02	392446	0.392	
18	6.157	5.749	0.005953	2.617	2.623	0.0026	2.741	2.653	2.609	2.668	2.661	2.661	2.646	2.656	2.656	3.489	3.093	0.00329	0.553	6.41	0.02	338109	0.338	
19	5.706	5.651	0.0056785	2.482	2.511	0.0025	2.505	2.609	2.507	2.540	2.515	2.661	2.529	2.568	2.568	3.166	3.083	0.00312	0.550	6.661	0.02	392110	0.392	
20	5.796	5.85	0.005823	2.46	2.585	0.0025	2.858	2.916	2.799	2.858	2.85	2.821	2.865	2.845	2.845	2.938	3.005	0.00297	0.510	5.286	0.02	259548	0.260	
			0.00571			0.00250				2.604				2.612					0.00311	0.543	6.16315			0.352
			0.00018			0.00008				0.093				0.105					0.000184	0.019	0.829851			0.058
			0.03096			0.03314				0.036				0.040					0.059129	0.036	0.134647			0.163

K1C data: hand-mixed G1s

SpectNo	W1 [mm]	W2 [mm]	W [mm]	B1 [mm]	B2 [mm]	B [mm]	C1.1	C1.2	C1.3	C1	C2.1	C2.2	C2.3	CZ	a1 [mm]	(W1-C1)a2 [mm]	(W2-C2)a [mm]	a/W	P [N]	L [m]	K1C [Nm <sup>-1.5</sup> ]	K1C [MNm <sup>-1</sup> ]
20%																						
1	5.946	5.996	0.005971	2.64	2.653	0.002647	2.464	2.588	2.529	2.527	2.414	2.464	2.464	2.447	3.419	3.549	0.00348	0.583	3.241	0.02	188077	0.188
2	6.06	5.869	0.0059645	2.65	2.63	0.00264	2.376	2.376	2.42	2.391	2.412	2.515	2.339	2.422	3.669	3.447	0.00356	0.597	3.577	0.02	218965	0.219
3	5.951	5.797	0.005874	2.669	2.662	0.002666	2.412	2.485	2.515	2.471	2.595	2.609	2.595	2.600	3.480	3.197	0.00334	0.568	4.246	0.02	237312	0.237
4	5.354	5.287	0.0053205	2.376	2.418	0.002397	2.375	2.388	2.414	2.392	2.552	2.526	2.408	2.495	2.962	2.792	0.00288	0.541	4.419	0.02	289132	0.289
5	5.465	5.418	0.0054415	2.402	2.461	0.002432	2.405	2.42	2.536	2.454	2.456	2.427	2.456	2.446	3.011	2.972	0.00299	0.550	4.334	0.02	278842	0.279
6	5.298	5.22	0.005259	2.341	2.328	0.002335	2.609	2.609	2.507	2.575	2.602	2.588	2.515	2.568	2.723	2.652	0.00269	0.511	3.616	0.02	224023	0.224
7	6.033	5.737	0.005885	2.622	2.531	0.002577	2.391	2.296	2.325	2.337	2.383	2.361	2.318	2.354	3.696	3.383	0.00354	0.601	3.476	0.02	226651	0.227
8	5.397	5.207	0.005302	2.29	2.333	0.002312	2.391	2.42	2.383	2.398	2.412	2.5	2.449	2.454	2.999	2.753	0.00288	0.542	3.748	0.02	257201	0.257
9	6.452	6.23	0.006341	2.713	2.716	0.002715	2.464	2.449	2.434	2.449	2.383	2.427	2.412	2.407	4.003	3.823	0.00391	0.617	4.174	0.02	245639	0.246
10	6.045	5.954	0.0059995	2.636	2.656	0.002646	2.412	2.58	2.515	2.502	2.5	2.412	2.464	2.459	3.543	3.495	0.00352	0.587	4.092	0.02	238545	0.239
11	5.507	5.152	0.0053295	2.304	2.349	0.002327	2.507	2.391	2.434	2.444	2.573	2.369	2.5	2.481	3.063	2.671	0.00287	0.538	3.695	0.02	246191	0.246
12	5.654	5.523	0.0055885	2.321	2.368	0.002345	2.515	2.522	2.493	2.510	2.525	2.515	2.529	2.523	3.144	3.000	0.00307	0.550	3.253	0.02	208510	0.209
13	5.783	5.75	0.0057665	2.388	2.4	0.002394	2.522	2.515	2.5	2.512	2.515	2.527	2.52	2.521	3.271	3.229	0.00325	0.564	3.541	0.02	222678	0.223
14	5.66	5.45	0.005555	2.4	2.431	0.002416	2.449	2.522	2.449	2.473	2.485	2.602	2.515	2.534	3.187	2.916	0.00305	0.549	4.321	0.02	270880	0.271
15	5.341	5.571	0.005456	2.399	2.3	0.00235	2.668	2.624	2.602	2.631	2.573	2.602	2.58	2.585	2.710	2.986	0.00285	0.522	4.095	0.02	247239	0.247
16	5.468	5.461	0.0054645	2.366	2.291	0.002329	2.588	2.274	2.361	2.408	2.325	2.354	2.325	2.335	3.060	3.126	0.00309	0.566	4.319	0.02	305399	0.305
17	6.033	5.856	0.0059445	2.427	2.492	0.00246	2.522	2.536	2.529	2.529	2.471	2.529	2.507	2.502	3.504	3.354	0.00343	0.577	3.021	0.02	185303	0.185
18	5.914	5.896	0.005905	2.595	2.566	0.002581	2.588	2.274	2.361	2.408	2.325	2.325	2.354	2.335	3.506	3.561	0.00353	0.598	4.067	0.02	260438	0.260
19	5.299	5.721	0.00551	2.488	2.315	0.002402	2.522	2.485	2.536	2.514	2.573	2.536	2.442	2.517	2.785	3.204	0.00299	0.543	6.006	0.02	375699	0.376
20	5.859	5.484	0.0056715	2.561	2.595	0.002578	2.624	2.609	2.522	2.585	2.777	2.568	2.544	2.630	3.274	2.854	0.00306	0.540	3.67	0.02	202587	0.203
			0.00568			0.00248				2.476				2.481					3.94555		0.246	
			0.00030			0.00014				0.075				0.084					0.028		0.044	
			0.05254			0.05541				0.030				0.034					0.051		0.179	